Final Technical Report
SERDP Project CU 1168

Characterization of the Aerobic Oxidation of *cis*-Dichloroethene and Vinyl Chloride in Support of Bioremediation of Chloroethene-Contaminated Sites

James M. Gossett, Timothy E. Mattes, and Deborah L. Sills

(School of Civil and Environmental Engineering, Cornell University, Ithaca NY)

Jim C. Spain, Shirley F. Nishino and Nicholas V. Coleman

(Air Force Research Laboratory—MLQL, Tyndall AFB, FL)

November 5, 2004

Report Documentation Page

Form Approved
OMB No. 0704-0188

1. REPORT DATE	2. REPORT TYPE	3. DATES COVERED
05 NOV 2004		**00-00-2004 to 00-00-2004**

4. TITLE AND SUBTITLE	5a. CONTRACT NUMBER
Characterization of the Aerobic Oxidation of cis-Dichloroethene and Vinyl Chloride in Support of Bioremediation of Chloroethene-Contaminated Sites	5b. GRANT NUMBER
	5c. PROGRAM ELEMENT NUMBER
6. AUTHOR(S)	5d. PROJECT NUMBER
	5e. TASK NUMBER
	5f. WORK UNIT NUMBER
7. PERFORMING ORGANIZATION NAME(S) AND ADDRESS(ES) **Air Force Research Laboratory,AFRL-MLQL,Tyndall AFB,FL,32403**	8. PERFORMING ORGANIZATION REPORT NUMBER
9. SPONSORING/MONITORING AGENCY NAME(S) AND ADDRESS(ES)	10. SPONSOR/MONITOR'S ACRONYM(S)
	11. SPONSOR/MONITOR'S REPORT NUMBER(S)

12. DISTRIBUTION/AVAILABILITY STATEMENT
Approved for public release; distribution unlimited

13. SUPPLEMENTARY NOTES

14. ABSTRACT

15. SUBJECT TERMS

16. SECURITY CLASSIFICATION OF:			17. LIMITATION OF ABSTRACT	18. NUMBER OF PAGES	19a. NAME OF RESPONSIBLE PERSON
a. REPORT **unclassified**	b. ABSTRACT **unclassified**	c. THIS PAGE **unclassified**	**Same as Report (SAR)**	**143**	

Table of Contents

List of Acronyms iii
List of Figures iv
List of Tables iv
Acknowledgements v
Executive Summary vi
Background 1
Objectives 1
Results and Accomplishments 2
Phylogenetic and Kinetic Diversity of Aerobic Vinyl-Chloride-Assimilating Bacteria from Contaminated Sites 2
Isolation and Characterization of a cDCE-Degrading Bacterium 5
Characterization of VC and ETH Oxidation in *Mycobacterium* strain JS60 6
Distribution of the Coenzyme M Pathway of Epoxide Metabolism among Ethene- and Vinyl Chloride-Degrading *Mycobacterium* Strains 8
A Linear Plasmid Carries Vinyl Chloride Biodegradation Genes in *Nocardioides* JS614 10
Characterization of the Vinyl Chloride and Ethene Starvation Response in *Nocardioides* Strain JS614 13
Site-Specific Study — Distribution and Activity of VC-Degraders at Moody AFB 14
Site Description 14
Field Sampling 15
Microcosm Preparation 16
Gas Chromatography 17
Results — Site Characterization 18
Results — Microcosm Studies 18
Inoculation of Moody Microcosms with JS621 and/or Nutrients 20
MPN Enumeration of VC- and ETH-Degraders in Moody AFB Samples 22
Moody AFB Well-Water Study 24
Moody AFB Discussion 26
Final Summary and Conclusions 27
References 29

Appendices 31

Appendix A: Coleman, N. V., T. E. Mattes, J. M. Gossett, and J. C. Spain 2002. Phylogenetic and kinetic diversity of aerobic vinyl chloride-assimilating bacteria from contaminated sites. *Appl. Environ. Microbiol.* 68:6162-6171. 31

Appendix B: Coleman, N. V., T. E. Mattes, J. M. Gossett, and J. C. Spain 2002. Biodegradation of *cis*-dichloroethene as the sole carbon source by a beta-proteobacterium. *Appl. Environ. Microbiol.* 68:2726-2730. 32

Appendix C: Coleman, N. V., and J. C. Spain 2003. Epoxyalkane:Coenzyme-M transferase in the ethene and vinyl-chloride biodegradation pathways of *Mycobacterium* strain JS60. *J. Bacteriol.* 185: 5536-5545 33

Appendix D: Coleman, N. V., and J. C. Spain 2003. Distribution of the Coenzyme-M pathway of epoxide metabolism among ethene- and vinyl-chloride-degrading *Mycobacterium* strains. *Appl. Environ. Microbiol.* 69:6041-6046. 34

Appendix E: Mattes, T. E., N. V. Coleman, J. C. Spain, and J. M. Gossett 2004. A linear plasmid carries vinyl chloride biodegradation genes in *Nocardioides* JS614. Manuscript submitted to *Archives of Microbiology*. 35

Appendix F: Mattes, T. E., N. V. Coleman, J. C. Spain, and J. M. Gossett 2004. Characterization of the vinyl chloride and ethene starvation response in *Nocardioides* Strain JS614. Manuscript submitted to *Archives of Microbiology*. 36

List of Acronyms

AkMO	alkene monoxygenase
bgs	below ground surface
cDCE	*cis*-1,2-dichloroethene
CoA	coenzyme A
DNA	deoxyribonucleic acid
DOD	U. S. Department of Defense
DOE	U.S. Department of Energy
EaCoMT	epoxyalkane coenzyme-M transferase
ETH	ethene
GC	gas chromatography
MS	mass spectrometry
PCE	tetrachloroethene (perchloroethylene)
PCR	polymerase chain reaction
SERDP	Strategic Environmental Research and Development Program
TCE	trichloroethene
VC	vinyl chloride

List of Figures

Figure 1. 16S rDNA sequence analysis of VC-, ETH-, and cDCE-degrading strains based on 459-bp ClustalX alignment. Bold font: Isolates from the present study, with isolation substrate. Italic font: Reference bacteria from GenBank. 4

Figure 2. Growth of *Mycobacterium* strain JS60 on VC (A) or ETH (B) as the sole carbon and energy sources at 30°C, pH 6.5. Growth rates (0.080 h^{-1} with ethene, 0.017 h^{-1} with VC) were calculated by plotting an exponential curve through a subset of the OD_{600} data (not shown). 6

Figure 3. Metabolism of ETH and VC by JS60 cell suspensions. A. ETH-grown cells, no inhibitor; B. ETH-grown cells +20 mM fluoroacetate; C. VC-grown cells, no inhibitor; D. VC-grown cells +20 mM fluoroacetate. Cells were suspended in phosphate buffer at a density (OD_{600}) of 5 (A, B) or 30 (C, D). 7

Figure 4. Schematic diagram of genes encoded on the 8364 bp *Nhe*I restriction fragment cloned from *Mycobacterium* strain JS60. *orf*1 and *orf*2 are likely to be involved in acyl-CoA ester metabolism, *etnE* encodes an EaCoMT, and the *etnABCD* genes encode a putative 4-component alkene monooxygenase. 8

Figure 5. Hypothetical pathway of VC and ETH assimilation in *Nocardioides* JS614 12

Figure 6. Map of vinyl chloride contaminant plume at Moody AFB LF04 site. Sample locations (AF1-AF11) are circled 15

Figure 7. Vinyl chloride vs. time for autoclaved-control and live microcosms from AF1 19

Figure 8. Ethene vs. time for autoclaved-control and live microcosms from AF1 19

Figure 9. Results from inoculation of Moody LF04 microcosms with JS621 21

Figure 10. Vinyl chloride vs. time for autoclaved-control and live microcosm bottles from MW9 25

Figure 11. Ethene vs. time for autoclaved-control and live microcosm bottles from MW9 25

List of Tables

Table 1. Site Characterization Parameters for Moody LF04. 18

Table 2. pH values for JS621 amendment experiment. 23

Acknowledgements

The following worked, on or assisted with, this research project:

In the environmental engineering laboratories of Cornell University

- Prof. James M. Gossett, PI
- Timothy E. Mattes, PhD student
- Deborah L. Sills, MS student
- Juli Rubin, undergraduate student
- Brian Weisenstein, PhD student in microbiology (doing temporary rotation through the Gossett lab)

Elsewhere at Cornell University

- Prof. Anthony Hay, microbiology, for technical advice
- Prof. Stephen Zinder, microbiology, for technical advice
- Prof. Ruth Richardson, civil/environmental engineering, for technical advice
- Linda Rankin, PhD student in the Zinder lab, for technical assistance

In the U.S. Air Force Research Laboratory, MLQL Tyndall AFB, FL

- Dr. Jim C. Spain, PI
- Dr. Nicolas V. Coleman, post-doctoral research associate
- Dr. Shirley Nishino, post-doctoral research associate
- Mike Allen and John Dunlap assisted with characterization of JS666
- Nathan Lo assisted with phylogenetic analyses
- Crystal Henley assisted with isolation of ethene degraders
- F. P. Guengerich advised on chorooxirane synthesis
- Heather Luckarift and Lloyd Nadeau assisted with MS analyses

Nicholas Coleman was supported by a postdoctoral fellowship from the Oak Ridge Institute for Science and Education (U.S. Department of Energy).

Many people supplied cultures and samples, including: Scott Ensign, Torin Weisbrod, Bill Jacobs, Petra Koziollek, Melinda Chambless, Mike Witt, Sandra Dworatzek, Evan Cox, Elizabeth Edwards, Lori Moser, Bella Chu, Jim Clarke, Todd Wiedemeier, Bob Davis, Merv Dale, Scott Glass, Rob Simcik, John Nash, Kandi Brown, and Mike Miracle.

Executive Summary

The lesser chlorinated ethenes, *cis*-1,2-dichloroethene (cDCE) and vinyl chloride (VC), are produced by anaerobic reductive dechlorination at subsurface sites contaminated by tetrachloroethene (PCE) and trichloroethene (TCE). Accumulation of VC and cDCE under anaerobic conditions limits the application of natural attenuation and enhanced reductive anaerobic biological in-situ treatment technologies (RABITT). Aerobic degradation of lesser-chlorinated ethenes has been demonstrated, suggesting that sequential anaerobic/aerobic conditions may result in complete mineralization of PCE/TCE. However, our present understanding of the aerobic transformation potentials of cDCE and VC is limited, thus limiting the reliability of — and confidence in — natural and enhanced biological alternatives for site remediation.

The objective of our project was to determine the prevalence and metabolic capabilities of microorganisms able to derive energy from aerobic oxidation of cDCE and/or VC in subsurface environments. The results help delineate the role of growth-coupled (vs. cometabolic) aerobic oxidation in the natural attenuation of lesser-chlorinated ethenes. Results provide the basis for improved site assessment, improved remedial-action decision-making, and more reliable bioremediation technologies.

Our findings indicate that aerobic bacteria (*Mycobacterium* and *Nocardioides* strains) capable of growth-linked VC oxidation are widespread in the environment, and commonly found at chlorinated-ethene-contaminated sites. Aerobic assimilation of VC as a carbon source is therefore an ecologically significant phenomenon of equal or greater importance than cometabolic VC degradation. Based on their distribution, growth rates and kinetic parameters, we believe that *Mycobacterium* strains are most likely to be responsible for the aerobic natural attenuation of VC that has been observed at many sites. The data suggest that biostimulation (e.g. addition of O_2 and/or inorganic nutrients) would be an appropriate strategy for accelerating VC attenuation at contaminated sites, because the appropriate microbial populations are likely to be already present in many cases.

Our discovery of a bacterium (*Polaromonas* strain JS666) able to grow on cDCE shows that aerobic biodegradation of cDCE in the absence of other carbon substrates is possible. From our results with enrichment cultures, these bacteria appear to be rare, and may presently exist only in highly selective 'artificial' environments such as the activated carbon filter that was the source of strain JS666. Our data suggest that it is unlikely that natural attenuation or biostimulation alone will be capable of remediation of cDCE contamination at most sites. Bioaugmentation with our isolate JS666 would be an appropriate strategy, and could lead to a self-sustaining, low-cost bioremediation method at sites where cDCE is a problem contaminant. Further investigation of JS666 is recommended — to delineate metabolic pathways; to determine the suite of substrates it can co-transform; to optimize culture conditions for field-bioaugmentation; to develop a molecular probe for field-monitoring after bioaugmentation; and, finally, to field-test the use of JS666 as bioaugmentation agent.

We have conclusively identified the enzyme (EaCoMT) responsible for bacterial epoxyethane metabolism, and obtained strong circumstantial evidence that the same enzyme is

also involved in chlorooxirane metabolism. In addition, we have cloned and sequenced genes involved in VC, ETH, epoxyethane and chlorooxirane metabolism. The results indicate that the EaCoMT and monooxygenase enzymes encoded by a single operon (*etnEABCD*) in *Mycobacterium* JS60 and *Nocardioides* JS614 catalyze the initial reactions in both the VC and ETH assimilation pathways. EaCoMT activity and genes were found in all the alkene-oxidizing strains that we examined, including strains isolated on VC and ethene. The EaCoMT-specific gene primers we have developed could be used for culture-independent monitoring of microbial populations during the natural attenuation or bioremediation of chlorinated ethenes. Such methods are particularly relevant for mycobacteria, which are slow-growing and sometimes difficult to isolate.

Based on our data, there was no DNA sequence (either 16S rDNA or EaCoMT gene) that distinguished VC- from ETH-degraders. However, the EaCoMT activity in cell extracts of the VC-degraders tended to be higher. This is particularly apparent when strains JS619 (VC) and JS625 (ETH) are compared – these strains had almost identical EaCoMT gene sequences, but the EaCoMT activity in cell extracts was 5-fold higher in JS619. Sequencing of complete EaCoMT genes and flanking DNA, and analysis of the activity of other catabolic enzymes may help to shed light on the factors that distinguish ethene- and VC-assimilating bacteria, and yield insights into the possible evolution of the latter group from the former.

The EaCoMT gene appears to be carried on large linear plasmids in the VC-degrading strains. Based on the gene organization in *Mycobacterium* strain JS60, it is likely that the alkene monooxygenase genes are also present on the same linear plasmids, which is apparently the case with *Nocardiodes* strain JS614. The present study is the first to our knowledge to associate a specific metabolic function with plasmids in *Mycobacterium* strains. Plasmid-borne genes for ethene- and VC- biodegradation could potentially be transferred among bacteria in the environment, and thus, further investigation of the such elements is warranted in light of the potential importance of the alkene-degrading phenotype to bioremediation and natural attenuation processes.

We note that *Nocardioides* JS614 may hold promise as a bioaugmentation agent at sites where other VC-oxidizers are absent. JS614 has very high growth and VC-utilization rates. It is also of a genus that, unlike mycobacteria, has no pathogenic brethren — a factor in gaining regulatory acceptance. The one, known drawback of JS614 is its peculiarly severe response to starvation. However, in studies reported herein, we were able to show that the starvation response can be virtually eliminated if small amounts of a readily degradable substrate (e.g., acetate) is administered along with VC following VC-starvation.

Finally, we note that two organisms isolated and identified from this research study — *Nocardioides* JS614 and *Polaromonas* strain JS666 — have been selected by DOE for genomic draft sequencing. We present this as evidence that the scientific community in general is enthusiastic about the outcome of our SERDP-sponsored research.

Background

The lesser chlorinated ethenes, *cis*-1,2-dichloroethene (cDCE) and vinyl chloride (VC), are produced by anaerobic reductive dechlorination at subsurface sites contaminated by tetrachloroethene (PCE) and trichloroethene (TCE). Accumulation of VC and cDCE under anaerobic conditions limits the application of natural attenuation and enhanced reductive anaerobic biological in-situ treatment technologies (RABITT). Aerobic degradation of lesser-chlorinated ethenes has been demonstrated, suggesting that sequential anaerobic/aerobic conditions may result in complete mineralization of PCE/TCE. However, our present understanding of the transformation potentials of cDCE and VC is limited, thus limiting the reliability of — and confidence in — natural and enhanced biological alternatives for site remediation.

Previous laboratory studies have revealed the existence of bacteria able to couple growth to aerobic oxidation of VC (Hartmans and deBont, 1992; Hartmans et al., 1985; Verce et al., 2000; Verce et al., 2001). Several field and microcosm studies (Bradley and Chapelle, 2000; Bradley and Chapelle, 1998; Klier et al., 1999) previously suggested that aerobic oxidation of cDCE occurs in the absence of cometabolic substrates (e.g., methane, ethene, or toluene). Questions remain concerning the environmental prevalence (and hence *relevance*) of growth-coupled, aerobic VC- and cDCE-oxidizing bacteria; pathways and biochemistry involved; the relationship between VC- and ethene (ETH)-degraders (i.e., do the former derive from the latter?); and the *in situ* activity and distribution of aerobic VC- and cDCE-oxidizing bacteria.

Objectives

The objective of our project was to determine the prevalence and metabolic capabilities of microorganisms able to derive energy from aerobic oxidation of cDCE and/or VC in subsurface environments. The results help delineate the role of growth-coupled (vs. cometabolic) aerobic oxidation in the natural attenuation of lesser-chlorinated ethenes. The findings shed much-needed light on the aerobic transformations of lesser-chlorinated ethenes — compounds currently limiting the efficacy of natural attenuation and enhanced bioremediation of candidate sites. Results provide the basis for improved site assessment, improved remedial-action decision-making, and more reliable bioremediation technologies.

By isolating bacteria capable of growth on chloroethenes and determining the biochemical differences between these strains and those that grow on ethene, we hoped to develop molecular methods of detecting such microbes at contaminated sites. In conjunction with an activity-based assay using microcosms, this strategy would provide the ability to both predict biodegradation and to monitor ongoing processes during natural attenuation or bioremediation. A better understanding of these oxidative pathways should expand the number of sites judged suitable for bioremediation alternatives (natural and enhanced), with potential savings to DoD in the millions of dollars.

The following questions were addressed through this research effort:

1. What is the prevalence of aerobic bacteria able to grow on cDCE and/or VC? It is clear that they are not ubiquitous. Are they present at contaminated sites? If so can their presence be taken as evidence of aerobic cDCE and/or VC degradation and consequent hazard reduction?
2. What are the requirements and capabilities of aerobic bacteria able to grow on cDCE and/or VC? What metabolic pathways are employed? Do such pathways differ from those employed by ethene (ETH) degraders? What other substrates can be transformed by cDCE- and/or VC-oxiders? What are the kinetic parameters (rate constants, thresholds) with respect to both the chlorinated-ethene substrates and oxygen? These are practical concerns that relate to the environmental niches occupied by the organisms.
3. How closely related are chloroethene degraders and ethene degraders? The previous studies suggest that chloroethene-degrading strains are derived from ETH-degrading strains by changes in the regulation of the pathway. The hypothesis would be simple to test if chloroethene-degrading strains and ETH-degrading strains could be isolated from the same ecosystem. The answer to the questions should provide the ability to predict chloroethene degradation when site conditions are known. In other words, can cDCE and/or VC degraders be expected to either be present or arise from indigenous ethene degraders when the conditions are appropriate?

Results and Accomplishments

Four papers arising from this SERDP-sponsored research project have been published in the refereed, scientific literature. In addition, two manuscripts have been submitted and are *in-review*. In the sections that follow, we provide only summaries of our work, where published papers or submitted manuscripts are available. For those readers desiring full details, the full papers/manuscripts can be found in Appendices A through F.

Phylogenetic and Kinetic Diversity of Aerobic Vinyl-Chloride-Assimilating Bacteria from Contaminated Sites

[See full paper in Appendix A]

Aerobic bacteria that grow on vinyl chloride (VC) have been isolated previously, but their diversity and distribution are largely unknown. It is also unclear whether such bacteria contribute to the natural attenuation of VC at chlorinated-ethene-contaminated sites. We detected aerobic VC biodegradation in 23 of 37 microcosms and enrichments inoculated with samples from various sites (Coleman et al., 2002b). Twelve different bacteria (11 *Mycobacterium* strains and 1 *Nocardioides* strain) capable of growth on VC as the sole carbon source were isolated, and 5 representative strains were examined further. All the isolates grew on ethene in addition to VC and contained VC-inducible ethene-monooxygenase activity. The *Mycobacterium* strains (JS60, JS61, JS616, and JS617) all had similar growth yields (5.4 to 6.6 g of protein/mol), maximum specific growth rates (0.17 to 0.23 day^{-1}), and maximum specific substrate utilization rates (9 to 16 nmol/min/mg of protein) with VC. The *Nocardioides* strain (JS614) had a higher growth yield (10.3 g of protein/mol), growth rate (0.71 day^{-1}), and substrate utilization rate (43 nmol/min/mg of protein) with VC but was much more sensitive to VC starvation. Half-velocity constant (K_s) values for VC were between 0.5 and 3.2 μM, while K_s values for oxygen ranged from 0.03 to 0.3

mg/liter. Oxygen threshold values (the concentration of oxygen below which it cannot be used) during VC oxidation were measurable, but very low — 0.02 to 0.1 mg/liter. The low oxygen half-velocity constants and thresholds suggest that VC oxidation can proceed in very low-oxygen environments. However, the VC-oxidizers we isolated are *not* microaerophiles — all tolerated even pure oxygen.

Since VC-oxidation rates are relatively rapid, VC may become depleted before it migrates very far into aerobic portion of the plume. It is quite possible, then, that growth-coupled-VC-oxidizers may operate principally within the low-oxygen boundary between anaerobic and aerobic zones in VC-contaminated aquifers.

Using soil samples with no history of chlorinated ethene contamination, we also isolated four ETH-assimilating bacteria (JS622, JS623, JS624 and JS625) that cannot grow on VC (Figure 1). Strains JS622 and JS623 were from sandy garden soil (Panama City, FL), strain JS624 was from grass rhizosphere soil (Central Park, New York City, NY), and strain JS625 was from decomposing tree bark (National Mall, Washington, D.C.). A remarkable conclusion of our study is that aerobic enrichments on both VC and ETH almost always yielded *Mycobacterium* strains, regardless of the sample type or geographical location.

Our isolation results indicate that VC- assimilating bacteria are present at a great many contaminated sites, and suggest that aerobic natural attenuation of VC via growth-coupled oxidation may be a widespread phenomenon. The implications for enhanced bioremediation are that a biostimulation strategy (e.g. addition of oxygen and inorganic nutrients) may be sufficient at some sites to enhance in situ VC oxidation.

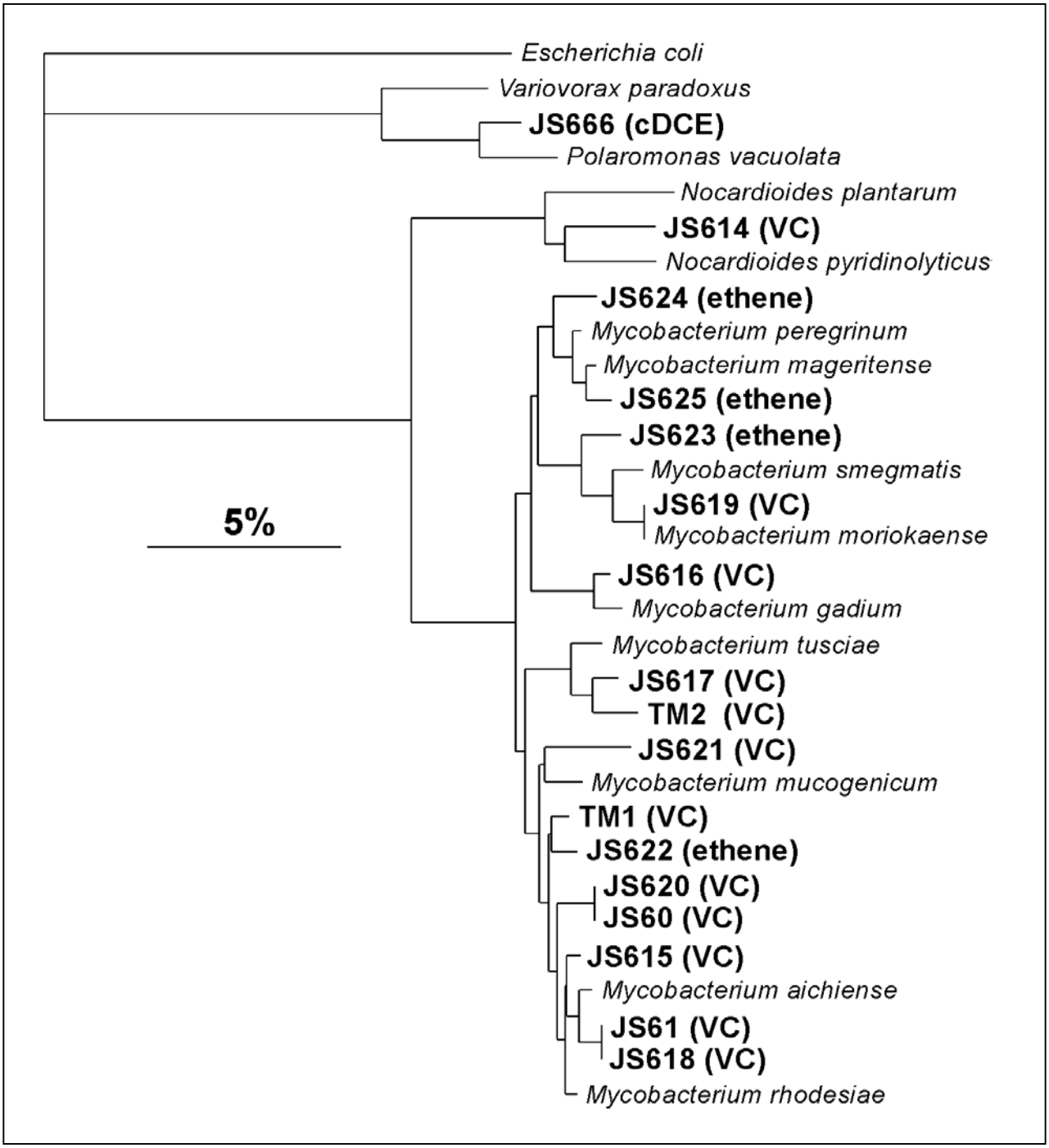

Figure 1. 16S rDNA sequence analysis of VC-, ETH-, and cDCE-degrading strains based on 459-bp ClustalX alignment. Bold font: Isolates from the present study, with isolation substrate. Italic font: Reference bacteria from GenBank.

Isolation and Characterization of a cDCE-Degrading Bacterium

[See full paper in Appendix B]

From 30 aerobic microcosms set up with cDCE as sole carbon source, two yielded cDCE-degrading activity that could be transferred repeatedly in minimal medium, indicating that microorganisms capable of growth on cDCE were present. A pure culture of cDCE-assimilating bacteria was successfully isolated (Coleman et al., 2002a) from one of the enrichments, which was inoculated with activated carbon from a pump-and-treat plant (Dortmund, Germany) processing chloroethene-contaminated groundwater.

The 16S ribosomal DNA sequence of the isolate (strain JS666) had 97.9% identity to the sequence from *Polaromonas vacuolata*, indicating that the isolate was a β-proteobacterium. At 20°C, strain JS666 grew on cDCE with a minimum doubling time of 73 ± 7 h and a growth yield of 6.1 g of protein/mol of cDCE. Chloride analysis indicated that complete dechlorination of cDCE occurred during growth (1.94 mol of Cl produced/mol of cDCE degraded). There was no detectable growth in JS666 cultures without cDCE, and there was no significant disappearance of cDCE in flasks inoculated with autoclaved cells. The pH optimum for growth of strain JS666 on cDCE was 7.2. Growth on cDCE was optimal at temperatures between 20 and 25°C and was not detectable at 30°C. The half-velocity constant (K_s) for cDCE transformation was 1.6 ± 0.2 μM, and the maximum specific substrate utilization rate (k) ranged from 12.6 to 16.8 nmol/min/mg of protein.

Cells grown on cDCE could transform (but not grow on) ethene, vinyl chloride, *trans*-dichloroethene, trichloroethene, and 1,2-dichloroethane. Epoxyethane was produced from ethene by cDCE-grown cells, suggesting that an epoxidation reaction is the first step in cDCE degradation.

The ability of cDCE-grown JS666 cells to transform other chloroethenes may prove to be very useful at contaminated sites, where mixtures of pollutants may be encountered. It is surprising that strain JS666 did not grow on ethene, which seems to be the most likely natural substrate of the cDCE-degrading enzymes, particularly considering the fact that the VC-assimilating bacteria isolated to date also use ethene as a carbon source (Coleman et al., 2002b) and at least in one case appear to have evolved directly from ethene-degrading bacteria (Verce et al., 2001).

The relatively low measured K_s value, considered in conjunction with the relatively high k value, is significant considering the possible participation of this organism in natural attenuation of cDCE. If JS666 were present and active at a cDCE-contaminated site, the cDCE utilization rate would be one-half the maximum rate at a cDCE concentration of 160 μg/liter. The Environmental Protection Agency-mandated maximum contaminant level for cDCE in drinking water is 70 μg/liter (http://www.epa.gov). Therefore, under appropriate conditions in the field, JS666 should easily be able to oxidize cDCE to obtain levels below drinking water standard levels. Perhaps more relevant is the observation that in the experiments described here, cDCE was degraded routinely to concentrations below 0.03 μg/liter. The discovery of a bacterium able to grow on cDCE shows that aerobic biodegradation of cDCE in the absence of other carbon substrates is possible. Our results with enrichment cultures indicate that such bacteria appear to

be rare and may exist only in highly selective artificial environments, such as the activated-carbon filter that was the source of strain JS666. The existence of cDCE-assimilating bacteria suggests that there is potential for bioaugmentation, which could lead to a self-sustaining, low-cost bioremediation strategy at sites where cDCE is a problem contaminant. Our results indicate that growth on cDCE as a carbon source could be a previously unrecognized factor in determining the environmental fate of this compound. Further characterization of JS666 should facilitate the search for similar strains and allow evaluation of the role of such strains in the natural attenuation of cDCE and other chlorinated ethenes.

Characterization of VC and ETH Oxidation in *Mycobacterium* strain JS60

[See full paper in Appendix C]

Growth conditions for *Mycobacterium* strain JS60 were optimized by increasing the temperature to 30°C and decreasing the pH to 6.5 (Figure 2). The modifications resulted in increases in the growth rates on ethene and VC of 3.3-fold and 1.9-fold respectively, compared to the rates at 20°C, pH 7.0 (Coleman et al., 2002b). Ethene was clearly a better substrate than VC, in terms of both growth rate and growth yield. The substrate utilization rates of whole cells at 30°C calculated from the growth rates (Fig. 2) and growth yields (Coleman et al., 2002b) were 118 nmol/min/mg protein (ethene) and 44 nmol/min/mg protein (VC).

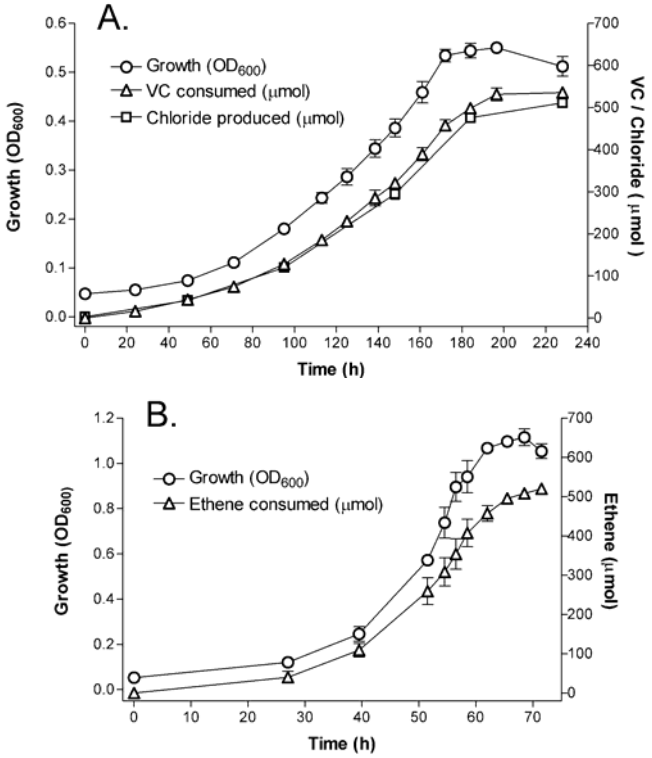

Figure 2. Growth of *Mycobacterium* strain JS60 on VC (A) or ETH (B) as the sole carbon and energy sources at 30°C, pH 6.5. Growth rates (0.080 h^{-1} with ethene, 0.017 h^{-1} with VC) were calculated by plotting an exponential curve through a subset of the OD_{600} data (not shown).

Initial characterization of strain JS60 focused on the alkene monooxygenase activity of cell suspensions grown on VC or ETH. Similar to the early findings of de Bont and co-workers (de Bont and Harder, 1978; Hartmans and de Bont, 1992), we observed that ETH- or VC-grown resting cells of JS60 transiently accumulated epoxyethane and chlorooxirane from ETH and VC, respectively, and that addition of the TCA-cycle inhibitor fluoroacetate caused prolonged accumulation of the epoxides (Figure 3). The data suggest that acetyl-CoA is a key intermendiate in the VC and ethene assimilation pathways.

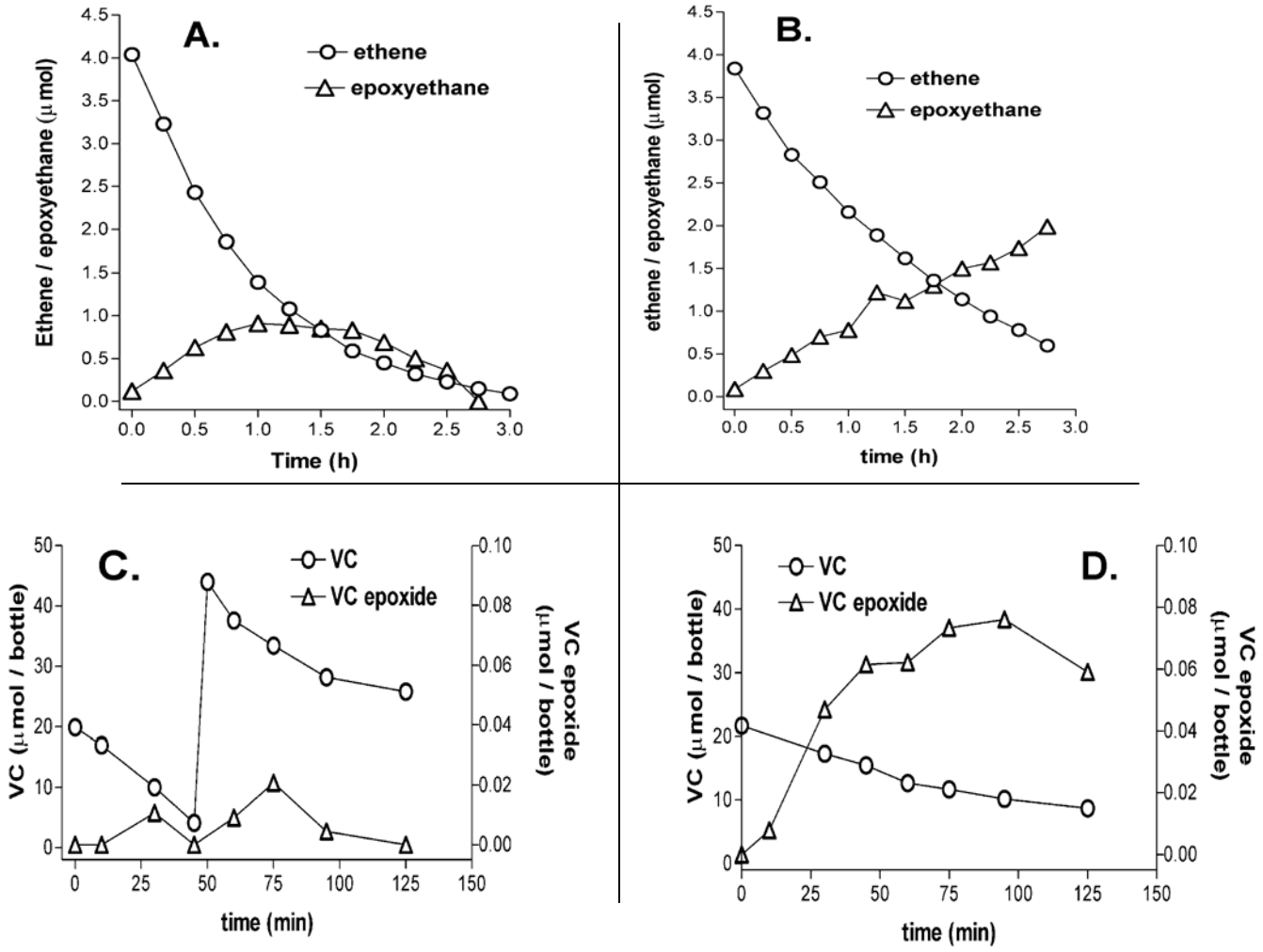

Figure 3. Metabolism of ETH and VC by JS60 cell suspensions. A. ETH-grown cells, no inhibitor; B. ETH-grown cells +20 mM fluoroacetate; C. VC-grown cells, no inhibitor; D. VC-grown cells +20 mM fluoroacetate. Cells were suspended in phosphate buffer at a density (OD_{600}) of 5 (A, B) or 30 (C, D).

We investigated epoxyethane metabolism in *Mycobacterium* strain JS60 and discovered a coenzyme M (CoM)-dependent enzyme activity in extracts from VC and ethene-grown cells

(Coleman and Spain, 2003a). PCR amplifications using primers targeted at epoxyalkane:CoM transferase (EaCoMT) genes yielded part of the JS60 EaCoMT gene, which was used to clone an 8.4-kb genomic DNA fragment. The complete EaCoMT gene (*etnE*) was recovered, along with genes (*etnABCD*) encoding a four-component monooxygenase and two genes possibly involved in acyl-CoA ester metabolism (Fig. 4).

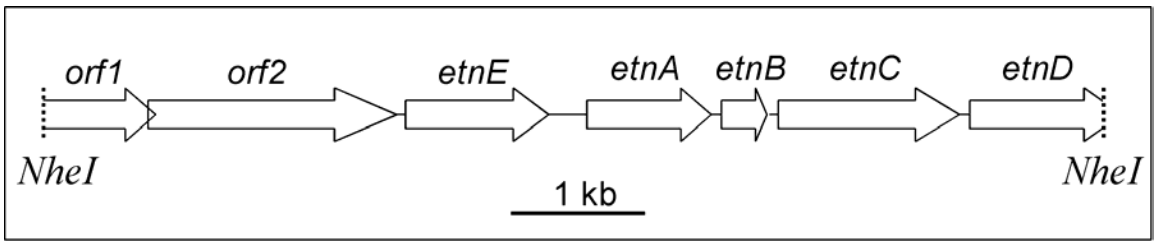

Figure 4. Schematic diagram of genes encoded on the 8364 bp *Nhe*I restriction fragment cloned from *Mycobacterium* strain JS60. *orf*1 and *orf*2 are likely to be involved in acyl-CoA ester metabolism, *etnE* encodes an EaCoMT, and the *etnABCD* genes encode a putative 4-component alkene monooxygenase.

Reverse transcription-PCR indicated that the *etnE* and *etnA* genes were co-transcribed and inducible by ethene and VC. Heterologous expression of the *etnE* gene in *Mycobacterium smegmatis* mc^2155 using the pMV261 vector gave a recombinant strain capable of transforming epoxyethane, epoxypropane, and chlorooxirane. A metabolite identified by mass spectrometry as 2-hydroxyethyl-CoM was produced from epoxyethane.

The results indicate that the EaCoMT and monooxygenase enzymes encoded by a single operon (*etnEABCD*) catalyze the initial reactions in both the VC and ethene assimilation pathways. CoM-mediated reactions appear to be more widespread in bacteria than was previously believed.

Distribution of the Coenzyme M Pathway of Epoxide Metabolism among Ethene- and Vinyl Chloride-Degrading *Mycobacterium* Strains

[See full paper in Appendix D]

An epoxyalkane:coenzyme M (CoM) transferase (EaCoMT) enzyme was found to be active in the aerobic vinyl chloride (VC) and ethene assimilation pathways of *Mycobacterium* strain JS60. EaCoMT activity and genes were next investigated in 10 different mycobacteria isolated on VC or ethene from diverse environmental samples. In all cases, epoxyethane metabolism in cell extracts was dependent on CoM, with average specific activities of EaCoMT between 380 and 2,910 nmol/min/mg of protein. PCR with primers based on conserved regions of EaCoMT genes from *Mycobacterium* strain JS60 and the propene oxidizers *Xanthobacter* strain Py2 and *Rhodococcus* strain B-276 yielded fragments (834 bp) of EaCoMT genes from all of the VC- and ethene-assimilating isolates. The *Mycobacterium* EaCoMT genes form a distinct cluster and are more closely related to the EaCoMT of *Rhodococcus* strain B-276 than that of *Xanthobacter* strain Py2. The incongruence of the EaCoMT and 16S rRNA gene trees and the fact that isolates from geographically distant locations possessed almost identical EaCoMT genes

suggest that lateral transfer of EaCoMT among the *Mycobacterium* strains has occurred. Pulsed-field gel electrophoresis revealed large linear plasmids (110 to 330 kb) in all of the VC-degrading strains. In Southern blotting experiments, the strain JS60 EaCoMT gene hybridized to many of the plasmids. The CoM-mediated pathway of epoxide metabolism appears to be universal in alkene-assimilating mycobacteria, possibly because of plasmid-mediated lateral gene transfer.

Our study with *Mycobacterium* strain JS60 is the first to indicate a role for coenzyme M in VC-oxidizing bacteria and also the first to obtain sequences of bacterial genes involved in growth-linked VC/ETH oxidation. These insights will be invaluable in further elucidating the pathways of aerobic VC- and ETH- biodegradation, and will also act as a foundation for the design of DNA-based tools for the detection of VC- and ETH-oxidizing bacteria in the environment.

We found EaCoMT activity and genes in all of the alkene-oxidizing mycobacteria that we examined, including strains isolated on both VC and ethene. EaCoMT genes were not found in BLAST database searches of *Mycobacterium* genomes (or any other genomes) that have been completed to date, indicating that EaCoMT is specific to the alkene-assimilation pathway. It remains to be determined whether EaCoMT is involved in the VC and ethene assimilation pathways of *Pseudomonas* (Verce et al., 2000; Verce et al., 2001) and *Nocardioides* (Coleman et al., 2002b) strains. The EaCoMT gene primers we have developed could be used to address this question. In addition, such primers will be very useful for culture-independent monitoring of microbial populations during the natural attenuation or bioremediation of chlorinated ethenes. Such methods are particularly relevant for mycobacteria, which are slow growing and sometimes difficult to isolate in pure culture.

The 10 VC and ethene degraders we studied were scattered throughout the genus *Mycobacterium*, with no apparent correspondence seen between phylogeny and alkene growth substrate. Although EaCoMT activities tended to be higher in the VC degraders than in the ethene degraders, it is difficult to compare these results because of the use of different growth substrates in experiments with each group of strains. Sequencing of EaCoMT genes did not reveal any signature regions that discriminated between the VC- and ethene-assimilating strains, and indeed, in the case of strains JS619 (VC) and JS625 (ethene), only a single nucleotide difference separated the EaCoMT PCR products. An important question arising from our work therefore concerns the distinction between bacteria that can grow on both VC and ethene and those that grow on ethene alone.

The EaCoMT gene appears to be carried on large linear plasmids in VC-degrading strains. On the basis of the gene organization in *Mycobacterium* strain JS60 (Coleman and Spain, 2003a), it is likely that the alkene monooxygenase genes are also present on the same plasmids. Cryptic linear plasmids have previously been identified in various pathogenic *Mycobacterium* strains (Le Dantec et al., 2001; Picardeau and Vincent, 1997, 1998) and in ethene-oxidizing *Mycobacterium* strain E-1-57 (Saeki et al, 1999). Only one previous study (Waterhouse et al., 1991) has associated a specific catabolic function (morpholine biodegradation) with plasmids in mycobacteria. Our results indicate that catabolic plasmids are more widespread in this genus than was previously believed. Plasmid-borne genes for ethene and VC biodegradation could potentially

be transferred among bacteria in the environment, and thus, further investigation of such elements is warranted in light of the potential importance of the alkene-degrading phenotype to bioremediation and natural attenuation processes (Coleman et al., 2002b).

A Linear Plasmid Carries Vinyl Chloride Biodegradation Genes in *Nocardioides* JS614

[See full paper in Appendix E]

Nocardioides strain JS614 grows on vinyl chloride (VC) and ethene (ETH) as carbon and energy sources. Bacteria such as JS614 could be influential in natural attenuation and biogeochemical ETH cycling, and useful for bioremediation, biocatalysis and metabolic engineering, but a lack of knowledge of the genetic basis of VC and ETH assimilation has limited these applications.

JS614 VC/ETH catabolic genes and flanking DNA (34.8 kb) were retrieved from a fosmid clone. Alkene monooxygenase (AkMO) and epoxyalkane:Coenzyme M transferase (EaCoMT) genes were found in a putative operon that also included CoA transferase, acyl-CoA synthetase, dehydrogenase and reductase genes. Adjacent to this gene cluster was a divergently transcribed gene cluster that encoded possible coenzyme M biosynthesis enzymes.

Reverse transcription (RT-) PCR demonstrated the VC- and ETH-inducible nature of several genes. Genes encoding possible plasmid conjugation, integration, and partitioning functions were also discovered on the fosmid clone. Pulsed field gel electrophoresis (PFGE) revealed a 290 kb linear plasmid (pNoc614) in JS614. Curing experiments and PCR indicated that pNoc614 encodes VC/ETH degradation genes, and that pNoc614 was the source of the sequenced fosmid clone. The results provide rigorous evidence that linear plasmids encode VC/ETH biodegradation genes, and greatly expand the database of useful genes for future *in situ* molecular studies of VC-degrading bacteria.

This is the first study to use a sequence-based approach to conclusively demonstrate that VC/ETH degradation genes are plasmid-borne, a finding which suggests horizontal transfer of VC biodegradation genes in the environment is possible. This is also the first study to obtain significant amounts of sequence data from an alkene catabolic plasmid. The gene cluster encoding VC and ETH biodegradation was found immediately adjacent to the putative CoM biosynthesis genes, and both gene clusters appeared to be under the control of sigma-54 promoters in a central non-coding region, suggesting that both gene clusters are coordinately regulated.

Hypothetical pathways of VC and ETH assimilation were generated based on the predicted functions of ORF7-15 (Fig.5). The pathways are based on analogy with *Mycobacterium* strains JS60 (Coleman and Spain, 2003a) and E20 (de Bont and Harder, 1978), as well as analogy with propene-oxidizing strains (Ensign, 2001) and similarity to sequences in GenBank. Despite the lack of biochemical evidence thus far, we believe it is useful to provide our best guess at the pathway so that hypotheses are available for future experimentation. An increased understanding of the biochemical pathway of VC and ETH oxidation is not only

important with respect to natural attenuation of VC, but might also facilitate a better understanding of biogeochemical cycling of ETH, a plant hormone and greenhouse gas.

Although the sequence data thus far suggest that the alkene degradation pathways are identical in *Nocardioides* strain JS614 and *Mycobacterium* strain JS60, the question of why the growth yield and growth rate on VC and ETH are higher in JS614 remains unanswered. Our discovery of a second EaCoMT allele in strain JS614 might be relevant to the question. If the JS614 *etnE1* gene encoded a functional enzyme, expression of this enzyme would lead to increased EaCoMT activity, and more efficient capture of reactive epoxides as CoM conjugates before they are lost to cell-damaging and non-growth supporting side-reactions.

The sequencing of a large fragment of genomic DNA from JS614 has greatly increased the database of genes from aerobic VC-assimilating bacteria, thus facilitating future *in situ* molecular studies of these bacteria. AkMO and other catabolic genes from JS614 could also be used in biocatalysis or metabolic engineering applications where expression of a highly active alkene monooxygenase or the design of novel biochemical pathways is desired. Our data provide many novel targets for PCR- or probe-based detection of VC/ETH-degraders. For example, the plasmid-associated genes such as TraA reported in this study could be used indicators of the presence of pNoc614-type plasmids, thus complementing data obtained from the use of traditional catabolic gene probes/primers.

Our results suggest that the genes encoding VC and ETH degradation are highly conserved, even between different genera, thus validating the use of such genes as indicators of the presence of VC/ETH degraders *in situ*. Unfortunately, our data do not allow us to distinguish between VC and ETH degraders on the basis of DNA sequence, which would be a prerequisite for determining whether growth-linked or cometabolic processes are responsible for VC degradation in the field. A detailed molecular analysis of ETH-degraders that cannot grow on VC is required to address this issue, and to shed light on the mechanism of evolution of VC-degraders from ETH-degraders.

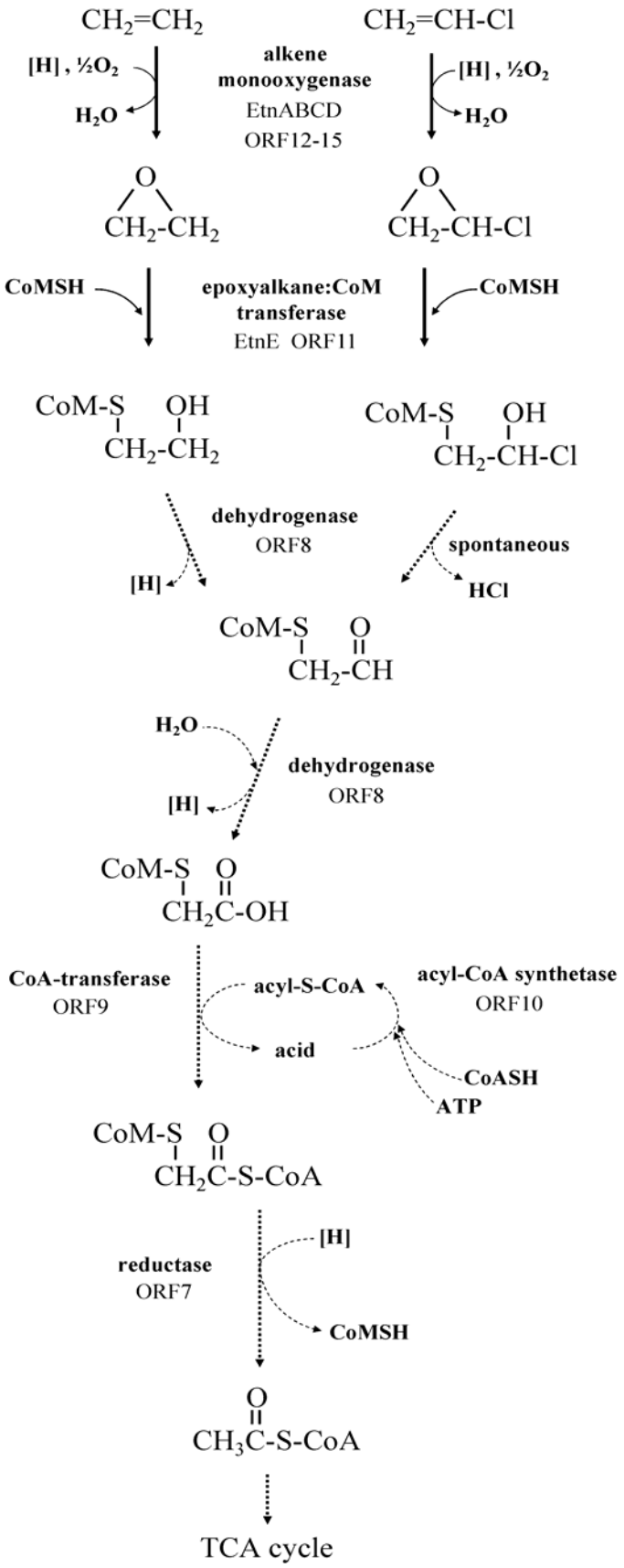

Figure 5. Hypothetical pathway of VC and ETH assimilation in *Nocardioides* JS614.

Characterization of the Vinyl Chloride and Ethene Starvation Response in *Nocardioides* Strain JS614

[See full paper in Appendix F]

Nocardioides strain JS614 exhibits an extended lag period for resumption of aerobic growth on VC or ETH after these substrates are withheld from the culture for longer than one day. This lag could affect application of JS614 in bioaugmentation and biocatalysis strategies and raises fundamental questions concerning mechanisms controlling the lag. Initial growth experiments indicate the lag is not due to cell death and is limited to starvation recovery on or adaptation to VC or ETH as growth substrates.

Assays of alkene monooxygenase (AkMO) and epoxyalkane:Coenzyme M transferase (EaCoMT) activities indicate rapid AkMO inactivation during starvation. Switching ETH-grown JS614 cultures to acetate for 24 h revealed elevated AkMO activities in comparison to starvation.

SDS-PAGE and MALDI-TOF MS experiments demonstrated that AkMO subunits were induced by VC and ETH, and were not degraded during starvation. Upon resumption of ETH degradation, SDS-PAGE results suggested that AkMO subunits were synthesized. Addition of acetate along with VC or ETH reduced the lag associated with VC or ETH starvation.

We conclude that AkMO inactivation, along with additional undefined mechanisms control the lag period associated with starvation recovery on VC or ETH. Our data suggest that depletion of reducing power contributes to the lag, but that toxic epoxide accumulation or rapid turnover of AkMO subunits are unlikely contributors.

It is of important, practical significance to note that the extended lag period is reduced or eliminated by addition of small amounts of a readily degradable substrate (e.g. acetate) along with VC or ETH. Based on the data presented in this paper (Appendix F), acetate is likely oxidized to regenerate the reducing equivalent pool, which allows existing AkMO to resume functioning, but could also be utilized for repair of damaged AkMO and/or for energy to synthesize new AkMO. Except for the observation that AkMO subunits are not degraded during starvation, the data presented in this paper do not conclusively implicate or rule out other possible mechanisms that might control the lag period, and therefore further work is required in this regard. Extended lag periods for adaptation to growth on alkene substrates appear to be controlled by a different mechanism than the lag period associated with alkene starvation, an observation that also warrants further investigation.

Site-Specific Study — Distribution and Activity of VC-Degraders at Moody AFB.

During the initial site survey, groundwater enrichments from different monitoring wells at Landfill 04 (LF04) at Moody AFB (Valdosta, GA) yielded four *Mycobacterium* isolates — strain JS621 (see Fig. 1) and three other apparently identical strains. The JS621-like strains were isolated from monitoring wells covering the length of the VC plume, suggesting a single VC-degrading strain dominates this site. On the basis of these observations, we chose the Moody AFB LF04 site for more detailed analysis**.**

A microcosm study was conducted using groundwater and soil from LF04. A diagram of the VC plume can be seen in Figure 6. The purpose of this study was to delineate the pattern of distribution of ETH and VC degraders inside and outside the plume and to isolate ETH- and VC-degraders and to ascertain via 16S RNA sequencing if the latter came from the former. The presence of cDCE and VC at this site indicated that microbial reductive dechlorination of PCE and TCE was (or had been) occurring. The break in the VC plume (see Figure 6) and the presence of oxygen in the area of the plume where no VC was present, as well as in other parts of the plume, suggested that oxidative degradation of vinyl chloride was possibly occurring. The variety of conditions at this site (reducing conditions in some regions and oxidative conditions in others) were the main reasons this site was chosen for study. Samples of groundwater and soil were taken from 11 locations (labeled AF1 through AF11 in Figure 6) within and beyond the edges of a VC plume located 30 feet below ground surface (bgs). Microcosms were prepared for samples from 10 of the 11 locations (none were prepared for AF5), and for each location, 8 microcosms were constructed, giving a total of 80 microcosms. Half of the microcosms were fed ETH and half were fed VC. VC and ETH were measured using headspace samples on a gas chromatograph.

Site Description. The contaminant plume at Moody AFB is the result of a landfill (Landfill 04) from which chlorinated ethenes (principally PCE) leached into the aquifer. The following site information comes from an unpublished study conducted in 1997. The subsurface geology of the site area is complex and consists primarily of interconnected zones of clayey silts, silty sands, and sandy clays. At 30-40 feet bgs, there is a continuous layer of sand/silty sand of approximately 9 feet. This sand/silty-sand layer has a much higher hydraulic conductivity than the surrounding silt, clayey-silt, and silty-clay layers. This differential in hydraulic conductivities causes preferential flow within this sand/silty-sand region in the aquifer. Laboratory analyses of groundwater that were conducted in 1997 (unpublished data) indicated that the primary zone of chlorinated-ethene contamination occurs at 30-40 feet bgs. TCE, cDCE, and VC are the primary contaminants detected at the site (with the latter two presumably the result of *in situ* reductive dechlorination of TCE) , and the plumes associated with these contaminants extend approximately 1,400 feet down-gradient from the landfill and have a width of approximately 600 feet transverse to the direction of groundwater flow. Results from sampling in 1997 showed that the highest concentrations of TCE, cDCE, and VC were 340, 615, and 3,100 μg/L, respectively.

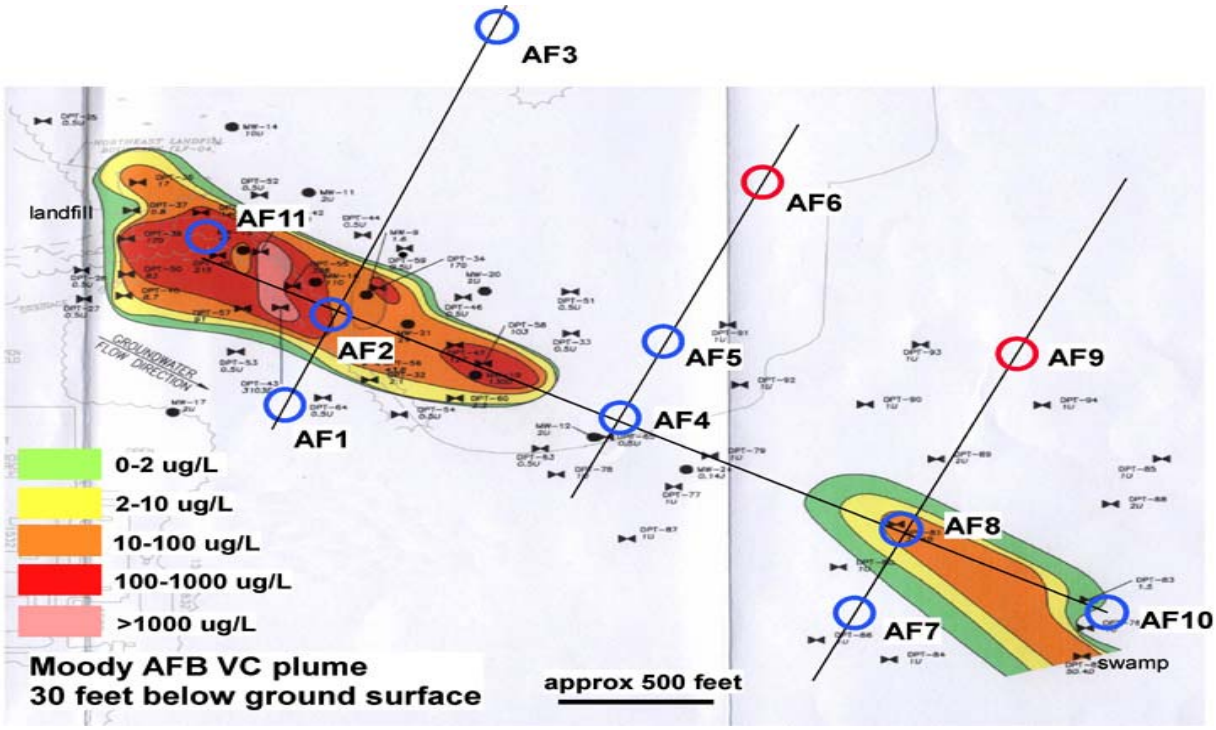

Figure 6. Map of vinyl chloride contaminant plume at Moody AFB LF04 site. Sample locations (AF1-AF11) are circled.

Electron-acceptor data were also collected in 1997 in order to further characterize the site and to interpret the changes that occurred in chlorinated-ethene concentrations over time and assess if other biodegradative pathways (such as oxidation of VC) were possible at the site. Average DO concentrations ranged from 2.9 mg/L up-gradient from the plume, 0.9 mg/L within the plume, 1.4 mg/L at the lateral edge of the plume, and 1.9 mg/L down-gradient from the plume, suggesting the presence of biological activity (depleting dissolved oxygen) within the plume. Average nitrate and sulfate concentrations were very low (<1.0 mg/L) throughout the site, suggesting that both nitrate and sulfate are not significant electron acceptors at the site. Differences in average concentrations of ferrous iron, resulting from ferric-iron reduction, were 5.4 mg/L up-gradient from the plume, 31.1 mg/L within the plume, 15.8 mg/L at the lateral edge of the plume, and 7.6 mg/L down-gradient from the plume. Average methane concentrations within the plume were 2.7 mg/L, indicating highly reducing conditions there.

Field Sampling. Ten groundwater and soil samples were extracted from 30 feet bgs using Geoprobe® direct-push technology. The locations were named (and samples labeled) AF1 … AF11. Sampling was conducted under aseptic conditions as much as possible (described below) in order to prevent cross-contamination. Each sample was extracted into an individual plastic core with a length of approximately 3 feet and diameter of 1.5 inches. Geoprobe® parts that came into contact with the soil samples were sanitized with an Alconox® washing in-between sampling points. Samples were extruded into unused plastic bags, ziplocked, and

kneaded in order to create a homogenous soil sample. Each soil sample was then divided into two portions — one for Cornell laboratory studies and one for Tyndall Air Force Base.

Groundwater samples were collected using a peristaltic pump attached to semi-rigid polyethylene tubing that ran through the Geoprobe® tubing to 30 feet bgs. The water samples were taken by overflow into sampling containers to avoid air pockets and ensure that each water sample was representative of its location. Both the polyethylene tubing and the flexible tubing in the peristaltic pump were changed between sampling locations to prevent cross contamination. Groundwater samples were taken for two purposes: (1) to construct microcosms; and (2) for VOC samples conducted by an independent lab. Water samples used for microcosm construction were stored in sterile 1-L Nalgene containers, and samples used for VOC analysis were stored in EPA-approved VOC vials.

The following parameters were field-measured at the time of sampling: dissolved oxygen (DO), temperature, ferrous iron, and total iron. DO and temperature were measured with a Yellow Springs Instrument Co. Inc. (YSI) Model 58 dissolved-oxygen meter and a YSI Model 5739 DO probe. For DO measurement, water samples were taken by overflow into a 250-mL erlenmeyer flask with marbles lying on the bottom. The probe was fitted fairly tightly into the opening of the flask with an O-ring that was placed around the probe; this prevented reaeration during DO measurement. The flask was swirled by hand, causing the marbles to roll around the bottom of the flask, creating mixing pattern not unlike that of a magnetic stir-bar; agitation below the probe membrane is a requirement for accurate DO measurement. The DO probe was calibrated using a one-point calibration in water-vapor-saturated air (i.e., the probe was inserted into the headspace of a sealed flask above a layer of water).

Ferrous iron was measured with Hach® chemical test # 26672 which uses a 1,10-phenanthroline indicator that reacts with ferrous iron to form an orange color proportional to the ferrous-iron concentration. Total iron were measured with Hach® chemical test kit #1464, which uses a reducing agent that converts all but the most resistant forms of iron to ferrous iron and then uses a 1,10-phenanthroline indicator to measure ferrous iron. pH measurement was attempted in the field, but two pH meter systems did not work properly. pH was then necessarily measured in the laboratory at Cornell three days after sampling; a Denver Instrument Model PO-10 pH meter was used.

Microcosm Preparation. Microcosms were prepared using sterile, 160-mL serum bottles and sterilized utensils, with a separate set of utensils used to prepare the eight microcosms from each sampling point and the bottles were sealed with a sterile Teflon-faced stopper and an aluminum crimp-cap. Each microcosm was constructed from 50 grams (dry weight) soil and 50 grams of adjacent groundwater. The actual amount of indigenous soil used was determined by measuring the moisture content of soil samples from each of the 10 locations (no microcosm were constructed for AF 5), and calculating the amount of wet soil needed to equal 50 grams of dry soil. For example, the soil sample from sampling site AF1 had a moisture content of 0.18 (w/w), and the microcosms were constructed from 61 (i.e., 50/0.82) grams of soil and 39 grams of groundwater. Soil moisture content is the mass of water found in a soil sample divided by the mass of the original soil sample. The mass of water was determined by weighing a soil sample prior to and after drying the soil and subtracting the mass of the dried soil sample from the mass

of the indigenous soil sample. Soil samples were dried in an oven set at 103-105^0 C for 12 hours and were placed in a desiccator for 3 hours after they were taken out of the oven.

Once microcosms were prepared, they were placed on an orbital shaker at 160 rpm at 25^{0}C for 24 hours to equilibrate gas, liquid, and solid phases. Microcosms were kept on the orbital shaker for the entire experiment. Two microcosms from each sampling location (a total of 20 microcosms) were sterilized in an autoclave for 2 hours at 121^{0}C. The same microcosms were sterilized in the same manner two days later. Headspace samples from one representative microcosm for each sampling location were analyzed by gas chromatography using the method described below for the following volatile organics: methane, ethane, ethene, propane, VC, cDCE, TCE, PCE, benzene, toluene, ethyl benzene, and xylenes. Four microcosms from each sampling location (one of which was sterile) were fed with 100 μmoles of VC and four microcosms from each sampling location (one of which was sterile) were fed with 400 μmoles of ETH.

Gas Chromatography. The total amounts of VC, ETH, and oxygen were measured for ongoing microcosm monitoring using a GC. Headspace analysis was conducted by a single 0.1-mL headspace injection via a gas-tight locking syringe into a Perkin Elmer Autosystem GC. The sample flowed through a column packed with 1% SP-1000 on 80/100 Carbopack B. . The carrier gas was N_2 (Airgas high purity). The flow rate was approximately 30 mL/min, and the column was kept isothermally at 90^{0}C for the entire run. During each analytical procedure, column effluent was routed to the TCD until the peak of oxygen had eluted (0.67 minutes); at that point, an automatic switching valve routed the effluent to the FID for the remainder of the analytical run, to quantify ETH (0.82 minutes) and VC (2.4 minutes).

Quantification of VC and ETH was the product of a predetermined calibration factor and the peak-area value given by the data integrator. Calibration factors were developed by examining dummy microcosm bottles with known amounts of VC and ETH. 2.5 mL of VC gas was injected into each VC-standard bottle and 10 mL of ETH gas was injected into each ETH-standard bottle. The moles of the gas delivered was determined by the ideal gas law, using the temperature and barometric pressure of the laboratory at the time of preparation. After the bottles were allowed to equilibrate to 25^{0}C on an orbital shaker running at 160 rpm, 0.1-mL headspace samples were injected to the GC. The calibration factor represented the peak area per total moles of compound in the bottle. Three standard dummy microcosm bottles for VC and three standard dummy microcosm bottles for ETH were prepared and analyzed, yielding triplicate values for calibration factors, from which a mean was calculated. The coefficient of variation (100 x standard deviation/mean) for VC was 1.9 percent. The coefficient of variation (100 x standard deviation/mean) for ETH was 2.9 percent.

Volatile organics that were measured prior to spiking microcosms with VC and ETH (i.e. methane, ethane, ethene, propane, VC, cDCE, TCE, PCE, benzene, toluene, ethyl benzene, and xylenes) were analyzed with the same GC setup described previously with the following changes. In this case only the FID detector was used, and the column was not kept isothermally during the entire run. The column was kept isothermally at 35^{0}C for the first 2.2 minutes of the run; the temperature was ramped at a rate of 8 degrees/min for the next 20 minutes, and was kept isothermally at 195^{0}C for the remaining 41.3 minutes of the run. Headspace samples of bottles

containing each of the mentioned VOCs were injected into the GC to verify retention times. No significant amounts of indigenous VOCs were detected in any of these microcosms prior to additions of VC or ETH.

Results — Site Characterization. Various water quality parameters were field-measured at the time of sampling (or in the case of pH as soon as possible after sampling due to equipment malfunction at the site) to characterize the site before setting up the microcosms. DO, temperature, pH, ferrous iron, and total iron measurements are shown in Table 1.

Table 1. Site Characterization Parameters for Moody LF04.

Sample Site	DO (mg/L)	Temperature (^{o}C)	pH	Ferrous Iron (mg/L)	Total Iron (mg/L)
AF 1	3.6	25.5	5.5	2.8	30
AF 2	0.9	23.7	5.5	5.0	30
AF 3	6.4	22.4	5.6	1.0	55
AF 4	1.6	23.4	6.2	1.5	24
AF 6	5.1	24.7	5.6	1.9	58
AF 7	3.7	21.1	5.5	4.0	30
AF 8	3.4	22.9	5.4	4	44
AF 9	5.9	23.5	5.7	2.8	25
AF 10	2.2	22.8	5.4	7.0	50
AF 11	0.5	22.4	5.9	45	270

Groundwater VOC analyses that were conducted by Severn Trent Laboratories Inc. in Knoxville, Tennessee. These data showed that locations within or on the edge of the plume (i.e. AF2, AF8, and AF 11) contained significant amounts ofthe following VOCs: VC (17 µg/L, 58 µg/L, and 1400 µg/L, respectively); cDCE (89 µg/L, 100 µg/L, and 980 µg/L respectively); TCE (2.3 µg/L, 82 µg/L, and 3100 µg/L, respectively); and 1,1-dichloroethane (5.8 µg/L, 7.1 µg/L, and 240 µg/L, respectively). AF 11, which is the sampling location found closest to the plume source, also contained significant amounts of the following, additional VOCs: benzene (19 µg/L), chlorobenzene (40 µg/L, 1,2,4-trimethylbenzene (18 µg/L), chloroethane (37 µg/L), 1,1-dichloroethene (73 µg/L), toluene (17 µg/L), and xylenes (52 µg/L). The other sampling locations (AF1, AF3, AF5, AF6, AF7, AF9, and AF10) which lie outside the plume did not contain significant amounts of VOCs.

Results — Microcosm Studies. Microcosms were sampled for VC, ETH, and oxygen over 140 days. They were monitored via GC every 24 hours for the first two days of the experiment, every 48 hours until between day 2 and day 10, every 3 days until between day 10 and day 26, every 10 days between day 26 and day 46, on day 66, and once a month for the next three months. All microcosms showed no degradation of VC, ETH, or oxygen over 140 days. Exemplary VC and ETH measurements from an autoclaved-control microcosm and a live microcosm constructed from soil and groundwater sampled from AF1 are depicted in Figures 7 and 8, respectively. All other microcosms from all 10 sampling locations behaved in a similar manner and exhibited no VC, ETH, or oxygen depletions.

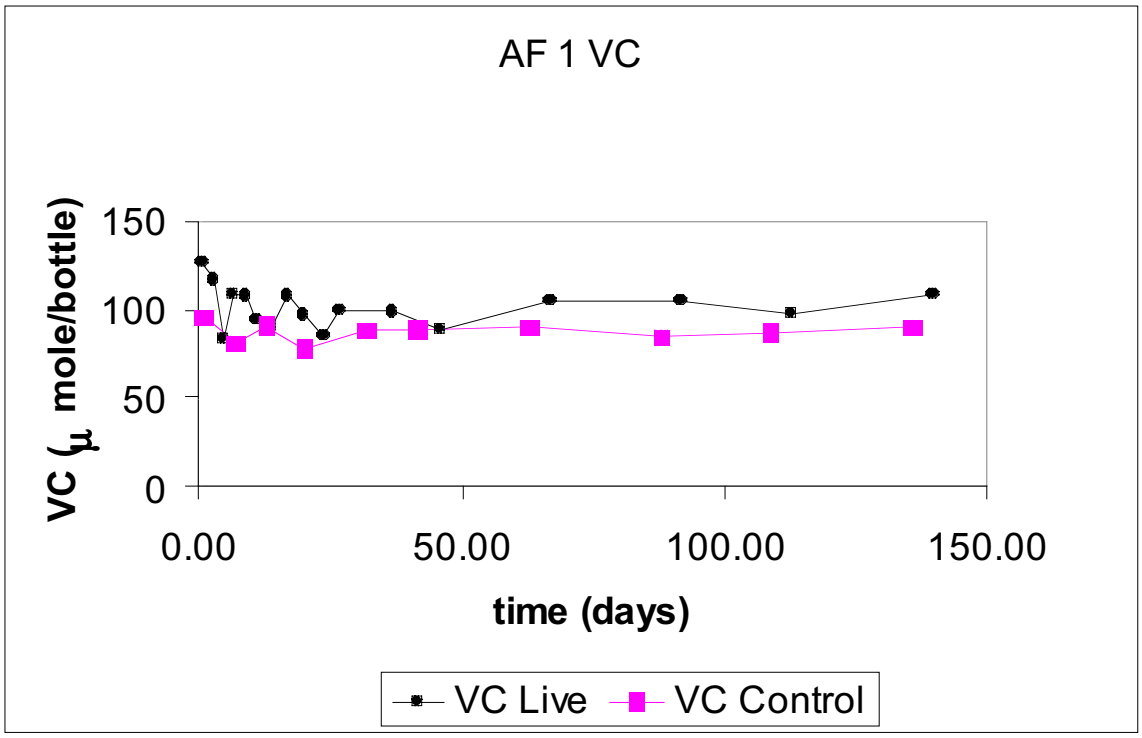

Figure 7. Vinyl chloride vs. time for autoclaved-control and live microcosms from AF1.

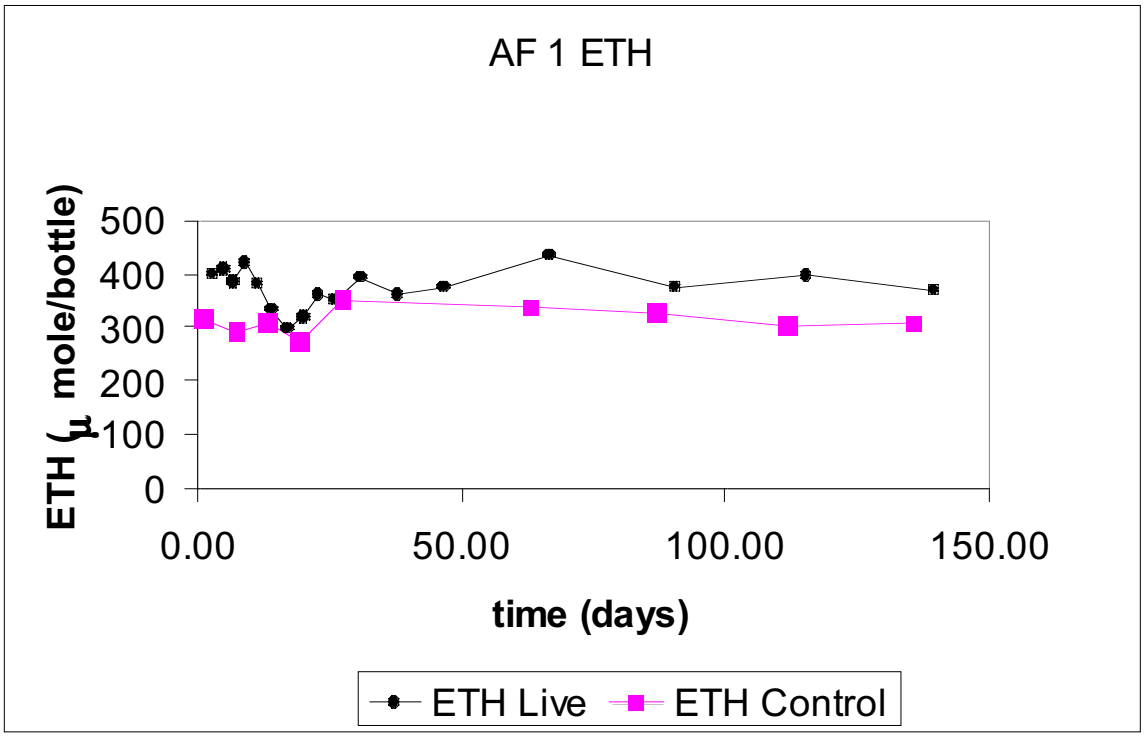

Figure 8. Ethene vs. time for autoclaved-control and live microcosms from AF1.

Inoculation of Moody Microcosms with JS621 and/or Nutrients. Since there was no VC, ETH, or oxygen depletion in any of the microcosms, the following study was conducted to investigate the reasons. This study was designed to determine if: (1) there was a lack of suitable ETH- and VC-degrading organisms on site; (2) there was a lack of nutrients in the microcosms; (3) environmental conditions in the microcosms were hostile to microorganisms; or (4) a combination of (1) and (2) or (1) and (3). The four following treatments were set up on day 107 of the Moody microcosm studies:

1. Four microcosms — AF 2 (VC and ETH) and AF 11 (VC and ETH) — were amended with JS621, a VC- and ETH-degrading microorganism that was previously isolated from a Moody well-water sample. 5 mL of microcosm liquid was removed and 5 mL of JS621 culture (OD600 0.08) was added to each of the microcosms under aseptic conditions. Due to the nature of the microcosm slurries from AF 2 and AF 11, the serum bottles had to be opened in order to remove microcosm liquid. Vinyl chloride and ethene levels were restored after the JS621 inocula were added.

2. Four microcosms — AF 10 (VC and ETH) and AF 11(VC and ETH) — were amended with nutrients. 5 mL of liquid was removed from each microcosm and 5 mL of a sterile nutrient solution was added to each using aseptic technique. The nutrient solution contained (per liter of distilled, deionized water): 6.7 g KH_2PO_4, 6.8 g $(NH_4)_2SO_4$, and 20 ml of a trace-metal solution that contained (per liter of distilled, deionized water): 60 g $MgSO_4 \bullet 7H_2O$, 6.37 g EDTA ($Na_2(H_2O)_2$), 1 g $ZnSO_4 \bullet 7H_2O$, 1 g $CaCl_2 \bullet 2H_2O$, $FeSO_4 \bullet 7H_2O$, 1 g $NaMoO_4 \bullet 2H_2O$, 1 g $CoCl_2 \bullet 6H_2O$, $MnSO_4 \bullet H_2O$. The pH of the sterile nutrient solution was adjusted to 5.5 with filter-sterilized NaOH.

3. Four microcosms — AF 2 (VC and ETH) and AF 10 (VC and ETH) — were amended with both JS621 and nutrients. 10 mL of liquid was removed from the microcosms and 5 mL of JS 621 culture and 5 mL of sterile nutrient solution were added to the microcosms using sterile technique.

4. Two control microcosms were prepared, using 50 grams of sand and 50 grams of distilled, deionized water. These were then autoclaved. The two then received treatment #3, and one was administered VC; the other, ETH. These positive controls were included to test the viability of JS621 inocula.

All microcosms and controls began with 100 μmoles of VC or 400 μmoles of ETH.. Figure 9 depicts the results. VC and ETH were degraded in the microcosms that were amended with JS621 and those amended with both JS621 and nutrients. VC and ETH were not degraded in the microcosms amended with nutrients only. VC and ETH were also degraded in the JS621+nutrient-amended "positive" controls (i.e., prepared from sand and water).

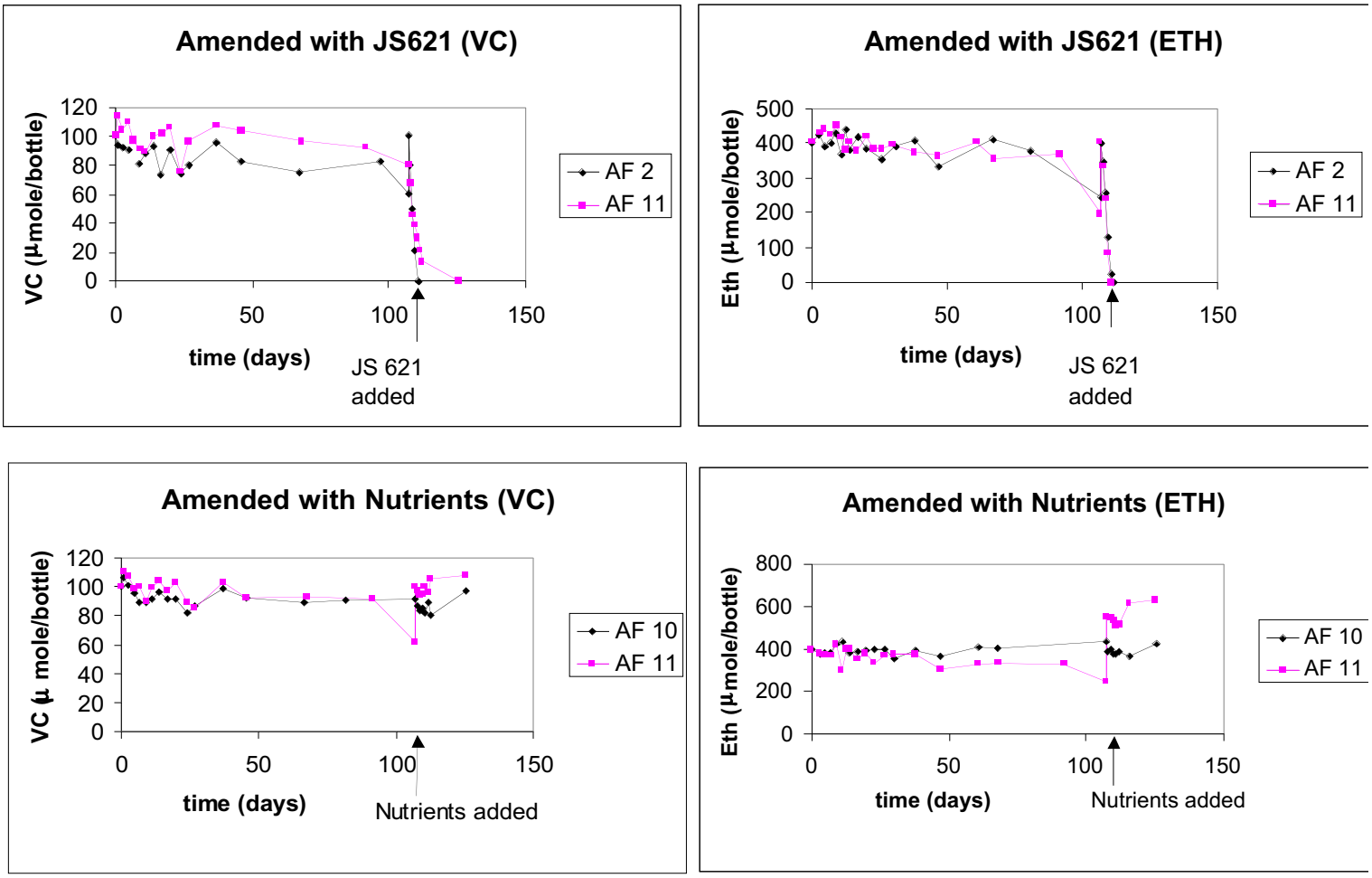

Figure 9. Results from inoculation of Moody LF04 microcosms with JS621.

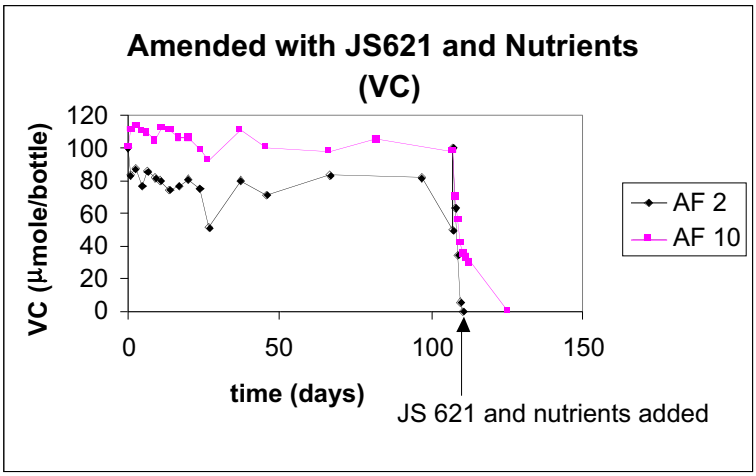

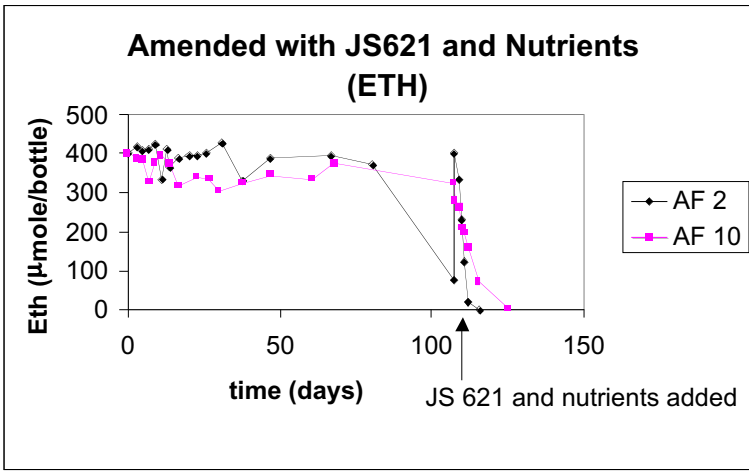

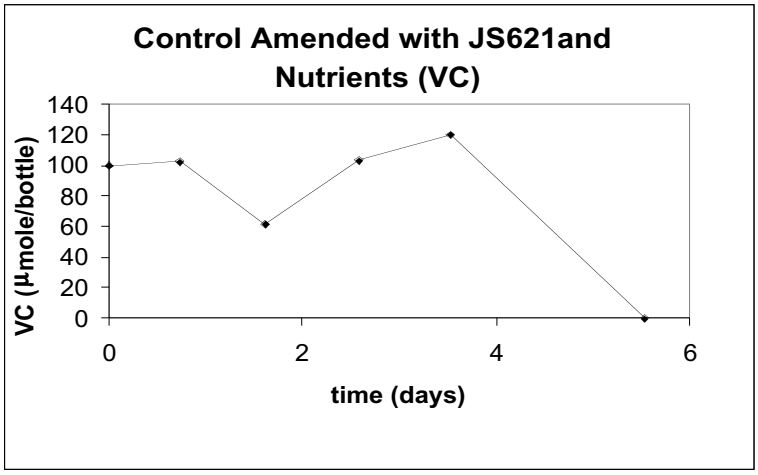

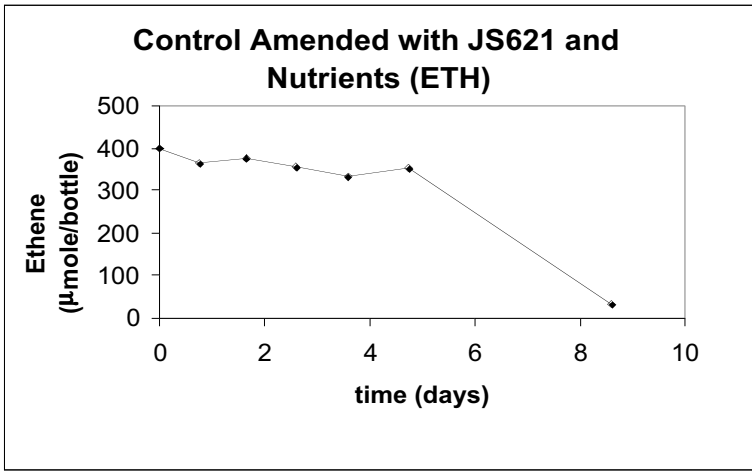

Figure 9 (continued). Results from inoculation of Moody LF04 microcosms with JS621.

Some pH data are shown in an accompanying Table 2. Though low (i.e., between pH 4.8 and 5.4), pH values were all maintained at values essentially similar to those *in situ*. Furthermore, there were no trend-differences in pH that would seem to explain results. Inactive microcosms ("initial" conditions in all microcosms, and "final" conditions of microcosms amended only with nutrients) had pH values similar to those in active microcosms (those amended with JS621 or JS621+ nutrients). pH does not appear to explain results.

MPN Enumeration of VC- and ETH-Degraders in Moody AFB Samples. Methods for the detection and enumeration of VC- and ETH-degraders in the Moody AFB aquifer sediments were developed based on the most-probable-number (MPN) principle. For these experiments, the Moody AFB groundwater isolate *Mycobacterium* JS621 was used as a model organism. Growth of strain JS621 under conditions similar to those at the site (pH 5.5, approx. 20°C) could be detected in the MPN medium via HCl production from VC, which caused a color change in the pH indicator bromophenol green. Growth on ETH under similar conditions was detectable by turbidity. MPN assays were set up in triplicate on VC and ETH with all 11 of the

LF04 aquifer sediment samples used to construct the microcosm studies. However, after 5 months incubation, no growth or activity was observed in any of the MPNs. Viable counts of the aquifer material on 1/10-trypticase soy agar yielded very few culturable bacteria ($<10^3$ cfu / g aquifer sediment).

DNA-based methods of detection and enumeration of VC oxidizing-bacteria could provide a rapid and sensitive alternative to microcosm studies in the assessment of the natural attenuation potential of a contaminated site. Such molecular methods would also be invaluable for bioaugmentation studies, in monitoring the survival and/or activity of inoculated bacteria. These strategies have not been employed thus far for VC-oxidizing bacteria due to lack of information about the genes of the VC pathway. Our earlier results indicated that molecular detection of VC-degraders by PCR amplification of the EaCoMT gene is a possibility, and we sought to detect VC-degraders in the Moody AFB sediment samples by this method. However, these experiments were not successful, due to difficulties in extracting DNA from the aquifer material.

Microcosm and MPN results agreed, and suggest that inactivity in Moody microcosms was the result of a lack of suitable microorganisms, and not the result of inhospitable conditions or lack of nutrients

Table 2. pH values for JS621 amendment experiment.

	Initial pH[1]	Final pH[2]
Amended with JS621		
AF2(VC)	5.1	5.4
AF11VC)		
AF2(ETH)		
AF11(ETH)	4.9	4.8
Amended with nutrients		
AF10(VC)	5.6	
AF11(VC)		5.2
AF10(ETH)		
AF11(ETH)		4.2
Amended with JS621 and nutrients		
AF2(VC)		
AF10(VC)		5.4
AF2(ETH)		
AF10(ETH)		5.5
Controls		
VC		5.1
ETH		5.4

[1]Initial pH = pH at time of amendment.

[2]Final pH = pH at conclusion of data period shown in preceding Figures.

Moody AFB Well-Water Study. The JS621-amendment study with inactive microcosms suggested that conditions on site were not inhospitable to VC or ETH degradation, but that suitable organisms simply were not present. This is curious, given that we had previously isolated *Mycobacterium*-like strain JS621 from wells MW9 and MW27 at this same site (Coleman et al., 2002b). Were VC- and ETH-degraders — once in evidence at this site — no longer so?

We decided to obtain fresh samples of groundwater from these same two wells (MW9 and MW27), plus another (MW19), to see if VC- or ETH-degrading activity could now be found. In addition to the possibility that VC- and ETH-degraders were now absent, it is also possible that our negative microcosm results (versus Coleman et al.'s positive finding of suitable organisms) were due to sampling differences. Groundwater pumped out of wells would be more apt to yield a sample integrated over a larger area than the point samples taken with the Geoprobe® for the microcosm study. In other words, we might have missed finding activity with our discrete, Geoprobe® sampling.

Geoprobe® sampling points for the microcosm study had been selected with the thought that at least some of them would be in a zone of biological activity, but no activity was detected in this study. VC- and ETH-degrading organisms require VC (or ETH) as well as oxygen, and thus would be expected to be active only where both VC (or ETH) and oxygen coexist. On the other hand, if rates of aerobic oxidation of VC (or ETH) are as significant in the field as Coleman et al. observed in their studies, the zone where both the VC (or ETH) and oxygen coexist may be rather narrow — essentially the boundary between the anaerobic zone in which VC (or ETH) is formed via reductive dechlorination, and the aerobic zone into which it is migrating. Further into the aerobic zone, the VC (or ETH) would have become nondetectable. This would complicate the search for VC- and ETH-degraders, if discrete sampling were employed. A further complication is caused by the much lower retardations of VC and ETH, compared to that of microorganisms. Locations of dissolved-concentration depletion may not coincide with locations of actual activity. The hope was that taking water samples from a well would thus sample over a larger area of the aquifer than the point-sampling that was conducted for the microcosm study and increase the probability of finding VC- and ETH-degrading organisms.

Six well-water microcosms from each sampling location (MW9, MW19, and MW27) were prepared in a manner similar to that of the earlier microcosms, except for the lack of soil in this later study. 100 mL of well water was placed in each sterile, 160-mL serum bottle, and the bottles were sealed with a sterile teflon-faced stopper and an aluminum crimp-cap. Two bottles from each sampling location were sterilized in an autoclave at 121^0C for one hour. Three serum bottles from each sampling location (one of which was sterile) were fed with 100 μmoles of VC and three serum bottles from each sampling location (one of which was sterile) were fed with 400 μmoles of ETH. The serum bottles were kept under the same conditions as the earlier microcosms (i.e. on an orbital shaker running at 160 rpm at 25˚C).

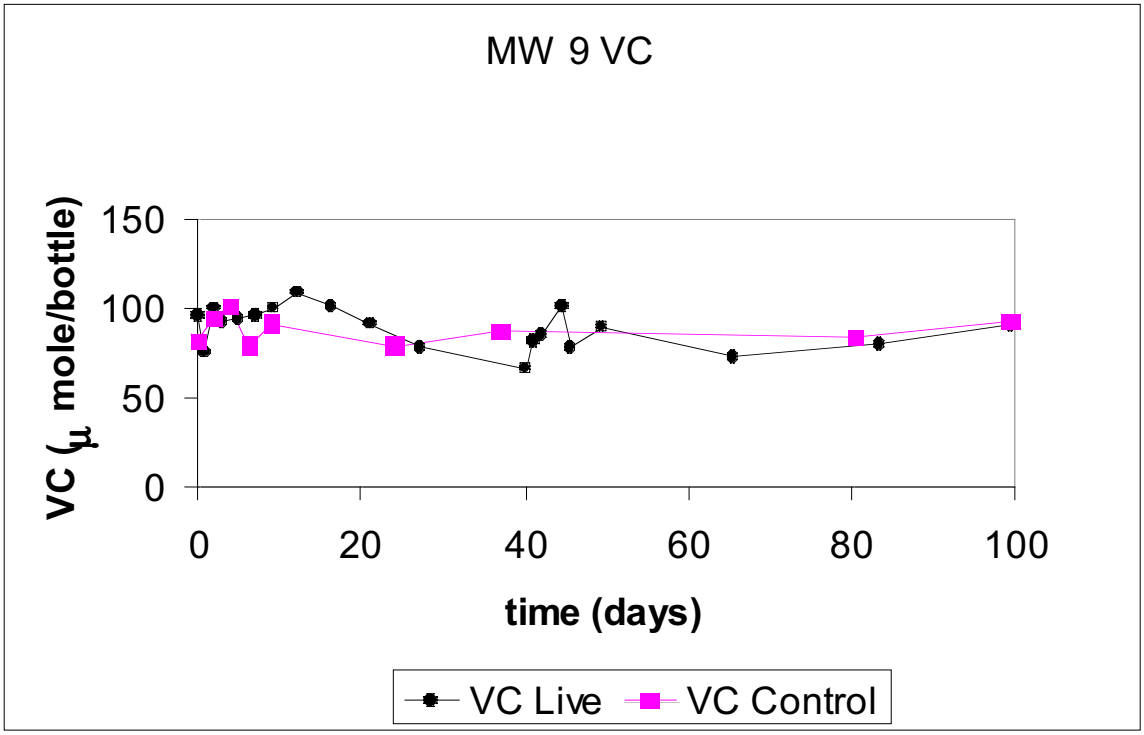

Figure 10. Vinyl chloride vs. time for autoclaved-control and live microcosm bottles from MW9.

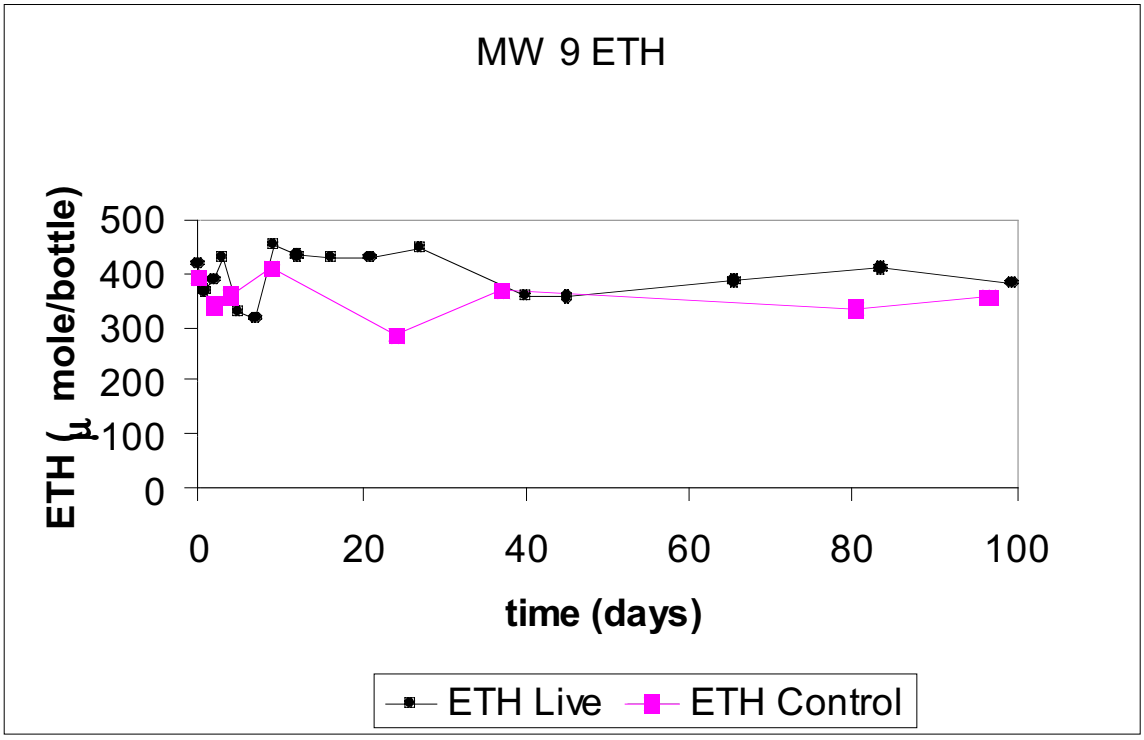

Figure 11. Ethene vs. time for autoclaved-control and live microcosm bottles from MW9.

The well-water microcosms were monitored for VC, ETH, and oxygen over a period of 100 days. They were sampled every 24 hours for the first 3 days of the study, every 48 hours until day 9, every 4 days between day 9 and day 21, every week between day 21 and day 45, and every 20 days between day 45 and day. None showed depletion of VC, ETH, or oxygen over 100 days. VC and ETH measurements from an autoclaved-control well-water microcosm and a live well-water microcosm constructed from MW9-samples are depicted in Figures 10 and 11, respectively. All other well-water microcosms from MW19 and MW27 behaved in a similar manner and exhibited no VC, ETH, or oxygen depletion.

Moody AFB Discussion. It is difficult to reconcile our failure to detect VC or ETH degraders in aquifer sediments at Moody AFB with our previously successful enrichments and isolations from groundwater samples taken at the same site. Addition of the VC-degrading strain JS621 to inactive microcosms yielded good VC- and ETH degradation, indicating that the lack of activity was not due to insufficient nutrients or the presence of inhibitory substances, but rather to the lack of degradative bacteria. In this case, the origin of JS621 and the JS621-like strains previously isolated from Moody AFB groundwater are brought into question. However, the 16s rDNA fingerprint of JS621 does not match that of any of the other isolates used in our labs, which seems to rule out "laboratory contamination" as an explanation.

These results are curious and point to the difficulty in finding biological activity at contaminated sites where there is evidence that such activity is occurring. VC and ETH degrading organisms require both VC (or ETH) and oxygen, but the zone where both the VC (or ETH) and oxygen coexist may be rather narrow and difficult to locate. In any case the results of this study suggest that the microorganisms we were looking for were not present at the locations sampled — at least at the time sampled.

Final Summary and Conclusions

Our findings indicate that aerobic bacteria (*Mycobacterium* and *Nocardioides* strains) capable of growth-linked VC oxidation are widespread in the environment, and commonly found at chlorinated-ethene-contaminated sites. Aerobic assimilation of VC as a carbon source is therefore an ecologically significant phenomenon of equal or greater importance than cometabolic VC degradation. Based on their distribution, growth rates and kinetic parameters, we believe that *Mycobacterium* strains are most likely to be responsible for the aerobic natural attenuation of VC that has been observed at many sites. The data suggest that biostimulation (e.g. addition of O_2 and/or inorganic nutrients) would be an appropriate strategy for accelerating VC attenuation at contaminated sites, because the appropriate microbial populations are likely to be already present in many cases.

Our discovery of a bacterium (*Polaromonas* strain JS666) able to grow on cDCE shows that aerobic biodegradation of cDCE in the absence of other carbon substrates is possible. From our results with enrichment cultures, these bacteria appear to be rare, and may presently exist only in highly selective 'artificial' environments such as the activated carbon filter that was the source of strain JS666. Our data suggest that it is unlikely that natural attenuation or biostimulation alone will be capable of remediation of cDCE contamination at most sites. Bioaugmentation with our isolate JS666 would be an appropriate strategy, and could lead to a self-sustaining, low-cost bioremediation method at sites where cDCE is a problem contaminant. Further investigation of JS666 is recommended — to delineate metabolic pathways; to determine the suite of substrates it can co-transform; to optimize culture conditions for field-bioaugmentation; to develop a molecular probe for field-monitoring after bioaugmentation; and, finally, to field-test the use of JS666 as bioaugmentation agent.

We have conclusively identified the enzyme (EaCoMT) responsible for bacterial epoxyethane metabolism, and obtained strong circumstantial evidence that the same enzyme is also involved in chlorooxirane metabolism. In addition, we have cloned and sequenced genes involved in VC, ETH, epoxyethane and chlorooxirane metabolism. The results indicate that the EaCoMT and monooxygenase enzymes encoded by a single operon (*etnEABCD*) in *Mycobacterium* JS60 and *Nocardioides* JS614 catalyze the initial reactions in both the VC and ETH assimilation pathways. EaCoMT activity and genes were found in all the alkene-oxidizing strains that we examined, including strains isolated on VC and ethene. The EaCoMT-specific gene primers we have developed could be used for culture-independent monitoring of microbial populations during the natural attenuation or bioremediation of chlorinated ethenes. Such methods are particularly relevant for mycobacteria, which are slow-growing and sometimes difficult to isolate.

There is good evidence in the literature in at least one case that VC-degraders evolved directly from ETH-degraders (Verce et al., 2001). The transition from ETH to VC assimilation could be due to recruitment of an additional catabolic enzyme, changes in enzyme specificity, or alteration of enzyme expression levels. Based on our data, there was no DNA sequence (either 16S rDNA or EaCoMT gene) that distinguished VC- from ETH-degraders. However, the EaCoMT activity in cell extracts of the VC-degraders tended to be higher. This is particularly apparent when strains JS619 (VC) and JS625 (ETH) are compared – these strains had almost

identical EaCoMT gene sequences, but the EaCoMT activity in cell extracts was 5-fold higher in JS619. Sequencing of complete EaCoMT genes and flanking DNA, and analysis of the activity of other catabolic enzymes may help to shed light on the factors that distinguish ethene- and VC-assimilating bacteria, and yield insights into the possible evolution of the latter group from the former.

The EaCoMT gene appears to be carried on large linear plasmids in the VC-degrading strains. Based on the gene organization in *Mycobacterium* strain JS60, it is likely that the alkene monooxygenase genes are also present on the same linear plasmids, which is apparently the case with *Nocardiodes* strain JS614. The present study is the first to our knowledge to associate a specific metabolic function with plasmids in *Mycobacterium* strains. Cryptic linear plasmids have previously been identified in various pathogenic mycobacteria (Le Dantec et al., 2001; Picardeau and Vincent, 1997, 1998), and linear plasmids were detected in the ethene-oxidizing *Mycobacterium* strain E-1-57 (Saeki et al, 1999), but in that case, no evidence for the plasmids' role in ethene metabolism was obtained. Plasmid-borne genes for ethene- and VC-biodegradation could potentially be transferred among bacteria in the environment, and thus, further investigation of the such elements is warranted in light of the potential importance of the alkene-degrading phenotype to bioremediation and natural attenuation processes.

We note that *Nocardioides* JS614 may hold promise as a bioaugmentation agent at sites where other VC-oxidizers are absent. JS614 has very high growth and VC-utilization rates. It is also of a genus that, unlike mycobacteria, has no pathogenic brethren — a factor in gaining regulatory acceptance. The one, known drawback of JS614 is its peculiarly severe response to starvation. However, in studies reported herein, we were able to show that the starvation response can be virtually eliminated if small amounts of a readily degradable substrate (e.g., acetate) is administered along with VC following VC-starvation.

Finally, we note that two organisms isolated and identified from this research study — *Nocardioides* JS614 and *Polaromonas* strain JS666 — have been selected by DOE for genomic draft sequencing. The notification from Dr. Daniel Drell stated as follows: "Your nomination of the beta-proteobacterium strain JS666 and *Nocardioides* strain JS614 were highly recommended for draft sequencing at the Joint Genome Institute (JGI), and, in light of that recommendation, has been selected for sequencing. The reviewer comments reflect the panel's enthusiasm for your microbe/community." We present this as evidence that the scientific community in general is enthusiastic about the outcome of our SERDP-sponsored research.

References

Bradley, P. M., and F. H. Chapelle 2000. Aerobic microbial mineralization of dichloroethene as sole carbon source. *Environ. Sci. Technol.* **34:**221-223.

Bradley, P. M., and F. H. Chapelle 1998. Microbial mineralization of VC and DCE under different terminal electron accepting conditions. *Anaerobe* **4:**81-87.

Coleman, N. V., T. E. Mattes, J. M. Gossett, and J. C. Spain 2002a. Biodegradation of *cis*-dichloroethene as the sole carbon source by a beta-proteobacterium. *Appl. Environ. Microbiol.* **68:**2726-2730.

Coleman, N. V., T. E. Mattes, J. M. Gossett, and J. C. Spain 2002b. Phylogenetic and kinetic diversity of aerobic vinyl chloride-assimilating bacteria from contaminated sites. *Appl. Environ. Microbiol.* **68:**6162-6171.

Coleman, N. V., and J. C. Spain 2003a. Epoxyalkane:Coenzyme-M transferase in the ethene and vinyl-chloride biodegradation pathways of *Mycobacterium* strain JS60. *J. Bacteriol.* **185**: 5536-5545.

Coleman, N. V., and J. C. Spain 2003b. Distribution of the Coenzyme-M pathway of epoxide metabolism among ethene- and vinyl-chloride-degrading *Mycobacterium* strains. *Appl. Environ. Microbiol.* **69:**6041-6046.

de Bont, J. A. M., and W. Harder 1978. Metabolism of ethylene by *Mycobacterium* E 20. *FEMS Microbiol. Lett.* **3:**89-93.

Ensign, S. A. 2001. Microbial metabolism of aliphatic alkenes. *Biochemistry* **40:** 5845-5853.

Hartmans, S., and J. A. M. de Bont 1992. Aerobic vinyl chloride metabolism in *Mycobacterium aurum* L1. *Appl. Environ. Microbiol.* **58:**1220-1226.

Hartmans, S., J. A. M. de Bont, J. Tramper, and K. C. A. M. Luyben 1985. Bacterial degradation of vinyl chloride. *Biotech. Lett.* **7:**383-388.

Klier, N. J., R. J. West, and P. A. Donberg 1999. Aerobic biodegradation of dichloroethylenes in surface and subsurface soils. *Chemosphere.* **38:**1175-88.

Le Dantec, C., N. Winter, B. Gicquel, V. Vincent, and M. Picardeau 2001. Genomic sequence and transcriptional analysis of a 23-kilobase mycobacterial linear plasmid: evidence for horizontal transfer and identification of plasmid maintenance systems. *J. Bacteriol.* **183:**2157-64.

Picardeau, M., and V. Vincent 1997. Characterization of large linear plasmids in mycobacteria. *J. Bacteriol.* **179:**2753-6.

Picardeau, M., and V. Vincent 1998. Mycobacterial linear plasmids have an invertron-like structure related to other linear replicons in actinomycetes. *Microbiology* **144:**1981-8.

Saeki, H., M. Akira, K. Furuhashi, B. Averhoff, and G. Gottschalk 1999. Degradation of trichloroethene by a linear-plasmid-encoded alkene monooxygenase in *Rhodococcus corallinus* (*Nocardia corallina*) B-276. *Microbiology*. **145:**1721-30.

Verce, M. F., R. L. Ulrich, and D. L. Freedman 2000. Characterization of an isolate that uses vinyl chloride as a growth substrate under aerobic conditions. *Appl. Environ. Microbiol.* **66:**3535-3542.

Verce, M. F., R. L. Ulrich, and D. L. Freedman 2001. Transition from cometabolic to growth-linked biodegradation of vinyl chloride by a *Pseudomonas* sp. isolated on ethene. *Environ. Sci. Technol.* **35:**4242-4251.

Waterhouse, K. V., A. Swain, and W. A. Venables. 1991. Physical characterization of plasmids in a morpholine-degrading *Mycobacterium*. *FEMS Microbiol. Lett.* **80:**305–310.

Appendix A

Coleman, N. V., T. E. Mattes, J. M. Gossett, and J. C. Spain 2002. Phylogenetic and kinetic diversity of aerobic vinyl chloride-assimilating bacteria from contaminated sites. *Appl. Environ. Microbiol*. 68:6162-6171.

APPLIED AND ENVIRONMENTAL MICROBIOLOGY, Dec. 2002, p. 6162–6171 Vol. 68, No. 12
0099-2240/02/$04.00+0 DOI: 10.1128/AEM.68.12.6162–6171.2002

Phylogenetic and Kinetic Diversity of Aerobic Vinyl Chloride-Assimilating Bacteria from Contaminated Sites

Nicholas V. Coleman,[1] Timothy E. Mattes,[2] James M. Gossett,[2] and Jim C. Spain[1]*

Air Force Research Laboratory—MLQL, Tyndall AFB, Florida 32403,[1] and School of Civil and Environmental Engineering, Cornell University, Ithaca, New York 14853[2]

Received 3 July 2002/Accepted 24 September 2002

Aerobic bacteria that grow on vinyl chloride (VC) have been isolated previously, but their diversity and distribution are largely unknown. It is also unclear whether such bacteria contribute to the natural attenuation of VC at chlorinated-ethene-contaminated sites. We detected aerobic VC biodegradation in 23 of 37 microcosms and enrichments inoculated with samples from various sites. Twelve different bacteria (11 *Mycobacterium* strains and 1 *Nocardioides* strain) capable of growth on VC as the sole carbon source were isolated, and 5 representative strains were examined further. All the isolates grew on ethene in addition to VC and contained VC-inducible ethene monooxygenase activity. The *Mycobacterium* strains (JS60, JS61, JS616, and JS617) all had similar growth yields (5.4 to 6.6 g of protein/mol), maximum specific growth rates (0.17 to 0.23 day^{-1}), and maximum specific substrate utilization rates (9 to 16 nmol/min/mg of protein) with VC. The *Nocardioides* strain (JS614) had a higher growth yield (10.3 g of protein/mol), growth rate (0.71 day^{-1}), and substrate utilization rate (43 nmol/min/mg of protein) with VC but was much more sensitive to VC starvation. Half-velocity constant (K_s) values for VC were between 0.5 and 3.2 μM, while K_s values for oxygen ranged from 0.03 to 0.3 mg/liter. Our results indicate that aerobic VC-degrading microorganisms (predominantly *Mycobacterium* strains) are widely distributed at sites contaminated with chlorinated solvents and are likely to be responsible for the natural attenuation of VC.

Vinyl chloride (VC) is a common groundwater contaminant (49) which is of concern due to its carcinogenicity (7). Although VC can be produced naturally at very low levels in some soils (32), the industrial synthesis of polyvinyl chloride plastics (27 million tons per year globally [33]) and the bacterial metabolism of chlorinated solvents (36, 41) are the most problematic sources of VC contamination. Many anaerobic bacteria can reductively dechlorinate the widely used solvents tetrachloroethene (PCE) and trichloroethene (TCE), producing *cis*-dichloroethene (cDCE), VC, or ethene (ETH) (19, 30, 35, 40, 59). However, microbes capable of reducing VC to ETH are often absent or inactive in subsurface ecosystems, and thus, VC commonly accumulates as an end product of anaerobic dechlorination (17, 37, 39).

VC can be oxidized to CO_2 under anaerobic conditions in the presence of Fe(III) or humic acids (4, 5), but the microbiology and biochemistry of such anaerobic oxidations have not been investigated. Aerobic bacteria can catalyze the cometabolic oxidation of VC in the presence of monooxygenase inducers such as methane (18), ethane (20), ETH (34), propane (38), propene (15), isoprene (16), toluene (48), and ammonia (56). Bioremediation strategies based on aerobic cometabolism have been examined for VC and other chlorinated ethenes (36, 47), but there are several problems with cometabolic systems—electron donors are required (2), the growth-supporting substrate and the pollutant compete for the same enzymes (15), and reactive toxic metabolites may accumulate and inhibit biodegradation (43, 61).

A few strains of *Mycobacterium* (25, 26) and *Pseudomonas* (57, 58) that can grow aerobically on VC as the sole carbon and energy source have been isolated from soil, river water, and activated sludge. Such bacteria are not subject to cometabolic limitations and may play a role in the natural attenuation of VC if they occur in the subsurface at contaminated sites. The origin of VC-assimilating bacteria is unclear, although evolution from strains that grow on ETH seems likely (58). ETH is produced via biosynthesis in plants and soil microorganisms, and aerobic ETH-assimilating bacteria appear to be fairly widespread and easily isolated (10, 23). The VC- and ETH-assimilation pathways in bacteria are not well understood, but there is evidence for an initial monooxygenase attack and the production of VC epoxide (chlorooxirane) (25) and epoxyethane (ethylene oxide) (11), respectively.

While several recent studies (17, 28, 29) have examined the distribution and diversity of anaerobic PCE-TCE-dechlorinating bacteria, similar studies on aerobic VC-assimilating bacteria are lacking, and it is not known whether such bacteria might contribute to the natural attenuation of VC. Evidence from the field (14) suggests that VC can disappear in the aerobic downgradient portions of chlorinated ethene plumes, but whether VC-assimilating bacteria are responsible for the effect is unknown. There is great variation in the kinetic parameters of the few aerobic VC degraders examined thus far, making it difficult to predict the rate and extent of in situ VC oxidation. To address the above issues, we investigated aerobic VC biodeg-

* Corresponding author. Mailing address: Air Force Research Laboratory—MLQL, Building 1117, 139 Barnes Dr., Tyndall AFB, FL 32403. Phone: (850) 283-6058. Fax: (850) 283-6090. E-mail: Jim.Spain@tyndall.af.mil.

radation in samples from chlorinated-ethene-contaminated sites and examined the phylogeny and kinetic parameters of VC-assimilating strains isolated from the site samples.

MATERIALS AND METHODS

Chemicals, media, and incubation conditions. The VC (99.5%) was from Fluka, and the ETH (99.5%) was from Scott. All other chemicals were reagent grade. A minimal salts medium (MSM) (24), modified as described previously (9), was used for both enrichments and pure cultures. One-tenth-strength Trypticase soy agar (1/10-TSA; pH 7.0) and 1/10-strength Trypticase soy broth (1/10-TSB; pH 7.0) were used as nonselective media and contained TSB (3 g/liter; Difco) and Bacto agar (20 g/liter; Difco) where required. In some cases, glucose (10 g/liter) and/or bovine serum albumin (Fraction V; 5 g/liter; Sigma) was added to 1/10-TSA and 1/10-TSB. All cultures were incubated aerobically. Broths were shaken at 150 to 165 rpm. Incubation temperatures ranged from 20 to 30°C, as listed specifically below.

Analytical methods. VC, ETH, and epoxyethane were analyzed in headspace samples by gas chromatography with flame-ionization detection as described previously (9). For analysis of kinetic data, aqueous concentrations of VC were calculated from total amounts, using a dimensionless Henry's constant of 0.9079 at 20°C (22). For ETH, a Henry's constant of 7.24 at 20°C was estimated by using the technique of Gossett (22). A Hewlett Packard HP 5890 Series II gas chromatograph equipped with a thermal conductivity detector and a 1/8-in.-diameter stainless steel column packed with a 60/80-mesh 5A molecular sieve (Supelco) was used to analyze oxygen in headspace samples (0.5 ml from 160-ml serum bottles). Protein concentrations were routinely measured by a UV absorbance assay based on previously described methods (31, 42). Samples of culture fluid (0.45 ml) were mixed with NaOH (0.15 ml, 10 M) and heated (90°C, 10 min). The samples were cooled, an HCl solution was added (400 μl; 10 M HCl and MSM in a 3:5 ratio), and the tubes were centrifuged (16,000 × *g*) for 5 min. The absorbance of the supernatants was measured at 230 and 260 nm, and the protein content was calculated in micrograms per milliliter as $(183 \times A_{230}) - (75.8 \times A_{260})$. Protein in neutralized lysates was also determined on occasion by using the MicroBCA assay kit (Pierce) as described previously (9). Dry-weight growth yields were determined with 700-ml cultures grown on 100 ml (4,167 μmol) of VC or ETH. Cells were washed in deionized water and then dried at 105°C to a constant weight. The optical density at 600 nm (OD_{600}) was also used to monitor growth in some cases.

Microcosms and enrichment cultures. Samples of groundwater (50% [vol/vol]), soil (5% [wt/vol]), sediment (5% [wt/vol]), or activated carbon (5% [wt/vol]) were mixed with MSM in 160-ml serum bottles (50-ml or 72-ml [liquid phase]) sealed with Teflon-faced rubber stoppers and aluminum crimp caps. In cases where samples contained solids and groundwater, initial microcosms were set up without the addition of medium. VC was added at 20 to 40 μmol/bottle (0.13 to 0.26 mM aqueous concentration) in the initial microcosms and at 100 to 400 μmol/bottle in later transfers (0.66 to 2.64 mM). The microcosms and enrichments were incubated with the bottles in an inverted position and with shaking at the ambient temperature (20 to 24°C), and active cultures (5% [vol/vol]) were transferred to fresh MSM at intervals. Sterile controls (autoclaved samples in MSM) were set up in accompaniment to the initial microcosms for the monitoring of abiotic losses.

Isolation and identification of VC degraders. Pure cultures were isolated from the enrichments by spreading dilutions on MSM plates and incubating in desiccators in a 1% (vol/vol) VC-air atmosphere. After incubation at ambient temperature for 1 to 3 months, representative colonies were restreaked on two MSM plates, one of which was reincubated with 1% VC and the other of which was reincubated in air alone. Isolates showing significantly more growth in the presence of VC were investigated further. In some cases, isolations were also done on 1/10-TSA plates both with and without added bovine serum albumin. Utilization of VC was confirmed by reinoculation of isolates into MSM-VC broths and the monitoring of VC consumption (gas chromatography [GC] analysis) and cell growth (OD_{600} or protein assay). Identification of strains was done by partial sequencing of amplified 16S rDNA (MIDI Labs, Newark, Del.). Phylogenetic analysis was done with ClustalX and TreeView software (see Fig. 1; see legend for details).

DNA extraction and repetitive extragenic palindromic (REP)-PCR analysis. Cultures were inoculated into 50 ml of 1/10-TSB–glucose (1%)–glycine (0.6%) at an OD_{600} of approximately 0.5 and grown for 16 to 24 h at 30°C to an OD_{600} of approximately 1.0 to 1.5. Cells were washed in STE buffer (as described previously (45), but with EDTA at 50 mM), treated with acetone (27), and incubated at 37°C overnight in lysozyme (5 mg in 1 ml of STE buffer). Cells were lysed with proteinase K (0.5 mg/ml), sodium dodecyl sulfate (1%), and heat (55°C, 2 to 16 h), and the DNA was purified via phenol-chloroform extraction, isopropanol precipitation, RNase treatment, and ethanol precipitation (45). Typical yields were 0.5 to 1.5 μg of genomic DNA/ml of culture. DNA was diluted to 50 ng/μl in water and used as the template for PCR with the REP1R-I and REP2-I primers as described by de Bruijn (13), except dNTPs were added at 0.2 mM.

Determination of growth rates and growth yields. VC-grown cells were washed with MSM and inoculated into 50 ml of MSM (OD_{600} = 0.05, protein = 7 to 11 μg/ml). VC was added at 150 μmol/bottle (1 mM), and the cultures were incubated at 20°C with sampling at intervals for determination of VC and protein concentrations. VC (150 μmol) was added as required. Another set of cultures inoculated with ETH-grown cells was similarly treated, except ETH was provided as the substrate (one addition of 600 μmol/bottle = 0.7 mM). Growth yields were calculated from the linear regression (milligrams of protein produced/mmol of substrate consumed). Maximum specific growth rates were subsequently calculated by fitting an exponential curve to a plot showing protein yield versus time. In this case, protein yield was calculated from substrate depletion data as $X_0 + Y\Delta S$, where X_0 is the initial biomass (milligrams of protein), Y is the growth yield (milligrams of protein/millimole of substrate), and ΔS is the cumulative substrate consumed (millimoles). This method of calculating the growth rate was used due to the availability of more substrate depletion data than protein data and because of the relatively large scatter in the protein measurements for some cultures. The growth yield of strain JS616 was determined by using 3-ml cultures in 10-ml serum bottles. The whole culture was lysed by injecting NaOH (1 ml, 10 M) into the bottle and heating (90°C, 15 min), and then the lysate was neutralized and assayed for protein by measurement of UV absorbance.

VC-ETH utilization kinetics. VC- or ETH-grown cells were washed in MSM and divided among three 160-ml serum bottles containing 72 ml of MSM each. The cultures were incubated with the bottles inverted at an angle at 20°C and with rotary shaking at 165 rpm, and the headspace gases were sampled at intervals for GC analysis. Estimates of the maximum specific substrate utilization rate (k) and the half-velocity constant (K_s) were obtained from VC or ETH depletion curves. The data were fitted to the Michaelis-Menten model by using the AQUASIM software program, as described previously (9). VC kinetics was determined with cultures pregrown on VC, while ETH kinetics was determined with cultures pregrown on ETH. Protein concentrations were measured at the end of each depletion experiment by lysing the entire contents of each culture bottle, as described previously. Experiments were designed such that biomass increases over the observed depletion curves were negligible (typically < 0.5%).

Oxygen utilization kinetics. The half-velocity constant with respect to oxygen ($K_s[O_2]$) was determined with 72-ml cultures in triplicate as described above for the VC-ETH kinetics study. After inoculation, the headspace was purged briefly with nitrogen to remove excess oxygen and then 300 μmol of VC or 800 μmol of ETH was added to the culture. $K_s(O_2)$ values were estimated using AQUASIM as described above. A zero-oxygen standard was prepared by adding excess sodium sulfite to a 160-ml serum bottle containing 72 ml of distilled water in the presence of cobalt catalyst. The oxygen peak area for the mixture from this bottle, as measured by GC, was defined as corresponding to 0 mg of dissolved oxygen/liter. Oxygen threshold levels (i.e., oxygen uptake levels too low to measure at oxygen concentrations greater than zero) were observed during the study, which required a modification of the Michaelis-Menten model for the AQUASIM program as follows:

$$V = \frac{V_{\max}(S - S_t)}{(K_s(O_2) + (S - S_t))}$$

where V is the rate of oxygen depletion, $V_{\max}$ is the maximum rate of oxygen depletion ($-dS/dt$), S is the oxygen concentration (in milligrams per liter), and S_t is the threshold oxygen concentration (in milligrams per liter). The model-fitting parameters were thus $V_{\max}$, $K_s(O_2)$, and S_t.

Epoxyethane production assay. Cells from 50-ml MSM cultures grown to mid-exponential phase on either VC or sodium acetate (20 mM) were washed in KP buffer (K_2HPO_4, 20 mM [pH 7.0]) and suspended to 0.2 ml with KP buffer in 10-ml serum bottles. The bottles were capped and an epoxypropane solution was added (2.5 mM in 0.8 ml of KP buffer), yielding 1-ml suspensions at an OD_{600} between 5 and 10 (protein = 0.7 to 2.3 mg/ml). ETH (3 μmol) was added, and the bottles were incubated with shaking (300 rpm) at 20°C. After 10 min of equilibration, 100-μl headspace samples were taken at intervals and analyzed by GC to determine the epoxyethane accumulation rate. At the end of the experiment, protein was assayed and monooxygenase activity was calculated as nanomoles of epoxyethane produced per minute per milligram of protein. In the case of strain JS616, Tween 80 (0.1% [vol/vol]) was added to cultures just before

harvesting and was included in the washing buffer to facilitate centrifugation and reduce clumping during the assay.

Bacterial strain accession numbers. Several of the VC-degrading strains have been deposited with the American Type Culture Collection, with accession numbers as follows: JS60, BAA-494; JS61, BAA-495; JS616, BAA-496; JS617, BAA-497; JS621, BAA-498; and JS614, BAA-499.

RESULTS AND DISCUSSION

Distribution of VC assimilation activity. Aerobic biodegradation of VC occurred in 23 of 37 samples from 22 sites (Table 1). Twenty of 31 chlorinated-ethene-contaminated samples yielded positive enrichments, while 3 of 6 uncontaminated samples were positive. The lag time before VC degradation began was highly variable, ranging from 20 to 110 days. In most cases, VC-degrading activity in the initial microcosms was readily transferable in enrichment cultures with VC as the sole carbon and energy source. It is unclear from our data whether the presence of VC degraders correlated with site contamination. This is due to the small number of uncontaminated samples investigated and the lack of rigorous site characterization in many cases.

One interesting trend noted with the samples from contaminated sites was that VC degraders were not detected in the two samples (Phoenix groundwater and Cecil Field sediment) that contained benzene in addition to chlorinated ethenes. It is possible that at such sampling locations, hydrocarbons interfered with the development of VC-degrading populations by exerting toxic effects or by acting as alternative carbon sources. Another unexpected result with the samples from Cecil Field was that a positive enrichment was obtained from groundwater outside the contaminant plume (sample MW16-13S), while no activity was seen in groundwater from a highly contaminated area of the site (MW3-13S). Active enrichments were also obtained from uncontaminated samples in two other cases (Moody Air Force Base [AFB] sample MW-14 groundwater and Ithaca activated sludge).

From our survey of sites, it appears that VC-degrading microorganisms are fairly widespread and arise wherever conditions are appropriate for their growth. The presence of chlorinated ethenes is apparently not the sole factor that determines whether VC degraders are present at a site. Other site conditions, such as redox potential, pH, and the presence of other contaminants and nutrients, would be expected to influence the development of VC-degrading microbial populations. The most favorable niches for the growth of VC degraders may be in aerobic areas downgradient of chlorinated ETH plumes, where anaerobic electron donors are depleted and the end products of anaerobic chloroethene metabolism (i.e., VC, ETH, and ethane) accumulate.

Isolation and characterization of bacteria. Pure cultures of VC-assimilating bacteria were isolated from 15 of the enrichments. All of the isolated strains grew on both VC and ETH as the sole carbon source and were relatively slow growing, requiring 1 to 3 weeks to form colonies on 1/10-TSA plates and 1 to 3 months to form colonies on MSM-VC plates. The optimum temperature and pH for the isolates was determined in two cases (i.e., those of strains JS60 and JS61) to be 30°C and pH 6.0 to 6.5. For the sake of consistency, however, further growth and kinetic experiments with the isolates were performed at 20°C with a pH of 7.0.

On 1/10-TSA plates, colonies of the VC-degrading strains were white, cream, yellow, or orange in color and ranged in form from smooth and circular to raised and irregular. Large- and small-colony variants were produced by pure cultures in several cases, a trait that was particularly noticeable with strain JS614. Strains JS61, JS617, and JS621 did not readily form single colonies on 1/10-TSA or MSM plates, despite growing well in broth medium. The addition of glucose and particularly albumin (as used in mycobacterial media such as Middlebrook 7H9) greatly facilitated colony development with such strains. In liquid culture, all of the isolates except strain JS614 showed some degree of hydrophobic behavior–either clumping or adhering to the walls of serum bottles.

In groundwater enrichments, there was a tendency for less hydrophobic strains (e.g., JS60, JS615, and JS620) related to *Mycobacterium rhodesiae* (see below) to dominate, while with solid sample types a diverse range of more hydrophobic strains (e.g., JS616, JS617, and JS619) tended to be isolated. The use of groundwater samples in many cases may have biased our survey against the more hydrophobic, possibly surface-associated bacteria at the sampling site. Future sampling efforts should therefore focus on samples of soil or aquifer solids to more fully investigate the diversity of VC-assimilating bacteria. The fact that we could not isolate pure cultures from some enrichments despite repeated attempts also indicates that the biodiversity of aerobic VC degraders is not fully represented by the isolates obtained thus far.

Phylogenetic analysis. Comparison of partial 16S rDNA sequences from the VC-degrading isolates with sequences from GenBank indicated that with one exception (strain JS614), all of the isolates were *Mycobacterium* species (Fig. 1). Many of the strains (i.e., TM1, JS60, JS61, JS615, JS618, JS620, and JS621) clustered in a loose group which includes *M. rhodesiae*, *M. sphagni*, *M. aichiense*, *M. fortuitum*, and *M. mucogenicum* (44, 52). This group also includes the ETH-degrading strain K1 (34), the trichloroethane-degrading strain TA27 (60), and several polyaromatic hydrocarbon-degrading bacteria (e.g., strains RJGII-135 [46] and SM7.6.1 [21]). Based on analysis of some near-full-length 16S rDNA sequences (1,420 bases), we have tentatively assigned strains TM1, JS60, JS615, and JS620 to *M. rhodesiae* and strains JS61 and JS618 to *M. aichiense*.

The strain JS621 partial 16S rDNA sequence (400 bp) was most similar to that of *M. mucogenicum* (Fig. 1), but comparison of near-full-length sequences (data not shown) revealed a closer relationship to *M. rhodesiae* (98.2% sequence identity). However, JS621 was slow growing and nonpigmented on plates, in contrast to *M. rhodesiae* (52), and the other *M. rhodesiae*-like VC degraders, which grew more rapidly and featured yellow pigmentation. Thus, strain JS621 may represent a novel species of mycobacterium. Based on 16S rDNA analysis, the mycobacterial isolates JS617 and TM2 are most likely to be strains of *M. tusciae* (51), while JS616 and JS619 are probably strains of *M. gadium* (8), and *M. moriokaense* (53), respectively. The 16S rDNA sequence from strain JS614 was most similar to sequences from *Nocardioides* strains. Analysis of near-full-length 16S rDNA sequences (1,469 bases) indicated that the JS614 gene was 97.4% identical to that of *Nocardioides pyridinolyticus*, the closest-matching well-established species. Based on these results, it is possible that strain JS614 represents a new *Nocardioides* species (50).

TABLE 1. VC biodegradation in aerobic microcosms and enrichments

Sample (location)	Contaminants present at site[a]	VC oxidation	Lag time (days)	Strain isolated
Groundwater (industrial site; Plaquemine, La.)	VC, cDCE, TCE, PCE	+	70	*Mycobacterium* sp. strain JS60
Activated sludge (Ithaca, N.Y.).	None identified	+	50	*Mycobacterium* sp. strain JS61
Soil (industrial site; Midland, Mich.)	None identified	−		None (no activity after 4 mo)
Pond water (Tyndall AFB, Fla.)	None identified	−		None (no activity after 4 mo)
Wastewater (Tyndall AFB, Fla.)	None identified	−		None (no activity after 4 mo)
Soil (industrial site; Boeblingen, Germany)	cDCE, TCE, PCE	+	50	None (isolation attempts failed)
Soil (industrial site; Dusseldorf, Germany)	VC, cDCE	+	40	*Mycobacterium* sp. strain JS618
Activated carbon (pump and treatment plant; Dortmund, Germany)	VC, cDCE, TCE, PCE	+	30	*Mycobacterium* sp. strain JS617
Sediment (industrial site; Carlyss, La.)[b]	VC, cDCE, 1, 1-DCE, TCE	+	20	*Mycobacterium* sp. strain JS616
Soil (Dover AFB, Del.)[b]	cDCE, TCE, TCA	+	110	None (no activity after 2nd transfer)
Soil (Hill AFB, Utah)[b]	TCE, TCA	+	90	None (low activity)
Groundwater (Phoenix, Ariz.)	VC, cDCE, TCE, TCA, benzene	−		None (no activity after 4 mo)
Soil (industrial site; Carson, Calif.)	VC, DCA	+	20	*Nocardioides* sp. strain JS614
Aquifer solids (Travis AFB, Calif.)[b]	VC, cDCE, TCE	+	50	*Mycobacterium* sp. strain JS619
Groundwater MW16-10S (Cecil Field NAS[c], Fla.)	VC, cDCE, TCE, DCA	+	60	*Mycobacterium* sp. strain JS615
Groundwater (Cecil Field NAS, Fla.) MW16-13S	None identified	+	90	None (enrichment frozen)
Groundwater (Cecil Field NAS, Fla.) MW3-13S	cDCE, TCE, DCA, TCA	−		None (no activity after 4 mo)
Sediment (Cecil Field NAS, Fla.) Rowell Ck.	cDCE, DCA, chloroform, benzene	−		None (no activity after 4 mo)
Groundwater (Cape Canaveral, Fla.) MW S-14	VC, cDCE	+	30	*Mycobacterium* sp. strain JS620
Groundwater (Cape Canaveral, Fla.) MW S-19	VC, cDCE	+	110	None (enrichment frozen)
Groundwater (Cape Canaveral, Fla.) MW I-11	VC, cDCE	−		None (no activity after 4 mo)
Groundwater (Moody AFB, Ga.) MW-14	None identified	+	90	*Mycobacterium* sp. strain JS621
Groundwater (Moody AFB, Ga.) MW-9	VC, cDCE, TCE	+	40	*Mycobacterium* sp. (JS621 like)
Groundwater (Moody AFB, Ga.) MW-12	VC, cDCE, TCE	+	70	*Mycobacterium* sp. (JS621 like)
Groundwater (Moody AFB, Ga.) MW-19	VC, cDCE, TCE	+	70	None (isolations in progress)
Groundwater (Moody AFB, Ga.) MW-27	VC, cDCE, TCE	+	50	*Mycobacterium* sp. (JS621 like)
Soil-groundwater (Cape Canaveral, Fla., site 1381)	VC, cDCE	−		None (no activity after 4 mo)
Soil-groundwater (Alameda NAS, Calif., site 4)	VC, cDCE, TCE	−		None (no activity after 4 mo)
Soil-groundwater Fort Lewis (Wash.)	VC, cDCE, TCE	+	50	*Mycobacterium* sp. strain TM2
Groundwater-fines (industrial site, Sydney, Australia)	Chlorinated methanes, ethanes, and ethenes	−		None (no activity after 4 mo)
Groundwater-fines (landfill, Voorhees, N.J.)	cDCE	+	70	*Mycobacterium* sp. strain TM1
Soil (Savannah River, Ga.)	TCE	−		None (no activity after 4 mo)
Groundwater (Camp LeJeune, N.C., site 73) MW-13	VC, cDCE, TCE	−		None (no activity after 4 mo)
Soil-groundwater (Camp LeJeune, N.C., site 73) MW-15	VC, cDCE, TCE	−		None (no activity after 4 mo)
Soil-groundwater (Camp LeJeune, N.C., site 73) MW-29	VC, cDCE, TCE	−		None (no activity after 4 mo)
Soil-groundwater (Camp LeJeune, N.C., site 73) A47/3-11	VC, cDCE, TCE	+	60	None (isolations in progress)
Soil-groundwater (Camp LeJeune, N.C., site 73) A47/3-8	VC, cDCE, TCE	+	80	None (isolations in progress)

[a] Information obtained from site managers and our own GC analyses. DCA, 1,2-dichloroethane; TCA, 1,1,2-trichloroethane.
[b] Sample was an experimental microcosm received from another laboratory.
[c] NAS, Naval Air Station.

In two cases, VC-degrading isolates from geographically distant sites had identical partial 16S rDNA sequences (isolates JS60 and JS620 and isolates JS61 and JS618). On the basis of phenotypic differences such as pigmentation and the results of REP-PCR amplification (Fig. 2), which showed all four strains to be distinct, we believe these strains to be independent isolates. The four isolates derived from Moody AFB groundwater (JS621 and three JS621-like strains) had identical partial 16S rDNA sequences and the same colony morphology. Further tests (e.g., REP-PCR assays) are required to determine the relationship between these isolates. The JS621-like strains were isolated from monitoring wells covering the entire length of the VC plume, suggesting that a single VC-degrading strain dominates this site. A similar phenomenon has been observed at Kelly AFB (Texas), where chlorobenzene-degrading bacteria isolated from different groundwater samples were all found to carry identical 16S rDNA genes and degradation pathways (54).

The fact that all our VC-degrading isolates were gram-positive bacteria (order *Actinomycetales*) seems unusual in light of the recent isolations of VC-degrading *Pseudomonas* strains (57, 58). As the media and temperatures used in our study were similar to those of Verce et al. (57, 58), the differences in phylogeny of isolates may be due to the sole use of VC for selection in our work rather than of ethane (57) or ETH (58) in initial enrichments. Differences in sample types (i.e., groundwater and soil versus sewage sludge) may also have influenced the types of isolates recovered, although it should

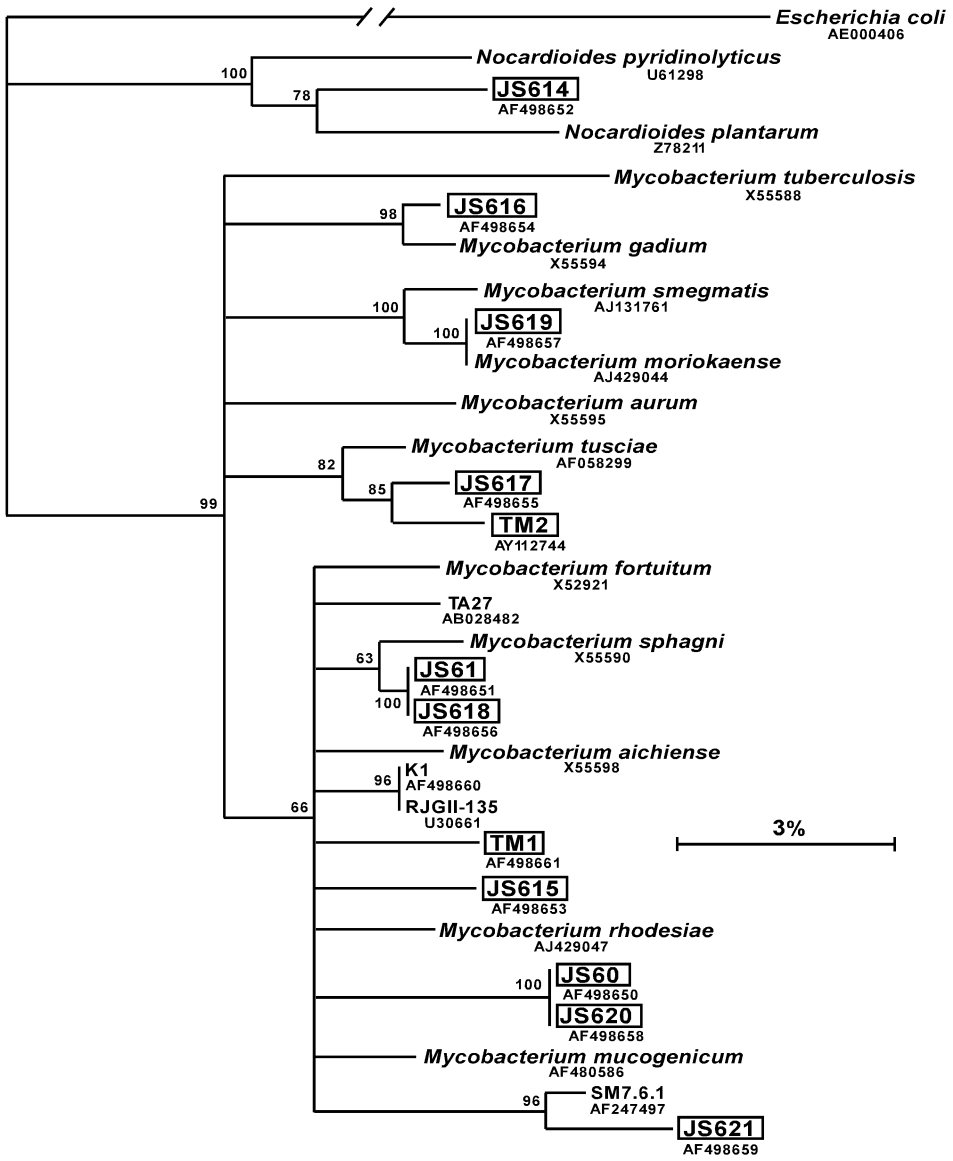

FIG. 1. Phylogeny of VC-assimilating isolates based on partial 16S rRNA gene sequences. Names of VC-degrading isolates from the present study are in boxes. A total of 400 bases were used for analysis after removal of positions containing gaps or ambiguous nucleotides. Bootstrap values from 100 neighbor-joining trees are indicated to the left of the nodes. Branch points with less than 50% bootstrap support were collapsed. The bar represents 3 nucleotide changes per 100 nucleotides. The consensus tree was rooted by using *Escherichia coli* as the outgroup. GenBank accession numbers are given below each strain.

be noted that we isolated *Mycobacterium* JS61 from activated sludge. Based on the results of our isolations, it appears that mycobacteria are more likely candidates than pseudomonads as the agents responsible for the natural attenuation of VC in the subsurface at contaminated sites.

Growth and kinetic parameters. Five representative strains were selected for more detailed analysis of growth and kinetic parameters with ETH and VC (Table 2). The growth yields and growth rates of the four *Mycobacterium* strains examined (JS60, JS61, JS616, and JS617) were similar, and all were lower than the values obtained for the *Nocardioides* strain (JS614). We considered the possibility that the apparent high yields of strain JS614 were due to biases in the lysis or protein quantitation methods used, but alternative protein assays (Micro-BCA) and measurement of dry-weight yields confirmed the initial data. The dry-weight growth yields with JS614 were 20.1 g/mol for VC and 29.4 g/mol for ETH compared to yields with JS60 of 10.8 g/mol for VC and 22.0 g/mol for ETH (averages of two experiments).

The growth yields of the *Mycobacterium* strains agreed fairly well with the yields of previously isolated *Mycobacterium* and *Pseudomonas* strains (57), assuming a value of 55% protein in dry weight of bacteria (6) (a ratio of 56% was calculated from the growth yields of strain JS60 in the present study). The higher growth yields of strain JS614 may reflect a different pathway of VC assimilation in this bacterium. For example,

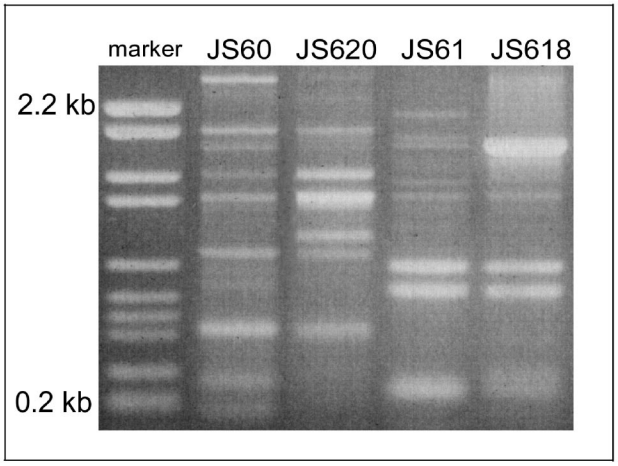

FIG. 2. Discrimination of closely related VC-degrading mycobacteria by REP-PCR.

carboxylation of the epoxides resulting from VC and ETH oxidation (1) would allow the net incorporation of more carbon per mole of VC utilized than alternatives such as conjugation to coenzyme A (11) or glutathione (55). Further investigation into the biochemistry of VC assimilation in strain JS614 and the other isolates is required to test this hypothesis.

The maximum specific growth rates on VC of our mycobacteria were about 5-fold lower than that for *Mycobacterium* sp. strain L1 (25), 5-fold higher than that for *Pseudomonas* sp. strain DL1, and 50-fold higher than that for *Pseudomonas* sp. strain MF1 (58). The comparison with strain L1 may not be entirely appropriate given the higher growth temperature used in that study (30°C), but the comparison with the *Pseudomonas* strains is appropriate. The more rapid growth of the *Mycobacterium* strains adds weight to our argument that this group is more likely to be influential in the natural attenuation of VC. The maximum specific growth rate of *Nocardioides* sp. strain JS614 at 20°C was 15 times higher than that of strain DL1 and 150 times higher than that of strain MF1. Although *Nocardioides*-type VC degraders appear to be rare based on the results of our site-screening study, they are likely to have a large impact on the natural attenuation of VC where they occur due to their rapid growth and high biomass yields.

In general, the substrate utilization kinetics of the four *Mycobacterium* strains were more similar to each other than they were to the *Nocardioides* strain (Table 2). The *k* values for VC utilization ranged from 9 to 16 nmol/min/mg of protein among the four *Mycobacterium* strains; however, the corresponding *k* value for the *Nocardioides* strain was 43 nmol/min/mg of protein. The *k* values for ETH were greater than those for VC with the *Mycobacterium* strains, but the reverse was true with the *Nocardioides* strain (JS614).

The K_s values of the VC-assimilating strains showed no apparent grouping by phylogeny and were generally similar (ca. 1 μM). The K_s values agreed fairly well with data from other bacteria that grow on VC (58) and were much lower than the K_s values reported for aerobic cometabolic chlorinated-ethene-degrading cultures (3). K_s values for ETH among the *Mycobacterium* strains were higher than K_s values for VC, suggesting that the enzymes involved have a somewhat greater affinity for VC than for ETH. No such difference in affinity between VC and ETH was apparent for the *Nocardioides* strain JS614. The low K_s values for VC (and the absence of a measurable VC threshold) suggests that these bacteria are capable of degrading VC to very low levels under appropriate field conditions and are therefore environmentally relevant strains. In terms of kinetic parameters, it appears that it matters very little which species of VC-degrading *Mycobacterium* resides at a contaminated site but the presence of an organism like *Nocardioides* JS614 would represent a significantly greater VC oxidation potential.

All five strains examined were able to oxidize ETH to epoxyethane after growth on VC but not after growth on acetate, indicating the presence of an inducible alkene monooxygenase (Table 2). The specific activities measured for epoxyethane production ranged from 7 to 22 nmol/min/mg of protein. The measured activities are lower than the true activity (*k* value for ETH oxidation; Table 2), probably due to the inhibitory presence of epoxypropane in the cell suspensions. The addition of epoxypropane was required to stop the metabolism of ep-

TABLE 2. Growth and kinetic parameters of VC-assimilating bacteria

Strain	Growth yield[a] (g of protein/mol of substrate)		Maximum specific growth rate (day^{-1})		*k* (nmol/min/mg of protein)		K_s (μM)		Epoxyethane production from ETH (nmol/min/mg of protein)	
	VC	ETH	VC	ETH	VC	ETH	VC	ETH	VC-grown	Acetate-grown
Mycobacterium										
JS60	6.6 ± 0.7	11.2 ± 0.6	0.22 ± 0.02	0.58 ± 0.05	9.7 ± 0.2	25.4 ± 0.8	0.5 ± 0.1	0.9 ± 0.1	12.1 ± 3.7	0
JS61	6.2 ± 1.5	12.1 ± 1.6	0.21 ± 0.02	0.76 ± 0.07	9.0 ± 0.2	43.5 ± 1.4	0.8 ± 0.2	4.0 ± 0.2	8.0 ± 2.8	0
JS616	5.4 ± 1.1	12.8 ± 1.1	0.17 ± 0.02	0.39 ± 0.02	15.4 ± 0.6	20.4 ± 1.0	3.2 ± 0.3	4.0 ± 0.5	13.9 ± 9.3	0
JS617	6.0 ± 0.6	11.1 ± 0.5	0.23 ± 0.02	0.64 ± 0.05	16.0 ± 0.4	30.6 ± 1.4	0.8 ± 0.1	1.5 ± 0.1	6.7 ± 0.7	0
Nocardioides sp. strain JS614	10.3 ± 0.8	21.2 ± 1.8	0.71 ± 0.04	0.91 ± 0.08	43.1 ± 4.2	21.5 ± 1.6	1.2 ± 0.2	1.0 ± 0.2	22.0 ± 4.1	0
Mycobacterium sp. strain L1[b]	7.6	11.9	0.96	NR[c]	100	NR	3.2	NR	NR	NR
Pseudomonas sp. strain DL1[b]	7.2 ± 0.3	13.1 ± 1.7	0.046	0.071	4.6 ± 0.2	3.8 ± 0.1	1.2 ± 0.2	18.8 ± 1.2	NR	NR

[a] All data from the present study are averages of three replicates; error values represent 95% confidence intervals.
[b] Data for strains L1 (25) and DL1 (58) were converted to units of protein, assuming a value of 55% protein in dry weight.
[c] NR, not reported.

TABLE 3. Oxygen half-velocity constants of VC-assimilating bacteria

Strain	$K_s(O_2)$ (mg/liter)[a]		O_2 threshold (mg/liter)	
	VC	ETH	VC	ETH
Mycobacterium				
JS60	0.17 ± 0.06	0.18 ± 0.1	0.02 ± 0.01	0.00
JS61	0.03 ± 0.04	0.25 ± 0.1	0.07 ± 0.01	0.00
JS616	0.30 ± 0.24	1.1 ± 1.0	0.10 ± 0.02	0.00
JS617	0.07 ± 0.06	0.2 ± 0.1	0.06 ± 0.02	0.02 ± 0.01
Nocardioides sp. strain JS614	0.11 ± 0.04	0.29 ± 0.1	0.06 ± 0.01	0.12 ± 0.02

[a] Data are averages of three replicates; error values represent 95% confidence intervals.

oxyethane (12) to allow an accumulation rate to be measured, but epoxypropane also partially inhibited ETH oxidation in experiments with strain JS60 (data not shown). In further experiments with JS60 (data not shown), ETH-grown cells also readily metabolized VC, suggesting that the same monooxygenase enzyme is active on VC and ETH and is inducible by both substrates. Alkene monooxygenase activity has also been detected in *Mycobacterium* sp. strain L1, *Pseudomonas* sp. strain MF1, and *Pseudomonas* sp. strain DL1 (25, 57, 58), indicating that monooxygenase-catalyzed epoxidation is common to all VC-assimilating bacteria. The monooxygenase activities calculated in the present study were significantly lower than the corresponding activities reported for *Mycobacterium* sp. strain L1 (25) and ETH-assimilating mycobacteria (23). This difference is at least partly due to the use of lower incubation temperatures in our experiments (20°C) and the inhibitory effects of epoxypropane.

Oxygen utilization kinetics. $K_s(O_2)$ values were determined for five of the VC-assimilating strains (Table 3). For each strain, the $K_s(O_2)$ value for VC was lower than the $K_s(O_2)$ value for ETH, similar to the pattern seen with the K_s values for substrate utilization (Table 2). The very low $K_s(O_2)$ values measured (0.03 to 0.30 mg/liter) during growth on VC indicate that these five strains can effectively biodegrade VC under conditions of low-oxygen tension similar to those commonly encountered in the subsurface. Although the $K_s(O_2)$ values were low, all the strains exhibited oxygen threshold behavior during growth on VC, in which O_2 uptake ceased when the O_2 concentration dropped below 0.02 to 0.1 mg/liter. The *Nocardioides* strain (JS614) was the only strain to exhibit any significant oxygen threshold behavior during growth on ETH. It is unlikely that the O_2 thresholds observed were analytical artifacts, as in every case elevated oxygen levels in experimental bottles were confirmed by comparison to an identically treated zero-oxygen standard. In addition, the cultures were not limited by lack of VC or ETH at the oxygen threshold point and respiking of oxygen (tested with strain JS616 on VC and strain JS614 on ETH) resulted in further O_2 uptake until a threshold was again reached. Thus, cessation of oxygen uptake at the measured threshold value was not a result of substrate depletion or cell death. We cannot explain these observations at present, but they could reflect some properties of the initial monooxygenase in the VC-ETH pathway.

Effect of starvation on VC degradation. To determine the response of the VC-assimilating isolates to periods of VC depletion, two representative strains were examined—*Mycobacterium* sp. strain JS60 and *Nocardioides* sp. strain JS614. VC starvation affected these two strains very differently (Fig. 3). Strain JS60 readily recovered from periods of VC starvation of at least 1 week of duration, and the time required for degradation of 150 μmol of VC increased in proportion to the length of the preceding starvation period. In its tolerance of VC starvation, strain JS60 resembled the pseudomonads of Verce et al. (57, 58) more than the *Mycobacterium* sp. strain L1 of Hartmans and de Bont (25), although it is difficult to directly

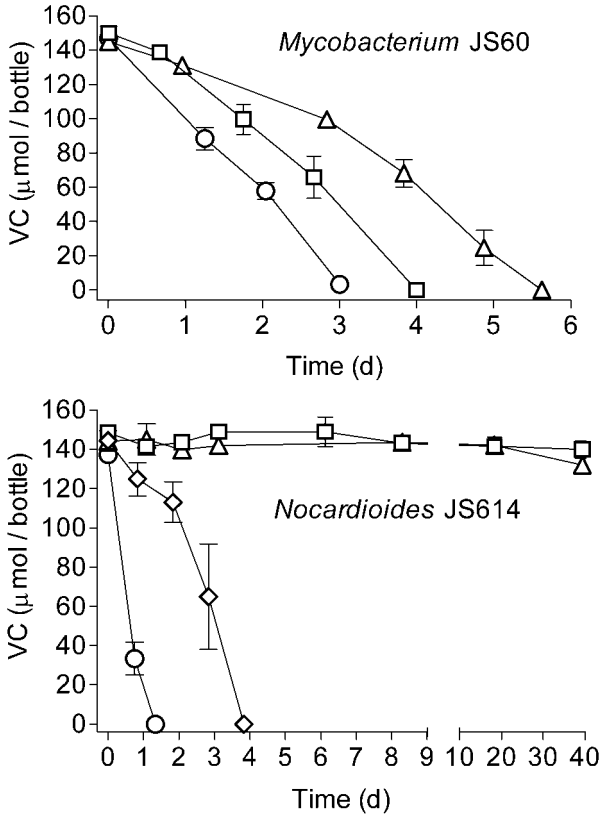

FIG. 3. Effect of VC starvation on VC degradation. Cultures of JS60 and JS614 were grown on VC in 50-ml MSM broths to mid-exponential phase (OD_{600} = 0.2 to 0.3; protein = 30 to 70 μg/ml) until the VC (additions of 2 × 150 μmol) was depleted. The cultures were then incubated for 0, 0.5, 1, or 7 days before readdition of VC (150 μmol = 1.0 mM initial aqueous concentration) and monitoring by GC analysis. ○, no starvation; ◇, 12 h of starvation; □, 1 day of starvation; △, 1 week of starvation. Data are averages of three replicate cultures; error bars represent standard deviations.

compare these starvation experiments due to differences in the experimental conditions (e.g., cell density, temperature, and batch versus continuous culture).

In contrast to JS60, strain JS614 did not recover from periods of VC starvation of 1 day or longer. The sensitivity of JS614 to starvation is also illustrated by the fact that during kinetics experiments, its maximum VC utilization rate was reduced by approximately 50% after less than 5 min of VC starvation (data not shown). The physiological basis of the different responses of strains JS60 and JS614 to VC starvation is unknown. The sensitivity of JS614 could be due to activity of alkene monooxygenase combined with a lack of activity of the epoxide-transforming enzymes, resulting in the accumulation of toxic VC epoxide (25). If these experiments were to be considered representative of the behavior of VC-assimilating strains in the environment, *Nocardioides* VC degraders would be expected to be ineffective in locations where VC is not constantly present while *Mycobacterium* strains would be more robust. It is possible that the sensitivity to VC starvation of *Nocardioides* VC degraders explains the paradox of their apparently limited distribution in the environment (Table 1) despite their impressive growth and kinetic parameters (Table 2).

Testing of ETH degraders for growth on VC. In light of the recent report describing an ETH-assimilating *Pseudomonas* strain that could adapt to growth on VC (58), we decided to investigate whether a similar adaptation can occur in gram-positive bacteria. *Mycobacterium* sp. strain K1 and *Corynebacterium* sp. strain K3, previously isolated from a consortium grown on ETH (34), were tested for their ability to grow on VC (Fig. 4). Strain K3 did not grow on VC, although cells from the same inoculum grew when ETH was used as the carbon source (data not shown). In contrast, strain K1 readily adapted to growth on VC as the sole carbon source, even after growth on nonselective medium. This finding was unexpected, as the consortium that was the source of strain K1 did not grow on VC (34). It is possible that in the present study, the use of a pure culture or the different experimental conditions permitted the growth of strain K1 on VC. Interestingly, the partial 16S rDNA sequence of strain K1 is similar to those of the *M. rhodesiae*-like strains we isolated on VC as the sole carbon source (Fig. 1).

The rapid growth of *Mycobacterium* strain K1 on VC is in contrast to the approximately 40-day lag period seen before an ETH-degrading *Pseudomonas* adapted to growth on VC (58), suggesting that in the case of strain K1, the ETH assimilation pathway functioned equally well for VC assimilation. This finding has significant implications for the natural attenuation of VC, because ETH-assimilating bacteria are likely to be present at chlorinated-ethene-contaminated sites, particularly when some ETH is produced as an end product of the anaerobic respiration of more highly chlorinated ethenes. It remains to be determined what proportion of ETH-assimilating bacteria can also grow on VC—our results with strain K3 and those of a previous study (25) suggest that the ability is not ubiquitous.

Conclusion. Our findings indicate that the bacterial assimilation of VC is an ecologically significant phenomenon of an importance equal to or greater than that of cometabolic VC degradation. Members of a diverse group of *Mycobacterium* strains are capable of growth on VC, and these bacteria are indigenous and widely distributed at chlorinated-ethene-contaminated sites. Based on their distribution, growth rates, and kinetic parameters, we believe that *Mycobacterium* strains are most likely to be responsible for the aerobic natural attenuation of VC that has been observed at many sites. Further characterization of the strains we have isolated will provide a basis for developing molecular methods for detecting VC degraders in the environment and assessing the natural attenuation potential of individual sites. Our VC-assimilating strains may also be useful for enhanced bioremediation by complementing the activities of anaerobic bacteria and providing a mechanism for the complete mineralization of chlorinated ETHs.

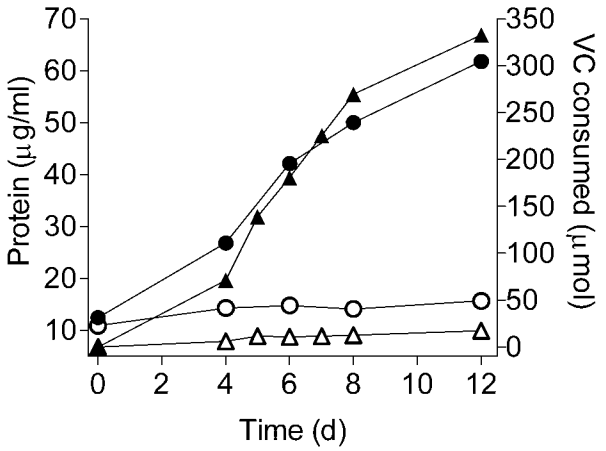

FIG. 4. Testing of ETH-assimilating bacteria for growth on VC as the carbon source. *Mycobacterium* sp. strain K1 and *Corynebacterium* sp. strain K3 (34) were grown on 1/10-TSA–1% glucose plates and inoculated into duplicate 50-ml MSM broth volumes at an initial OD_{600} of 0.10 (protein = 10 to 15 μg/ml). VC was added (150 μmol = 1.0 mM initial aqueous concentration), and the cultures were incubated at 20°C and sampled at intervals to quantify VC and protein. In the case of strain K1, VC was added again (2 × 150 μmol) after the initial amount had been degraded. ▲, VC-strain K1; ●, protein-strain K1; △, VC-strain K3; ○, protein-strain K3. Data are averages of two replicate cultures.

ACKNOWLEDGMENTS

We thank Shirley Nishino for help with sample collection and setup of enrichments and Juli Rubin and Sue Broxson for technical assistance. We are also grateful to the many people who provided information or material from chloroethene-contaminated sites: Petra Koziollek (who also provided strains K1 and K3), Melinda Chambless, Mike Witt, Sandra Dworatzek, Evan Cox, Elizabeth Edwards, Lori Moser, Bella Chu, Jim Clarke, Todd Wiedemeier, Bob Davis, Merv Dale, Scott Glass, Rob Simcik, John Nash, Kandi Brown, and Mike Miracle. This work was funded by the U.S. Strategic Environmental Research and Development Program.

N.V.C. was supported by a postdoctoral fellowship from the Oak Ridge Institute for Science and Education (U.S. Department of Energy).

REFERENCES

1. **Allen, J. R., and S. A. Ensign.** 1997. Purification to homogeneity and reconstitution of the individual components of the epoxide carboxylase multiprotein enzyme complex from *Xanthobacter* strain Py2. J. Biol. Chem. **272:** 32121–32128.
2. **Alvarez-Cohen, L., and P. L. McCarty.** 1991. Effects of toxicity, aeration, and reductant supply on trichloroethylene transformation by a mixed methanotrophic culture. Appl. Environ. Microbiol. **57:**228–235.
3. **Alvarez-Cohen, L., and G. E. Speitel, Jr.** 2001. Kinetics of aerobic cometabolism of chlorinated solvents. Biodegradation **12:**105–126.

4. **Bradley, P. M., and F. H. Chapelle.** 1996. Anaerobic mineralization of vinyl chloride in Fe(III)-reducing aquifer sediments. Environ. Sci. Technol. **30:** 2084–2086.
5. **Bradley, P. M., F. H. Chapelle, and D. R. Lovley.** 1998. Humic acids as electron acceptors for anaerobic microbial oxidation of vinyl chloride and dichloroethene. Appl. Environ. Microbiol. **64:**3102–3105.
6. **Brock, T. D., and M. T. Madigan.** 1991. Biology of microorganisms, 6th ed. p. 121. Prentice-Hall, Englewood Cliffs, N.J.
7. **Bucher, J. R., G. Cooper, J. K. Haseman, C. W. Jameson, M. Longnecker, F. Kamel, R. Maronpot, H. B. Matthews, R. Melnick, R. Newbold, R. W. Tennant, C. Thompson, and M. Waalkes.** 2001. Ninth report on carcinogens. National Toxicology Program, U.S. Dept. of Health and Human Services, Washington, D.C. [Online.] http://ehis.niehs.nih.gov/roc/ninth/known/vinylchloride.pdf.
8. **Casal, M., and J. R. Calero.** 1974. *Mycobacterium gadium* sp. nov., a new species of rapid-growing scotochromogenic mycobacteria. Tubercle **55:**299–308.
9. **Coleman, N. V., T. E. Mattes, J. M. Gossett, and J. C. Spain.** 2002. Biodegradation of *cis*-dichloroethene as the sole carbon source by a β-proteobacterium. Appl. Environ. Microbiol. **68:**2726–2730.
10. **de Bont, J. A. M.** 1976. Oxidation of ethylene by soil bacteria. Antonie Leeuwenhoek **42:**59–71.
11. **de Bont, J. A. M., and W. Harder.** 1978. Metabolism of ethylene by *Mycobacterium* E 20. FEMS Microbiol. Lett. **3:**89–93.
12. **de Bont, J. A. M., M. M. Atwood, S. B. Primrose, and W. Harder.** 1979. Epoxidation of short-chain alkenes in *Mycobacterium* E20: the involvement of a specific monooxygenase. FEMS Microbiol. Lett. **6:**183–188.
13. **de Bruijn, F. J.** 1992. Use of repetitive (repetitive extragenic palindromic and enterobacterial repetitive intergeneric consensus) sequences and the polymerase chain reaction to fingerprint the genomes of *Rhizobium meliloti* isolates and other soil bacteria. Appl. Environ. Microbiol. **58:**2180–2187.
14. **Edwards, E. A., and E. E. Cox.** 1997. Field and laboratory studies of sequential anaerobic-aerobic chlorinated solvent biodegradation, p. 261–265. *In* B. C. Alleman, and A. Leeman, (ed.), In situ and on-site bioremediation, vol. 3. Battelle Press, Columbus, Ohio.
15. **Ensign, S. A., M. R. Hyman, and D. J. Arp.** 1992. Cometabolic degradation of chlorinated alkenes by alkene monooxygenase in a propylene-grown *Xanthobacter* strain. Appl. Environ. Microbiol. **58:**3038–3046.
16. **Ewers, J., D. Freier-Schröder, and H.-J. Knackmuss.** 1990. Selection of trichloroethene (TCE) degrading bacteria that resist inactivation by TCE. Arch. Microbiol. **154:**410–413.
17. **Fennell, D. E., A. B. Carroll, J. M. Gossett, and S. H. Zinder.** 2001. Assessment of indigenous reductive dechlorinating potential at a TCE-contaminated site using microcosms, polymerase chain reaction analysis, and site data. Environ. Sci. Technol. **35:**1830–1839.
18. **Fox, B. G., J. G. Borneman, L. P. Wackett, and J. D. Lipscomb.** 1990. Haloalkene oxidation by the soluble methane monooxygenase from *Methylosinus trichosporium* OB3b: mechanistic and environmental implications. Biochemistry **29:**6419–6427.
19. **Freedman, D. L., and J. M. Gossett.** 1989. Biological reductive dechlorination of tetrachloroethylene and trichloroethylene to ethylene under methanogenic conditions. Appl. Environ. Microbiol. **55:**2144–2151.
20. **Freedman, D. L., and S. D. Herz.** 1996. Use of ethylene and ethane as primary substrates for aerobic cometabolism of vinyl chloride. Water Environ. Res. **68:**320–328.
21. **Friedrich, M., R. J. Grosser, E. A. Kern, W. P. Inskeep, and D. M. Ward.** 2000. Effect of model sorptive phases on phenanthrene biodegradation: molecular analysis of enrichments and isolates suggests selection based on bioavailability. Appl. Environ. Microbiol. **66:**2703–2710.
22. **Gossett, J. M.** 1987. Measurement of Henry's Law constants for C_1 and C_2 chlorinated hydrocarbons. Environ. Sci. Technol. **21:**202–208.
23. **Habets-Crützen, A. Q. H., L. E. S. Brink, C. G. van Ginkel, J. A. M. de Bont, and J. Tramper.** 1984. Production of epoxides from gaseous alkenes by resting-cell suspensions and immobilized cells of alkene-utilizing bacteria. Appl. Microbiol. Biotechnol. **20:**245–250.
24. **Hartmans, S., A. Kaptein, J. Tramper, and J. A. M. de Bont.** 1992. Characterization of a *Mycobacterium* sp. and a *Xanthobacter* sp. for the removal of vinyl chloride and 1,2-dichloroethane from waste gases. Appl. Microbiol. Biotechnol. **37:**796–801.
25. **Hartmans, S., and J. A. M. de Bont.** 1992. Aerobic vinyl chloride metabolism in *Mycobacterium aurum* L1. Appl. Environ. Microbiol. **58:**1220–1226.
26. **Hartmans, S., J. A. M. de Bont, J. Tramper, and K. C. A. M. Luyben.** 1985. Bacterial degradation of vinyl chloride. Biotechnol. Lett. **7:**383–388.
27. **Heath, L. S., G. L. Sloan, and H. E. Heath.** 1986. A simple and generally applicable procedure for releasing DNA from bacterial cells. Appl. Environ. Microbiol. **51:**1138–1140.
28. **Hendrickson, E. R., J. A. Payne, R. M. Young, M. G. Starr, M. P. Perry, S. Fahnestock, D. E. Ellis, and R. C. Ebersole.** 2002. Molecular analysis of *Dehalococcoides* 16S ribosomal DNA from chloroethene-contaminated sites throughout North America and Europe. Appl. Environ. Microbiol. **68:**485–495.
29. **Hohnstock-Ashe, A. M., S. M. Plummer, R. M. Yager, P. Baveye, and E. L. Madsen.** 2001. Further biogeochemical characterization of a trichloroethene-contaminated fractured dolomite aquifer: electron source and microbial communities involved in reductive dechlorination. Environ. Sci. Technol. **35:**4449–4456.
30. **Holliger, C., D. Hahn, H. Harmsen, W. Ludwig, W. Schumacher, B. Tindall, F. Vasquez, N. Weiss, and A. J. Zehnder.** 1998. *Dehalobacter restrictus* gen. nov. and sp. nov., a strictly anaerobic bacterium that reductively dechlorinates tetra- and trichloroethene in an anaerobic respiration. Arch. Microbiol. **169:**313–321.
31. **Kalb, V. F., and R. W. Bernlohr.** 1977. A new spectrophotometric assay for protein in cell extracts. Anal. Biochem. **82:**362–371.
32. **Keppler, F., R. Borchars, J. Pracht, S. Rheinberger, and H. Scholer.** 2002. Natural formation of vinyl chloride in the terrestrial environment. Environ. Sci. Technol. **36:**2479–2483.
33. **Kielhorn, J., C. Melber, U. Wahnschaffe, A. Aitio, and I. Mangelsdorf.** 2000. Vinyl chloride: still a cause for concern. Environ. Health Perspect. **108:**579–588.
34. **Koziollek, P., D. Bryniok, and H.-J. Knackmuss.** 1999. Ethene as an auxiliary substrate for the cooxidation of *cis*-dichloroethene and vinyl chloride. Arch. Microbiol. **172:**240–246.
35. **Krumholz, L. R., R. Sharp, and S. S. Fishbain.** 1996. A freshwater anaerobe coupling acetate oxidation to tetrachloroethylene dehalogenation. Appl. Environ. Microbiol. **62:**4108–4113.
36. **Lee, M. D., J. M. Odom, and R. J. Buchanan, Jr.** 1998. New perspectives on microbial dehalogenation of chlorinated solvents: insights from the field. Annu. Rev. Microbiol. **52:**423–452.
37. **Lorah, M. M., and L. D. Olsen.** 1999. Degradation of 1,1,2,2-tetrachloroethane in a freshwater tidal wetland: field and laboratory evidence. Environ. Sci. Technol. **33:**227–234.
38. **Malachowsky, K. J., T. J. Phelps, A. B. Teboli, D. E. Minnikin, and D. C. White.** 1994. Aerobic mineralization of trichloroethylene, vinyl chloride, and aromatic compounds by *Rhodococcus* species. Appl. Environ. Microbiol. **60:**542–548.
39. **Maymó-Gatell, X., T. Anguish, and S. H. Zinder.** 1999. Reductive dechlorination of chlorinated ethenes and 1,2-dichloroethane by "*Dehalococcoides ethenogenes*" 195. Appl. Environ. Microbiol. **65:**3108–3113.
40. **Maymó-Gatell, X., Y.-T. Chien, J. M. Gossett, and S. H. Zinder.** 1997. Isolation of a bacterium that reductively dechlorinates tetrachloroethene to ethene. Science **276:**1568–1571.
41. **McCarty, P. L.** 1997. Breathing with chlorinated solvents. Science **276:**1521–1522.
42. **Meyers, P. R., W. R. Bourn, L. M. Steyn, P. D. van Helden, A. D. Beyers, and G. D. Brown.** 1998. Novel method for rapid measurement of growth of mycobacteria in detergent-free media. J. Clin. Microbiol. **36:**2752–2754.
43. **Newman, L. M., and L. P. Wackett.** 1997. Trichloroethylene oxidation by purified toluene 2-monooxygenase: products, kinetics, and turnover-dependent inactivation. J. Bacteriol. **179:**90–96.
44. **Pitulle, C., M. Dorsch, J. Kazda, J. Wolters, and E. Stackebrandt.** 1992. Phylogeny of rapidly growing members of the genus *Mycobacterium.* Int. J. Syst. Bacteriol. **42:**337–343.
45. **Sambrook, J., and D. W. Russell.** 2001. Molecular cloning: a laboratory manual, 3rd ed. Cold Spring Harbor Laboratory Press, New York, N.Y.
46. **Schneider, J., R. Grosser, K. Jayasimhulu, W. Xue, and D. Warshawsky.** 1996. Degradation of pyrene, benz[*a*]anthracene, and benzo[*a*]pyrene by *Mycobacterium* sp. strain RJGII-135, isolated from a former coal gasification site. Appl. Environ. Microbiol. **62:** 13–19.
47. **Semprini, L.** 1997. Strategies for the aerobic co-metabolism of chlorinated solvents. Curr. Opin. Biotechnol. **8:**296–308.
48. **Shim, H., D. Ryoo, P. Barbieri, and T. K. Wood.** 2001. Aerobic degradation of mixtures of tetrachloroethylene, trichloroethylene, dichloroethylenes, and vinyl chloride by toluene-*o*-xylene monooxygenase of Pseudomonas stutzeri OX1. Appl. Microbiol. Biotechnol. **56:**265–269.
49. **Squillace, P. J., M. J. Moran, W. W. Lapham, C. V. Price, R. M. Clawges, and J. S. Zogorski.** 1999. Volatile organic compounds in untreated ambient groundwater of the United States, 1985–1995. Environ. Sci. Technol. **33:** 4176–4187.
50. **Stackebrandt, E., and B. M. Goebel.** 1994. A place for DNA-DNA reassociation and 16S rRNA sequence analysis in the present species definition in bacteriology. Int. J. Syst. Bacteriol. **44:**846–849.
51. **Tortoli, E., R. M. Kroppenstedt, A. Bartoloni, G. Caroli, I. Jan, J. Pawlowski, and S. Emler.** 1999. *Mycobacterium tusciae* sp. nov. Int. J. Syst. Bacteriol. **49:**1839–1844.
52. **Tsukamura, M., and S. Mizuno.** 1977. Numerical analysis of relationships among rapidly growing, scotochromogenic mycobacteria. J. Gen. Microbiol. **98:**511–517.
53. **Tsukamura, M., and S. Ichiyama.** 1986. Numerical classification of rapidly growing nonphotochromogenic mycobacteria. Microbiol. Immunol. **30:**863–882.
54. **van der Meer, J. R., C. Werlen, S. F. Nishino, and J. C. Spain.** 1998. Evolution of a pathway for chlorobenzene metabolism leads to natural attenuation in contaminated groundwater. Appl. Environ. Microbiol. **64:**4185–4193.

55. **van Hylckama Vlieg, J. E. T., J. Kingma, A. J. van den Wijngaard, and D. B. Janssen.** 1998. A glutathione *S*-transferase with activity towards *cis*-dichloroepoxyethane is involved in isoprene utilization by *Rhodococcus* sp. strain AD45. Appl. Environ. Microbiol. **64:**2800–2805.
56. **Vannelli, T., M. Logan, D. M. Arciero, and A. B. Hooper.** 1990. Degradation of halogenated aliphatic compounds by the ammonia-oxidizing bacterium *Nitrosomonas europaea.* Appl. Environ. Microbiol. **56:**1169–1171.
57. **Verce, M. F., R. L. Ulrich, and D. L. Freedman.** 2000. Characterization of an isolate that uses vinyl chloride as a growth substrate under aerobic conditions. Appl. Environ. Microbiol. **66:**3535–3542.
58. **Verce, M. F., R. L. Ulrich, and D. L. Freedman.** 2001. Transition from cometabolic to growth-linked biodegradation of vinyl chloride by a *Pseudomonas* sp. isolated on ethene. Environ. Sci. Technol. **35:**4242–4251.
59. **Vogel, T. M., and P. L. McCarty.** 1985. Biotransformation of tetrachloroethylene to trichloroethylene, dichloroethylene, vinyl chloride, and carbon dioxide under methanogenic conditions. Appl. Environ. Microbiol. **49:**1080–1083.
60. **Yagi, O., A. Hashimoto, K. Iwasaki, and M. Nakajima.** 1999. Aerobic degradation of 1,1,1-trichloroethane by *Mycobacterium* spp. isolated from soil. Appl. Environ. Microbiol. **65:**4693–4696.
61. **Yeager, C. M., P. J. Bottomley, and D. J. Arp.** 2001. Cytotoxicity associated with trichloroethylene oxidation in *Burkholderia cepacia* G4. Appl. Environ. Microbiol. **67:**2107–2115.

Appendix B

Coleman, N. V., T. E. Mattes, J. M. Gossett, and J. C. Spain 2002. Biodegradation of *cis*-dichloroethene as the sole carbon source by a beta-proteobacterium. *Appl. Environ. Microbiol.* 68:2726-2730.

APPLIED AND ENVIRONMENTAL MICROBIOLOGY, June 2002, p. 2726–2730 Vol. 68, No. 6
0099-2240/02/$04.00+0 DOI: 10.1128/AEM.68.6.2726–2730.2002

Biodegradation of *cis*-Dichloroethene as the Sole Carbon Source by a β-Proteobacterium

Nicholas V. Coleman,[1] Timothy E. Mattes,[2] James M. Gossett,[2] and Jim C. Spain[1]*

Air Force Research Laboratory–MLQL, Tyndall AFB, Florida 32403,[1] and School of Civil and Environmental Engineering, Cornell University, Ithaca, New York 14853[2]

Received 10 December 2001/Accepted 18 March 2002

An aerobic bacterium capable of growth on *cis*-dichloroethene (cDCE) as a sole carbon and energy source was isolated by enrichment culture. The 16S ribosomal DNA sequence of the isolate (strain JS666) had 97.9% identity to the sequence from *Polaromonas vacuolata*, indicating that the isolate was a β-proteobacterium. At 20°C, strain JS666 grew on cDCE with a minimum doubling time of 73 ± 7 h and a growth yield of 6.1 g of protein/mol of cDCE. Chloride analysis indicated that complete dechlorination of cDCE occurred during growth. The half-velocity constant for cDCE transformation was 1.6 ± 0.2 μM, and the maximum specific substrate utilization rate ranged from 12.6 to 16.8 nmol/min/mg of protein. Resting cells grown on cDCE could transform cDCE, ethene, vinyl chloride, *trans*-dichloroethene, trichloroethene, and 1,2-dichloroethane. Epoxyethane was produced from ethene by cDCE-grown cells, suggesting that an epoxidation reaction is the first step in cDCE degradation.

The extensive use of chloroethenes as solvents and synthetic feedstocks has resulted in widespread environmental contamination (22), which is of concern due to the toxicity and carcinogenicity of such compounds. Microbial metabolism is an important factor in determining the fate of chloroethenes in the biosphere (14). Several anaerobic bacteria use tetrachloroethene (perchloroethene) and trichloroethene (TCE) as electron acceptors, producing *cis*-1,2-dichloroethene (cDCE), vinyl chloride (VC), and ethene as end products (10, 15, 16, 17). Under aerobic conditions, ethene and VC can serve as carbon and energy sources for bacterial growth (3, 8), but thus far, no conclusive evidence exists for aerobic growth on any of the dichloroethenes (*cis*-dichloroethene, *trans*-dichloroethene [tDCE], or 1,1-dichloroethene).

Because cDCE accumulation is often a limiting factor in the biodegradation of chloroethenes in subsurface ecosystems, aerobic bacteria capable of growth on cDCE would provide a crucial missing link in the chain of microbial metabolism for this class of compounds. Thermodynamic calculations suggest that cDCE contains sufficient energy to support aerobic growth (4), and enzymes active on cDCE are known in hydrocarbon-oxidizing bacteria (5, 6, 13, 20, 24, 25). In addition, aerobic oxidation of cDCE to CO_2 has been observed in microcosm and enrichment culture studies (2, 12). Encouraged by the facts described above, we hypothesized that aerobic growth on cDCE was possible and searched at a variety of contaminated sites for microorganisms able to use this compound as a sole source of carbon and energy.

* Corresponding author. Mailing address: Air Force Research Laboratory–MLQL Building 1117, 139 Barnes Dr., Tyndall AFB, FL 32403. Phone: (850) 283-6058. Fax: (850) 283-6090. E-mail: Jim.Spain@tyndall.af.mil.

MATERIALS AND METHODS

Chemicals and media. *cis*-Dichloroethene (97%), tDCE (98%), TCE (99.5%), and 1,2-dichloroethane (1,2-DCA) (99.8%) were obtained from Sigma-Aldrich. VC (99.5%) was obtained from Fluka, and ethene (99.5%) was obtained from Scott. All other chemicals were reagent grade. A minimal salts medium (MSM) based on that of Hartmans et al. (9) was used for enrichment cultures, with the following modifications: the phosphate concentration was reduced to 20 mM, the ammonium concentration was reduced to 10 mM, and the chloride concentration was reduced to 0.02 mM. The pH of MSM was adjusted to 7.0. Trypticase soy agar in which the nutrient content was one-quarter strength (1/4-TSA) (Difco) was used as a nonselective medium; the agar (Difco) concentration was 20 g/liter.

Enrichment cultures. Samples of soil (5%, wt/vol), sediment (5%, wt/vol), granular activated carbon (5%, wt/vol), or groundwater (50%, vol/vol) were mixed with MSM to give a total volume of 50 ml in 160-ml serum bottles (headspace, 110 ml of air), which were crimp sealed with Teflon-faced butyl rubber stoppers (Wheaton). cDCE (3 μl of undiluted liquid) was added as the sole carbon source at a concentration of 40 μmol per bottle (initial aqueous concentration, 0.6 mM). Enrichment cultures were incubated at 20°C with shaking at 150 rpm.

Isolation and identification of strain JS666. Repeated isolation attempts with minimal medium plates containing cDCE were unsuccessful, so an approach based on the dilution-to-extinction principle was adopted. Serial 10-fold dilutions of an enrichment culture (10^{-5} to 10^{-8}) were prepared in triplicate in phosphate buffer, and 100 μl of each dilution was used to inoculate fresh MSM. cDCE was added, and the bottles were incubated as described above for the enrichments. After turbidity appeared in the cultures, samples were spread plated on 1/4-TSA plates, and the purity was evaluated. One resultant isolate (strain JS666) was characterized by standard bacteriological methods (9) and by amplification and sequencing of the 16S rRNA gene (MIDI Labs, Newark, Del.). Clustal-X software (21) was used for sequence alignment and generation of phylogenetic trees.

Growth of strain JS666. Several colonies from a 1/4-TSA plate were inoculated into 50 ml of MSM and grown on cDCE (four 50-μmol additions) until the late exponential phase. The cells were washed twice in phosphate buffer (20 mM, pH 7.0) and suspended in 700 ml of MSM in a 2,240-ml flask (headspace, 1,540 ml of air) that was crimp sealed as described above. cDCE (60 μl) was added to the culture three to five times, with each addition equivalent to 790 μmol of cDCE/flask (initial aqueous concentration, 0.90 mM). The growth substrate range of strain JS666 was investigated by using various compounds as carbon sources (40 μmol/bottle) in 50 ml of MSM. Growth of cultures and transformation of substrates were monitored as described below. All JS666 cultures were grown at 20°C with shaking at 150 rpm.

Substrate range of resting cells. Strain JS666 was grown on either succinate (disodium salt, 20 mM) or cDCE in 700 ml of MSM as described above. Cells were harvested in the exponential phase, washed twice in phosphate buffer, and suspended in 0.2 ml of buffer. The cells were transferred to a 10-ml serum vial, and substrate (3 μmol) was added, either dissolved in 0.8 ml of buffer or added as a gas directly to the headspace. In the latter case, the volume of the suspension was adjusted to 1 ml with buffer. Cells were suspended at an optical density at 600 nm (OD_{600}) of 2.5 to 3.0 (1.1 to 1.4 mg of protein/ml) for the substrate range tests and at an OD_{600} of 15.1 to 15.5 (5.6 to 5.9 mg of protein/ml) for detailed analysis of ethene metabolism. The cell suspension vials were incubated horizontally at 20°C with shaking at 300 rpm. Substrate disappearance and protein concentrations were measured as described below. Abiotic losses (determined with sterile water controls) were subtracted from the observed rates of substrate disappearance before calculation of specific activities.

Kinetic study. An inoculum (4 ml) from a cDCE-grown JS666 culture was transferred to 68 ml of fresh MSM in a 160-ml serum bottle. The culture was allowed to degrade approximately 100 μmol of cDCE in order to produce a sufficient amount of active biomass for kinetic experiments. Three sequential substrate depletion curves were generated at 20°C for the same serum bottle, which was kept inverted at an angle on a rotary shaker with shaking at 165 rpm between the times when headspace samples were removed. Estimates of the maximum specific substrate utilization rate (k) and the half-velocity constant (K_s) for cDCE transformation were obtained from headspace-based cDCE depletion curves. The data were fitted to the Monod model by using the Aquasim software program, as described previously (18, 26), with a diffusive link (19) included to account for the fact that both the liquid and gaseous phases could act as reservoirs of cDCE. The possibility of mass transfer limitation was addressed by constructing a nonequilibrium model with Aquasim, incorporating a mass transfer coefficient ($K_L a$) measured as described previously (21). The depletion curves predicted by the nonequilibrium model coincided with those of the equilibrium model, which demonstrated the adequacy of our phase equilibrium assumption.

Protein was measured at the beginning of the first depletion curve and at the end of each depletion curve. Because of the relatively large amounts of cDCE (7 to 13 μmol) added at the beginning of each sequential depletion curve, biomass increased significantly during the course of the experiment (from 9.1 to 12.6 mg of protein/liter). However, because most of the batch depletion data were gathered near the end of each curve, the change in biomass within each intensive, data-gathering period was relatively small (<2%, as estimated by using the growth yield coefficient which we report here).

Analytical methods. cDCE was analyzed in headspace samples (100 or 250 μl) by gas chromatography with flame ionization detection, and either a capillary column (GSQ; Agilent) or a packed column (10% SP-1000 on 100/120 Supelcoport [Supelco]). Both columns separated cDCE from tDCE, which was present as an impurity in the cDCE source at a concentration of approximately 2%. cDCE was quantified (micromoles per bottle) by comparison to a standard curve derived from known quantities of cDCE in serum bottles with the same gas and liquid volumes as the experimental bottles. For the kinetic studies, cDCE concentrations were converted to micromolar concentrations by methods described previously (7) by using a dimensionless Henry's constant of 0.1232 for cDCE at 20°C.

Protein concentrations were measured with the Micro-BCA reagent (Pierce Chemical Company). Culture fluid (0.9 ml) was mixed with 0.1 ml of 10 M NaOH, heated to 90°C for 10 min to effect cell lysis, and cooled to room temperature, and 1 ml of Micro-BCA working reagent was added. Samples were then incubated at 60°C for 60 min and cooled to room temperature, and the absorbance at 562 nm was read with a spectrophotometer (Hewlett Packard 8452A or Varian Cary 3E). Absorbance values were compared to the values for bovine serum albumin standards treated identically. The growth rate was calculated by fitting an exponential function to the plot of protein versus time. The growth yield was calculated from a linear regression of protein versus amount of cDCE consumed.

Chloride was quantified by the colorimetric method of Bergmann and Sanik (1), which we modified by using 1-ml samples, 0.2 ml of iron reagent, and 0.4 ml of thiocyanate reagent. Cells were removed by centrifugation (16,000 × g, 2 min) before the supernatant was used in the chloride assay.

RESULTS AND DISCUSSION

Despite extended incubation times and the use of inocula (soil, water, sediments) from chloroethene-contaminated sites, only two active cultures were obtained from 18 aerobic enrichments (20°C) initiated with cDCE as the sole carbon source.

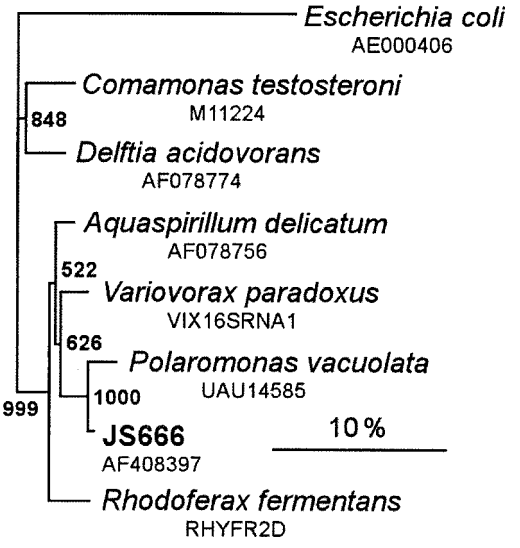

FIG. 1. Phylogeny of strain JS666 based on 16S rRNA gene comparison. GenBank accession numbers are given below the species names. Positions containing gaps or ambiguous nucleotides were removed, leaving sequences consisting of 1,434 bases for analysis. Bootstrap confidence values (from 1,000 neighbor-joining trees) are indicated at the nodes. Bar = 10 inferred nucleotide changes per 100 nucleotides. The consensus tree was rooted by using *Escherichia coli* as the outgroup.

One of the active enrichments was chosen for further study. The inoculum for the culture was granular activated carbon from a pump-and-treat plant (Dortmund, Germany) processing groundwater contaminated with perchloroethene, TCE, and cDCE. Biodegradation of cDCE in the enrichment began after 50 days, and cDCE-degrading activity was subsequently maintained for 7 months in the absence of other carbon sources through 11 transfers (5%, vol/vol) transfers in minimal medium.

A pure culture that grew on cDCE was obtained from serial dilutions of the Dortmund enrichment culture. The cDCE-degrading isolate, strain JS666, is a yellow-pigmented, gram-negative, nonmotile, oxidase-positive, catalase-negative rod. Phylogenetic analysis of the 16S rRNA gene (GenBank accession no. AF408397) indicated that JS666 is a member of the family *Comamonadaceae* in the β-proteobacteria, with 97.9% sequence identity to the Antarctic isolate *Polaromonas vacuolata* (Fig. 1). It is unclear whether JS666 is truly a *Polaromonas* strain due to many phenotypic differences, including differences in motility, the catalase reaction, pigmentation, and the optimum temperature (11). Assignment of strain JS666 to a genus is difficult at present due to the lack of taxonomic data for the isolate and to the uncertain phylogeny of some members of the *Comamonadaceae* (28).

Strain JS666 grew on cDCE as the sole carbon and energy source (Fig. 2). Batch cultures grown on cDCE as the sole carbon source did not reach high optical densities, but protein measurements (Fig. 2, inset) confirmed that growth was coupled to cDCE degradation, with a calculated growth yield of 6.1 ± 0.4 g of protein/mol of cDCE. The doubling time on cDCE calculated from the protein data was 74 ± 8 h at 20°C (data not shown). The growth rate and yield with cDCE are

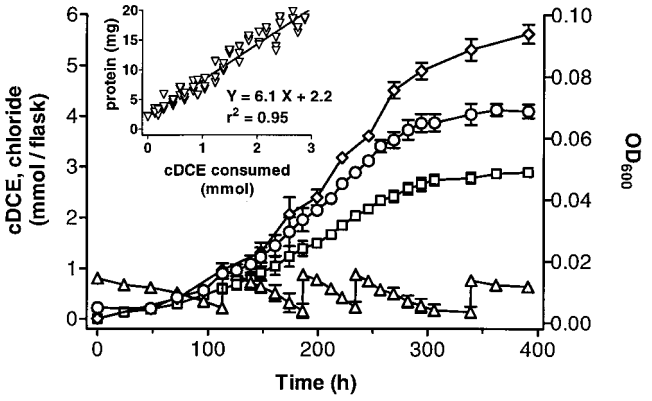

FIG. 2. Growth of strain JS666 on cDCE as the sole carbon and energy source. Symbols: △, cDCE content; □, cumulative amount of cDCE consumed; ○, biomass expressed as OD_{600}; ◇, chloride content. Due to partitioning between the headspace and the liquid phase, cDCE concentrations are expressed in millimoles per flask. The aqueous cDCE concentration after each addition should be 0.9 mM, based on the Henry's constant (7). The data points are averages based on three replicate cultures, and the error bars indicate the standard deviations. (Inset) Growth yield on cDCE calculated from linear regression of the amount of protein (▽) in cultures versus the cumulative amount of cDCE consumed. Individual data points from three replicate cultures are shown. The growth yield indicated by the linear regression is 6.1 ± 0.4 g of protein per mol of cDCE (error based on 95% confidence interval).

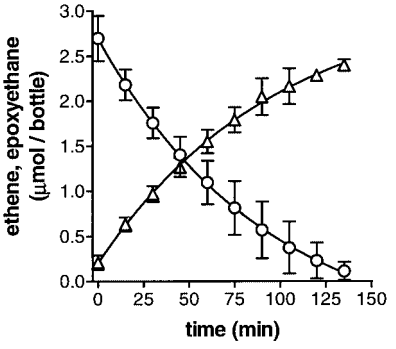

FIG. 3. Production of epoxyethane (△) from ethene (○) by cDCE-grown JS666 cells. Due to partitioning of both compounds between the headspace and the liquid phase, the concentrations are expressed in micromoles per bottle. The data points are averages based on three separate experiments, and the error bars indicate the standard deviations. Epoxyethane was identified by its characteristic gas chromatography retention time.

both lower than corresponding values for growth on 1,2-DCA (23) or VC (8), probably due to the lower incubation temperature used in this study and the lower energy content of cDCE (4).

The stoichiometry of chloride production (Fig. 2) indicates that cDCE was completely dechlorinated (1.94 mol of Cl^- produced/mol of cDCE degraded). There was no detectable growth in JS666 cultures without cDCE, and there was no significant disappearance of cDCE in flasks inoculated with autoclaved cells (data not shown). The pH optimum for growth of strain JS666 on cDCE was 7.2. Growth on cDCE was optimal at temperatures between 20 and 25°C and was not detectable at 30°C. tDCE was present as an impurity (approximately 2%) in the cDCE used in this work, but tDCE was not metabolized during growth on cDCE. In other experiments (data not shown), some of the tDCE impurity was transformed after cDCE was depleted.

Strain JS666 did not grow on tDCE, TCE, VC, 1,2-DCA, or ethene as a carbon source, but cells could transform all these compounds after growth on cDCE (Table 1). The enzymes involved are inducible, as indicated by the lower activity in succinate-grown cells. The ability of cDCE-grown JS666 cells to transform other chloroethenes may prove to be very useful at contaminated sites, where mixtures of pollutants may be encountered (22). It is surprising that strain JS666 did not grow on ethene, which seems to be the most likely natural substrate of the cDCE-degrading enzymes, particularly considering the fact that the VC-assimilating bacteria isolated to date also use ethene as a carbon source (8, 26) and at least in one case appear to have evolved directly from ethene-degrading bacteria (27).

TABLE 1. Activity of cDCE-grown and succinate-grown JS666 cells with chloroethenes, ethene, and 1,2-DCA as substrates

Test substrate	Sp act (nmol/min/mg of protein)	
	cDCE-grown cells	Succinate-grown cells
cDCE	16.8 ± 4.8	0.9 ± 0.6
tDCE	4.0 ± 0.7	0
TCE	5.2 ± 0.9	0.4 ± 0.4
VC	6.6 ± 0.6	1.5 ± 0.7
1,2-DCA	12.5 ± 1.9	1.1 ± 0.8
Ethene	2.9 ± 1.7	0.6 ± 0.7

[a] Data are averages ± standard deviations based on three experiments.

Dense suspensions of cDCE-grown cells oxidized ethene stoichiometrically to epoxyethane (Fig. 3) and also oxidized propene to epoxypropane (data not shown). Succinate-grown cells also catalyzed ethene transformation, but the rate was only 40% of the rate observed with cells grown on cDCE (data not shown). At this time we cannot explain the observed differences in the activity of succinate-grown cells in the epoxyethane accumulation experiment and the substrate range assays (Table 1), although it should be noted that the former experiment was performed with much denser cell suspensions, which may have affected activity.

The ability of JS666 cells to convert ethene to epoxyethane suggests that oxidation of cDCE to the corresponding epoxide is the first step in cDCE biodegradation in strain JS666. cDCE epoxide was not detected when cells were incubated with cDCE, however, which could have been due to further metabolism of the epoxide by the cells. Monooxygenase-catalyzed epoxidations appear to be a universal initial step in the aerobic metabolism of chloroethenes in bacteria (5, 6, 8, 24, 25). Further work will be required to determine rigorously whether strain JS666 uses the same strategy.

The kinetics of cDCE metabolism in strain JS666 at 20°C with continuous agitation were studied by simultaneously fitting depletion curves to three sets of data (Fig. 4). A k of 12.6 ± 0.3 nmol/min/mg of protein and a K_s of 1.6 ± 0.2 μM best fit all three data sets. The k value calculated from depletion curves (Fig. 4) agreed fairly well with the cDCE utilization rate

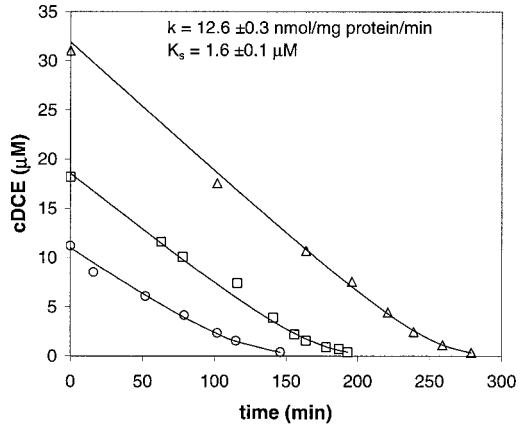

FIG. 4. Three sequential depletion curves for cDCE at 20°C obtained for JS666 (value ± 95% confidence interval). Symbols: ○, experiment 1 measured values; □, experiment 2 measured values; △, experiment 3 measured values. The lines indicate the model-predicted fit.

seen in substrate range assays (Table 1). However, by using the *k* value and growth yield (*Y*) (Fig. 2), a doubling time (ln2/*Yk*) of 150 h was estimated, which is at odds with the doubling time determined directly from protein measurements during growth (74 h). The discrepancy suggests that there was underestimation of *k* in the substrate depletion experiments, probably due to a lower active fraction of protein (i.e., protein measurements probably overestimated the active biomass) under the conditions of the substrate depletion assay compared to cells in exponential-phase cultures. Note that differences in the active fraction of protein would not have affected estimates of K_s.

The relatively low measured K_s value, considered in conjunction with the relatively high *k* value, is significant considering the possible participation of this organism in natural attenuation of cDCE. If JS666 were present and active at a cDCE-contaminated site, the cDCE utilization rate would be one-half the maximum rate at a cDCE concentration of 160 μg/liter. The Environmental Protection Agency-mandated maximum contaminant level for cDCE in drinking water is 70 μg/liter (http://www.epa.gov). Therefore, under appropriate conditions in the field, JS666 should easily be able to oxidize cDCE to obtain levels below drinking water standard levels. Perhaps more relevant is the observation that in the experiments described here, cDCE was degraded routinely to concentrations below 0.03 μg/liter.

The discovery of a bacterium able to grow on cDCE shows that aerobic biodegradation of cDCE in the absence of other carbon substrates is possible. Our results with enrichment cultures indicate that such bacteria appear to be rare and may exist only in highly selective artificial environments, such as the activated carbon filter that was the source of strain JS666. The existence of cDCE-assimilating bacteria suggests that there is potential for bioaugmentation, which could lead to a self-sustaining, low-cost bioremediation strategy at sites where cDCE is a problem contaminant. Our results indicate that growth on cDCE as a carbon source could be a previously unrecognized factor in determining the environmental fate of this compound. Further characterization of JS666 should facilitate the search for similar strains and allow evaluation of the role of such strains in the natural attenuation of cDCE and other chlorinated ethenes.

ACKNOWLEDGMENTS

We thank Petra Koziollek for providing the activated carbon sample. Mike Allen and John Dunlap helped with phenotypic characterization of JS666.

This work was funded by the U.S. Strategic Environmental Research and Development Program. N.V.C. was supported by a postdoctoral fellowship from the Oak Ridge Institute for Science and Education (U.S. Department of Energy).

REFERENCES

1. **Bergmann, J. G., and J. Sanik.** 1957. Determination of trace amounts of chlorine in naphtha. Anal. Chem. **29:**241–243.
2. **Bradley, P. M., and F. H. Chapelle.** 2000. Aerobic microbial mineralization of dichloroethene as sole carbon source. Environ. Sci. Technol. **34:**221–223.
3. **de Bont, J. A. M., and W. Harder.** 1978. Metabolism of ethylene by *Mycobacterium* E 20. FEMS Microbiol. Lett. **3:**89–93.
4. **Dolfing, J., A. J. van den Wijngaard, and D. B. Janssen.** 1993. Microbiological aspects of the removal of chlorinated hydrocarbons from air. Biodegradation **4:**261–282.
5. **Ensign, S. A., M. R Hyman, and D. J. Arp.** 1992. Cometabolic degradation of chlorinated alkenes by alkene monooxygenase in a propylene-grown *Xanthobacter* strain. Appl. Environ. Microbiol. **58:**3038–3046.
6. **Fox, B. G., J. G. Bornemann, L. P. Wackett, and J. D. Lipscomb.** 1990. Haloalkene oxidation by the soluble methane monooxygenase from *Methylosinus trichosporium* OB3b: mechanistic and environmental implications. Biochemistry **29:**6419–6427.
7. **Gossett, J. M.** 1987. Measurement of Henry's Law constants for C_1 and C_2 chlorinated hydrocarbons. Environ. Sci. Technol. **21:**202–208.
8. **Hartmans, S., and J. A. M de Bont.** 1992. Aerobic vinyl chloride metabolism in *Mycobacterium aurum* L1. Appl. Environ. Microbiol. **58:**1220–1226.
9. **Hartmans, S., A. Kaptein, J. Tramper, and J. A. M. de Bont.** 1992. Characterization of a *Mycobacterium* sp. and a *Xanthobacter* sp. for the removal of vinyl chloride and 1,2-dichloroethane from waste gases. Appl. Microbiol. Biotechnol. **37:**796–801.
10. **Holliger, C., D. Hahn, H. Harmsen, W. Ludwig, W. Schumacher, B. Tindall, F. Vazquez, N. Weiss, and A. J. Zehnder** . 1998. *Dehalobacter restrictus* gen. nov. and sp. nov., a strictly anaerobic bacterium that reductively dechlorinates tetra- and trichloroethene in an anaerobic respiration. Arch. Microbiol. **169:**313–321.
11. **Irgens, R. L., J. J. Gosink, and J. T. Staley.** 1996. *Polaromonas vacuolata* gen. nov., sp. nov., a psychrophilic, marine, gas-vacuolate bacterium from Antarctica. Int. J. Syst. Bacteriol. **46:**822–826.
12. **Klier, N. J., R. J. West, and P. A. Donberg.** 1999. Aerobic biodegradation of dichloroethylenes in surface and subsurface soils. Chemosphere **38:**1175–1188.
13. **Koziollek, P., D. Bryniok, and H.-J. Knackmuss.** 1999. Ethene as an auxiliary substrate for the cooxidation of *cis*-dichloroethene and vinyl chloride. Arch. Microbiol. **172:**240–246.
14. **Lee, M. D., J. M. Odom, and R. J. Buchanan, Jr.** 1998. New perspectives on microbial dehalogenation of chlorinated solvents: insights from the field. Annu. Rev. Microbiol. **52:**423–452.
15. **Maymó-Gatell, X., Y. Chien, J. M. Gossett, and S. H. Zinder.** 1997. Isolation of a bacterium that reductively dechlorinates tetrachloroethene to ethene. Science **276:**1568–1571.
16. **Maymó-Gatell, X., I. Nijenhuis, and S. H. Zinder.** 2001. Reductive dechlorination of cis-1,2-dichloroethene and vinyl chloride by "*Dehalococcoides ethenogenes*." Environ. Sci. Technol. **35:**516–521.
17. **Neumann, A., H. Scholz-Murumatsu, and G. Diekert.** 1994. Tetrachloroethene metabolism of *Dehalospirillum multivorans.* Arch. Microbiol. **162:** 295–301.
18. **Reichert, P. R.** 1994. AQUASIM–a tool for simulation and data analysis of aquatic systems. Water Sci. Technol. **2:**21–30.
19. **Reichert, P. R.** 1998. AQUASIM 2.0–user manual. Swiss Federal Institute for Environmental Science and Technology. Dubendorf, Switzerland.
20. **Semprini, L.** 1997. Strategies for the aerobic co-metabolism of chlorinated solvents. Curr. Opin. Biotechnol. **8:**296–308.
21. **Smatlak, C. R.** 1995. Comparative kinetics of H_2 utilization for dechlorination of tetrachloroethene and methanogenesis by an anaerobic enrichment culture. M.S. thesis. Cornell University, Ithaca, N.Y.
22. **Squillace, P. J., M. J. Moran, W. W. Lapham, C. V. Price, R. M. Clawges, and J. S. Zogorski.** 1999. Volatile organic compounds in untreated ambient groundwater of the United States, 1985–1995. Environ. Sci. Technol. **33:** 4176–4187.
23. **van den Wijngaard, A. J., R. D. Wind, and D. B. Janssen.** 1993. Kinetics of bacterial growth on chlorinated aliphatic compounds. Appl. Environ. Microbiol. **59:**2041–2048.

24. **van Hylckama Vlieg, J. E. T., J. Kingma, A. J. van den Wijngaard, and D. B. Janssen.** 1998. A glutathione *S*-transferase with activity towards *cis*-dichloroepoxyethane is involved in isoprene utilization by *Rhodococcus* sp. strain AD45. Appl. Environ. Microbiol. **64:**2800–2805.
25. **van Hylckama Vlieg, J. E. T., W. de Koning, and D. B. Janssen.** 1996. Transformation kinetics of chlorinated ethenes by *Methylosinus trichosporium* OB3b and detection of unstable epoxides by on-line gas chromatography. Appl. Environ. Microbiol. **62:**3304–3312.
26. **Verce, M. F., R. L. Ulrich, and D. L. Freedman.** 2000. Characterization of an isolate that uses vinyl chloride as a growth substrate under aerobic conditions. Appl. Environ. Microbiol. **66:**3535–3542.
27. **Verce, M. F., R. L. Ulrich, and D. L. Freedman.** 2001. Transition from cometabolic to growth-linked biodegradation of vinyl chloride by a *Pseudomonas* sp. isolated on ethene. Environ. Sci. Technol. **35:**4242–4251.
28. **Wen, A., M. Fegan, C. Hayward, S. Chakraborty, and L. I. Sly.** 1999. Phylogenetic relationships among members of the *Comamonadaceae*, and description of *Delftia acidovorans* (den Dooren de Jong 1926 and Tamaoka *et al.* 1987) gen. nov., comb. nov. Int. J. Syst. Bacteriol. **49:**567–576.

Appendix C

Coleman, N. V., and J. C. Spain 2003. Epoxyalkane:Coenzyme-M transferase in the ethene and vinyl-chloride biodegradation pathways of *Mycobacterium* strain JS60. *J. Bacteriol.* 185: 5536-5545.

JOURNAL OF BACTERIOLOGY, Sept. 2003, p. 5536–5545 Vol. 185, No. 18
0021-9193/03/$08.00+0 DOI: 10.1128/JB.185.18.5536–5545.2003

Epoxyalkane:Coenzyme M Transferase in the Ethene and Vinyl Chloride Biodegradation Pathways of *Mycobacterium* Strain JS60

Nicholas V. Coleman† and Jim C. Spain*

Air Force Research Laboratory-MLQL, Tyndall AFB, Florida 32403

Received 7 April 2003/Accepted 3 July 2003

Mycobacterium **strains that grow on ethene and vinyl chloride (VC) are widely distributed in the environment and are potentially useful for biocatalysis and bioremediation. The catabolic pathway of alkene assimilation in mycobacteria is not well characterized. It is clear that the initial step is a monooxygenase-mediated epoxidation that produces epoxyethane from ethene and chlorooxirane from VC, but the enzymes involved in subsequent transformation of the epoxides have not been identified. We investigated epoxyethane metabolism in *Mycobacterium* strain JS60 and discovered a coenzyme M (CoM)-dependent enzyme activity in extracts from VC- and ethene-grown cells. PCR amplifications using primers targeted at epoxyalkane:CoM transferase (EaCoMT) genes yielded part of the JS60 EaCoMT gene, which was used to clone an 8.4-kb genomic DNA fragment. The complete EaCoMT gene (*etnE*) was recovered, along with genes (*etnABCD*) encoding a four-component monooxygenase and two genes possibly involved in acyl-CoA ester metabolism. Reverse transcription-PCR indicated that the *etnE* and *etnA* genes were cotranscribed and inducible by ethene and VC. Heterologous expression of the *etnE* gene in *Mycobacterium smegmatis* mc^{2}155 using the pMV261 vector gave a recombinant strain capable of transforming epoxyethane, epoxypropane, and chlorooxirane. A metabolite identified by mass spectrometry as 2-hydroxyethyl-CoM was produced from epoxyethane. The results indicate that the EaCoMT and monooxygenase enzymes encoded by a single operon (*etnEABCD*) catalyze the initial reactions in both the VC and ethene assimilation pathways. CoM-mediated reactions appear to be more widespread in bacteria than was previously believed.**

Ethene and vinyl chloride (VC) are important industrial chemicals and are also produced naturally by abiotic (22) and biosynthetic (14, 53) reactions. Anaerobic bacteria such as *Dehalococcoides* spp. produce VC and ethene during dehalorespiration of the chlorinated solvents perchloroethene and trichloroethene (29, 30), thus VC and/or ethene can accumulate in anaerobic subsurface zones at contaminated sites (12, 56). Monooxygenases, such as liver cytochrome P-450 (16, 44), oxidize VC and ethene to highly reactive epoxides that pose potential health risks. Whereas uncertainty exists concerning the dangers of low-level ethene exposure (43), VC is known to be a human carcinogen (23).

Mycobacterium strains capable of aerobic growth on ethene as the sole carbon and energy source were first isolated almost 30 years ago (8). More recently, strains of *Mycobacterium* (7, 18), *Nocardioides* (7), and *Pseudomonas* (50, 51) capable of growth on both ethene and VC have been discovered. The VC- and ethene-assimilating bacteria may be useful for the bioremediation of sites contaminated with chlorinated solvents (38). In addition, several ethene-assimilating strains have been evaluated as biocatalysts for the production of epoxides (17, 46). Much research has focused on the kinetics of VC and ethene oxidation and on the cometabolism of related substrates (7, 24, 49), while fundamental questions concerning the catabolic pathways and enzymes involved have been somewhat neglected. The biochemical traits that distinguish bacteria that grow on both substrates from those that grow on ethene alone are unknown, as are most of the metabolic intermediates in both pathways.

In bacteria, the initial enzymatic attack on VC and ethene is similar to the reactions observed in mammalian systems, i.e., a monooxygenase catalyzes the formation of epoxyethane (ethylene oxide) from ethene and the formation of chlorooxirane (VC epoxide) from VC (18, 50). The ethene monooxygenase from *Mycobacterium* strain E3 has been examined in some detail (19) and is a multicomponent enzyme, most likely with a binuclear iron active site similar to those of methane and propene monooxygenases (13, 39). The reductase component of the monooxygenase from strain E3 has been purified (55), but the other monooxygenase components have not been characterized. None of the genes encoding VC or ethene monooxygenases have been cloned or sequenced.

Epoxide metabolism in the VC and ethene catabolic pathways has been investigated in a few cases, but the results are inconclusive. Early work with the ethene-assimilating *Mycobacterium* strain E20 (10) suggested the involvement of a coenzyme A (CoA)- and NAD^+-dependent enzyme that converted epoxyethane into acetyl-CoA, but the specific activities reported were very low (approximately 2 nmol/min/mg of protein). This "epoxyethane dehydrogenase" activity was also detected in the VC-assimilating *Mycobacterium* strain L1 (18), but further investigations in that case were hampered by the

* Corresponding author. Mailing address: Air Force Research Laboratory-MLQL, Bldg. 1117, 139 Barnes Dr., Tyndall AFB, FL 32403. Phone: (850) 283-6058. Fax: (850) 283-6090. E-mail: Jim.Spain@tyndall.af.mil.

† Present address: School of Molecular and Microbial Biosciences, University of Sydney, NSW, 2006, Australia.

TABLE 1. Bacterial strains, plasmids, and oligonucleotides

Material	Relevant characteristics	Reference or Source
Strains		
Mycobacterium rhodesiae JS60	Grows on VC and ethene as sole carbon sources	7
Mycobacterium smegmatis mc^{2}155	Highly electrotransformable derivative of ATCC 607	40
Escherichia coli JM109	*recA1 supE44 endA1 hsdR17 gyrA96 relA1 thi* Δ(*lac-proAB*) F′[*traD36 proAB*$^+$ *lacI*^{q} *lacZ* ΔM15]	58
Plasmids		
pK18	Km^r, 2.7 kb, general purpose cloning vector	34
pGEM-T Easy	Ap^r, 3.0 kb, T/A cloning vector	Promega
pMV261	Km^r, 4.5 kb, *E. coli-Mycobacterium* shuttle vector	41
pMV-CoM	Km^r, 5.8 kb, pMV261 carrying JS60 EaCoMT gene (*etnE*)	This study
Oligonucleotides (5′-3′)		
CoM-F1	ATGGTGGGGAACTACCCGAATCC	This study
CoM-R1	ATGAGGCCGCAGTCGGTGGACA	This study
CoM-F1L	AACTACCCSAAYCCSCGCTGGTACGAC	This study
CoM-R2	TCGTCGGCAGTTTCGGTGATCGTGCTCTT	This study
60M-F2	GGGGATATCAGTGATCGCCATACAGCAATTAAGGAG	This study
60M-R2	GGGAAGCTTTTGTGTCCGGACAGGCCGATAGTC	This study
RTM-F1	AAGGAGTGCATCATGAAGGTTGGGG	This study
RTβ-R1	TTGGCTGATACCGGGTCGAGGTTGAG	This study

instability of the activity in cell extracts and because of practical difficulties in working with chlorooxirane.

Various other bacterial enzymes can transform epoxides, and such alternative reactions must also be considered with respect to epoxyethane and chlorooxirane metabolism. Epoxide hydrolases play a role in many biodegradative pathways, including those involving chlorinated aliphatic compounds. The epichlorohydrin hydrolase from *Agrobacterium* strain AD1 is the best-studied example (35). Glutathione *S*-transferase (GST) enzymes are also widely distributed among bacteria. Notably, the GST from the isoprene degrader *Rhodococcus* strain AD45 can transform *cis*-dichloroepoxyethane (48), a substrate similar to the epoxides of VC and ethene. In the propene-assimilating bacteria *Xanthobacter* strain Py2 and *Rhodococcus* strain B-276, an epoxide carboxylase enzyme complex catalyzes the conversion of epoxypropane into acetoacetate. This unusual system consists of epoxyalkane:CoM transferase (EaCoMT), two stereoselective dehydrogenases, and an oxidoreductase-carboxylase (11).

The aim of the present study was to investigate the initial reactions of the VC and ethene assimilation pathways in *Mycobacterium* strain JS60, a bacterium previously isolated from groundwater (7). In particular, our focus was on determining the mechanism of epoxide metabolism.

MATERIALS AND METHODS

Chemicals, enzymes, and media. Most chemicals and media were described previously (7). CoM (98%), CoA (95%), NAD (98%), glutathione (98%), epoxyethane (99.5%), and epoxypropane (99%) were from Sigma-Aldrich. All molecular biology enzymes were from Roche except for DNase-free RNase, which was from Qiagen. MSM minimal medium (7) or 1/10-strength trypticase-soy medium with 1% glucose (7) was used for growing *Mycobacterium* strain JS60. MSM medium was modified by increasing the phosphate concentration to 40 mM and decreasing the pH to 6.5. Luria-Bertani (LB) medium (37) was used for both *Escherichia coli* strain JM109 and *Mycobacterium* strain mc^{2}155. Transformants of JM109 were plated on LB containing kanamycin (Km; 50 μg/ml) or ampicillin (Ap; 100 μg/ml). 5-Bromo-4-chloro-3-indolyl-β-d-galactopyranoside (X-Gal) and isopropyl-β-D-thiogalactopyranoside (IPTG) (37) were added where required. Transformants of mc^{2}155 were plated on LB with 20 μg of Km/ml or grown in LB broths containing 10 μg of Km/ml and 0.05% Tween 80. Strain mc^{2}155(pMV-CoM) was grown in LB-Tween-Km medium containing 0.1 mM $ZnSO_4$.

Plasmids, bacterial strains, and incubation conditions. Plasmids and bacterial strains used in this study are described in Table 1. Strain JS60 was grown in 50 or 700 ml of MSM medium in crimp-sealed flasks (7). VC was added at 2% (vol/vol) of the total flask volume and resupplied as necessary. Ethene was added once at 10% (vol/vol), and potassium acetate was added at 20 mM. *Mycobacterium* strains JS60 and mc^{2}155 were grown at 30°C; *E. coli* strain JM109 was grown at 37°C. All cultures were incubated aerobically with shaking at 200 rpm.

General analytical methods. VC, ethene, epoxyethane, and epoxypropane were analyzed in headspace samples (250 μl) by gas chromatography (HP 5890 series II) on a megabore capillary column (GSQ; Agilent) with flame-ionization detection. The growth of cultures was followed by measurement of the optical density at 600 nm (OD_{600}). Protein concentrations in cell extracts were measured by a UV absorbance assay, as described previously (7) but omitting the lysis and neutralization steps. Chloride was analyzed as described previously (6).

Preparation of cell extracts. Cultures of JS60 cells were grown to early exponential phase (OD_{600} = 0.2 to 0.3) in MSM with VC, ethene, or acetate as carbon sources. Tween 80 was added to 0.05%, and the cells were harvested by centrifugation, washed in buffer (20 mM K_2HPO_4, 0.05% Tween 80; pH 7.0), and suspended in 2 ml of morpholinepropanesulfonic acid (MOPS)-glycerol-dithiothreitol (DTT) buffer (3). The cells were broken by three passages through a chilled French pressure cell (130,000 kPa), and the lysate was centrifuged (16,000 × *g* for 15 min). The supernatant was retained and diluted to 2.0 mg of protein/ml in the same buffer.

EaCoMT assay. Serum bottles (25 ml) containing 900 μl of Tris-HCl (50 mM; pH 8.0) and 50 μl of CoM (200 mM) were crimp sealed. Epoxyethane (5 μmol) was added, and the bottles were incubated at 30°C with shaking at 300 rpm. After 15 min, cell extract (50 μl) was added, and after a further 5 min of equilibration headspace samples were analyzed at intervals to quantify epoxyethane. Specific activity was calculated as nanomoles of epoxyethane consumed per minute per milligram of protein.

DNA extraction, PCR, and T/A cloning. Extraction of genomic DNA from strain JS60 was performed essentially as described previously (7), except that ethene-grown cultures (700 ml) were used and ampicillin (200 μg/ml) was included with glycine in the overnight incubation. Plasmid extraction from *E. coli* strains was done by alkaline lysis (37). A Qiaquick kit (Qiagen) was used for purification of plasmid DNA and PCR products, while the Qiaex II kit (Qiagen) was used for the purification of genomic DNA fragments. PCR mixtures (25 μl) contained 1.5 mM Mg^{2+}, 50 pmol of each primer, 2.5 U of *Taq* polymerase, and 5 to 50 ng of template DNA. Primers used in this work are listed in Table 1. Unless indicated otherwise, the thermocycling protocol was 95°C for 2 min, then

30 cycles of 94°C (30 s), 60°C (30 s), and 72°C (1 min), followed by a final extension cycle (72°C, 10 min). In initial PCR experiments with JS60, the primers CoM-F1 and CoM-R1 were used. A band of the expected size (981 bp) was excised from the gel, purified, ligated to the pGEM-T-Easy vector (Promega), and introduced into strain JM109 by electroporation. Recombinant clones were screened by restriction digestion, and several representatives containing inserts of the expected size were sequenced (Roswell Park Cancer Institute Biopolymer Facility; PE-ABI model 373A Stretch sequencer).

Southern blotting and construction of clone library. Restriction digests (80 μl) containing 10 to 15 μg of JS60 genomic DNA and 60 to 80 U of restriction enzyme were incubated for 16 h at 37°C. After gel electrophoresis, Southern blotting was done according to standard methods (37), using the ECL kit (Pharmacia) for detection. The probe consisted of an 893-bp fragment of the EaCoMT gene of strain JS60, amplified by PCR using the primers CoM-F1L and CoM-R2. For clone library construction, *Nhe*I restriction digests were repeated at a five-fold-larger scale and DNA fragments (7 to 10 kb) were excised, purified, and ligated to *Xba*I-cut, phosphatase-treated pK18 vector. The ligation mixture was electroporated into strain JM109, which was plated on LB–Km–X-Gal–IPTG medium.

Screening of clone library. Recombinant JM109(pK18) clones (480 white colonies) were transferred to five microtiter plates containing LB-Km broth (100 μl), and the plates were incubated with shaking overnight. Cultures (30 μl) from eight wells of a microtiter plate were pooled and centrifuged (16,000 × *g*, 1 min), and the cells were suspended in 200 μl of Tris-HCl buffer (5 mM; pH 8.0), yielding 60 clone pools. Each cell suspension was heat treated (95°C, 5 min) and centrifuged (16,000 × *g*, 2 min), and then 1 μl of the supernatant was used in PCR amplifications with the CoM-F1L and CoM-R2 primers, as described above. Individual cultures from pools containing positive clones were subsequently screened by a similar method, except that the template was 1 μl of culture from each well. Several positive clones were analyzed by restriction digestion, and the insert DNA (8.4 kb) from one representative was sequenced on both strands.

RNA extraction and RT-PCR. Cultures of strain JS60 were grown on VC, ethene, or acetate to mid-exponential phase. The cells were washed in TE buffer (37), suspended in the same buffer (OD_{600} = 30), and frozen in 500-μl aliquots at −80°C. The RNeasy kit (Qiagen) was used for RNA extraction, with modifications as follows. Cells from one frozen aliquot were thawed, pelleted, suspended in 500 μl of buffer RLT, and added to a 2-ml screw-cap tube containing 1.5 ml of buffer RLT-saturated zirconia-silica beads (0.1-mm diameter). The mixture was subjected to beadbeating (Mini-Beadbeater; BioSpec Products) for 1 min at high speed. The supernatant (350 μl) was column purified according to the RNeasy protocol for bacteria, and the eluate was treated with DNase (30 U; 15 min; 20°C) and then repurified using the RNeasy protocol for RNA cleanup. The final RNA solutions were diluted to 5 ng/μl in water, and 2 μl of each was used for reverse transcription-PCR (RT-PCR) with the Titan One-Tube kit (Roche). Thermocycling was done with the RTM-F1 and RTβ-R1 primers, with annealing at 60°C (30 s), extension at 68°C (2 min), and other parameters according to the kit instructions. Negative controls (no reverse transcriptase) were prepared with Expand DNA polymerase mixture, and a positive control contained JS60 DNA (1 ng) instead of RNA.

Construction of *Mycobacterium* strain mc^{2}155(pMV-CoM). The JS60 EaCoMT gene *etnE* was amplified using the primers 60 M-F2 and 60 M-R2. The product (1.3 kb) was digested with *Eco*RV and *Hin*dIII, ligated into *Pvu*II-*Hin*dIII-digested pMV261, and electroporated into strain JM109. The recombinant plasmid was designated pMV-CoM. Electrocompetent cells of *Mycobacterium* strain mc^{2}155 were prepared essentially as described previously (21). Competent mc^{2}155 cells (100 μl) were electroporated with plasmid pMV-CoM, recovered for 4 h with shaking in 1 ml of LB-Tween broth, and plated on LB-Km medium. Clones were screened by PCR with the 60 M-F2 and 60 M-R2 primers, using as the template 1 μl of cell lysate obtained from beadbeating a loopful of cells in 500 μl of Tris-HCl (5 mM; pH 8.0). The size of the plasmid in one PCR-positive clone was checked by electroporating 1 μl of beadbeater lysate into JM109, followed by plasmid extraction and restriction digestion. One clone, designated mc^{2}155(pMV-CoM), was used for subsequent experiments. A transformant of mc^{2}155 containing the pMV261 vector without insert DNA was prepared by similar methods for use as a negative control.

Expression of JS60 EaCoMT in strain mc^{2}155(pMV-CoM). *Mycobacterium* strain mc^{2}155(pMV-CoM) and mc^{2}155(pMV261) cultures were grown in LB-Tween-Km-Zn medium to an OD_{600} of 1.0 to 1.5, and EaCoMT expression was induced by heat shock (45°C for 30 min). Cell lysis and EaCoMT assays were as described above for JS60, except that 0.5% Tween was added to the lysis buffer. The protein concentration in the extracts was standardized to 3.0 to 3.5 mg/ml unless indicated otherwise. The activities of mc^{2}155(pMV-CoM) and mc^{2}155 (pMV261) extracts with epoxypropane were assayed by similar methods.

Chlorooxirane transformation by cell extracts. Chlorooxirane was synthesized by photochlorination of epoxyethane with *tert*-butyl hypochlorite (16, 20, 32, 52). Liquid epoxyethane (20 ml) and *tert*-butyl hypochlorite (1 ml) were reacted under N_2 at 0°C for 45 min, illuminated by a 150 W incandescent bulb. Epoxyethane was removed by sparging with N_2 at room temperature for 10 min. The resultant mixture of chlorooxirane and *tert*-butyl alcohol was diluted in anhydrous tetrahydrofuran (THF) and used immediately. Reactions were set up in crimp-sealed 10-ml bottles containing 755 μl of Tris-acetate buffer (50 mM; pH 8), 200 μl of cell extract [13 mg of protein/ml, from either mc^{2}155(pMV-CoM) or mc^{2}155(pMV261)], 20 μl of CoM (0.2 M), and 25 μl of chlorooxirane (12 mM in THF), with magnetic stirring. A control containing only Tris-acetate buffer (775 μl), MOPS-glycerol-DTT buffer (200 μl), and chlorooxirane (25 μl) was also included. The assays were conducted at 20°C to slow the rate of reactions and allow reasonable sampling times. At appropriate intervals, samples of the reaction mixtures (100 μl) were added to 4-(*p*-nitrobenzyl)pyridine reagent (500 μl) (16), and after 5 min triethylamine reagent (400 μl) (16) was added. The absorbance at 550 nm was measured, and the chlorooxirane concentration was calculated using the molar extinction coefficient (ε = 14,300 M/cm at 550 nm [5]).

Analysis of metabolites by MS. Cell extract (12 mg of protein in 2 ml) from strain mc^{2}155(pMV-CoM) was added to dialysis tubing (15-kDa cutoff) and dialyzed overnight at 4°C in 500 ml of MOPS-glycerol-DTT buffer. Dialyzed extract (50 μl) was added to crimp-sealed 25-ml serum bottles containing ammonium acetate (900 μl; 50 mM; pH 8.0) and CoM (50 μl; 200 mM). Epoxyethane (360 μl; 15 μmol) was added, and the bottles were incubated at 30°C with shaking at 300 rpm. At intervals, reaction mixtures were added to chilled prerinsed filters (5-kDa cutoff; Ultrafree-MC; Sigma) and centrifuged (5,000 × *g*; 20 min; 0°C). The eluates were injected directly into an LCQ Advantage mass spectrometer (Thermo Finnigan) operated in negative ionization electrospray injection mode. Tandem mass spectrometry (MS-MS) analysis was performed on the *m/z* 141 and 185 parent ions to determine their fragmentation patterns. Metabolites produced by extracts of mc^{2}155(pMV261) cultures and in abiotic controls (no cell extract) were analyzed by similar methods.

RESULTS

Growth of *Mycobacterium* strain JS60 on VC and ethene. Near-stoichiometric production of inorganic chloride from VC (0.95 mol/mol) occurred during growth of strain JS60 on VC as the sole carbon source (Fig. 1B). Ethene was clearly a better substrate than VC in terms of both growth rate and growth yield (Fig. 1A). The maximum specific substrate utilization rates of whole cells calculated from the growth rates (Fig. 1) and growth yields (7) were 118 nmol/min/mg of protein (ethene) and 44 nmol/min/mg of protein (VC). The increases in growth rates and substrate utilization rates compared to those reported previously (7) are most likely due to optimization of culture conditions (the temperature was increased from 20 to 30°C, and the pH was decreased from 7.0 to 6.5).

Epoxyethane metabolism in cell extracts. Various cofactors were tested for the ability to stimulate epoxyethane metabolism in extracts of ethene-grown *Mycobacterium* strain JS60. There was no significant loss of epoxyethane in the absence of cofactors (Fig. 2), and neither glutathione (48) nor a combination of NAD^+ and CoA (10) stimulated activity under the assay conditions used (data not shown). Epoxyethane metabolism was rapid when CoM (2-mercaptoethanesulfonate) was added to cell extracts (Fig. 2), suggesting the presence of an EaCoMT enzyme (4). The specific activities of EaCoMT in extracts from VC-grown, ethene-grown, and acetate-grown cells were calculated to be 980 ± 50, 990 ± 60, and 0 ± 50 nmol/min/mg of protein (errors from 95% confidence intervals of linear regressions in Fig. 2) after the abiotic rate of epoxyethane loss was subtracted (13 ± 2 nmol/min in Tris buffer

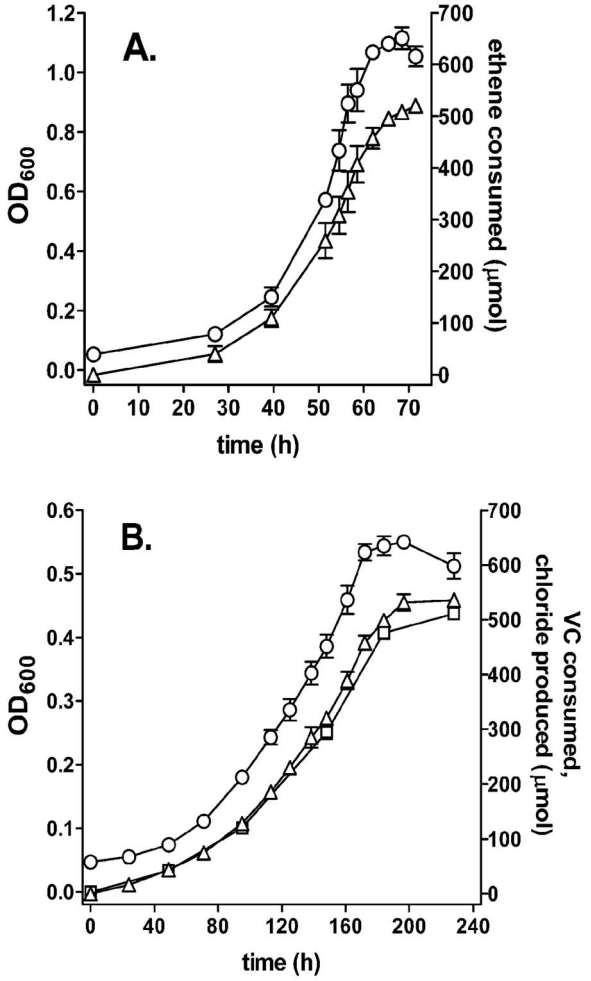

FIG. 1. Growth of *Mycobacterium* strain JS60 on ethene (A) and VC (B) as sole carbon and energy sources. ○, biomass measured as OD_{600}; Δ, cumulative amount of substrate consumed; □, cumulative amount of chloride produced. Growth rates (0.080 h^{-1} with ethene, 0.017 h^{-1} with VC) were calculated by plotting an exponential curve through a subset of the OD_{600} data (results not shown). The inoculum for both experiments was a frozen stock of washed, VC-grown cells. Data are averages of three replicates, and error bars are the standard deviations.

with CoM [data not shown]). The EaCoMT activity in extracts was an order of magnitude higher than the alkene oxidation rates calculated for whole cells (above), and it is more than sufficient to account for the measured growth rates on VC and ethene. The high EaCoMT activity in cell extracts is probably due in part to the high concentrations of reduced CoM and epoxyethane available to the enzyme under the assay conditions.

Cloning of the EaCoMT gene from strain JS60. PCR primers (CoM-F1 and CoM-R1) based on conserved regions of the EaCoMT genes of *Xanthobacter* strain Py2 (X79863) and *Rhodococcus* strain B-276 (AF426826) yielded several products in PCR amplifications with JS60 DNA. A major product at the expected size (981 bp) had very high sequence identity to the EaCoMT gene from strain B-276. Improved primers (CoM-F1L and CoM-R2) yielded a single strong EaCoMT

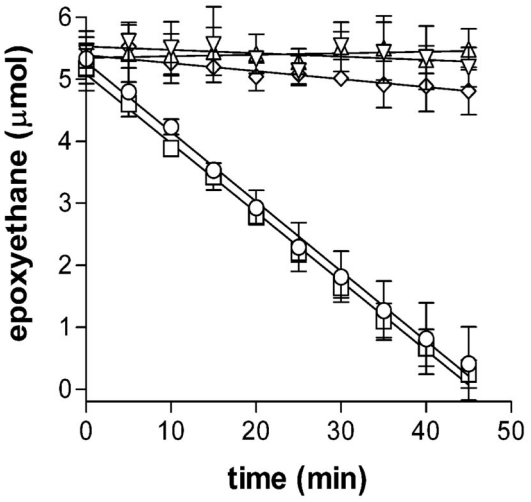

FIG. 2. Effect of CoM on epoxyethane metabolism in JS60 cell extracts. ○, ethene-grown cell extract with CoM; □, VC-grown cell extract with CoM; ◇, acetate-grown cell extract with CoM; ▽, ethene-grown cell extract with no cofactor; Δ, VC-grown cell extract with no cofactor. Data are the averages of three independent experiments, and error bars are the standard deviations.

PCR product (893 bp), which was subsequently used as a probe in Southern blotting experiments. Genomic DNA from JS60 digested with enzymes that did not cut within the 893-bp sequence (*Pst*I, *Kpn*I, *Nsi*I, *Sph*I, and *Nhe*I) gave one hybridizing band in all cases (data not shown), indicating that a single EaCoMT allele was present. The *Nhe*I fragment (8.4 kb) was cloned into *E. coli* strain JM109 using the pK18 vector, positive clones were detected by PCR screening, and the insert DNA from one representative clone (E4H) was sequenced.

Sequence analysis of the JS60 EaCoMT gene and flanking DNA. The *Nhe*I fragment of JS60 DNA (8,364 bp) (GenBank accession number AY243034) had an overall GC content of 59%, which is slightly lower than typical for *Mycobacterium* (54). Seven open reading frames (ORFs), the first and last of which were incomplete, were identified on one strand of the DNA (Fig. 3). Five of the ORFs started with ATG, one started with TTG, and all were preceded by plausible ribosome binding sites. Two genes possibly involved in acyl-CoA ester metabolism (ORF1 and ORF2) were located upstream of the EaCoMT gene, while genes likely to encode a four-component monooxygenase were located downstream (Table 2).

The monooxygenase genes were similar in sequence and identical in arrangement to the propene monooxygenase genes

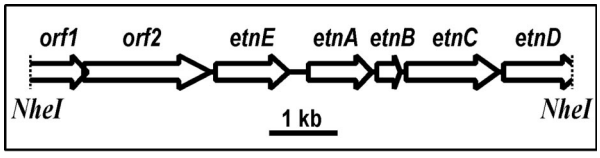

FIG. 3. Schematic diagram of genes on the 8,364-bp *Nhe*I restriction fragment cloned from *Mycobacterium* strain JS60. *orf1* and *orf2* are likely to be involved in acyl-CoA ester metabolism, *etnE* encodes an EaCoMT, and the *etnABCD* genes encode a putative four-component alkene monooxygenase.

TABLE 2. Gene products of the *etn* locus: predicted functions and database similarities

ORF	Position in sequence (nucleotides)	Predicted molecular mass (Da)	Predicted function	Similar protein	Organism	Amino acid identity (%)	Protein accession no.
ORF1[a]	0–795	28,767	CoA transferase	GctB	*Acidaminococcus fermentans*	29.9	Q59112
				CatJ	*Pseudomonas* strain B13	27.8	AAL02406
ORF2	783–2771	70,192	Acyl-CoA synthetase	CAA10043	*Pseudomonas mendocina* strain 35	30.4	CAA10043
				FerA	*Sphingomonas* strain SYK6	28.3	BAB86294
etnE	2887–3996	40,928	EaCoMT	AAL28081	*Rhodococcus* strain B-276	71.3	AAL28081
				XecA	*Xanthobacter* strain Py2	47.3	CAA56241
etnA	4315–5367	39,732	Monooxygenase β-subunit	AmoA	*Rhodococcus* strain B-276	39.1	D37875
				ThmB	*Pseudonocardia* strain K1	31.6	CAC10509
etnB	5391–5720	12,334	Monooxygenase coupling-effector protein	AmoB	*Rhodococcus* strain B-276	50.8	D37875
				MmoB	*Methylocystis* strain WI14	28.3	AAF01270
etnC	5767–7269	56,926	Monooxygenase α-subunit	AmoC	*Rhodococcus* strain B-276	59.4	BAA07114
				MmoX	*Methylosinus* strain OB3b	35.1	P27353
etnD[a]	7389–8364	35,149	Monooxygenase reductase	AmoD	*Rhodococcus* strain B-276	41.8	BAA07115
				DmpP	*Pseudomonas* strain CF600	40.4	P19734

[a] Incomplete ORF.

(*amoABCD*) of *Rhodococcus* strain B-276. The sequence similarity, inducibility by VC and ethene (see below), and proximity to a gene involved in epoxyethane and chlorooxirane metabolism (see below) provide strong evidence that the four genes encode the VC-ethene monooxygenase of JS60. Due to the likelihood that ethene rather than VC was the original substrate of the putative monooxygenase, we designated the genes *etnABCD*. Because the JS60 EaCoMT gene was functional in epoxide metabolism and cotranscribed with at least *etnA* (see below), it was designated *etnE*.

Sequence alignment (data not shown) of the EtnC gene product with α-subunit components from methane (MmoX), propene (AmoC, XamoA), butane (BmoX), isoprene (IsoA), THF (ThmA), benzene (BmoA), phenol (DmpN), and toluene (TomA3) monooxygenases confirmed the presence of four conserved glutamate residues and two conserved histidine residues involved in binding nonheme iron atoms at the active site (15, 36, 39, 59). The sequence comparison therefore indicates that the JS60 ethene-VC monooxygenase is a binuclear iron enzyme. The National Center for Biotechnology Information conserved domain database (CDD) detected the presence of binding sites for FAD, NAD, and a 2Fe-2S iron-sulfur cluster in the EtnD gene product, as would be expected for a monooxygenase reductase (28, 55).

A sequence alignment of the EaCoMTs from JS60, Py2, and B-276 (Fig. 4) emphasized the high similarity of these enzymes, particularly those from JS60 and B-276. The His-X-Cys-X_n-Cys motif involved in zinc binding in the Py2 EaCoMT enzyme (26) and in the more distantly related methionine synthases and methanogenic CoM transferases (60) is conserved in the

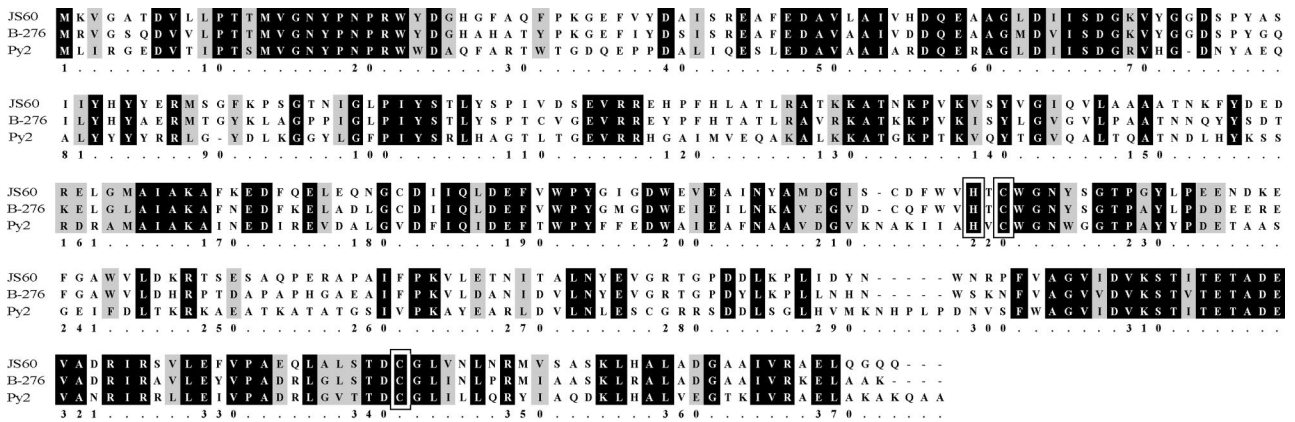

FIG. 4. Sequence alignment of EaCoMT proteins from *Mycobacterium* strain JS60, *Rhodococcus* strain B-276, and *Xanthobacter* strain Py2. Identical residues are shaded black, while similar residues are shaded gray. The conserved histidine (220) and cysteine (222, 343) residues likely to be involved in zinc binding are boxed.

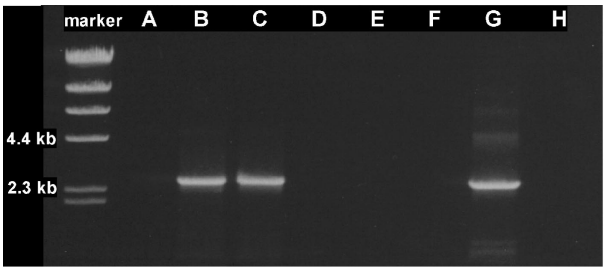

FIG. 5. RT-PCR analysis of *etnEA* expression in strain JS60. Lanes: A, acetate-grown cells; B, VC-grown cells; C, ethene-grown cells; D, acetate-grown cells (no RT); E, VC-grown cells (no RT); F, ethene-grown cells (no RT); G, DNA template; H, no template.

EaCoMT from strain JS60, which suggests that this enzyme also possesses a zinc cofactor.

RT-PCR of *etn* locus genes. Primers (RTM-F1 and RTβ-R1) were designed to amplify a 2.5-kb region of the *etn* locus from the start of the EaCoMT gene *etnE* to the end of the putative monooxygenase β-subunit gene *etnA*. A product of the expected size was seen in RT-PCRs with RNA extracted from VC- or ethene-grown JS60 cultures, whereas no products were seen in reactions using RNA from acetate-grown JS60 cultures (Fig. 5). Negative controls lacking reverse transcriptase gave no detectable products, indicating that the amplicons observed in RT-PCRs were derived from RNA and not DNA. The results indicate that the *etnE* and *etnA* genes are cotranscribed and are inducible by ethene and VC.

Heterologous expression of the JS60 EaCoMT gene. Based on the work of Krum and Ensign with the EaCoMT from *Xanthobacter* strain Py2 (25), we initially attempted to express the JS60 EaCoMT gene *etnE* in *E. coli* by using a T7-based expression system [pET-21a vector, C43(DE3) host], but the experiments were unsuccessful (data not shown). We hypothesized that heterologous expression in a more closely related host strain might be more successful and, therefore, we cloned the *etnE* gene into *Mycobacterium smegmatis* mc^{2}155 (40) under the control of the *hsp60* promoter in the pMV261 vector (41). Good EaCoMT activity was obtained in cell extracts of the recombinant strain, designated mc^{2}155(pMV-CoM).

In contrast to previously published work (41), we observed better expression of the cloned gene (increase in specific activity of approximately 30% [data not shown]) in extracts from mc^{2}155(pMV-CoM) cultures that were heat shocked (45°C, 30 min) before harvest, and therefore cell extracts from heat-shocked cultures were used for all subsequent work. Our results indicate that the *hsp* promoter in the pMV261 vector is partially inducible above a basal constitutive expression level. The EaCoMT activity in mc^{2}155(pMV-CoM) cell extracts with epoxyethane as a substrate (Table 3) was 62% of the activity in cell extracts of JS60 (Fig. 2). Epoxypropane was also transformed by mc^{2}155(pMV-CoM) cell extracts, although the specific activity was only 23% of that seen with epoxyethane. Apart from the slow abiotic reaction between epoxide and CoM, no significant transformation of epoxyethane or epoxypropane was seen in cell extracts of strain mc^{2}155 (pMV261), confirming that the EaCoMT activities were due to expression of the cloned JS60 *etnE* gene. EaCoMT-like genes were not found in BLAST searches of the in-progress genome sequence of *M. smegmatis* strain mc^{2}155.

TABLE 3. EaCoMT activity in cell extracts of strains mc^{2}155(pMV-CoM) and mc^{2}155(pMV261)

Substrate	EaCoMT activity (nmol/min/mg of protein)[a,b] (*n*)	
	mc^{2}155(pMV-CoM)	mc^{2}155(pMV261)
Epoxyethane	615 ± 98 (6)	12 ± 20 (3)
Epoxypropane	143 ± 23 (4)	1 ± 3 (4)

[a] Averages and standard deviations derived from several independent experiments.

[b] Activities calculated from substrate depletion rate, after subtraction of abiotic rates of substrate loss in controls without cell extract. The abiotic rates of epoxyethane and epoxypropane loss were 13 ± 2 and 12 ± 2 nmol/min, respectively.

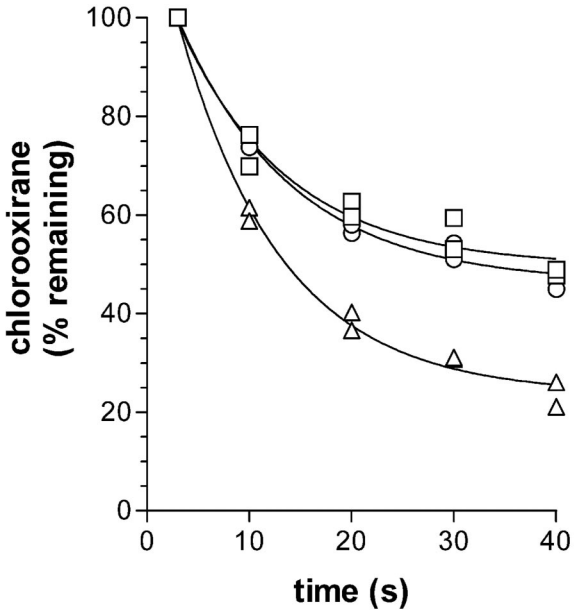

FIG. 6. Chlorooxirane transformation in cell extract reactions. ○, buffer alone; □, buffer, CoM, and cell extract from strain mc^{2}155(pMV261); Δ, buffer, CoM, and cell extract from strain mc^{2}155(pMV-CoM). Data from two experiments are shown. Chlorooxirane was quantified by the absorbance (550 nm) of its 4-(*p*-nitrobenzyl)pyridine adduct. Initial concentrations of chlorooxirane in the assays ranged from 0.2 to 0.3 mM.

Chlorooxirane metabolism in cell extracts. Transformation of chlorooxirane was more extensive, and the initial rate more rapid, in reactions containing strain mc^{2}155(pMV-CoM) extracts than in reactions containing strain mc^{2}155(pMV261) extracts or buffer alone (Fig. 6). Based on the data between 3 and 20 s, the enzyme-catalyzed rate of reaction was calculated to be 57 nmol/min/mg of protein at 20°C. This specific activity should be considered an approximation, due to both the nonlinearity of the data and the very high rate of abiotic chlorooxirane decomposition. Although much lower than the activity with epoxyethane (Fig. 2), the EaCoMT activity with chlorooxirane is sufficient to account for VC oxidation (10 nmol/min/mg of protein in whole cells at 20°C [7]), which would be essential to avoid any accumulation of the highly reactive chlorooxirane in the cells. The reason for the incomplete metabolism of

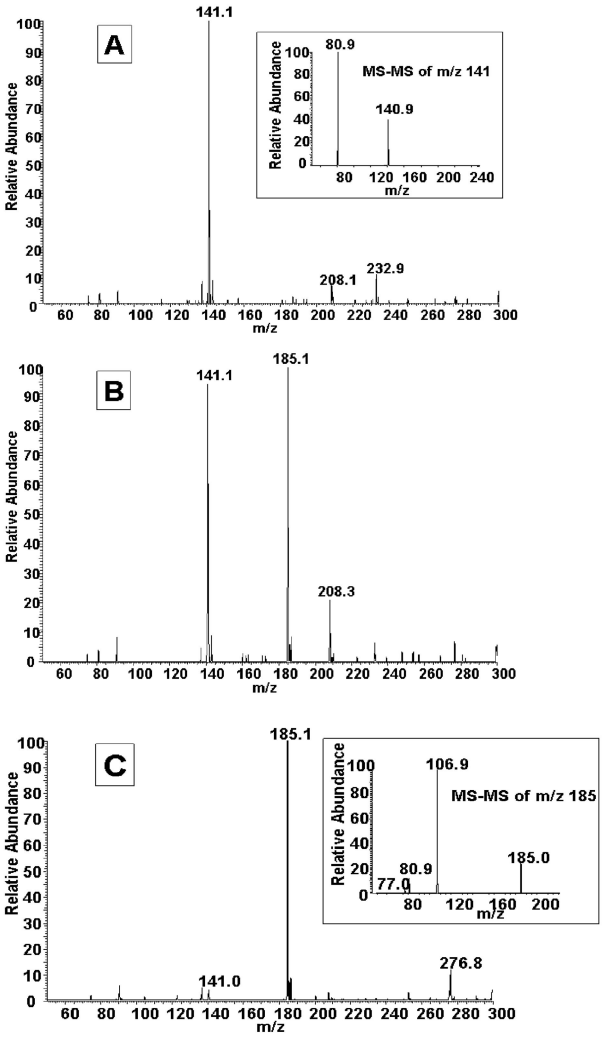

FIG. 7. MS analysis of metabolites formed from epoxyethane during EaCoMT reaction. (A) Zero time sample; (B) 30-min sample; (C) 1-h sample.

chlorooxirane in the assay is unknown. CoM was present in 10-fold excess and, thus, is not expected to be limiting. Either a high K_m or inactivation of the EaCoMT enzyme by chlorooxirane could be responsible. Respiking of chlorooxirane or desalting of the mixture and repeating the assay would distinguish between these possibilities. In combination with the results from JS60 cell extracts (Fig. 2) and RT-PCR (Fig. 5), the results indicate that the JS60 EaCoMT enzyme, EtnE, can catalyze the transformation of chlorooxirane in addition to epoxyethane and thus plays a role in both the ethene and VC catabolic pathways.

Analysis of metabolites produced from epoxyethane. Reactions between CoM and epoxyethane were analyzed by MS (Fig. 7), using dialyzed cell extracts from strain mc^{2}155(pMV-CoM) assayed in ammonium acetate buffer. Under these conditions, the EaCoMT activity was approximately 75% of that seen with undialyzed extracts in Tris buffer (data not shown). A strong peak at *m/z* 141 that yielded a fragment ion at *m/z* 81 was present at the start of the reactions. The spectrum matched that of a CoM standard, and thus *m/z* 141 and *m/z* 81 are probably HS-CH_2-CH_2-SO_3^- and HSO_3^-, respectively. After 1 h, the *m/z* 141 peak was almost undetectable and a peak at *m/z* 185 was dominant. Based on analogy with the CoM adduct in the propene assimilation pathway (4), the *m/z* 185 ion is consistent with 2-hydroxyethyl-CoM (HO-CH_2-CH_2-S-CH_2-CH_2-SO_3^-). The proposed structure is supported by the fragmentation pattern, assuming that *m/z* 77 is HO-CH_2-CH_2-S^-, *m/z* 81 is HSO_3^-, and *m/z* 107 is CH_2═CH-SO_3^-. Several minor peaks also appeared during the course of the EaCoMT reaction. The ion at *m/z* 208 could be derived from MOPS buffer. The peaks at *m/z* 233 and 277 are possibly glycerol adducts (sulfonate esters) of *m/z* 141 and 185, respectively.

The *m/z* 185 ion did not appear in reactions when either CoM or epoxyethane was omitted, but it was seen in reactions containing cell extract from strain mc^{2}155(pMV261) and also in abiotic reactions containing only buffer, CoM, and epoxyethane (data not shown). In these latter two cases, the intensity of the *m/z* 185 ion after 1 h of incubation was approximately 10% of that observed with cell extract from strain mc^{2}155(pMV-CoM). The data suggest that the JS60 EaCoMT enzyme increases the rate of a reaction that also occurs spontaneously between epoxyethane and CoM.

DISCUSSION

We have conclusively determined the mechanism responsible for bacterial epoxyethane metabolism, and we obtained strong circumstantial evidence that the same mechanism is also involved in chlorooxirane metabolism. Three lines of investigation support the latter conclusion: the JS60 *etnE* gene was expressed in response to both VC and ethene; there were equal levels of EaCoMT activity in extracts from VC- and ethene-grown JS60 cells; and chlorooxirane was transformed more rapidly by cell extracts of strain mc^{2}155(pMV-CoM) than of strain mc^{2}155(pMV261). Our finding of EaCoMT in strain JS60 adds *Mycobacterium* to the small group of eubacterial genera (*Xanthobacter*, *Rhodococcus*) thus far known to use CoM in catabolic reactions (25). The fact that *Mycobacterium* strain JS60 contains an active EaCoMT enzyme and grows on alkenes in minimal medium indicates that the strain can biosynthesize CoM, although we did not obtain direct evidence of this.

Our results suggest answers to questions raised by earlier studies on epoxyethane metabolism in other *Mycobacterium* strains. It is likely that CoM is the unknown heat-stable, dialyzable cofactor that was required for epoxyethane metabolism in cell extracts of *Mycobacterium* strain E20 (10). The authors of that study noted that only extracts from ethene-grown cells contained the stimulatory cofactor, which agrees with the more recent finding of inducible CoM biosynthesis in *Xanthobacter* strain Py2 and *Rhodococcus* strain B-276 (25). It is also possible that EaCoMT is responsible for epoxyethane metabolism in the dibromoethane-degrading *Mycobacterium* strain GP1 (33), which is phylogenetically similar to strain JS60. In strain GP1, epoxyethane is produced from 2-bromoethanol through the action of a haloalcohol dehalogenase, but the mechanism of subsequent epoxyethane transformation was not elucidated.

Early experiments with ethene- and VC-assimilating mycobacteria indicated that epoxyethane metabolism was depen-

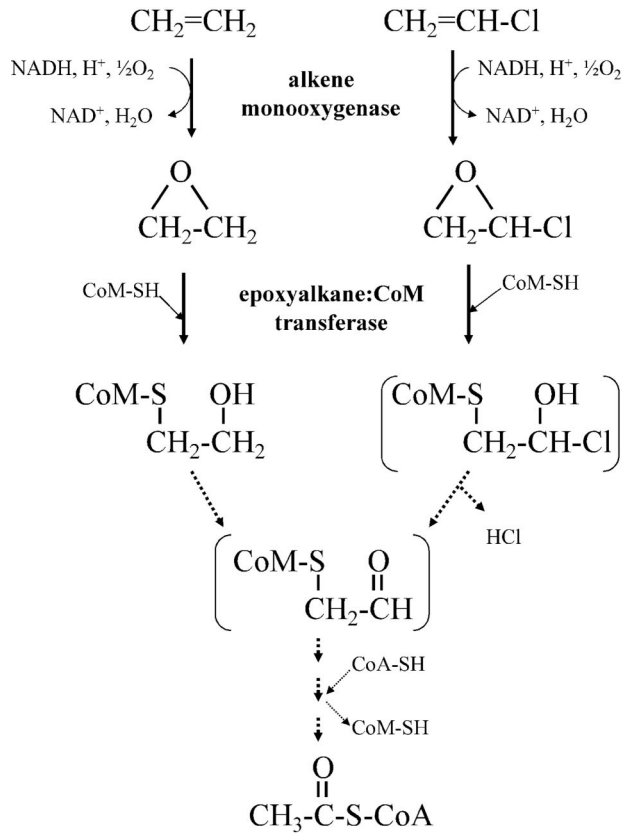

FIG. 8. Proposed pathways of VC and ethene assimilation in *Mycobacterium* strains. Intermediates that have not been identified are in brackets, and hypothetical reactions are indicated by dotted lines.

dent on NAD and CoA (10, 18). Although we saw no evidence of a requirement for such cofactors, our reaction conditions were very different in that they contained an exogenous supply of CoM, 10- to 50-fold less protein, and 10- to 50-fold more epoxyethane. Different strains of alkene-utilizing mycobacteria could possess different mechanisms of epoxide metabolism, but based on preliminary results from several other strains (unpublished data) we believe this is unlikely. NAD and CoA could play a role in the downstream reactions of the ethene pathway, e.g., in regenerating the reduced form of CoM. In our reactions that contained an excess of CoM, recycling of the cofactor would not be expected to affect the initial reaction rate, unlike in earlier studies where CoM would have been extremely rate limiting.

The JS60 EaCoMT accepted epoxypropane as a substrate, although the strain does not grow on propene (data not shown). The activities of the EaCoMTs from the propene-oxidizing strains with epoxyethane have not been reported, but such activity might be expected at least in strain Py2, which can grow (albeit slowly) on ethene as a carbon source (45). The amino acid identity (71.3%) between the EaCoMTs of strains JS60 and B-276 was much higher than that between the Py2 and B-276 enzymes (49.2%). This is unusual in light of the fact that the enzymes from Py2 and B-276 are both part of a propene assimilation pathway, whereas the JS60 enzyme is part of an ethene and VC assimilation pathway. It appears that, in this case, the similarity of the catabolic enzymes was better predicted by the phylogeny of the strains than by the substrates of the pathways. The correspondence between JS60 and B-276 held also for the alkene monooxygenase genes in terms of gene sequence and gene organization. The alkene monooxygenases of strains JS60 and B-276 are both more similar to each other than to anything else currently in GenBank.

Strong evidence that we have identified the VC-ethene monooxygenase genes comes from the sequence and operon similarity of *etnABCD* to the strain B-276 propene monooxygenase (*amoABCD*), the expression of *etnA* in response to growth on ethene and VC, and the cotranscription of *etnA* with the EaCoMT gene *etnE*. We attempted to express the *etnABC* genes with the pMV261/mc^{2}155 cloning system, but we did not detect any activity against ethene (data not shown). This failure could be due to the need for a monooxygenase reductase in addition to the alpha, beta, and coupling protein components (*etnD* was incomplete in the DNA fragment we cloned). It is conceivable that additional monooxygenase genes are found downstream of *etnABCD*, but based on the high sequence similarity and identical gene organization of the JS60 and B-276 systems we believe that the JS60 monooxygenase is a four-component enzyme.

The genetic organization of the *etn* locus in strain JS60 was considerably different from that of the alkene catabolic genes of *Xanthobacter* strain Py2 (27). In JS60, the EaCoMT gene *etnE* is located upstream of the alkene monooxygenase genes *etnABCD*, and it is cotranscribed with at least *etnA*. In contrast, the Py2 EaCoMT gene *xecA* is in an operon with the other three components of the epoxide carboxylase complex, and it is not immediately adjacent to the alkene monooxygenase genes. The organization of the *etn* locus in JS60 is more reminiscent of the isoprene gene cluster of *Rhodococcus* strain AD45 (47), where the GST gene *isoI* responsible for epoxide metabolism is just upstream of the alkene monooxygenase genes *isoABC DEF*. However, in strain AD45 a transcriptional terminator is present between the GST and monooxygenase genes, unlike in JS60, where transcription of the alkene monooxygenase and EaCoMT genes appears to be coupled.

We found no evidence for epoxide carboxylase genes (1, 2) near the *etnE* gene of strain JS60, but we did not attempt to find such genes elsewhere in the genome or assay for the corresponding enzyme activities. Based on the propene assimilation pathway determined by Ensign (11), the most likely product of a carboxylase reaction with 2-hydroxyethyl–CoM would be malonate semialdehyde, which can readily support bacterial growth (31, 57). Downstream metabolism in the VC and ethene pathways most likely occurs via acetyl-CoA, based on the results of previous work with *Mycobacterium* strain E20 (9, 10). Similar fluoroacetate inhibition effects to those reported in strain E20 were also seen in strain JS60 (i.e., epoxide accumulation in resting cell assays [data not shown]). Clues to the metabolic intermediates between 2-hydroxyethyl–CoM and acetyl-CoA may be found in the genes (*orf1*, *orf2*) upstream of the JS60 EaCoMT gene. The products of these two genes are similar to CoA transferase and acyl-CoA synthetase, respectively, and thus it is plausible that ORF1 and ORF2 transfer the alkene-derived two-carbon unit from CoM to CoA.

Our enzyme assays and RT-PCR experiments indicate that the alkene monooxygenase and EaCoMT enzymes of strain

JS60 are active in both the VC and ethene assimilation pathways. The point at which the two pathways converge is unclear at present: of key importance is the mechanism and timing of chloride release in the VC pathway. Several different metabolites could result from the nucleophilic attack of CoM on chlorooxirane. Consideration of metabolic economy leads us to believe that 2-chloro-2-hydroxyethyl–CoM is most likely, because it could spontaneously eliminate HCl (42) to give an aldehyde that could readily feed into the ethene assimilation pathway. VC and ethene catabolic pathways consistent with our results are shown in Fig. 8.

The cloning and sequencing of EaCoMT and alkene monooxygenase genes reported in the present study provide a foundation for the development of DNA-based methods of detecting VC- and ethene-assimilating mycobacteria in the environment. Such methods would be invaluable for monitoring natural attenuation and bioaugmentation processes at chlorinated-ethene-contaminated sites. The alkene monooxygenase and EaCoMT of *Mycobacterium* strain JS60 could also have applications in biocatalysis, for example in the stereoselective synthesis of epoxides.

ACKNOWLEDGMENTS

We thank Torin Weisbrod and Bill Jacobs for supplying pMV261 and mc^{2}155. F. P. Guengerich advised on chlorooxirane synthesis. Heather Luckarift and Lloyd Nadeau assisted with MS analyses. George Paoli and Glenn Johnson are thanked for stimulating discussions on molecular biology.

This work was funded by the U.S. Strategic Environmental Research and Development Program. N.V.C. was supported by a postdoctoral fellowship from the Oak Ridge Institute for Science and Education (U.S. Department of Energy).

REFERENCES

1. **Allen, J. R., and S. A. Ensign.** 1997. Characterization of three protein components required for functional reconstitution of the epoxide carboxylase multienzyme complex from *Xanthobacter* strain Py2. J. Bacteriol. **179:** 3110–3115.
2. **Allen, J. R., and S. A. Ensign.** 1998. Identification and characterization of epoxide carboxylase activity in cell extracts of *Nocardia corallina* B276. J. Bacteriol. **180:**2072–2078.
3. **Allen, J. R., and S. A. Ensign.** 1997. Purification to homogeneity and reconstitution of the individual components of the epoxide carboxylase multiprotein enzyme complex from *Xanthobacter* strain Py2. J. Biol. Chem. **272:** 32121–32128.
4. **Allen, J. R., D. D. Clark, J. G. Krum, and S. A. Ensign.** 1999. A role for coenzyme M (2-mercaptoethanesulfonic acid) in a bacterial pathway of aliphatic epoxide carboxylation. Proc. Natl. Acad. Sci. USA **96:**8432–8437.
5. **Barbin, A., J.-C. Bériziat, A. Croisy, I. K. O'Neill, and H. Bartsch.** 1990. Nucleophilic selectivity and reaction kinetics of chloroethylene oxide assessed by the 4-(*p*-nitrobenzyl)pyridine assay and proton nuclear magnetic resonance spectroscopy. Chem. Biol. Interact. **73:**261–277.
6. **Coleman, N. V., T. E. Mattes, J. M. Gossett, and J. C. Spain.** 2002. Biodegradation of *cis*-dichloroethene as the sole carbon source by a beta-proteobacterium. Appl. Environ. Microbiol. **68:**2726–2730.
7. **Coleman, N. V., T. E. Mattes, J. M. Gossett, and J. C. Spain.** 2002. Phylogenetic and kinetic diversity of aerobic vinyl chloride-assimilating bacteria from contaminated sites. Appl. Environ. Microbiol. **68:**6162–6171.
8. **de Bont, J. A. M.** 1976. Oxidation of ethylene by soil bacteria. Antonie Leeuwenhoek **42:**59–71.
9. **de Bont, J. A. M., and R. A. J. M. Albers.** 1976. Microbial metabolism of ethylene. Antonie Leeuwenhoek **42:**73–80.
10. **de Bont, J. A. M., and W. Harder.** 1978. Metabolism of ethylene by *Mycobacterium* E 20. FEMS Microbiol. Lett. **3:**89–93.
11. **Ensign, S. A.** 2001. Microbial metabolism of aliphatic alkenes. Biochemistry **40:**5845–5853.
12. **Fennell, D. E., A. B. Carroll, J. M. Gossett, and S. H. Zinder.** 2001. Assessment of indigenous reductive dechlorinating potential at a TCE-contaminated site using microcosms, polymerase chain reaction analysis, and site data. Environ. Sci. Technol. **35:**1830–1839.
13. **Fox, B. G., W. A. Froland, J. E. Dege, and J. D. Lipscomb.** 1989. Methane monooxygenase from *Methylosinus trichosporium* OB3b. Purification and properties of a three-component system with high specific activity from a type II methanotroph. J. Biol. Chem. **264:**10023–10033.
14. **Fukuda, H., T. Ogawa, and S. Tanase.** 1993. Ethylene production by microorganisms. Adv. Microb. Physiol. **35:**275–306.
15. **Gallagher, S. C., R. Cammack, and H. Dalton.** 1997. Alkene monooxygenase from *Nocardia corallina* B-276 is a member of the class of dinuclear iron proteins capable of stereospecific epoxygenation reactions. Eur. J. Biochem. **247:**635–641.
16. **Guengerich, F. P., W. M. Crawford, Jr., and P. G. Watanabe.** 1979. Activation of vinyl chloride to covalently bound metabolites: roles of 2-chloroethylene oxide and 2-chloroacetaldeyhde. Biochemistry **18:**5177–5182.
17. **Habets-Crützen, A. Q. H., L. E. S. Brink, C. G. van Ginkel, J. A. M. de Bont, and J. Tramper.** 1984. Production of epoxides from gaseous alkenes by resting-cell suspensions and immobilized cells of alkene-utilizing bacteria. Appl. Microbiol. Biotechnol. **20:**245–250.
18. **Hartmans, S., and J. A. M. de Bont.** 1992. Aerobic vinyl chloride metabolism in *Mycobacterium aurum* L1. Appl. Environ. Microbiol. **58:**1220–1226.
19. **Hartmans, S., F. J. Weber, D. P. M. Somhorst, and J. A. M. de Bont.** 1991. Alkene monooxygenase from *Mycobacterium*: a multicomponent enzyme. J. Gen. Microbiol. **137:**2555–2560.
20. **Holt, S., T. Y. Yen, R. Sangaiah, and J. A. Swenberg.** 1998. Detection of 1,N^6-ethenoadenine in rat urine after chloroethylene oxide exposure. Carcinogenesis **19:**1763–1769.
21. **Jacobs, W. R., G. V. Kalpana, J. D. Cirillo, L. Pascopella, S. B. Snapper, R. A. Udani, W. Jones, R. G. Barletta, and B. R. Bloom.** 1991. Genetic systems for mycobacteria. Methods Enzymol. **204:**537–555.
22. **Keppler, F., R. Borchars, J. Pracht, S. Rheinberger, and H. Scholer.** 2002. Natural formation of vinyl chloride in the terrestrial environment. Environ. Sci. Technol. **36:**2479–2483.
23. **Kielhorn, J., C. Melber, U. Wahnschaffe, A. Aitio, and I. Mangelsdorf.** 2000. Vinyl chloride: still a cause for concern. Environ. Health Perspect. **108:**579–588.
24. **Koziollek, P., D. Bryniok, and H.-J. Knackmuss.** 1999. Ethene as an auxiliary substrate for the cooxidation of *cis*-dichloroethene and vinyl chloride. Arch. Microbiol. **172:**240–246.
25. **Krum, J. G., and S. A. Ensign.** 2000. Heterologous expression of bacterial epoxyalkane:coenzyme M transferase and inducible coenzyme M biosynthesis in *Xanthobacter* strain Py2 and *Rhodococcus rhodochrous* B276. J. Bacteriol. **182:**2629–2634.
26. **Krum, J. G., H. Ellsworth, R. R. Sargeant, G. Rich, and S. A. Ensign.** 2002. Kinetic and microcalorimetric analysis of substrate and cofactor interactions in epoxyalkane:CoM transferase, a zinc-dependent epoxidase. Biochemistry **41:**5005–5014.
27. **Krum, J. G., and S. A. Ensign.** 2001. Evidence that a linear megaplasmid encodes enzymes of aliphatic alkene and epoxide metabolism and coenzyme M (2-mercaptoethanesulfonate) biosynthesis in *Xanthobacter* strain Py2. J. Bacteriol. **183:**2172–2177.
28. **Lund, J., M. P. Woodland, and H. Dalton.** 1985. Electron transfer reactions in the soluble methane monooxygenase of *Methylococcus capsulatus* (Bath). Eur. J. Biochem. **147:**297–305.
29. **Maymó-Gatell, X., T. Anguish, and S. H. Zinder.** 1999. Reductive dechlorination of chlorinated ethenes and 1, 2-dichloroethane by "*Dehalococcoides ethenogenes*" 195. Appl. Environ. Microbiol. **65:**3108–3113.
30. **Maymó-Gatell, X., Y.-T. Chien, J. M. Gossett, and S. H. Zinder.** 1997. Isolation of a bacterium that reductively dechlorinates tetrachloroethene to ethene. Science **276:**1568–1571.
31. **Menendez, C., Z. Bauer, H. Huber, N. Gad'on, K. O. Stetter, and G. Fuchs.** 1999. Presence of acetyl coenzyme A (CoA) carboxylase and propionyl-CoA carboxylase in autotrophic *Crenarchaeota* and indication for operation of a 3-hydroxypropionate cycle in autotrophic carbon fixation. J. Bacteriol. **181:** 1088–1098.
32. **Mintz, M. J., and C. Walling.** 1969. tert-Butyl hypochlorite. Organic Syntheses **49:**9–12.
33. **Poelarends, G. J., J. E. T van Hylckama Vlieg, J. R. Marchesi, L. M. Freitas dos Santos, and D. B. Janssen.** 1999. Degradation of 1, 2-dibromoethane by *Mycobacterium* sp. strain GP1. J. Bacteriol. **181:**2050–2058.
34. **Pridmore, R. D.** 1987. New and versatile cloning vectors with kanamycin-resistance marker. Gene **56:**309–312.
35. **Rink, R., M. Fennema, M. Smids, U. Dehmel, and D. B. Janssen.** 1997. Primary structure and catalytic mechanism of the epoxide hydrolase from *Agrobacterium radiobacter* AD1. J. Biol. Chem. **272:**14650–14657.
36. **Rosenzweig, A. C., C. A. Frederick, S. J. Lippard, and P. Nordlund.** 1993. Crystal structure of a bacterial non-haem iron hydroxylase that catalyses the biological oxidation of methane. Nature **366:**537–543.
37. **Sambrook, J., and D. W. Russell.** 2001. Molecular cloning: a laboratory manual, 3rd ed. Cold Spring Harbor Laboratory Press, Cold Spring Harbor, N.Y.
38. **Semprini, L.** 1995. In situ bioremediation of chlorinated solvents. Environ. Health Perspect. **103:**101–105.
39. **Small, F. J., and S. A. Ensign.** 1997. Alkene monooxygenase from *Xanthobacter* strain Py2. J. Biol. Chem. **272:**24913–24920.

40. **Snapper, S. B., R. E. Melton, S. Mustafa, T. Kieser, and W. R. Jacobs.** 1990. Isolation and characterization of efficient plasmid transformation mutants of *Mycobacterium smegmatis*. Mol. Microbiol. **4:**1911–1919.
41. **Stover, C. K., V. F. de la Cruz, T. R. Fuerst, J. E. Burlein, L. A. Benson, L. T. Bennett, G. P. Bansal, J. F. Young, M. H. Lee, G. F. Hatfull, S. B. Snapper, R. G. Barletta, W. R. Jacobs, and B. R. Bloom.** 1991. New use of BCG for recombinant vaccines. Nature **351:**456–460.
42. **Stucki, G., U. Krebser, and T. Leisinger.** 1983. Bacterial growth on 1,2-dichloroethane. Experientia **39:**1271–1273.
43. **Thier, R., and H. M. Bolt.** 2000. Carcinogenicity and genotoxicity of ethylene oxide: new aspects and recent advances. Crit. Rev. Toxicol. **30:**595–608.
44. **Tornqvist, M.** 1994. Is ambient ethene a cancer risk factor? Environ. Health Perspect. **102:**157–160.
45. **van Ginkel, C. G., and J. A. M. de Bont.** 1986. Isolation and characterization of alkene-utilizing *Xanthobacter* spp. Arch. Microbiol. **145:**403–407.
46. **van Ginkel, C. G., H. G. J. Welten, and J. A. M. de Bont.** 1987. Oxidation of gaseous and volatile hydrocarbons by selected alkene-utilizing bacteria. Appl. Environ. Microbiol. **53:**2903–2907.
47. **van Hylckama Vlieg, J. E., H. Leemhuis, J. H. L. Spelberg, and D. B. Janssen.** 2000. Characterization of the gene cluster involved in isoprene metabolism in *Rhodococcus* sp. strain AD45. J. Bacteriol. **182:**1956–1963.
48. **van Hylckama Vlieg, J. E. T., J. Kingma, A. J. van den Wijngaard, and D. B. Janssen.** 1998. A glutathione *S*-transferase with activity towards *cis*-dichloroepoxyethane is involved in isoprene utilization by *Rhodococcus* sp. strain AD45. Appl. Environ. Microbiol. **64:**2800–2805.
49. **Verce, M. F., C. K. Gunsch, A. S. Danko, and D. L. Freedman.** 2002. Cometabolism of cis-1,2-dichloroethene by aerobic cultures grown on vinyl chloride as the primary substrate. Environ. Sci. Technol. **36:**2171–2177.
50. **Verce, M. F., R. L. Ulrich, and D. L. Freedman.** 2000. Characterization of an isolate that uses vinyl chloride as a growth substrate under aerobic conditions. Appl. Environ. Microbiol. **66:**3535–3542.
51. **Verce, M. F., R. L. Ulrich, and D. L. Freedman.** 2001. Transition from cometabolic to growth-linked biodegradation of vinyl chloride by a *Pseudomonas* sp. isolated on ethene. Environ. Sci. Technol. **35:**4242–4251.
52. **Walling, C., and P. S. Fredericks.** 1962. Positive halogen compounds. IV. Radical reactions of chlorine and t-butyl hypochlorite with some small ring compounds. J. Am. Chem. Soc. **84:**3326–3331.
53. **Wang, K. L., H. Li, and J. R. Ecker.** 2002. Ethylene biosynthesis and signaling networks. Plant Cell **14:**131–151.
54. **Wayne, L. G., and G. P. Kubica.** 1986. Genus *Mycobacterium*, p. 1436–1457. *In* P. H. A. Sneath, N. S. Mair, M. E. Sharpe, and J. G. Holt (ed.), Bergey's manual of systematic bacteriology, vol. 2. Williams & Wilkins, Baltimore, Md.
55. **Weber, F. J., W. J. H. van Berkel, S. Hartmans, and J. A. M. de Bont.** 1992. Purification and properties of the NADH reductase component of alkene monooxygenase from *Mycobacterium* strain E3. J. Bacteriol. **174:**3275–3281.
56. **Witt, M. E., G. M. Klecka, E. J. Lutz, T. A. Ei, N. R. Grosso, and F. H. Chapelle.** 2002. Natural attenuation of chlorinated solvents at Area 6, Dover Air Force Base: groundwater biogeochemistry. J. Contam. Hydrol. **57:**61–80.
57. **Yamada, E. W., and W. B. Jakoby.** 1960. Aldehyde oxidation. V. Direct conversion of malonic semialdehyde to acetyl-coenzyme A. J. Biol. Chem. **235:**589–594.
58. **Yanisch-Perron, C., J. Vieira, and J. Messing.** 1985. Improved M13 phage cloning vectors and host strains: nucleotide sequences of the M13mp18 and pUC19 vectors. Gene **33:**103–119.
59. **Zhou, N. Y., A. Jenkins, C. K. Chan Kwo Chion, and D. J. Leak.** 1998. The alkene monooxygenase from *Xanthobacter* Py2 is a binuclear non-haem iron protein closely related to toluene 4-monooxygenase. FEBS Lett. **430:**181–185.
60. **Zhou, Z. S., K. Peariso, J. E. Penner-Hahn, and R. G. Matthews.** 1999. Identification of the zinc ligands in cobalamin-independent methionine synthase (MetE) from *Escherichia coli*. Biochemistry **38:**15915–15926.

Appendix D

Coleman, N. V., and J. C. Spain 2003. Distribution of the Coenzyme-M pathway of epoxide metabolism among ethene- and vinyl-chloride-degrading *Mycobacterium* strains. *Appl. Environ. Microbiol.* 69:6041-6046.

APPLIED AND ENVIRONMENTAL MICROBIOLOGY, Oct. 2003, p. 6041–6046 Vol. 69, No. 10
0099-2240/03/$08.00+0 DOI: 10.1128/AEM.69.10.6041–6046.2003

Distribution of the Coenzyme M Pathway of Epoxide Metabolism among Ethene- and Vinyl Chloride-Degrading *Mycobacterium* Strains

Nicholas V. Coleman† and Jim C. Spain*

Air Force Research Laboratory—MLQL, Tyndall Air Force Base, Florida 32403

Received 7 April 2003/Accepted 9 July 2003

An epoxyalkane:coenzyme M (CoM) transferase (EaCoMT) enzyme was recently found to be active in the aerobic vinyl chloride (VC) and ethene assimilation pathways of *Mycobacterium* strain JS60. In the present study, EaCoMT activity and genes were investigated in 10 different mycobacteria isolated on VC or ethene from diverse environmental samples. In all cases, epoxyethane metabolism in cell extracts was dependent on CoM, with average specific activities of EaCoMT between 380 and 2,910 nmol/min/mg of protein. PCR with primers based on conserved regions of EaCoMT genes from *Mycobacterium* strain JS60 and the propene oxidizers *Xanthobacter* strain Py2 and *Rhodococcus* strain B-276 yielded fragments (834 bp) of EaCoMT genes from all of the VC- and ethene-assimilating isolates. The *Mycobacterium* EaCoMT genes form a distinct cluster and are more closely related to the EaCoMT of *Rhodococcus* strain B-276 than that of *Xanthobacter* strain Py2. The incongruence of the EaCoMT and 16S rRNA gene trees and the fact that isolates from geographically distant locations possessed almost identical EaCoMT genes suggest that lateral transfer of EaCoMT among the *Mycobacterium* strains has occurred. Pulsed-field gel electrophoresis revealed large linear plasmids (110 to 330 kb) in all of the VC-degrading strains. In Southern blotting experiments, the strain JS60 EaCoMT gene hybridized to many of the plasmids. The CoM-mediated pathway of epoxide metabolism appears to be universal in alkene-assimilating mycobacteria, possibly because of plasmid-mediated lateral gene transfer.

Aerobic bacteria that grow on ethene and vinyl chloride (VC) are widely distributed in the environment and have attracted interest because of their potential applications in bioremediation and biocatalysis (5, 6, 11, 12, 32, 33). The first step in ethene and VC assimilation is known to be a monooxygenase reaction yielding epoxyethane from ethene (5, 7) and chlorooxirane from VC (12, 33), but the downstream pathways are not well understood. Our recent work (5a) has revealed that an epoxyalkane:coenzyme M (CoM) transferase (EaCoMT) enzyme is involved in epoxyethane and chlorooxirane metabolism in *Mycobacterium* strain JS60, a strain isolated from contaminated groundwater by enrichment on VC as the sole carbon source (5). The EaCoMT reaction is a key step that channels the initial intermediates into central metabolic pathways and also guards against the accumulation of highly toxic and reactive epoxides in the cytoplasm.

EaCoMT enzymes have previously been found only in the propene-oxidizing bacteria *Xanthobacter* strain Py2 and *Rhodococcus* strain B-276. In such strains, EaCoMT is part of an unusual epoxide carboxylase enzyme complex consisting of EaCoMT, two stereoselective dehydrogenases, and an oxidoreductase/carboxylase (1, 2, 9, 16). In addition to unique biochemical reactions, the propene assimilation pathway is also distinguished by unusual genetic elements. In both strains Py2 and B-276, the propene monooxygenase genes are carried on linear megaplasmids, and in strain Py2, the epoxide carboxylase system and CoM biosynthesis genes are also plasmid borne (18, 26).

As part of the study that yielded strain JS60, we isolated many other mycobacteria that grew on VC (5). It is not known whether these isolates or similar *Mycobacterium* strains isolated on ethene (6, 7) possess EaCoMT enzymes. The relationship between strains isolated on VC and ethene is unclear, and the role of factors such as site contamination and geography in the dissemination and evolution of both groups is unknown. On the basis of the recent finding that the EaCoMT gene in *Xanthobacter* Py2 is carried by a linear plasmid, it might be speculated that similar elements are involved in ethene and VC metabolism. To address these questions, we investigated 10 mycobacteria isolated on VC (6 strains) or ethene (4 strains) from a diverse range of environmental samples. EaCoMT genes and enzyme activities were found in all of the strains. In the VC degraders, the EaCoMT enzymes appear to be encoded on linear megaplasmids.

MATERIALS AND METHODS

Isolation and growth of bacteria. The growth methods and media used were described previously (5, 5a). Six *Mycobacterium* strains (JS60, JS61, JS616, JS617, JS619, and JS621) that grow on VC and ethene were previously isolated (5) from groundwater (Plaquemine, La.), activated sludge (Ithaca, N.Y.), pond sediment (Carlyss, La.), activated carbon (Dortmund, Germany), aquifer sediment (Travis Air Force Base, Calif.), and groundwater (Moody Air Force Base, Ga.), respectively. Several mycobacteria that grow on ethene (but not VC) were isolated by enrichment culture as described previously (5), except that ethene was added to the headspace as the sole carbon source (16 ml/160-ml bottle) and incubation was at 30°C. Strains JS622 and JS623 were derived from sandy garden soil (Panama City, Fla.), strain JS624 was from grass rhizosphere soil (Central Park, New York, N.Y.), and strain JS625 was from decomposing tree bark (Washington, D.C.). The isolates were identified by 16S rRNA gene (rDNA) sequencing.

* Corresponding author. Mailing address: Air Force Research Laboratory—MLQL, Building 1117, 139 Barnes Dr., Tyndall AFB, FL 32403. Phone: (850) 283-6058. Fax: (850) 283-6090. E-mail: Jim.Spain@tyndall.af.mil.

† Present address: School of Molecular and Microbial Biosciences, University of Sydney, NSW 2006, Australia.

Effects of CoM on growth and enzyme activity. EaCoMT activity was assayed in cell extracts as described elsewhere (5a). Extracts from strains JS61, JS616, JS617, JS619, and JS621 were prepared from VC-grown cells, whereas extracts from strains JS622, JS623, JS624, and JS625 were prepared from ethene-grown cells. The effect of CoM on growing cultures of strain JS623 was investigated by monitoring ethene consumption and epoxyethane accumulation in 50-ml cultures growing on ethene (10%, vol/vol) as the sole carbon source, either with or without CoM (10 μM) added. Ethene and epoxyethane were quantified by gas chromatography of headspace samples (5a). Control cultures of strain JS623 containing glucose (1%) and Tween 80 (0.05%) in the presence and absence of CoM were monitored by measurement of optical density at 600 nm.

DNA extraction and PCR amplification of EaCoMT genes. Genomic DNA was extracted either by a previously reported method (5) or by bead beating as follows. Cultures were grown for 3 to 6 weeks on 1/10-strength Trypticase soy agar plates containing 1% glucose (5). Cells scraped from one plate were washed in 1 ml of STE-Tween buffer (100 mM NaCl, 10 mM Tris, 50 mM EDTA, 0.1% Tween 80, pH 8.0), suspended in 1 ml of the same buffer, and added to a screw-cap tube containing 1 ml of STE-Tween-saturated silica-zirconia beads (0.1-mm diameter). The mixture was subjected to bead beating (Mini-Beadbeater; BioSpec Products) at high speed for 2 min, and the lysate was purified by phenol-chloroform extraction and ethanol precipitation (27). The bead beating method was superior to the enzymatic-chemical lysis method (5) in terms of DNA yield and time, but the recovered DNA was of somewhat lower quality, presumably because of shearing forces. PCR was done essentially as described elsewhere (Coleman and Spain, submitted), with annealing at 60°C for 30 s and 5 ng of genomic DNA added as the template. Primers CoM-F1L (5′-AACTAC CCSAAYCCSCGCTGGTACGAC-3′) and CoM-R2E (5′-GTCGGCAGTTTC GGTGATCGTGCTCTTGAC-3′) were designed from conserved regions of the EaCoMT genes of *Mycobacterium* strain JS60, *Rhodococcus* strain B-276, and *Xanthobacter* strain Py2 (GenBank accession numbers AY243034, AF426826, and X79863).

Preparation of cell plugs and PFGE. Cultures (700 ml) of *Mycobacterium* strains JS60, JS61, JS616, JS617, JS619, and JS621 were grown on ethene until mid-exponential phase, glycine (0.5%) and ampicillin (200 μg/ml) were added, and then incubation was continued overnight. Cells were pelleted and frozen in aliquots at −80°C. After thawing, the cell pellets (50 to 100 μl) were washed in STE-Tween, suspended in molten agarose (0.5 to 1.0 ml, 1% in 0.5× TBE buffer) (27), and pipetted into plug molds. The optical density at 600 nm of cells in the plugs ranged from 20 to 80, requiring individual optimization for each strain. Plugs (typically 5 to 10) were treated with lysozyme (50 mg in 5 ml of STE) at 37°C overnight, rinsed in wash buffer (20 mM Tris, 50 mM EDTA, pH 8), and then treated with proteinase K (5 mg in 5 ml of sodium lauryl sarcosinate [1%], sodium deoxycholate [0.2%], EDTA [0.1 M, pH 8]) for 24 h at 60°C. Plugs were rinsed three times in wash buffer and stored in the same buffer at 4°C. Contour-clamped homogeneous electric field (CHEF) pulsed-field gel electrophoresis (PFGE) was done in 1% agarose gels (0.5× TBE) at 14°C, 6 V/cm, and a 120° angle, with the switching time ramped from 10 to 40 s over 18 h (CHEF-DRIII system; Bio-Rad). Lambda phage concatemers (Bio-Rad) used as molecular weight markers were regenerated by heating at 45°C for 25 min before use.

Southern blotting. Southern blot assays were performed via standard methods (28), and the ECL kit (Amersham-Pharmacia) was used for detection. In Southern blots from standard agarose gels, acid depurination was omitted, while for PFGE gels, this step was replaced with a nicking procedure (CHEF-DRIII instructions; Bio-Rad), in which the gel was stained for 30 min in 1 μg of ethidium bromide per ml and then subjected to UV radiation at 60 mJ/cm^2 (Stratagene UV cross-linker). The probe used for Southern blotting in all cases was an 891-bp region of the strain JS60 EaCoMT gene, amplified by PCR with the CoM-F1L and CoM-R2E primers.

RESULTS AND DISCUSSION

Isolation of ethene-assimilating bacteria. To complement a previously isolated set of VC-assimilating bacteria (5), four bacteria that grow on ethene were isolated from soil samples with no known exposure to chlorinated ethenes. Partial sequencing of 16S rDNA indicated that all four isolates were distinct and were strains of *Mycobacterium*. On the basis of a 421-bp alignment of the 16S rDNAs, the closest species matches were JS622-*M. rhodesiae* (98.3% identity), JS623-*M. smegmatis* (96.7% identity), JS624-*M. peregrinum* (97.9% identity), and JS625-*M. mageritense* (99.0% identity). The GenBank accession numbers of the 16S rDNA sequences of the four strains are AY162027 to AY162030. None of the four isolates grew on VC (data not shown).

TABLE 1. EaCoMT activity in cell extracts of alkene-assimilating *Mycobacterium* strains

Strain	Isolation and growth substrate	EaCoMT activity[a] (nmol/min/mg of protein)	
		CoM added	No cofactor
JS60	VC	980 (930–1,060)[b]	0 (0)[b]
JS61	VC	2,910 (2,330–3,490)	110 (70–160)
JS616	VC	1,800 (1,710–1,890)	10 (0–20)
JS617	VC	900 (710–1,090)	30 (20–40)
JS619	VC	1,920 (1,880–1,960)	130 (130)
JS621	VC	790 (780–800)	110 (110)
JS622	Ethene	930 (850–1,000)	50 (0–100)
JS623	Ethene	590 (400–780)	60 (0–120)
JS624	Ethene	470 (440–500)	10 (0–20)
JS625	Ethene	380 (290–460)	0 (0)

[a] The results are averages of two assays, and the ranges are in parentheses. Reaction mixtures (1 ml) contained 0.1 mg of protein, 5 μmol of epoxyethane, and 10 μmol of CoM. Specific activities were calculated from the epoxyethane depletion rate after subtraction of the appropriate abiotic rate of epoxyethane loss (either 2.5 nmol/min in Tris buffer or 13 nmol/min in Tris buffer plus CoM).
[b] From a previous study (5a).

EaCoMT activity is widespread in alkene-assimilating mycobacteria. CoM-dependent epoxyethane metabolism was found in cell extracts of all of the VC- and ethene-assimilating *Mycobacterium* strains examined (Table 1). Very little epoxyethane transformation occurred in reaction mixtures without added CoM. The low activities in some reaction mixtures that were not supplemented with CoM may have been due to endogenous levels of CoM in the cell extracts or to the activity of other epoxide-transforming enzymes. Extracts from VC-grown cells of the strains originally isolated on VC had generally higher levels of EaCoMT activity (1,550 ± 821 nmol/min/mg of protein) than extracts from ethene-grown cells of the strains isolated on ethene (592 ± 241 nmol/min/mg of protein).

Previous work (5a) indicated almost identical levels of EaCoMT activity in ethene- and VC-grown cells of strain JS60. Therefore, the higher activities in extracts from VC-grown cells (Table 1) are more likely due to the fact that these strains were originally isolated on VC, rather than because VC was used as the growth substrate in this particular experiment. Higher EaCoMT activities might be expected in the VC-assimilating strains if EaCoMT plays a role in chlorooxirane metabolism (5a) because chlorooxirane is much more unstable and reactive than epoxyethane (aqueous half lives of 90 s [15] and 13 days [35], respectively). Higher EaCoMT activity is unlikely to be the sole reason for the ability of some strains to grow on VC in addition to ethene. For example, strain JS622 displayed higher EaCoMT activity than did strains JS617 and JS621, yet the latter two strains can grow on VC, whereas strain JS622 cannot.

CoM stimulates ethene metabolism in growing cultures of strain JS623. Cultures of *Mycobacterium* strain JS623 accumulated large amounts of epoxyethane during growth on ethene, in contrast to almost all of the other VC and ethene degraders. On the basis of the finding of EaCoMT in all of the strains

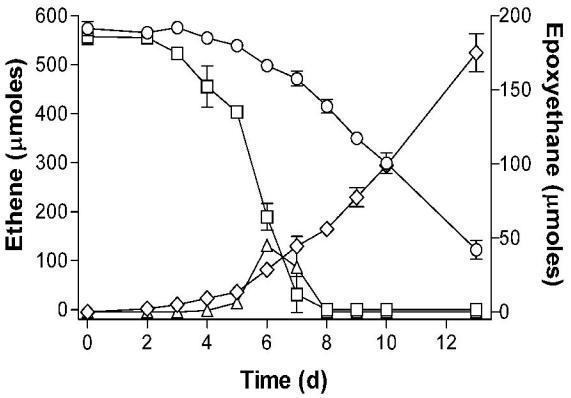

FIG. 1. Effect of CoM on ethene metabolism in growing cultures of strain JS623. Symbols: ○, ethene in cultures without CoM; □, ethene in cultures with 10 μM CoM; ◇, epoxyethane in cultures without CoM; △, epoxyethane in cultures with 10 μM CoM. The data shown are averages of three replicate cultures, and the error bars show the standard deviations. d, days.

(above), we hypothesized that an inadequate supply of CoM in the culture might be responsible for epoxyethane accumulation. Addition of 10 μM CoM to the MSM minimal medium accelerated ethene consumption in cultures of strain JS623 and eliminated the accumulation of epoxyethane (Fig. 1). CoM did not stimulate the growth of strain JS623 on glucose (data not shown), suggesting that the effect was specific to ethene metabolism. While an EaCoMT enzyme is present in all of the VC and ethene degraders examined, the ability of the strains to biosynthesize CoM may vary. It should therefore be noted that the EaCoMT activities measured in cell extract experiments with excess CoM (Table 1) may be higher than the in vivo activities in growing cultures, where limitations in the biosynthesis or recycling of CoM could affect the reaction rate.

PCR amplification of EaCoMT genes from *Mycobacterium* strains. PCR with primers CoM-F1L and CoM-R2E yielded strong products of the expected size (891 bp) from all of the VC- and ethene-assimilating *Mycobacterium* strains tested (Fig. 2). The 891-bp PCR products were cloned and sequenced, and all were revealed to be partial EaCoMT genes (GenBank accession numbers AY243035 to AY243043). The

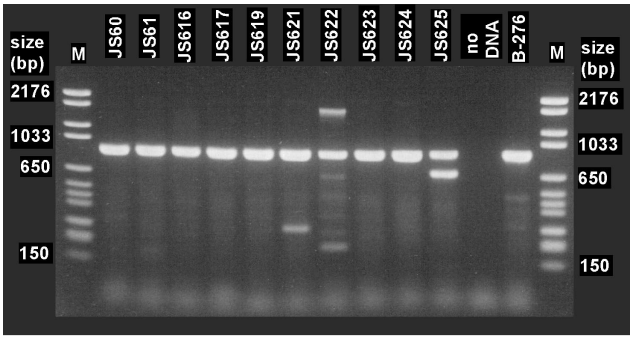

FIG. 2. PCR amplification of EaCoMT gene fragments from ethene- and VC-assimilating mycobacteria with the CoM-F1L and CoM-R2E primers. The propene degrader *Rhodococcus* strain B-276 was included as a positive control. Molecular size markers are in lanes M.

680-bp amplicon from strain JS625 was primed at both ends with CoM-F1L and bore no resemblance to EaCoMT genes. This sequence contained one large partial open reading frame (183 amino acids) that was somewhat similar to hypothetical protein Rv2624c from *Mycobacterium tuberculosis* (26.4% identity). The faint secondary products seen in amplifications with the strain JS621 and JS622 DNAs were not investigated further.

Only one EaCoMT sequence was obtained from each of the 891-bp PCR products (two or three cloned amplicons were sequenced in each case), but it is possible that multiple EaCoMT genes exist in the strains. Thus, the enzyme activities in Table 1 cannot be attributed rigorously to the EaCoMT genes that were sequenced. To address this issue, we prepared Southern blots from *Eco*RV or *Sph*I digests of genomic DNAs from the strains and probed them with the 891-bp EaCoMT PCR product from strain JS60. In the *Eco*RV digests of strains JS61, JS617, JS619, and JS621 and the *Sph*I digests of strains JS61 and JS621, a single strongly hybridizing band was seen (data not shown). In blots from restriction digests of the other strains, a smear of hybridizing DNA was seen but there were no discrete bands. Such results could be due to bead beater-induced DNA shearing or to nonspecific nuclease activity. Further experiments with higher-quality DNA preparations and a wider range of restriction enzymes are required to clarify our initial data, but the results obtained thus far suggest that a single EaCoMT allele is present in strains JS61, JS617, JS619, and JS621. Similar methods used in a previous study (5a) indicated that only a single EaCoMT gene was present in strain JS60.

Sequence analysis of *Mycobacterium* EaCoMT genes. In silico translation of the EaCoMT gene fragments revealed a 278-amino-acid open reading frame in all cases. The histidine and the first cysteine residue of the His-X-Cys-X_n-Cys motif involved in zinc binding in the *Xanthobacter* strain Py2 EaCoMT enzyme (17) were identified in each of the deduced amino acid sequences (the second cysteine residue lay outside the region amplified). Phylogenetic analysis of the *Mycobacterium*, *Xanthobacter* strain Py2, and *Rhodococcus* strain B-276 EaCoMT genes (Fig. 3) showed that the *Mycobacterium* sequences clustered together, having 80.5 to 99.9% sequence identity with each other, 68.7 to 70.5% identity with the B-276 gene, and 52.6 to 55.9% identity with the strain Py2 gene (percentages from a PHYLIP DNA distance similarity table (10). In several cases, almost identical EaCoMT sequences were obtained from strains derived from geographically distant samples. For example, three base changes or fewer (0.12 to 0.36% difference) separated the EaCoMT sequences of strains JS619 (California), JS624 (New York), and JS625 (Washington, D.C.), whereas the 16S rDNA sequences of these three strains were separated by 1.79 to 5.13%. Similar observations of highly conserved catabolic genes in phylogenetically diverse bacterial strains are not uncommon in the biodegradation literature (13, 23).

The tree topologies estimated from the EaCoMT and 16S rDNA sequences have numerous differences (Fig. 3). Assuming vertical inheritance of 16S rDNA, this suggests that lateral gene transfer (LGT) of EaCoMT genes has occurred (30). The LGT hypothesis is supported by the fact that the EaCoMT genes are in many cases more similar to each other than are the

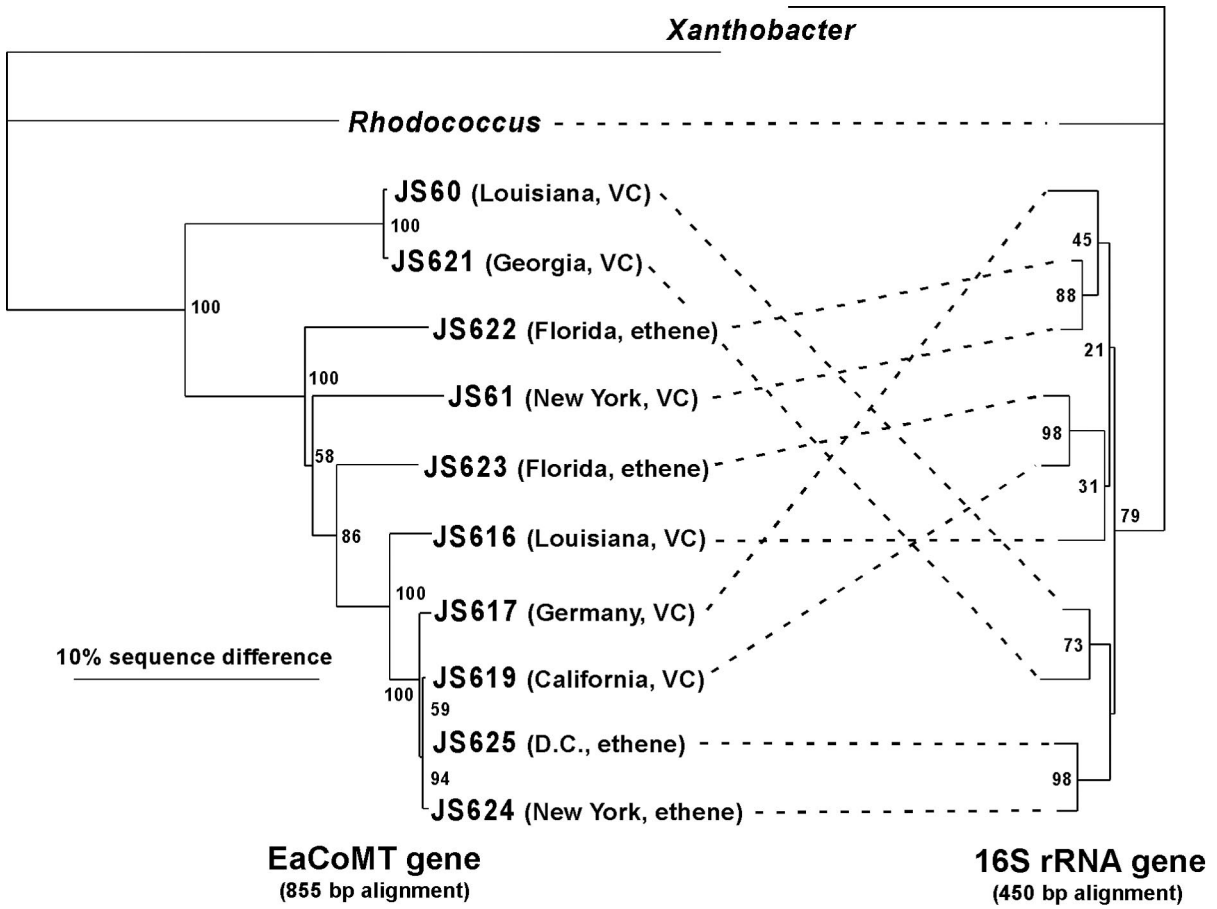

FIG. 3. Comparative phylogeny of EaCoMT and 16S rDNAs from alkene-oxidizing bacteria. The geographical origins and isolation substrates of the JS strains (all *Mycobacterium* spp.) are shown. Alignments and neighbor-joining trees were generated with ClustalX and TreeView, with *Xanthobacter* as the outgroup. The 16S rDNA alignment was manually adjusted by removing nucleotides at ambiguous positions. Percent bootstrap values from 100 trees are shown at the nodes. Because 16S rDNA sequences for *Rhodococcus* strain B-276 and *Xanthobacter* strain Py2 were not available, the sequences from *Rhodococcus rhodochrous* ATCC 271^T and *Xanthobacter autotrophicus* JW33 were substituted.

(slow-evolving) 16S rDNAs. We used the maximum-likelihood-based Shimodaira-Hasegawa test (28) in PAUP*b10 (29) to test the null hypothesis that the two genes in each strain have the same evolutionary history. On the basis of the 16S rDNA data set, the likelihood scores of the two topologies shown in Fig. 3 were estimated (GTR+I+G model in Modeltest) (24) to be −1,508.37 (16S rDNA) and −1,550.33 (EaCoMT). The latter is significantly lower than the former ($P < 0.0001$), and thus it is unlikely that the two genes have the same evolutionary history. On the basis of bootstrap values (Fig. 3), the strongest case for LGT concerns the EaCoMT genes of strains JS623 and JS619. Indeed, when these strains were removed from the data sets and the Shimodaira-Hasegawa test was repeated, no significant differences between the likelihood scores were found (likelihood scores of −1,419.10 and −1,418.65; $P = 0.381$). We conclude that rigorous statistical support for LGT only exists in the cases of strains JS619 and JS623.

Analysis of plasmids by PFGE and Southern blotting. On the basis of the phylogenetic evidence of lateral transfer of *Mycobacterium* EaCoMT genes (above) and the finding of plasmid-borne propene metabolism genes in *Rhodococcus* strain B-276 and *Xanthobacter* strain Py2 (18, 26), we hypothesized that catabolic plasmids were present in the VC- and ethene-assimilating strains and searched for such plasmids by PFGE. Because of difficulties in preparing DNA plugs from some of the strains isolated on ethene, we focused our analysis on the six VC-assimilating strains. CHEF-PFGE revealed one strong plasmid band and several fainter plasmid bands in each of the six strains investigated (Fig. 4A). All of the bands migrated at the same positions relative to the linear markers when the pulse conditions were altered (20 to 80 s over 18 h; data not shown), indicating that the plasmids were linear rather than circular (4).

After Southern blotting of the pulsed-field gels, probing with the strain JS60 EaCoMT gene resulted in hybridization signals with the strong plasmid band in most of the strains (Fig. 4B). The simplest hypothesis (i.e., that the genes are plasmid borne) is complicated by the additional strong probe binding at the "compression zone" (3, 20) and because of the weak probe hybridization with some of the smaller plasmids. The multiple signals could be due to multiple copies of the EaCoMT gene in the *Mycobacterium* strains, the resolution of different forms of the same plasmid in the gel, or nonspecific binding of the

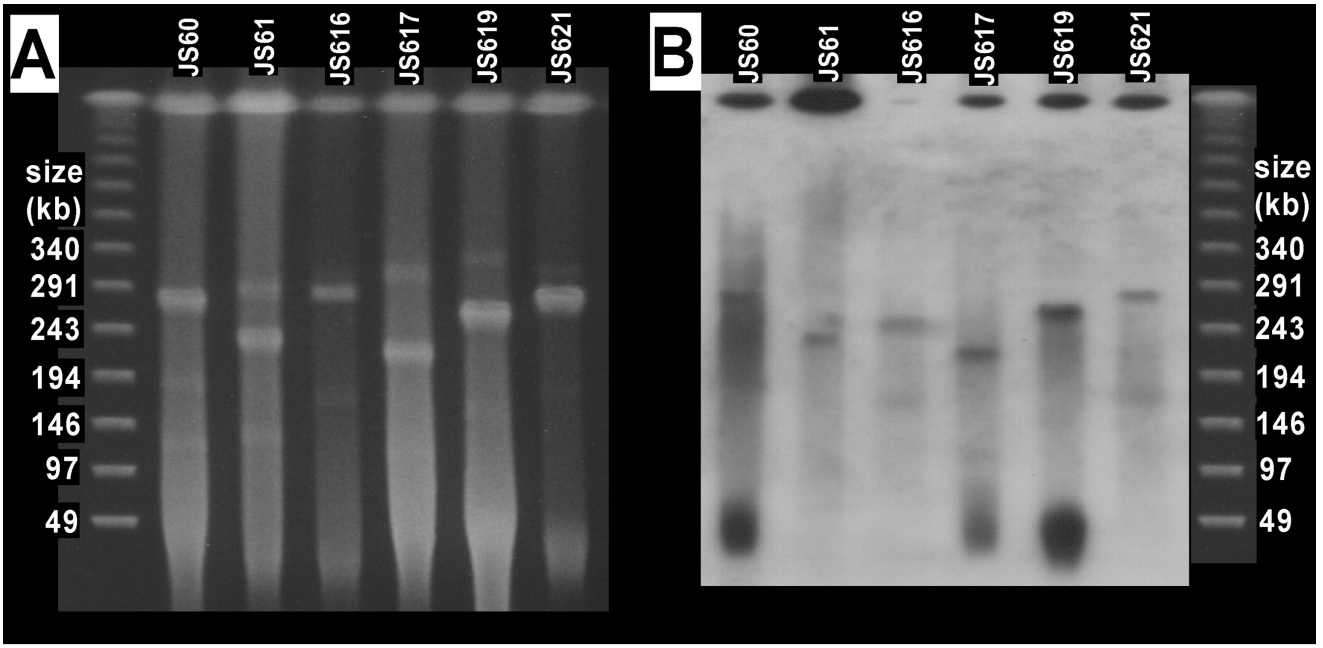

FIG. 4. (A) Ethidium bromide-stained CHEF-PFGE gel showing plasmids in VC-assimilating *Mycobacterium* strains. (B) Southern blot prepared from a PFGE gel by using the JS60 EaCoMT gene as the probe. Lambda concatemer markers are shown on the left and right and apply to both the blot and the gel.

probe. Southern blots from restriction digests of total DNA (above) seem to eliminate the possibility of multiple EaCoMT gene locations, but duplication of a large region of DNA would be consistent with both results. The presence of multiple plasmid forms is also a possibility. Concatemers of circular plasmids occur in *Streptomyces* strains (14), and a combination of linear and circular forms of the same plasmid in a single bacterium is common (3). Signals from both the compression zone and plasmid band were seen in Southern blotting experiments with *Rhodococcus* strain B-276 (26), in which the alkene monooxygenase genes were clearly plasmid borne (on the basis of the lack of plasmid in propene-negative mutants). The authors of that study attributed the probing result to nonspecific binding at the compression zone because of the larger amount of DNA there. It is possible that the signal from the compression zone in our study is due to the EaCoMT probe hybridizing to chromosomal methionine synthase (*metE*), which encodes a zinc-dependent enzyme with some sequence similarity to EaCoMT (17).

Implications of this study. We found EaCoMT activity and genes in all of the alkene-oxidizing mycobacteria that we examined, including strains isolated on both VC and ethene. EaCoMT genes were not found in BLAST database searches of *Mycobacterium* genomes (or any other genomes) that have been completed to date, indicating that EaCoMT is specific to the alkene-assimilation pathway. It remains to be determined whether EaCoMT is involved in the VC and ethene assimilation pathways of *Pseudomonas* (33, 34) and *Nocardioides* (5) strains. The EaCoMT gene primers we have developed could be used to address this question. In addition, such primers will be very useful for culture-independent monitoring of microbial populations during the natural attenuation or bioremediation of chlorinated ethenes. Such methods are particularly relevant for mycobacteria, which are slow growing and sometimes difficult to isolate in pure culture (5).

The 10 VC and ethene degraders we studied were scattered throughout the genus *Mycobacterium*, with no apparent correspondence seen between phylogeny and alkene growth substrate. Although EaCoMT activities tended to be higher in the VC degraders than in the ethene degraders, it is difficult to compare these results because of the use of different growth substrates in experiments with each group of strains. Sequencing of EaCoMT genes did not reveal any signature regions that discriminated between the VC- and ethene-assimilating strains, and indeed, in the case of strains JS619 (VC) and JS625 (ethene), only a single nucleotide difference separated the EaCoMT PCR products. An important question arising from our work therefore concerns the distinction between bacteria that can grow on both VC and ethene and those that grow on ethene alone.

There is good evidence in at least one case that VC degraders evolved directly from ethene-degraders—this was observed in vitro with *Pseudomonas* strain DL1 (34). The transition from ethene to VC assimilation could be due to recruitment of an additional catabolic enzyme (23), changes in enzyme specificity (25), or alteration of enzyme expression levels (31). With respect to enzyme specificity and expression level, it is interesting that although the EaCoMT gene sequences of strains JS619 and JS625 were almost identical, the EaCoMT activity in cell extracts was fivefold higher in strain JS619. Sequencing of complete EaCoMT genes and flanking DNA and analysis of the activity of other catabolic enzymes may help to shed light on the factors that distinguish ethene- and VC-assimilating bacteria and yield insights into the possible evolution of the latter group from the former.

The EaCoMT gene appears to be carried on large linear

plasmids in VC-degrading strains. On the basis of the gene organization in *Mycobacterium* strain JS60 (5a), it is likely that the alkene monooxygenase genes are also present on the same plasmids. Cryptic linear plasmids have previously been identified in various pathogenic *Mycobacterium* strains (19, 21, 22) and in ethene-oxidizing *Mycobacterium* strain E-1-57 (26). Only one previous study (36) has associated a specific catabolic function (morpholine biodegradation) with plasmids in mycobacteria. Our results indicate that catabolic plasmids are more widespread in this genus than was previously believed. Plasmid-borne genes for ethene and VC biodegradation could potentially be transferred among bacteria in the environment (8, 13), and thus, further investigation of such elements is warranted in light of the potential importance of the alkene-degrading phenotype to bioremediation and natural attenuation processes (5).

ACKNOWLEDGMENTS

We thank Nathan Lo for help with phylogenetic analyses and Crystal Henley for assistance with the isolation of ethene degraders. Scott Ensign kindly provided strain B-276.

This work was funded by the U.S. Strategic Environmental Research and Development Program. N.V.C. was supported by a postdoctoral fellowship from the Oak Ridge Institute for Science and Education (U.S. Department of Energy).

REFERENCES

1. **Allen, J. R., and S. A. Ensign.** 1997. Purification to homogeneity and reconstitution of the individual components of the epoxide carboxylase multiprotein enzyme complex from *Xanthobacter* strain Py2. J. Biol. Chem. **272:** 32121–32128.
2. **Allen, J. R., D. D. Clark, J. G. Krum, and S. A. Ensign.** 1999. A role for coenzyme M (2-mercaptoethanesulfonic acid) in a bacterial pathway of aliphatic epoxide carboxylation. Proc. Natl. Acad. Sci. USA **96:**8432–8437.
3. **Barton, B. M., G. P. Harding, and A. J. Zuccarelli.** 1995. A general method for detecting and sizing large plasmids. Anal. Biochem. **226:**235–240.
4. **Birren, B., and E. Lai.** 1993. Pulsed-field gel electrophoresis: a practical guide. Academic Press., San Diego, Calif.
5. **Coleman, N. V., T. E. Mattes, J. M. Gossett, and J. C. Spain.** 2002. Phylogenetic and kinetic diversity of aerobic vinyl chloride-assimilating bacteria from contaminated sites. Appl. Environ. Microbiol. **68:**6162–6171.

5a. **Coleman, N. V., and and J. C. Spain.** 2003. Epoxyalkane:coenzyme M transferase in the ethene and vinyl chloride biodegradation pathways of *Mycobacterium* strain JS60. J. Bacteriol. **185:**5536–5545.

6. **de Bont, J. A. M.** 1976. Oxidation of ethylene by soil bacteria. Antonie van Leeuwenhoek **42:**59–71.
7. **de Bont, J. A. M., and W. Harder.** 1978. Metabolism of ethylene by *Mycobacterium* E 20. FEMS Microbiol. Lett. **3:**89–93.
8. **Dejonghe, W., J. Goris, S. El Fantroussi, M. Hofte, P. De Vos, W. Verstraete, and E. M. Top.** 2000. Effect of dissemination of 2,4-dichlorophenoxyacetic acid (2,4-D) degradation plasmids on 2,4-D degradation and on bacterial community structure in two different soil horizons. Appl. Environ. Microbiol. **66:**3297–3304.
9. **Ensign, S. A.** 2001. Microbial metabolism of aliphatic alkenes. Biochemistry **40:**5845–5853.
10. **Felsenstein, J.** 1989. PHYLIP—phylogeny inference package (version 3.2). Cladistics **5:**164–166.
11. **Habets-Crützen, A. Q. H., L. E. S. Brink, C. G. van Ginkel, J. A. M. de Bont, and J. Tramper.** 1984. Production of epoxides from gaseous alkenes by resting-cell suspensions and immobilized cells of alkene-utilizing bacteria. Appl. Microbiol. Biotechnol. **20:**245–250.
12. **Hartmans, S., and J. A. M. de Bont.** 1992. Aerobic vinyl chloride metabolism in *Mycobacterium aurum* L1. Appl. Environ. Microbiol. **58:**1220–1226.
13. **Herrick, J. B., K. G. Stuart-Keil, W. C. Ghiorse, and E. L. Madsen.** 1997. Natural horizontal transfer of a naphthalene dioxygenase gene between bacteria native to a coal tar-contaminated field site. Appl. Environ. Microbiol. **63:**2330–2337.
14. **Kieser, T.** 1984. Factors affecting the isolation of CCC DNA from *Streptomyces lividans* and *Escherichia coli*. Plasmid **12:**19–36.
15. **Kline, S. A., J. J. Solomon, and B. L. van Duuren.** 1978. Synthesis and reactions of chloroalkene epoxides. J. Org. Chem. **43:**3596–3600.
16. **Krum, J. G., and S. A. Ensign.** 2000. Heterologous expression of bacterial epoxyalkane:coenzyme M transferase and inducible coenzyme M biosynthesis in *Xanthobacter* strain Py2 and *Rhodococcus rhodochrous* B276. J. Bacteriol. **182:**2629–2634.
17. **Krum, J. G., H. Ellsworth, R. R. Sargeant, G. Rich, and S. A. Ensign.** 2002. Kinetic and microcalorimetric analysis of substrate and cofactor interactions in epoxyalkane:CoM transferase, a zinc-dependent epoxidase. Biochemistry **41:**5005–5014.
18. **Krum, J. G., and S. A. Ensign.** 2001. Evidence that a linear megaplasmid encodes enzymes of aliphatic alkene and epoxide metabolism and coenzyme M (2-mercaptoethanesulfonate) biosynthesis in *Xanthobacter* strain Py2. J. Bacteriol. **183:**2172–2177.
19. **Le Dantec, C., N. Winter, B. Gicquel, V. Vincent, and M. Picardeau.** 2001. Genomic sequence and transcriptional analysis of a 23-kilobase mycobacterial linear plasmid: evidence for horizontal transfer and identification of plasmid maintenance systems. J. Bacteriol. **183:**2157–2164.
20. **Mathew, M. K., C. L. Smith, and C. R. Cantor.** 1988. High-resolution separation and accurate size determination in pulsed-field gel electrophoresis of DNA. 2. Effect of pulse time and electric field strength and implications for models of the separation process. Biochemistry **27:**9210–9216.
21. **Picardeau, M., and V. Vincent.** 1997. Characterization of large linear plasmids in mycobacteria. J. Bacteriol. **179:**2753–2756.
22. **Picardeau, M., and V. Vincent.** 1998. Mycobacterial linear plasmids have an invertron-like structure related to other linear replicons in actinomycetes. Microbiology **144:**1981–1988.
23. **Poelarends, G. J., M. Zandstra, T. Bosma, L. A. Kulakov, M. J. Larkin, J. R. Marchesi, A. J. Weightman, and D. B. Janssen.** 2000. Haloalkane-utilizing *Rhodococcus* strains isolated from geographically distinct locations possess a highly conserved gene cluster encoding haloalkane catabolism. J. Bacteriol. **182:**2725–2731.
24. **Posada, D., and K. A. Crandall.** 1998. Modeltest: testing the model of DNA substitution. Bioinformatics **14:**817–818.
25. **Pries, F., A. J. van den Wijngaard, R. Bos, M. Pentenga, and D. B. Janssen.** 1994. The role of spontaneous cap domain mutations in haloalkane dehalogenase specificity and evolution. J. Biol. Chem. **269:**17490–17494.
26. **Saeki, H., M. Akira, K. Furuhashi, B. Averhoff, and G. Gottschalk.** 1999. Degradation of trichloroethene by a linear-plasmid-encoded alkene monooxygenase in *Rhodococcus corallinus* (*Nocardia corallina*) B-276. Microbiology **145:**1721–1730.
27. **Sambrook, J., and D. W. Russell.** 2001. Molecular cloning: a laboratory manual, 3rd ed. Cold Spring Harbor Laboratory Press, Cold Spring Harbor, N.Y.
28. **Shimodaira, H., and H. Hasegawa.** 1999. Multiple comparisons of log-likelihoods with applications to phylogenetic inferences. Mol. Biol. Evol. **16:**964–969.
29. **Swofford, D. L.** 2000. PAUP*: phylogenetic analysis using parsimony (*and other methods). Sinauer Associates, Sunderland, Mass.
30. **Syvanen, M.** 1994. Horizontal gene flow: evidence and possible consequences. Annu. Rev. Genet. **28:**237–261.
31. **van der Ploeg, J. R., J. Kingma, E. J. De Vries, J. G. Van der Ven, and D. B. Janssen.** 1996. Adaptation of *Pseudomonas* sp. GJ1 to 2-bromoethanol caused by overexpression of an NAD-dependent aldehyde dehydrogenase with low affinity for halogenated aldehydes. Arch. Microbiol. **165:**258–264.
32. **Verce, M. F., C. K. Gunsch, A. S. Danko, and D. L. Freedman.** 2002. Cometabolism of *cis*-1,2-dichloroethene by aerobic cultures grown on vinyl chloride as the primary substrate. Environ. Sci. Technol. **36:**2171–2177.
33. **Verce, M. F., R. L. Ulrich, and D. L. Freedman.** 2000. Characterization of an isolate that uses vinyl chloride as a growth substrate under aerobic conditions. Appl. Environ. Microbiol. **66:**3535–3542.
34. **Verce, M. F., R. L. Ulrich, and D. L. Freedman.** 2001. Transition from cometabolic to growth-linked biodegradation of vinyl chloride by a *Pseudomonas* sp. isolated on ethene. Environ. Sci. Technol. **35:**4242–4251.
35. **Washington, J. W.** 1995. Hydrolysis rates of dissolved volatile organic compounds: principles, temperature effects and literature review. Ground Water **33:**415–424.
36. **Waterhouse, K. V., A. Swain, and W. A. Venables.** 1991. Physical characterization of plasmids in a morpholine-degrading *Mycobacterium*. FEMS Microbiol. Lett. **80:**305–310.

Appendix E

Mattes, T. E., N. V. Coleman, J. C. Spain, and J. M. Gossett 2004. A linear plasmid carries vinyl chloride biodegradation genes in *Nocardioides* JS614. Manuscript submitted to *Archives of Microbiology*.

A linear plasmid carries vinyl chloride biodegradation genes in *Nocardioides* JS614

Authors: Timothy E. Mattes[1*], Nicholas V. Coleman[2], Jim C. Spain[3], and James M. Gossett[4]

1. Department of Civil and Environmental Engineering, 4105 Seamans Center, The University of Iowa, Iowa City, IA, 52242, USA
2. School of Molecular and Microbial Biosciences, University of Sydney, Australia
3. AFRL-MLQL, Tyndall AFB, Florida, 32403, USA.
4. School of Civil and Environmental Engineering, Hollister Hall, Cornell University, Ithaca, NY, 14853, USA

* Corresponding author: Fax: (319) 335-5660
E-mail: tem8@cornell.edu

ABSTRACT

Nocardioides strain JS614 grows on vinyl chloride (VC) and ethene (ETH) as carbon and energy sources. Bacteria such as JS614 could be influential in natural attenuation and biogeochemical ETH cycling, and useful for bioremediation, biocatalysis and metabolic engineering, but a lack of knowledge of the genetic basis of VC and ETH assimilation has limited these applications. JS614 VC/ETH catabolic genes and flanking DNA (34.8 kb) were retrieved from a fosmid clone. Alkene monooxygenase (AkMO) and epoxyalkane:Coenzyme M transferase (EaCoMT) genes were found in a putative operon that also included CoA transferase, acyl-CoA synthetase, dehydrogenase and reductase genes. Adjacent to this gene cluster was a divergently transcribed gene cluster that encoded possible coenzyme M biosynthesis enzymes. Reverse transcription (RT-) PCR demonstrated the VC- and ETH-inducible nature of several genes. Genes encoding possible plasmid conjugation, integration, and partitioning functions were also discovered on the fosmid clone. Pulsed field gel electrophoresis (PFGE) revealed a 290 kb linear plasmid (pNoc614) in JS614. Curing experiments and PCR indicated that pNoc614 encodes VC/ETH degradation genes, and that pNoc614 was the source of the sequenced fosmid clone. The results provide rigorous evidence that linear plasmids encode VC/ETH biodegradation genes, and greatly expand the database of useful genes for future *in situ* molecular studies of VC-degrading bacteria.

Keywords: Linear plasmid, alkene oxidation, bioremediation, vinyl chloride

INTRODUCTION

Vinyl chloride (VC), a known human carcinogen (Bucher 2001) and common groundwater contaminant (Squillace 1999), is derived mainly from incomplete reductive dechlorination of the widely used chlorinated solvents tetrachloroethene (PCE) and trichloroethene (TCE), also common groundwater contaminants (Squillace 1999). VC tends to accumulate in anaerobic groundwater zones but often degrades readily if the VC plume migrates into aerobic groundwater zones (Davis 1990; Edwards 1997; Lee 1998). It seems likely that microorganisms are responsible for the observed aerobic attenuation, because *Mycobacterium, Nocardioides* and *Pseudomonas* strains that grow on VC as a carbon and energy source are widespread, and have been isolated from soil (Coleman et al. 2002), groundwater (Coleman et al. 2002), sediment (Hartmans 1992), and sewage sludge samples (Hartmans 1992; Verce 2000; Coleman et al. 2002).

All of the VC-assimilating bacteria isolated to date use both VC and ethene (ETH) as carbon sources, and it has been proposed that VC-degraders (Verce 2001; Coleman et al. 2002) evolved from ETH-degraders (van Ginkel 1986; van Ginkel 1987). However, the mechanism and genetic basis of the adaptation is unknown.

The presence of aerobic VC- and ETH-assimilating bacteria at a contaminated site is a crucial line of evidence for demonstrating natural attenuation, but it is not clear whether the isolates obtained to date are representative of microbes active under field conditions. There is currently no sequence-based method to distinguish an ETH-degrading bacterium from a VC-degrading bacterium, which is a serious shortcoming for site assessment and bioremediation studies. Molecular tools such as PCR (Fennell et al. 2001), reverse transcriptase (RT)-PCR,

stable isotope probing (Radajewski et al. 2000), and fluorescent *in situ* hybridization (FISH)(Richardson et al. 2002) would allow identification of active VC-degraders *in situ*, and potentially facilitate discrimination of VC- and ETH-degraders, but application of such methods requires a database of relevant genes, and thus far, our knowledge of the genetic basis of VC and ETH degradation is rudimentary.

The genes that encode enzymes responsible for catabolism of VC and ETH, including an alkene monooxygenase (AkMO) *etnABCD*, and an epoxyalkane:coenzyme M transferase (EaCoMT) *etnE*, have been identified in *Mycobacterium* strain JS60. The monooxygenase catalyzes the initial oxidation of ETH to epoxyethane and VC to chlorooxirane, which are further metabolized by EaCoMT (Coleman et al. 2002). The closest homologs of the mycobacterial *etnE* and *etnABCD* genes are the propene monooxygenase and EaCoMT genes of *Rhodococcus* strain B276 (Coleman and Spain 2003b), which indicates that the initial steps in the VC-, ETH- and propene-degradation pathways share a common origin. The identity of remaining enzymes and metabolic intermediates in the proposed VC and ETH pathway (Coleman and Spain 2003b) are uncertain due to speculation based on very preliminary evidence. Linear plasmids have been implicated in alkene metabolism in VC-degraders (Coleman and Spain 2003a; Danko et al. 2003) and propene-degraders (Saeki et al. 1999; Krum and Ensign 2001), but little is known of the plasmids, apart from their size (180-320 kb), linear topology, and apparent association with the alkene-degrading phenotype.

Nocardioides strain JS614 is unusual among VC-degraders due to its high growth yields and growth rates on alkenes, and its physiological response to VC and ETH starvation (Coleman et al. 2002). Although EaCoMT genes have been identified in other mycobacteria (Coleman and Spain 2003a), the genetic basis of VC and ETH biodegradation in *Nocardioides* JS614 (Coleman

et al. 2002) is unknown. Other members of the genus *Nocardioides* (division Actinobacteria) biodegrade atrazine (Topp et al. 2000), butane (Hamamura and Arp 2000), methyl chloride (McAnulla et al. 2001), p-nitrophenol (Yoon et al. 1999), trinitrophenol (Rajan et al. 1996), jet fuel (Jung et al. 2002), 2,4,5-trichlorophenoxyacetic acid (Golovleva et al. 1990), and phenanthrene (Iwabuchi et al. 1998), and can biosynthesize antibiotics (Kubota et al. 2003), steroid building blocks (Fokina and Donova 2003) and chemotherapy drug precursors (Hanson et al. 2003). Despite the interesting metabolic abilities of *Nocardioides* strains, only in a few cases have the relevant genes been identified.

Many questions remain unanswered with respect to VC/ETH degradation in bacteria such as JS614. What are the final steps in the assimilation pathway? What is the difference between VC- and ETH-degraders? Are the genes definitely plasmid-borne, and if so, what type of catabolic plasmids are involved? Are there key marker genes that could serve as indicators of the presence of VC degraders? To begin addressing these questions, we investigated in detail the genetic basis of VC/ETH-degradation in *Nocardioides* JS614. We report here the sequencing and analysis of a 35 kb JS614 DNA fragment containing the alkene oxidation and assimilation genes, and we demonstrate that these genes are carried on a 290 kb linear plasmid.

MATERIALS AND METHODS

Bacterial strains, media, culture conditions. Plasmids and bacterial strains used in this study are shown in Table 1. For RNA extraction, *Nocardioide*s strain JS614 was grown on MSM broth, prepared as described previously (Coleman et al. 2002), containing either VC, ETH, or acetate at 22°C . For DNA extraction, strain JS614 was grown on 1/10 TSA + 1% glucose at 30°C. The pNoc614-negative JS614 strain was grown on 1/10 trypticase soy medium (TSB) at

30°C. *Escherichia coli* strains JM109, EZ, and EPI300-T1^{R} were grown on Luria Bertani medium (LB) at 37°C. All cultures were incubated aerobically with shaking at 165-250 rpm. *E. coli* transformants were plated on LB agar containing either Kanamycin (Km; 35 μg/ml) or chloramphenicol (Cm; 12.5 μg/ml). 5-Bromo-4-chloro-3-indolyl-β-d-galactopyranoside (X-gal; 80 μg/ml) and isopropyl-β-D-thiogalactopyranoside (IPTG; 12 μg/ml) were added where required.

Chemicals. ETH (99%) was from Matheson and VC (99.5%) was from Sigma. All other chemicals were reagent grade.

General molecular methods. JS614 genomic DNA was extracted as described previously (Coleman et al. 2002), except that glycine was not used, and the lysozyme incubation was 30 min. Plasmids and fosmids were extracted from *E. coli* strains by alkaline lysis (Sambrook 2001), and purified using the Miniprep spin kit (Qiagen). PCR products were extracted from agarose gels using the Minelute kit (Qiagen), and genomic DNA from CHEF gels was extracted using the QiaexII kit (Qiagen).

Standard PCR mixtures (25 μl) contained 1.5 mM Mg^{2+}, 50 pmol of each primer, approximately 400 ng of template DNA, and 0.3 U of Taq Polymerase. Standard PCR thermocycling parameters were 94°C for 3 min, then 30 cycles at 94°C for 1 min, 55-65°C for 30s (depending on primer pair), 72°C for 1 min, and 72°C for 10 min. Degenerate PCR thermocycling parameters were 94°C for 3 min, then 45 cycles at 94°C for 1 min, 52°C for 1 min, 72°C for 1 min, 72°C for 10 min. Primers used in this study are listed in Table 1. PCR products were T/A-cloned into the pDRIVE vector (Qiagen), and transformed either by heatshock into EZ competent cells or electroporation into strain JM109. Ligation-mediated PCR was done with the Genomewalker kit (Clontech), using JS614 genomic DNA digested with SspI

and NruI. Thermocycling parameters for genomewalker PCR were as specified in the kit instructions.

PCR products and genomic DNA were visualized by standard gel electrophoresis. DNA sequencing was performed at the Cornell University BioResource Center using an Applied Biosystems Automated 3730 DNA Analyzer or at the Roswell Park Cancer Institute Biopolymer Facility using a PE-ABI model 373A stretch sequencer. PCR products were sequenced from both DNA strands, while fosmid insert DNA was sequenced on one strand only. Southern blotting was performed as described previously (Coleman and Spain 2003b). The probes consisted of an 831 bp fragment of the EaCoMT gene in strain JS614, amplified by PCR using the primers CoM-F3 and CoM-R3, and a 635 bp fragment of the AkMO alpha subunit, amplified by PCR using the primers Alpha-F5 and Alpha R-5 (Table 1).

Preparation and screening of fosmid library. JS614 genomic DNA was randomly sheared using a syringe and 25-gauge needle, end-repaired with a T4 DNA Polymerase and T4 polynucleotide kinase enzyme mix (Epicentre), and separated by CHEF-PFGE (1% low melting point agarose, 0.5x TBE, 14°C, 6 V/cm, 120° angle), with switching times ramped from 1-6 s over 11 h. DNA fragments approximately 40 kb in size was excised, purified, and ligated into pCC1FOS (Epicentre). Packaged fosmids were incubated with *E. coli* strain EPI300-T1^{R} (Epicentre), and plated onto LB-Cm. Individual clones were transferred to a 96-well microtiter plate and grown in 100 µl of LB-Cm broth. Clones were pooled and screened by PCR as described previously (Coleman and Spain 2003b) using alpha-F5/R5 primers (Table 1).

Pulsed-field gel electrophoresis (PFGE). Preparation of agarose cell plugs and PFGE were performed as described previously (Coleman and Spain 2003a), with the following modifications: JS614 cells were suspended in agarose at OD_{600} = 10, lysozyme was used at 1

mg/ml for 2 h, proteinase K incubation was at 50°C, and lambda concatemers were regenerated at 45°C for 10 min.

RNA extraction and RT-PCR. JS614 cultures grown on VC, ETH, and acetate to mid-exponential phase were washed, resuspended in MSM (OD_{600} 10-50) and frozen in aliquots at –80°C. The RNeasy kit (Qiagen) was used for RNA extraction. Purified RNA was digested with DNAse (28U; 40 min, 22°C) and then repurified using the RNeasy protocol for RNA cleanup. Reverse-transcription PCR (RT-PCR) was performed with the Qiagen One-Step RT-PCR kit using 0.5 ng (*etnC* primers), 5 ng (16S and *comA* primers), or 10 ng (CoAT primers) of RNA as template. RT-PCR parameters were according to the kit instructions except that the annealing temperature for *etnC* primers was 62°C. Negative controls (no reverse transcriptase) were prepared with Taq PCR Core kit (Qiagen), and the positive control contained JS614 genomic DNA instead of RNA.

RESULTS AND DISCUSSION

PCR amplification of *etn*EABCD genes. Working under the hypothesis that the VC/ETH monooxygenase in strain JS614 was an alkene monooxygenase, we designed degenerate PCR primers (mono-F2, mono-R2) based on conserved regions of propene monooxygenases (Py2 and B-276). These primers yielded a band near the expected size in reactions with JS614 genomic DNA. The protein sequence encoded by the 740 bp product was very similar to the deduced protein sequence of *etn*C, the gene that encodes the putative monooxygenase alpha subunit from *Mycobacterium* strain JS60 and we thus designated the JS614 gene *etnC*. A similar approach (primers CoM-F1/CoM-R2) was used to retrieve the EaCoMT gene of JS614. Two different PCR products (950 bp and 980 bp) were obtained, and

sequencing indicated they were fragments of two different EaCoMT genes, sharing 92% identity (data not shown). The 950 bp EaCoMT amplicon was primed correctly, but the 980 bp product was primed at both ends by CoM-R2. The 950 bp product contains a 7 bp deletion that could render it non-functional via a frameshift (data not shown). PCR, cloning and sequencing performed independently in two laboratories produced the same results – i.e. two different EaCoMT amplicons, one with a 7 bp deletion. Based on the JS60 nomenclature, we designated the genes *etnE* (980 bp) and *etnE1* (950 bp).

Based on the above evidence we assumed that *etnE* is the functional EaCoMT in JS614, and designed a new primer pair (CoM-F3/CoM-R3) specific for the allele (Table 1). A new, non-degenerate primer pair (Alpha-F5/Alpha-R5) was also designed to amplify 635 bp of *etnC* (Table 1). The *etnE* amplicon (831 bp) was sequenced to confirm its identity, and then used to probe Southern blots of DNA digested with enzymes that did not cut the probe sequence. The results were two hybridizing bands in most cases (Fig. 2), supporting the initial hypothesis that two EaCoMT alleles exist in this strain. Southern hybridization experiments using the *etnC* amplicon as a probe indicated that only one copy of *etnC* is present in strain JS614 (Fig. 1). The proximity of *etnE* and *etnC* in the JS60 *etn* locus (Coleman and Spain 2003b) suggested that PCR could be used to recover the sequence between the JS614 *etnE* and *etnC* genes. PCR with the primer pair CoM-F3/Alpha-R5 produced a 4 kb PCR product. Sequencing confirmed that a fragment of the *etnEABCD* operon had been amplified. Sequencing of ligation-mediated PCR products was successful in recovering 831 bp that extends beyond the 3' end of the initial region (primer AkMO_GSP1).

Sequencing of a fosmid clone containing the *etn* locus. In order to rapidly recover DNA flanking the *etnEABCD* locus we prepared a fosmid library of JS614 total genomic DNA,

and screened the clones using AkMO PCR primers (alpha-F5/alpha-R5). From 96 recombinant fosmids screened, one positive clone, designated P1, was obtained. Clone P1 was sequenced via primer walking, both inward from the vector DNA, and outward from the *etnE* and *etnD* genes. All the sequences obtained from JS614 were assembled into a contiguous 34.8 kb DNA region designated JS614-P1 (Fig. 2).

General description of JS614-P1 DNA sequence. JS614-P1 (34,814 bp) had an overall GC content of 66%, which is slightly lower than in some other *Nocardioides* strains (Yoon et al. 1997; Yoon et al. 1999), but typical for high GC Gram-positive bacteria (Brock 1991). We identified 30 ORFs in the JS614-P1 nucleotide sequence (Fig. 2), 11 on one DNA strand and 19 on the other, the first and last of which were incomplete. Eighteen of the ORFs began with ATG, four with GTG, three with TTG, three with CTG and all were preceded by plausible ribosome binding sites. Of the 30 predicted protein sequences, ten had no significant database match, and one was related to a conserved hypothetical protein of unknown function. Of the remaining ORFs, we have assigned catabolic functions to nine, cofactor biosynthesis to five, plasmid or phage-related functions to four, leaving one miscellaneous gene. The average GC content of ORFs 1-11 was 65%, ORFs 12-21 was 63%, ORFs 22-26 was 71%, and ORFs 27-30 was 67%. The patterning of GC content across the 34.8 kb DNA fragment suggests that ORFs 12-26 might have been acquired by JS614 through lateral gene transfer.

Genes associated with alkene and epoxide metabolism. We began analyzing the JS614-P1 DNA sequence with the hypothesis that putative VC/ETH pathway genes would be clustered, as has been observed in other alkene-degrading bacteria (Saeki 1994; Swaving 1995; van Hylckama Vlieg 2000). ORFs 11-15 corresponded to *etnEABCD* identified by PCR (above). The high sequence identity of the JS614 *etnEABCD* genes to the AkMO and EaCoMT genes of

Mycobacterium JS60 EaCoMT and *Gordonia rubripertinctus* (hereafter referred to as *Rhodococcus rhodochrous*) B-276, (Table 2), is strong evidence that *etnABCD* encodes the VC/ETH-monooxygenase system and *etnE* encodes the EaCoMT of strain JS614. RT-PCR (Fig. 3) demonstrated expression of *etnC* in response to ETH and VC, and very high levels of EaCoMT activity were found in JS614 cell extracts (Mattes et al. 2004). The *etnABCD* genes of JS614 are most similar to the AkMO genes of *Mycobacterium* JS60, and based on strong sequence similarity to methane (Cardy et al. 1991), propene (Saeki 1994; Zhou 1996), propane (Kotani et al. 2003), and butane (Sluis et al. 2002) monooxygenases, the enzyme is likely to be a soluble di-iron monooxygenase (Leahy et al. 2003). The JS614 EaCoMT is most similar to that of B-276, rather than that of JS60, despite the fact that both JS60 and JS614 were isolated on VC, and B-276 was isolated on propene. In addition, preliminary experiments indicated that JS614 did not grow on propene or epoxypropane (data not shown), suggesting differences between VC/ETH and propene biodegradation enzymes exist despite the similarities in gene sequence. EaCoMT gene sequences are therefore not reliable indicators of the growth substrate of their host, and would need to be used with caution in attempts to detect VC-degraders *in situ* at contaminated sites. The AkMO genes might be a better target in this respect, but because AkMO genes are not yet available from strains isolated on ETH, it is difficult to say whether JS614- or JS60- based AkMO gene primers or probes would discriminate VC-assimilating bacteria from ETH-degraders.

Located just upstream of the JS614 EaCoMT gene are ORF9 and ORF10, encoding a putative acyl-CoA transferase and acyl-CoA synthetase. RT-PCR showed expression of ORF9 in response to ETH and VC (Fig. 3), indicating a role for the acyl-CoA transferase in alkene metabolism**.** ORF9 and ORF10 are homologous to the ORF1 and ORF2 found upstream of *etnE*

in *Mycobacterium* JS60 (Coleman and Spain 2003b) (Table 2), and in both strains, the 5' end of the synthetase overlaps by 13 nucleotides with the 3' end of the transferase, suggesting translational coupling. The discovery of similar genes in both JS614 and JS60 coupled with the above RT-PCR results provides strong albeit circumstantial evidence that proteins encoded by ORFs 9 and 10 participate in the VC/ETH pathway. Proteins encoded by ORFs 1 and 2 from JS60 were previously proposed to facilitate transfer of CoA to the VC and ETH-derived two-carbon unit (Coleman and Spain 2003b). Based on the apparent translational coupling of ORF9 and ORF10, an intriguing possibility is that a CoA-transferase/synthetase cycle exists in the VC pathway (Van Hellemond et al. 1998; Sanchez et al. 2000). The protein encoded by ORF9 would use an acyl-CoA intermediate as the CoA donor, and the protein encoded by ORF10 would catalyze the regeneration of the acyl-CoA from the acid using CoA-SH and ATP. Such a reaction would also fit with the previously observed stimulatory effect of CoA on epoxyethane metabolism in *Mycobacterium* E20 and L1 cell extracts (de Bont 1978; Hartmans 1992).

Enzymes related to those encoded by ORF9 and ORF10 act on dicarboxylic acids (pimelate, glutaconate) that possess some structural similarity to carboxymethyl-CoM (HOOC-CH_2-S-CH_2-CH_2-SO_3H), a possible intermediate of the VC/ETH pathway. It is a plausible hypothesis that the ORF9 and ORF10 gene products act to transform carboxymethyl-CoM into CoM-S-acetyl-S-CoA (Fig. 6). Subsequent reductive elimination of CoM from the intermediate would be facilitated by addition of the electron-withdrawing CoA thioester group, as previously noted for glutathione metabolism (van Hylckama Vlieg 2000).

The NCBI Conserved Domain Database (CDD)(Marchler-Bauer et al. 2003) identified the protein encoded by ORF8 as a member of the short-chain dehydrogenase family (Table 2). A well-characterized homologous protein is 2-(S)-hydroxypropyl-CoM dehydrogenase from the

propene-degrading *Xanthobacter* strain Py2 (Table 2), which catalyzes the stereospecific oxidation of 2-(S)-hydroxypropyl-CoM to 2-(S)-ketopropyl-CoM during propene assimilation (Allen 1999). The substrate of the ORF8 gene product in strain JS614 is most likely 2-hydroxyethyl-CoM (Coleman and Spain 2003b) which would yield either 2-ketoethyl-CoM or carboxymethyl-CoM, depending on whether one or two oxidation steps occur. The fact that the substrates of CoA transferases and synthetases (above) are usually acids suggests that the protein encoded by ORF8 catalyzes two oxidation steps in the VC/ETH pathway, linking the EaCoMT (ORF11) and CoA-transferase/synthetase (ORF9, ORF10) reactions, and yielding two reducing equivalents (Fig.6). The possibility also exists that an aldehyde dehydrogenase encoded elsewhere on the JS614 genome catalyzes the oxidation of 2-ketoethyl-CoM to carboxymethyl-CoM. In the propene assimilation pathway, two stereoselective dehydrogenases are present due to production of chiral alcohol intermediates by EaCoMT (Allen 1999). The presence of only one dehydrogenase in the VC and ETH pathway is expected because the alcohol intermediate is achiral. Dehydrogenase activity by the putative protein encoded by ORF8 would be expected to regenerate NADH from NAD^+, thus requiring NAD^+ for activity in cell-free extracts. The dependence of epoxyethane degradation on NAD^+ was observed in cell extracts of *Mycobacterium* E20 (de Bont 1978) and *Mycobacterium aurum* L1 (Hartmans 1992) suggesting that a dehydrogenase is active in the ETH-assimilation pathway in mycobacteria. The evidence for the participation of a dehydrogenase in the VC/ETH pathway in strain JS614 is currently based on sequence analysis and comparison to biochemical experiments with ETH-degrading mycobacteria and is therefore largely circumstantial.

CDD predicted that protein encoded by ORF7 is a member of the pyridine dinucleotide-disulfide oxidoreductase superfamily, and that the N-terminal portion of the putative protein

contains a smaller NAD(P)H binding domain within a larger FAD binding domain. The closest related protein of known function was coenzyme A disulfide reductase from *Staphylococcus aureus* (delCardayre and Davies 1998) (Table 2), but the sequence of ORF7 is also similar to that of 2-oxopropyl-CoM reductase in *Xanthobacter* Py2 (Table 2), an FAD-containing enzyme that catalyzes the reductive cleavage of 2-ketopropyl-coenzyme M. In strain Py2, the products of the reductase reaction are CoM-SH and either acetone or acetoacetate (Nocek et al. 2002), depending on the availability of CO_2. The results presented here suggest that by analogy, the protein encoded by ORF7 catalyzes the final step in the VC/ETH pathway in JS614, cleaving CoM-Acetyl-CoA into CoM-SH and acetyl-CoA. FAD stimulated epoxyethane degradation in cell-free extracts of ETH-grown *Mycobacterium* E20 (de Bont 1978), an observation which is consistent with the participation of a flavoprotein in the ETH-assimilation pathway.

The ORF7 gene product could function as an epoxide carboxylase, catalyzing the conversion of 2-ketoethyl-CoM to malonate semialdehyde, but because the product of the reaction is usually metabolized in bacteria by an energetically neutral decarboxylation to give acetyl-CoA, it is difficult to see the benefit of carboxylation in this case. An alignment of the deduced amino acid sequence of ORF7 with reductases of potentially similar function and the 2-oxopropyl-CoM reductase from *Xanthobacter* Py2 revealed that the Py2 reductase/carboxylase has an extended N-terminus and a 19 aa insertion not seen in the putative protein encoded by ORF7 or the other reductases (data not shown), suggesting the ORF7 gene product functions only as a reductase and not a carboxylase. Further biochemical experiments are required to test this hypothesis.

ORFs 1-6 might participate in coenzyme M biosynthesis. CoM is an unusual cofactor used only in a few biochemical reactions and only bacteria that use CoM in key

metabolic reactions seem to be able to produce CoM. Thus, it seems reasonable to expect that the genes for CoM biosynthesis would be linked to those that encode the enzymes that require CoM as a cofactor. Using this reasoning we postulated that CoM biosynthesis genes might be encoded near VC/ETH pathway genes in strain JS614. The discovery of glutathione biosynthesis genes next to glutathione S-transferase genes in isoprene-degrading *Rhodococcus* AD45 (van Hylckama Vlieg 2000) supports this hypothesis. Sequence analysis revealed that the protein encoded by ORF6 is similar to (2R)-phospho-3-sulfolactate synthase (ComA), the enzyme that catalyzes the first step in Coenzyme M biosynthesis in methanogens by the addition of a sulfite molecule to phosphoenolpyruvate, forming (2R)-phospho-3-sulfolactate (Graham et al. 2002). RT-PCR showed increased expression of ORF6 in response to ETH and VC (Fig. 3), suggesting that ORF6 is associated with VC/ETH metabolism**.** The propene-oxidizing *Xanthobacter* Py2 also contains a putative *comA* gene (Krum and Ensign 2001) near the alkene catabolic genes. In methanogens, five proteins (ComA synthase (EC 4.4.1.19), ComB hydrolase (EC 3.1.3.71), ComC dehydrogenase (EC 1.1.1.272), and ComDE decarboxylase (EC 4.1.1.79)) convert phosphoenolpyruvate into sulfoacetaldehyde, which reacts with cysteine, eventually yielding CoM (Graham et al. 2002). It is unclear if the same CoM biosynthetic pathway operates in methanogens and aerobic alkene-oxidizers, but our finding of a gene similar to *comA* in a second alkene-degrader suggests that the initial step in the pathway is similar.

ORF1 encodes a putative phosphoadenosine phosphosulfate (PAPS) reductase, which catalyzes the reduction of sulfate to sulfite as a first step in aerobic sulfate assimilation (Bick et al. 2000). Since ComA requires sulfite, it is possible that the putative PAPS reductase provides sulfite to protein encoded by ORF6 for CoM biosynthesis. ORF5 encodes a conserved hypothetical protein with similarity to proteins from methanogens (Table 2). Since the protein

encoded by ORF5 is related to a methanogenic protein, it is tempting to speculate that it also involved in CoM biosynthesis. ORF4 encodes a putative adenylosuccinate lyase (Table 2), an enzyme that catalyzes the cleavage of adenylosuccinate to phosphoadenosine (AMP) and fumarate as a step in *de novo* purine biosynthesis (Ratner 1973). It is unclear how the protein encoded by ORF4 could participate in CoM biosynthesis, but it is possible that it supplies AMP for production of PAPS, a possible substrate of the ORF1 gene product.

ORF3 encodes a putative 1-aminocyclopropane-1-carboxylate (ACC) deaminase, an enzyme catalyzing the degradation of ACC, which is an intermediate of ETH biosynthesis in plants (Klee et al. 1991). The putative function of ORF3 in the context of CoM biosynthesis is also uncertain, but it is intriguing to consider that strain JS614, a microorganism capable of growth on ETH, also possesses an enzyme that might degrade the biochemical precursor of ETH. The presence of both ACC deaminase and ETH monooxygenase in JS614 could suggest a plant-associated lifestyle. ACC deaminase interferes with plant ETH metabolism, promoting root elongation, and thus increasing the size of the rhizosphere niche available to the bacteria.

ORF2 encodes a putative argininosuccinate lyase (Table 2), which in other systems catalyzes the final step in arginine biosynthesis by cleaving argininosuccinate to arginine and fumarate (Ratner 1973). Interestingly, a putative argininosuccinate lyase gene was found immediately adjacent to *xecG* (a putative ComA gene) in *Xanthobacter* Py2 (Krum and Ensign 2001), suggesting involvement in CoM biosynthesis. At this stage it is difficult to define the function of the protein encoded by ORF2 with respect to CoM biosynthesis. In the putative operon consisting of ORFs 1-6, ORF6 is the only gene similar to methanogenic CoM biosynthesis genes, suggesting either that ComBCDE homologs are present elsewhere in the genome, or that ORFs 1-5 encode an alternate CoM biosynthesis pathway. Further work is

required to test these hypotheses. Interestingly, a gene similar to *comA* (*yitD*) is found in the *Bacillus subtilis* genome (Kunst et al. 1997). The function of the gene has not been investigated to our knowledge, but sporulating *Bacillus* cells accumulate sulfolactate (Bonsen et al. 1969), suggesting a role for ComA and perhaps CoM synthesis in sporulation. Other genes in the *Bacillus subtilis yit* cluster might participate in CoM biosynthesis. For example, YitC is a putative phosphosulfolactate phosphatase, possibly related to ComB, which catalyzes the second step in CoM biosynthesis in methanogens (Graham et al. 2001). YitA, a putative sulfate adenylate transferase and YitB, a possible PAPS reductase, could participate in production of sulfite, a predicted substrate of YitD. The proximity of a predicted PAPS reductase gene and phosphosulfolactate synthase gene in the *yit* operon parallels the proximity of similar genes in JS614. Additionally, YitF, a possible muconate cycloisomerase, could be related to the protein encoded by ORF4 (Table 2). Overall, the similarities between *yit* cluster genes in *Bacillus subtilis* and ORFs 1-6 in JS614-P1 suggest these gene clusters are involved in a novel pathway of CoM biosynthesis. At this point, evidence for a novel CoM biosynthetic pathway in JS614 and *Bacillus* is based wholly on the above putative gene sequence analysis.

Plasmid-related genes. Recent evidence that implicate plasmids in propene-(Saeki et al. 1999; Krum and Ensign 2001) and VC/ETH-assimilation (Coleman and Spain 2003a; Danko et al. 2003) prompted us to search for plasmid-related genes on JS614-P1. ORF23 is predicted to encode a 1818 aa protein with several possible functions. A large portion of the ORF23 sequence is related to putative TraA-like protein sequences from plasmids in *cis*-1,4-polyisoprene-degrading *Gordonia westfalica* (Broker et al. 2004), atrazine-degrading *Arthrobacter aurescens*, and foal pathogen *Rhodococcus equi* (Takai et al. 2000). TraA proteins function as DNA relaxases, which initiate conjugative plasmid transfer by cleaving DNA within

the plasmid origin of transfer (OriT) (Grohmann et al. 2003). ORF23 also contains two partial conserved protein domains RecD (COG0507), a putative exonuclease, and DnaG (COG0358), a putative primase. In *E.coli*, RecD confers exonuclease activity to the RecBCD enzyme during homologous recombination (Snyder and Champness 1997), but the purpose of the RecD domain in ORF23 is unclear. The DnaG domain is associated with DNA primases, which are well-known to be involved in plasmid replication.

Immediately upstream of ORF23 is a region rich in inverted and tandem repeat sequences. A protein might be encoded here (ORF22), but there is evidence that the region is actually the OriT of the JS614 VC/ETH catabolic plasmid. The putative JS614 OriT region contains a sequence (AGGGCGCGGGTA) very similar to the consensus OriT core sequence identified in RSF1010, pTF1, and Ti plasmids (AGGGCGCACTTA) (Cook and Farrand 1992). In addition, the putative JS614 OriT core sequence is found at the start of a DNA repeat in a repeat-rich region next to a likely plasmid transfer gene, similar to the pattern observed with Gram-negative plasmid OriTs.

BLAST analysis indicated that sequence of ORF25 is similar to those of plasmid partitioning proteins (ParA, ParB) from various actinomycetes, including those of the atrazine catabolic plasmid pAA1 of *Arthrobacter aurescens* and the nicotine catabolic plasmid pAO1 of *Arthrobacter nicotinivorans*. In well-studied elements such as the *E.coli* F plasmid, ParA and ParB homologs help to evenly distribute the low-copy number plasmid among the daughter cells at cell division (Bignell and Thomas 2001).

ORF33 encodes a putative DNA integrase-recombinase most similar to that found on a 210 kb linear megaplasmid in isopropylbenzene-degrading *Rhodococcus erythropolis* strain BD2 (Stecker et al. 2003). The next closest BLAST hit was another plasmid-encoded integrase-

recombinase from *Streptomyces coelicolor* A3(2) (Table 2). Based on sequence similarity, and the fact that it contains a conserved RHRY tetrad, the protein encoded by ORF33 is likely to be a member of the tyrosine recombinase family, which catalyze site-specific integration and excision reactions in prokaryotes, eukaryotes and mobile genetic elements (Nunes-Duby et al. 1998) The presence of an integrase gene implies that the JS614-P1 DNA region could integrate into the chromosome. The simultaneous presence of integrated and free plasmids in a culture could explain why an EaCoMT probe hybridized to both plasmid and chromosomal DNA on PFGE gels prepared from mycobacterial VC-degraders (Coleman and Spain 2003a).

Miscellaneous genes. Based on BLAST results, the protein encoded by ORF21 is very likely a molybdopterin-containing oxidoreductase, and CDD detected a molybdopterin binding site at the 3' end of the deduced protein sequence of ORF21. Genes with the closest match to ORF21 and encode proteins with known functions are biotin sulfoxide reductase and dimethyl sulfoxide (DMSO)/ trimethylamine N-oxide (TMAO) reductase from *Rhodobacter sphaeroides* (Pollock V. V. and Barber M. J. 1995; Mouncey et al. 1997) but the overall closest BLAST matches to ORF21 (e=0) were to ORFs from the genomes of *Pseudomonas syringae, Azotobacter vinelandii, Bradyrhizobium japonicum,* and *Mesorhizobium* sp. If acting as a DMSO/TMOA reductase, the protein encoded by ORF21 could allow anaerobic growth of JS614 on alternative terminal electron acceptors apart from O_2.

Putative promoter sequences and transcriptional terminators. Reports that toluene monooxygenase gene clusters were under the control of sigma 54-dependent promoters (Byrne and Olsen 1996; Arenghi et al. 1999) prompted us to search for putative sigma-54 promoter sequences in JS614-P1. A possible sigma-54 promoter sequence ***GG***CACCCTCCGTT***GC***TG (conserved -24 and –12 elements in bold italics) was found 143 bp

upstream of the ORF7 start codon. Another possible sigma-54 promoter sequence ***GG***AACGCTAGAT***GC***GC was found on the complementary strand 164 bp upstream of the ORF6 start codon. The location of these putative sigma-54 promoter sequences in the non-coding region between the VC/ETH catabolic genes and putative coenzyme M biosynthesis genes suggests that a single regulatory protein could control both operons, although we did not find any obvious regulatory genes in the DNA region sequenced.

The noncoding region between *etnC* and *etnD* (GATCACCGTCGG**GTCGGGA GCTTGGGGCTCCCGAC**GGCAGCGCAGACCTTCTGAACTTGTCGACAAAGAATGGC GAACGCTCC) was extremely resistant to DNA sequencing and the possibility exists that additional DNA remains unsequenced in this region. Analysis of the sequence suggested that an inverted repeat (bold) is present. Inverted repeats can cause hairpin loops in single stranded DNA that can interfere with sequencing (Ishikawa et al. 2003). The corresponding hairpin in the nascent mRNA strand can act as a rho-independent transcription terminator if an AT-rich region is also found downstream (Snyder and Champness 1997). A fairly AT-rich region is located immediately downstream of the JS614 inverted repeat, suggesting that this repeat is indeed part of a transcriptional terminator, and implying that the reductase gene *etnD* could be regulated independently of the rest of the *etn* operon.

The linear plasmid of strain JS614. The discovery of both plasmid genes and VC/ETH catabolic genes in the JS614-P1 DNA region provides strong evidence that VC/ETH-biodegradation in JS614 is a plasmid-encoded trait, and prompted us to investigate the possibility in more detail. CHEF-PFGE experiments with undigested JS614 genomic DNA revealed the presence of an extrachromosomal element, designated pNoc614 (Fig. 4). Increasing the switching time from 10-40s to 20-80s had no effect on pNoc614 migration relative to the linear

markers (data not shown). The plasmid topology of pNoc614 was therefore assumed to be linear, and a size of 290 kb was estimated. Due to previous difficulties in interpreting Southern blots of pulsed-field gels prepared from VC-degrading mycobacteria, we tested a PCR-based approach (Krum and Ensign 2001) to determine the location of the alkene degradation genes.

Chromosomal DNA and pNoc614 DNA from JS614 were separated by CHEF-PFGE, and purified. PCR with AkMO-specific primers (Alpha-F5 and Alpha-R5) and 2 ng DNA template indicated that the *etn*C template concentration was highest in pNoc614 DNA, providing strong evidence that *etn*C, and by inference, the entire JS614-P1 region are carried on pNoc614 (Fig. 5). Faint AkMO PCR products were occasionally seen with PFGE gel slices taken from chromosomal DNA, and above and below the plasmid band, which might be a result of insufficient resolution of plasmid DNA from chromosomal DNA during electrophoresis, integration of plasmid DNA into the chromosome by phage integrases, and/or a background of DNA fragments resulting from nuclease activity. It was difficult to obtain clear PFGE gels with JS614, despite the easier lysis of this strain compared to the VC-degrading mycobacteria (Coleman and Spain 2003a). Unusual nuclease activity and smearing during PFGE has also been observed in *Streptomyces* and other actinomycete strains (Ray et al. 1992; Coleman and Spain 2003a).

A plasmid-cured JS614 strain does not grow on VC or ETH. Repeated subculturing of JS614 on 1/10 TSA + 1% glucose plates and PCR screening of single colonies (alpha-F5/alpha-R5 primers) led to the isolation of a strain that appeared to lack *etnC* (Fig. 5). This strain was designated JS614-C. The 16S rDNA (first 500 bp) of JS614-C was sequenced and found to be 100% identical to that of strain JS614, indicating that JS614-C was not a contaminant. PFGE analysis of JS614-C indicated that it lacked not only *etnC*, but also the

whole plasmid pNoc614 (Fig. 4). Strain JS614-C did not degrade VC or ETH in minimal growth media after more than 30 days of incubation (data not shown). The lack of growth of JS614-C was not due to the unusual starvation response of JS614, because the wild-type strain grown in non-selective media degraded ETH after several days lag time under the same conditions (Mattes et al. 2004). Although the non-selective media used to grow the inocula of JS614 and JS614-C differed in this experiment, in other experiments, we have observed no significant difference between acetate-grown and TSB-grown JS614 cells with respect to lag time before alkene degradation begins. Strain JS614-C grew well on acetate in minimal medium (data not shown), ruling out the possibility of an auxotrophic mutation causing the observed lack of growth. The finding that loss of *etnC* coincides with curing of the pNoc614 plasmid and lack of growth on VC and ETH provides compelling evidence that the VC and ETH biodegradation genes are carried on pNoc614 in strain JS614.

The JS614 fosmid clone representing a fragment of pNoc614 contained VC and ETH biodegradation genes, possible CoM biosynthesis genes, and plasmid-associated genes. This is the first study to use a sequence-based approach to conclusively demonstrate that VC/ETH degradation genes are plasmid-borne, a finding which suggests horizontal transfer of VC biodegradation genes in the environment is possible. This is also the first study to obtain significant amounts of sequence data from an alkene catabolic plasmid. The gene cluster encoding VC and ETH biodegradation was found immediately adjacent to the putative CoM biosynthesis genes, and both gene clusters appeared to be under the control of sigma-54 promoters in a central non-coding region, suggesting that both gene clusters are coordinately regulated. While our evidence that ORF1-ORF6 encode CoM biosynthesis is not rigorous, there are three lines of circumstantial evidence supporting this conclusion: 1) ORF6 is similar to a

known CoM biosynthetic gene, 2) ORF6 is transcribed in response to VC and ETH, and 3) ORF1-ORF6 are located immediately adjacent to genes encoding a catabolic pathway known to require CoM. It is likely that ORF7-ORF15 encode the enzymes that catalyze the complete pathway of VC and ETH assimilation to central metabolites. Hypothetical pathways of VC and ETH assimilation were generated based on the predicted functions of ORF7-15 (Fig.6). The pathways (Fig. 6) are based on analogy with *Mycobacterium* strains JS60 (Coleman and Spain 2003b) and E20 (de Bont 1978), as well as analogy with propene-oxidizing strains (Ensign 2001) and similarity to sequences in GenBank. Despite the lack of biochemical evidence thus far, we believe it is useful to provide our best guess at the pathway so that hypotheses are available for future experimentation. An increased understanding of the biochemical pathway of VC and ETH oxidation is not only important with respect to natural attenuation of VC, but might also facilitate a better understanding of biogeochemical cycling of ETH, a plant hormone and greenhouse gas.

Although the sequence data thus far suggest that the alkene degradation pathways are identical in *Nocardioides* strain JS614 and *Mycobacterium* strain JS60, the question of why the growth yield and growth rate on VC and ETH are higher in JS614 remains unanswered. Our discovery of a second EaCoMT allele in strain JS614 might be relevant to the question. If the JS614 *etnE1* gene encoded a functional enzyme, expression of this enzyme would lead to increased EaCoMT activity, and more efficient capture of reactive epoxides as CoM conjugates before they are lost to cell-damaging and non-growth supporting side-reactions.

The sequencing of a large fragment of genomic DNA from JS614 has greatly increased the database of genes from aerobic VC-assimilating bacteria, thus facilitating future *in situ* molecular studies of these bacteria. AkMO and other catabolic genes from JS614 could also be used in biocatalysis or metabolic engineering applications where expression of a highly active

alkene monooxygenase or the design of novel biochemical pathways is desired. Our data provide many novel targets for PCR- or probe-based detection of VC/ETH-degraders. For example, the plasmid-associated genes such as TraA reported in this study could be used indicators of the presence of pNoc614-type plasmids, thus complementing data obtained from the use of traditional catabolic gene probes/primers. Our results suggest that the genes encoding VC and ETH degradation are highly conserved, even between different genera, thus validating the use of such genes as indicators of the presence of VC/ETH degraders *in situ*. Unfortunately, our data do not allow us to distinguish between VC and ETH degraders on the basis of DNA sequence, which would be a prerequisite for determining whether growth-linked or cometabolic processes are responsible for VC degradation in the field. A detailed molecular analysis of ETH-degraders that cannot grow on VC is required to address this issue, and to shed light on the mechanism of evolution of VC-degraders from ETH-degraders.

ACKNOWLEDGEMENTS

We thank Anthony Hay, Ruth Richardson, and Steve Zinder for use of their laboratories and for technical advice. We thank Michelle Detwiler at RPCI for her DNA sequencing expertise and persistence in attempts to sequence the hairpin loop. We also thank Juli Rubin and Brian Weisenstein for technical assistance. The U.S. Strategic Environmental Research and Development Program funded this work.

REFERENCES

Allen JR, and S. A. Ensign (1999) Two short-chain dehydrogenases confer stereoselectivity for enantiomers of epoxypropane in the multiprotein epoxide carboxylating systems of *Xanthobacter* strain Py2 and *Nocardia corallina* B276. Biochemistry 38:247-256

Arenghi FLG, Pinti M, Galli E, Barbieri P (1999) Identification of the *Pseudomonas stutzeri* OX1 toluene-o-xylene monooxygenase regulatory gene (touR) and of its cognate promoter. Appl. Environ. Microbiol. 65:4057-4063

Bick JA, Dennis JJ, Zylstra GJ, Nowack J, Leustek T (2000) Identification of a new class of 5'-Adenylylsulfate (APS) reductases from sulfate-assimilating bacteria. J. Bacteriol. 182:135-142

Bignell C, Thomas CM (2001) The bacterial ParA-ParB partitioning proteins. J. Biotechnol. 91:1-34

Bonsen PP, Spudich JA, Nelson DL, Kornberg A (1969) Biochemical studies of bacterial sporulation and germination. XII. A sulfonic acid as a major sulfur compound of *Bacillus subtilis* spores. J. Bacteriol. 98:62-68.

Brock TD, and Madigan, M. T. (1991) Biology of Microorganisms. In, 7th edn. Prentice-Hall, Englewood Cliffs, NJ, p 148

Broker D, Arenskotter M, Legatzki A, Nies DH, Steinbuchel A (2004) Characterization of the 101-kilobase-pair megaplasmid pKB1, isolated from the rubber-degrading bacterium *Gordonia westfalica* Kb1. J. Bacteriol. 186:212-225

Bucher JR, Cooper, G., Haseman, J. K., Jameson, C. W., Longnecker, M., Kamel, F., Maronpot, R., Matthews, H.B., Melnick, R., Newbold, R., Tennant, R.W., Thompson, C., Waalkes, M. (2001) Ninth report on carcinogens. In. U.S. Dept. of Health and Human Services, National Toxicology Program. [http://ehis.niehs.nih.gov/roc/ninth/known/vinylchloride.pdf]

Byrne A, Olsen R (1996) Cascade regulation of the toluene-3-monooxygenase operon (tbuA1UBVA2C) of *Burkholderia pickettii* PKO1: role of the tbuA1 promoter (PtbuA1) in the expression of its cognate activator, TbuT. J. Bacteriol. 178:6327-6337

Cardy DL, Laidler V, Salmond GP, Murrell JC (1991) Molecular analysis of the methane monooxygenase (MMO) gene cluster of *Methylosinus trichosporium* OB3b. Mol. Microbiol. 5:335-342.

Coleman NV, Mattes TE, Gossett JM, Spain JC (2002) Phylogenetic and kinetic diversity of aerobic vinyl chloride-assimilating bacteria from contaminated sites. Appl. Environ. Microbiol. 68:6162-6171.

Coleman NV, Spain JC (2003a) Distribution of the coenzyme M pathway of epoxide metabolism among ethene- and vinyl chloride-degrading *Mycobacterium* strains. Appl. Environ. Microbiol. 69:6041-6046

Coleman NV, Spain JC (2003b) Epoxyalkane:Coenzyme M transferase in the ethene and vinyl chloride biodegradation pathways of *Mycobacterium* strain JS60. J. Bacteriol. 185:5536-5545

Cook DM, Farrand SK (1992) The oriT region of the *Agrobacterium tumefaciens* Ti plasmid pTiC58 shares DNA sequence identity with the transfer origins of RSF1010 and RK2/RP4 and with T-region borders. J. Bacteriol. 174:6238-6246.

Danko AS, Meizhong L, Freedman DL (2003) Involvement of a mega-linear plasmid in aerobic biodegradation of vinyl chloride. Abstracts of the Seventh International Symposium of In Situ and On-site Bioremediation, Orlando, FL

Davis JW, and C. L. Carpenter (1990) Aerobic degradation of vinyl chloride in groundwater samples. Appl. Environ. Microbiol. 56:3878-3880

de Bont JAM, and W. Harder (1978) Metabolism of ethylene by *Mycobacterium* E 20. FEMS Microbiol. Lett. 3:89-93

delCardayre SB, Davies JE (1998) *Staphylococcus aureus* Coenzyme A Disulfide Reductase, a new subfamily of pyridine nucleotide-disulfide oxidoreductase. J. Biol. Chem. 273:5752-5757

Edwards EA, and Cox, E. E. (1997) Field and laboratory studies of sequential anaerobic-aerobic chlorinated solvent biodegradation. In: Alleman BC, and Leeman, A. (ed) In Situ and On-Site Bioremediation. Battelle Press, Columbus, OH, pp 261-265

Ensign SA (2001) Microbial metabolism of aliphatic alkenes. Biochemistry 40:5845-5853.

Fennell DE, Carroll AB, Gossett JM, Zinder SH (2001) Assessment of indigenous reductive dechlorinating potential at a TCE-contaminated site using microcosms, polymerase chain reaction analysis, and site data. Environ. Sci. Technol. 35:1830-1839.

Fokina VV, Donova MV (2003) 21-Acetoxy-pregna-4(5),9(11),16(17)-triene-21-ol-3,20-dione conversion by *Nocardioides simplex* VKM Ac-2033D. J. Ster. Biochem. Molec. Biol. 87:319-325

Golovleva LA, Pertsova RN, Evtushenko LI, Baskunov BP (1990) Degradation of 2,4,5-trichlorophenoxyacetic acid by a *Nocardioides* simplex culture. Biodegradation 1:263-271

Graham DE, Graupner M, Xu H, White RH (2001) Identification of coenzyme M biosynthetic 2-phosphosulfolactate phosphatase. A member of a new class of Mg^{2+}-dependent acid phosphatases. Eur. J. Biochem. 268:5176-5188

Graham DE, Xu H, White RH (2002) Identification of Coenzyme M Biosynthetic Phosphosulfolactate Synthase. J. Biol. Chem. 277:13421-13429

Grohmann E, Muth G, Espinosa M (2003) Conjugative Plasmid Transfer in Gram-Positive Bacteria. Microbiol. Mol. Biol. Rev. 67:277-301

Hamamura N, Arp DJ (2000) Isolation and characterization of alkane-utilizing Nocardioides sp. strain CF8. FEMS Microbiol. Lett. 186:21-26

Hanson RL, Kant J, Patel RN (2003) Conversion of 7-Deoxy-10-deacetylbaccatin III to 6-alpha-Hydroxy-7-deoxy-10-deacetylbaccatin III by *Nocardioides luteus*. Biotechnol. Appl. Biochem. 4:4

Hartmans S, and J. A. M. de Bont (1992) Aerobic vinyl chloride metabolism in *Mycobacterium aurum* L1. Appl. Environ. Microbiol. 58:1220-1226

Ishikawa T et al. (2003) Use of transcriptional sequencing in difficult to read areas of the genome. Analytical Biochemistry 316:202-207

Iwabuchi T, Inomata YY, Katsuta A, Harayama S (1998) Isolation and characterization of marine *Nocardioides* capable of growing and degrading phenanthrene at 42 degrees C. J. Marine Biotech. 6:86-90

Jung CM, Broberg C, Giuliani J, Kirk LL, Hanne LF (2002) Characterization of JP-7 jet fuel degradation by the bacterium *Nocardioides luteus* strain BAFB. J. Basic Microbio. 42:127-131

Klee HJ, Hayford MB, Kretzmer KA, Barry GF, Kishore GM (1991) Control of ethylene synthesis by expression of a bacterial enzyme in transgenic tomato plants. Plant Cell 3:1187-1193.

Kotani T, Yamamoto T, Yurimoto H, Sakai Y, Kato N (2003) Propane monooxygenase and NAD+-dependent secondary alcohol dehydrogenase in propane metabolism by *Gordonia* sp. strain TY-5. J. Bacteriol. 185:7120-7128

Krum JG, Ensign SA (2001) Evidence that a linear megaplasmid encodes enzymes of aliphatic alkene and epoxide metabolism and coenzyme M (2-mercaptoethanesulfonate) biosynthesis in Xanthobacter strain Py2. J. Bacteriol. 183:2172-2177.

Kubota NK et al. (2003) Piericidins C5 and C6: new 4-pyridinol compounds produced by *Streptomyces* sp. and *Nocardioides* sp. Bioorg. Med. Chem. 11:4569-4575

Kunst F et al. (1997) The complete genome sequence of the gram-positive bacterium *Bacillus subtilis*. Nature 390:249-256.

Lane DJ (1991) 16S/23S rRNA sequencing. In: Stackbrandt E, Goodfellow M (eds) Nucleic acid techniques in bacterial systematics. John Wiley and Sons, Chichester, U.K., pp 177-203

Leahy JG, Batchelor PJ, Morcomb SM (2003) Evolution of the soluble diiron monooxygenases. FEMS Microbiology Reviews 27:449-479

Lee MD, J. M. Odom, and R. J. Buchanan, Jr. (1998) New perspectives on microbial dehalogenation of chlorinated solvents: insights from the field. Annu. Rev. Microbiol. 52:423-452

Marchler-Bauer A et al. (2003) CDD: a curated Entrez database of conserved domain alignments. Nucl. Acids. Res. 31:383-387

Mattes TE, Coleman NV, Spain JC, Gossett JM (2004) Characterization of the vinyl chloride and ethene starvation response in *Nocardioides* strain JS614. Submitted

McAnulla C, McDonald IR, Murrell JC (2001) Methyl chloride utilising bacteria are ubiquitous in the natural environment. FEMS Microbiol. Lett. 201:151-155

Mouncey N, Choudhary M, Kaplan S (1997) Characterization of genes encoding dimethyl sulfoxide reductase of *Rhodobacter sphaeroides* 2.4.1T: an essential metabolic gene function encoded on chromosome II. J. Bacteriol. 179:7617-7624

Nocek B, Jang SB, Jeong MS, Clark DD, Ensign SA, Peters JW (2002) Structural basis for CO_2 fixation by a novel member of the disulfide oxidoreductase family of enzymes, 2-ketopropyl-coenzyme M oxidoreductase/carboxylase. Biochemistry 41:12907-12913.

Nunes-Duby S, Kwon H, Tirumalai R, Ellenberger T, Landy A (1998) Similarities and differences among 105 members of the Int family of site-specific recombinases. Nucl. Acids. Res. 26:391-406

Pollock V. V., Barber M. J. (1995) Molecular cloning and expression of biotin sulfoxide reductase from *Rhodobacter sphaeroides* forma sp. denitrificans. Archives of Biochemistry and Biophysics 318:322-332

Radajewski S, Ineson P, Parekh NR, Murrell JC (2000) Stable-isotope probing as a tool in microbial ecology. Nature 403:646-649.

Rajan J et al. (1996) Mineralization of 2,4,6-trinitrophenol (picric acid): Characterization and phylogenetic identification of microbial strains. J. Ind. Microbiol. 16:319-324

Ratner S (1973) Argininosuccinases and Adenylosuccinases. In: Boyer PD (ed) The Enzymes, 3rd edn. Academic Press, New York, pp 167-197

Ray T, Weaden J, Dyson P (1992) Tris-dependent site-specific cleavage of *Streptomyces lividans* DNA. FEMS Microbiology Letters 96:247-252

Richardson RE, Bhupathiraju VK, Song DL, Goulet TA, Alvarez-Cohen L (2002) Phylogenetic characterization of microbial communities that reductively dechlorinate TCE based upon a combination of molecular techniques. Environ. Sci. Technol. 36:2652-2662.

Saeki H, Akira M, Furuhashi K, Averhoff B, Gottschalk G (1999) Degradation of trichloroethene by a linear-plasmid-encoded alkene monooxygenase in *Rhodococcus corallinus* (*Nocardia corallina*) B-276. Microbiology 145:1721-1730.

Saeki H, and K. Furuhashi (1994) Cloning and characterization of a *Nocardia corallina* B-276 gene cluster encoding alkene monooxygenase. J. Ferment. Bioeng. 78:399-406

Sambrook J, and D. W. Russell (2001) Molecular cloning: a laboratory manual, 3rd edn. Cold Spring Harbor Laboratory Press, New York

Sanchez LB, Galperin MY, Muller M (2000) Acetyl-CoA synthetase from the Amitochondriate eukaryote *Giardia lamblia* belongs to the newly recognized superfamily of acyl-CoA synthetases (nucleoside diphosphate-forming). J. Biol. Chem. 275:5794-5803

Sluis MK, Sayavedra-Soto LA, Arp DJ (2002) Molecular analysis of the soluble butane monooxygenase from '*Pseudomonas butanovora*'. Microbiology 148:3617-3629

Snyder L, Champness W (1997) Molecular Genetics of Bacteria. ASM Press, Washington D.C.

Squillace PJ, M. J. Moran, W. W. Lapham, C. V. Price, R. M. Clawges, and J. S. Zogorski (1999) Volatile organic compounds in untreated ambient groundwater of the United States, 1985-1995. Environ. Sci. Technol. 33:4176-4187

Stecker C, Johann A, Herzberg C, Averhoff B, Gottschalk G (2003) Complete nucleotide sequence and genetic organization of the 210-kilobase linear plasmid of *Rhodococcus erythropolis* BD2. J. Bacteriol. 185:5269-5274

Swaving J, C. A. G. M. Weijers, A. J. J. van Ooyen, and J. A. M. de Bont (1995) Complementation of *Xanthobacter* Py2 mutants defective in epoxyalkane degradation, and expression and nucleotide sequence of the complementing DNA fragment. Microbiology 141:477-484

Takai S et al. (2000) DNA Sequence and Comparison of Virulence Plasmids from *Rhodococcus equi* ATCC 33701 and 103. Infect. Immun. 68:6840-6847

Topp E, Mulbry WM, Zhu H, Nour SM, Cuppels D (2000) Characterization of s-triazine herbicide metabolism by a *Nocardioides* sp. isolated from agricultural soils. Appl. Environ. Microbiol. 66:3134-3141

van Ginkel CG, H. G. J. Welten, and J. A. M. de Bont (1986) Epoxidation of alkenes by alkene-grown *Xanthobacter* spp. Appl. Microbiol. Biotechnol. 24:334-337

van Ginkel CG, H. G. J. Welten, and J. A. M. de Bont (1987) Oxidation of gaseous and volatile hydrocarbons by selected alkene-utilizing bacteria. Appl. Environ. Microbiol. 53:2903-2907

Van Hellemond JJ, Opperdoes FR, Tielens AGM (1998) Trypanosomatidae produce acetate via a mitochondrial acetate:succinate CoA transferase. Proc. Natl. Acad. Sci. USA 95:3036-3041

van Hylckama Vlieg JE, H. Leemhuis, J. H. L. Spelberg, and D. B. Janssen (2000) Characterization of the gene cluster involved in isoprene metabolism in *Rhodococcus* sp. strain AD45. J. Bacteriol. 182:1956-1963

Verce MF, R. L. Ulrich, and D. L. Freedman (2000) Characterization of an isolate that uses vinyl chloride as a growth substrate under aerobic conditions. Appl. Environ. Microbiol. 66:3535-3542

Verce MF, R. L. Ulrich, and D. L. Freedman (2001) Transition from cometabolic to growth-linked biodegradation of vinyl chloride by a *Pseudomonas* sp. isolated on ethene. Environ. Sci. Technol. 35:4242-4251

Yanisch-Perron C, Vieira J, Messing J (1985) Improved M13 phage cloning vectors and host strains: nucleotide sequences of the M13mp18 and pUC19 vectors. Gene 33:103-119.

Yoon J, Rhee S, Lee J, Park Y, Lee S (1997) *Nocardioides pyridinolyticus* sp. nov., a pyridine-degrading bacterium isolated from the oxic zone of an oil shale column. Int. J. Syst. Bacteriol. 47:933-938

Yoon JH, Cho YG, Lee ST, Suzuki Ki, Nakase T, Park YH (1999) *Nocardioides nitrophenolicus* sp. nov., a p-nitrophenol-degrading bacterium. Int. J. Syst. Bacteriol. 49:675-680

Zhou NY, C. K. Chion, and D. J. Leak (1996) Cloning and expression of the genes encoding the propene monooxygenase from *Xanthobacter* Py2. Appl. Microbiol. Biotechnol. 44:582-588

Table 1. Bacterial strains, plasmids and oligonucleotides

Material	Relevant characteristics	Reference
Strains		
Nocardioides sp., strain JS614	Grows on VC and ethene as sole carbon sources	(Coleman et al. 2002)
Nocardioides sp., strain JS614-C (pNoc614-negative)	Mutant JS614 strain unable to grow on VC or ETH	This study
Escherichia coli strain JM109	*recA*1 *supE*44 *endA*1 *hsdR*17 *gyrA*96 *relA*1 *thi* Δ(*lac-proAB*) F′[*traD*36 *proAB*$^{+}$ *lacI*^{q} *lacZ* ΔM15]	(Yanisch-Perron et al. 1985)
Escherichia coli strain EZ	[F'::Tn *10* Tc^{r}) *proA*$^{+}$*B*$^{+}$*lacI*^{q}Z Δ*M15*] *recA1 endA1 hsdR17* ($r_{K12}^{-}m_{K12}^{+}$)*lac glnV44 thi*$^{-}$*1 gyrA96 relA1*	Qiagen
Escherichia coli strain EPI300™-T1^{R}	[F^{-} mcrA _(*mrr-hs*dRM*S-mc*rBC) _80*dlac*Z_M15 _*lac*X74 *rec*A1 *en*dA1 *ara*D1*39* _(*ara*, *leu*)7697 *gal*U *gal*K _$^{-}$ *rps*L *nup*G *trf*A *ton*A]	Epicentre
Plasmids and fosmids		
pDRIVE	Km^{R}, Ap^{R}, 3.9 kb, T/A-cloning vector	Qiagen
pCC1FOS	Cm^{R}, 8.2 kb, Copycontrol™ Fosmid vector	Epicentre
Oligonucleotides (5'– 3')		
CoM-F1	ATGGTGGGGAACTACCCGAATCC	(Coleman and Spain 2003b)
CoM-R2	TCGTCGGCAGTTTCGGTGATCGTGCTCTT	(Coleman and Spain 2003b)
CoM-F3	GCTCTCAAGATGTGCTTCTGCCAACCA	This study
CoM-R3	CGGTGCGTCCGACCTCGTAGTTCAG	This study
Mono-F2	CGKCRMGMMCCWGGAGC	This study
Mono-R2	GTKGTTCWCGWWCYRCTCG	This study
Alpha-F5	GCAGGTCAGATGCTGGACGAGGTTC	This study
Alpha-R5	GCGATGGCGACGGAATGGTGC	This study
AkMO_GSP1	CGGTTCGTCGAGGACATGCACCATTC	This study
*etnC*_F	CTTGAAACCGTCCACGAGAAGAG	This study
*etnC*_R	AGCGGGTCCTTGATCTCGTACTT	This study
*comA*_F	GGCCCGAACCGGCTGACGAAC	This study
*comA*_R	AGAAGCCTGACTTTCTCGACTTG	This study
CoAT_F	TTCTTCATGGACACCGACAAACTC	This study
CoAT_R	CTCCCGACCCATGCTCAAAGAC	This study

Table 2. Gene products from JS614-P1- predicted functions and database similarities

ORF	No. of amino acids	Coding sequence position (start-codon-stop codon)	Gene or function of closest relative (source), gene(s) of closest relative(s) with known function(s)(source), identified protein domains	Genbank accession number	No. of amino acids with identity/total (%)	E value
1[a]	63	0-194	Probable phosphoadenosine phosphosulfate reductase (*Rhodococcus erythropolis*)	BAB96810	36/64 (56%)	9e-14
			5' adenylylsulfate reductase (*Burkholderia cepacia*) COG0175	AAD50979	32/66 (48%)	2e-08
2	500	180-1682c	Putative argininosuccinate lyase (*Ralstonia metallidurans*)	ZP_00025364	154/487 (31%)	1e-42
			Argininosuccinate lyase (EC 4.3.2.1) - fission yeast (*Schizosaccharomyces pombe*) COG0165	S32580	103/391 (26%)	8e-31
3	322	1679-2647c	Putative 1-aminocyclopropane-1-carboxylate deaminase (*Pyrococcus abyssi*)	NP_125755	122/320 (38%)	7e-51
			1-aminocyclopropane-1-carboxylate deaminase (*Pseudomonas* sp. 6G5) COG2515	P30297	111/337 (32%)	3e-33
4	451	2644-3999c	Putative adenylosuccinate lyase (*Pseudomonas aeruginosa* PA01)	NP_252207	189/453 (41%)	7e-81
			Beta-carboxy-cis,cis-muconate cycloisomerase (*Acinetobacter calcoaceticus*) COG0015	1Q5N_A	128/390 (32%)	2e-45
5	253	3996-4757c	Predicted protein (*Methanosarcina acetivorans* str. C2A)	NP_618623	68/238 (28%)	1e-07
6	275	4923-5709c	Uncharacterized conserved protein (*Cytophaga hutchinsonii*)	ZP_00119544	80/229 (34%)	3e-38
			Phosphosulfolactate synthase (*Methanococcus jannaschii*)	1QWG_A	79/215 (36%)	2e-30
			Phosphosulfolactate synthase (*Xanthobacter* Py2) COG1809	Q9AF21	46/137 (33%)	3e-18
7	455	5874-7241	Hypothetical protein (*Chloroflexus aurantiacus*)	ZP_00019145	200/447 (44%)	1e-79
			Coenzyme A disulfide reductase	AAB97073	119/421	2e-45

			(*Staphylococcus aureus)*		(28%)	
			NADPH:2-ketopropyl-CoM carboxylase/oxidoreductase (*Xanthobacter* Py2) COG0446	Q56839	100/403 (24%)	5e-09
8	257	7380-8153	Short-chain alcohol dehydrogenase (*Novosphingobium aromaticivorans*),	ZP_00093213	112/261 (42%)	7e-46
			2-(S)-hydroxypropyl-CoM dehydrogenase (*Xanthobacter* Py2) COG1028	Q56841	119/253 (47%)	5e-33
9	580	8165-9907	Putative CoA transferase (*Mycobacterium rhodesiae* JS60)	AAO48571	182/264 (68%)	1e-94
			Glutaconate CoA-transferase subunits A and B (*Acidaminococcus fermentans*) COG1788	Q59111, Q59112	66/126 (30%), 75/256 (29%)	3e-14, 1e-11
10	691	9901-11976	Putative acyl-CoA synthetase (*Mycobacterium rhodesiae* JS60) COG1042	AAO48572	257/686 (37%)	e-100
			Pimeloyl-CoA synthetase (*Pseudomonas mendocina*)	CAA10043	223/690 (32%)	8e-70
11	370	12125-13237	Epoxyalkane:coenzyme M transferase (*Rhodococcus rhodochrous* B-276)	AAL28081	306/368 (83%)	0.0
			Epoxyalkane:coenzyme M transferase *etn*E (*Mycobacterium rhodesiae* JS60)	AAO48573	281/369 (76%)	e-169
12	349	13351-14400	Putative alkene monooxygenase beta subunit *etn*A (*Mycobacterium rhodesiae* JS60)	AAO48574	224/344 (65%)	e-133
			Epoxidase subunit *amoA* (*Gordonia rubripertinctus* B-276) pfam02332	BAA07112	139/340 (40%)	3e-67
13	105	14415-14732	Putative alkene monooxygenase coupling/effector protein *etn*B (*Mycobacterium rhodesiae* JS60)	AAO48575	77/102 (75%)	2e-35
			Coupling protein (*Gordonia rubripertinctus* B-276) pfam02406	BAA07113	54/93 (58%)	7e-21
14	501	14750-16255	Putative alkene monooxygenase alpha subunit *etn*C (*Mycobacterium rhodesiae* JS60)	AAO48576	416/500 (83%)	0.0

			Epoxidase subunit *amoC* (*Gordonia rubripertinctus* B-276) pfam02332	BAA07114	293/492 (59%)	e-180
15	346	16339-17379	Putative alkene monooxygenase reductase *etn*D (*Mycobacterium rhodesiae* JS60)	AAO48577	196/327 (59%)	e-108
			Reductase *amoD* (*Gordonia rubripertinctus* B-276) COG0543	BAA07115	146/342 (42%)	7e-69
16	163	17479-17970	Hypothetical protein; no similarity			
17	32	18101-18199	Hypothetical protein; no similarity			
18	226	18232-18912	Hypothetical protein; no similarity			
19	108	19028-19354	Hypothetical protein; no similarity			
20	90	19737-20009	Hypothetical protein; no similarity			
21	796	20184-22574	Molybdopterin oxidoreductase (*Pseudomonas syringae* pv. syringae B728a)	ZP_00127422	395/766 (51%)	0.0
			Dimethyl sulfoxide reductase (*Rhodobacter capsulatus*) COG0243	1DMS	315/777 (40%)	e-160
22	175	22556-23084c	Possible *OriT* region, Hypothetical protein, related to putative retroelement (*Oryza sativa*)	NP_920563	25/73 (34%)	0.12
23	1818	23202-28658c	Putative TraA protein (*Gordonia westfalica*)	NP_954808	631/1456 (43%)	0.0
			Putative TraA protein (*Arthrobacter aurescens*); COG0358, pfam01751	AAS20177	579/1476 (39%)	0.0
24	294	28917-29801c	Hypothetical protein; no similarity			
25	480	29918-31348c	Putative ParB partitioning protein (plasmid pAA1, *Arthrobacter aurescens*);	AAS20140	102/300 (34%)	3e-17
			Putative partitioning protein (plasmid pAO1, *Arthobacter nicotinivorans*)	CAD47867	43/160 (25%)	6e-08
			Putative ParA partitioning protein (virulence plasmid, *Rhodococcus equi*)	NP_066815	40/140 (28%)	1e-07
26	170	31753-32265	Hypothetical protein; no similarity			
27	64	32583-32777	Hypothetical protein; no similarity			
28	88	32794-33060	Hypothetical protein; no similarity			
29	219	33150-33809c	Hypothetical protein; no similarity			

[a]30	273	33991-34814c	Putative DNA integrase-recombinase (*Rhodococcus erythropolis*)	NP_898680	123/247 (49%)	2e-62
			Putative DNA integrase/recombinase (*Streptomyces coelicolor* A3(2)); pfam00589	NP_639594	116/267 (43%)	2e-56

[a] Incomplete ORFs.

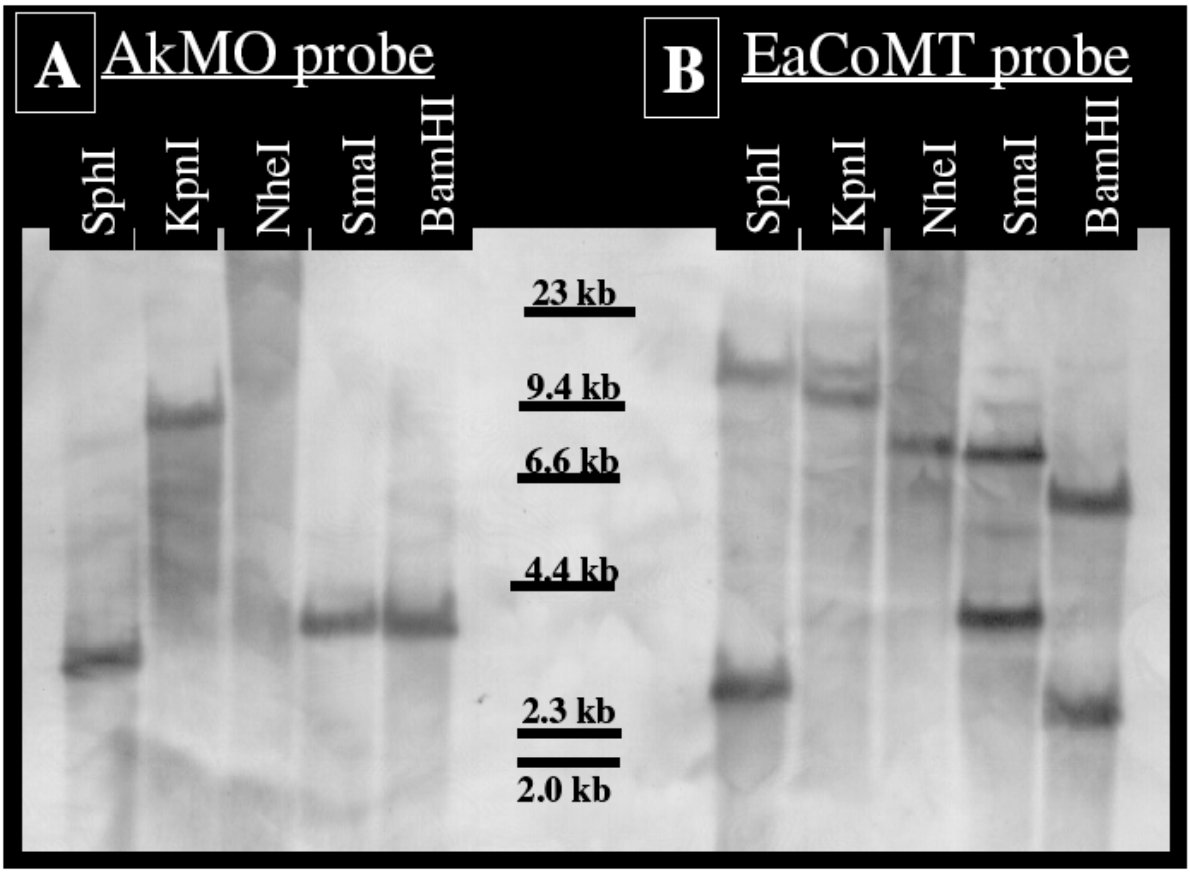

Figure 1. Southern blot of JS614 genomic DNA using A) JS614 AkMO alpha subunit gene *etnC* (635 bp) and B) JS614 EaCoMT gene *etnE* (831bp) as a probe. Lanes are labeled by restriction enzyme used.

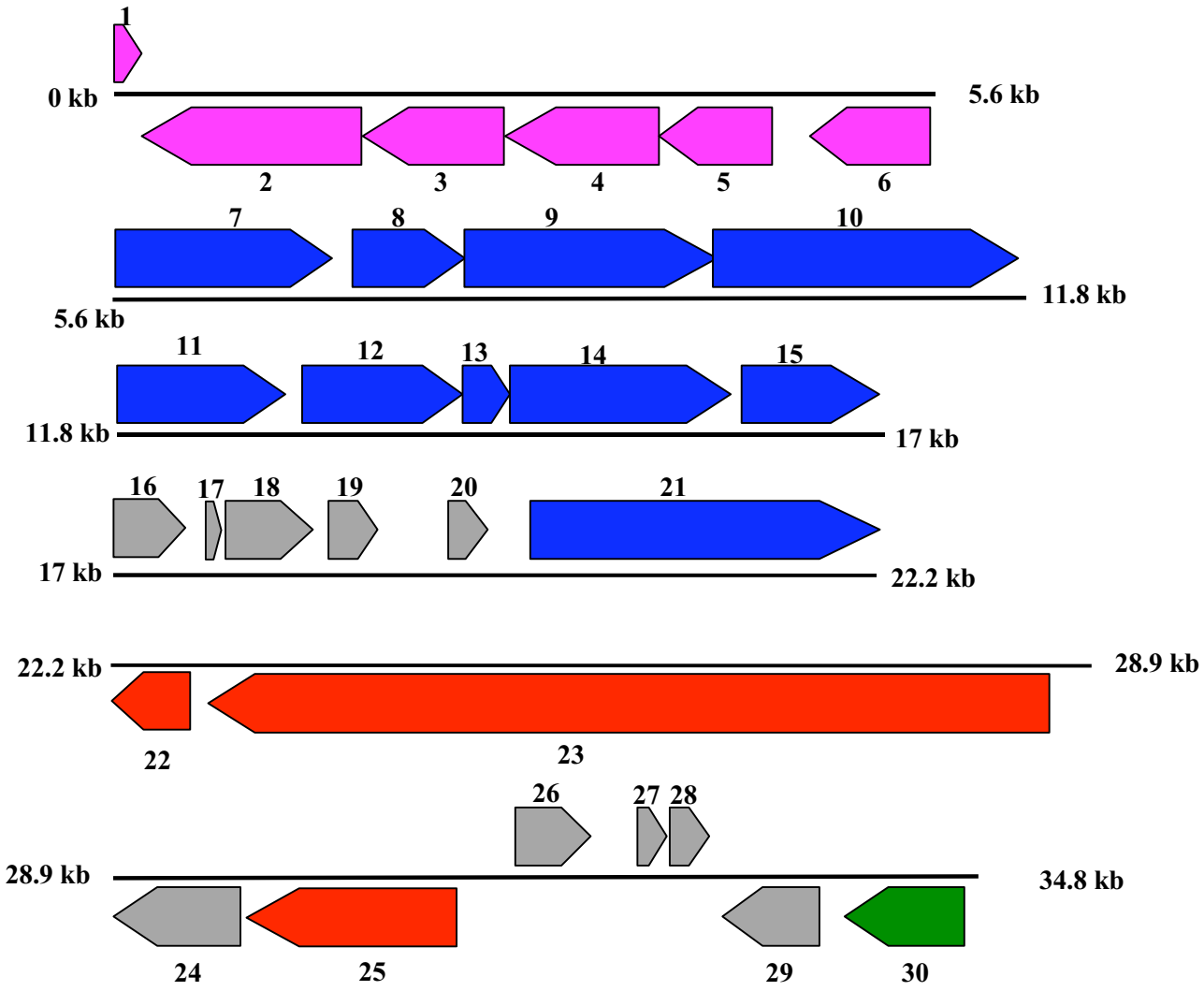

Figure 2. Schematic representation of ORFs on the 38.4 kb JS614-P1 region sequenced from *Nocardioides* strain JS614. Predicted ORFs are shown as arrows. The direction of the arrows indicates which DNA strand contains the ORF. ORFs shown in magenta are assigned to biosynthetic functions, blue ORFs are assigned catabolic functions, red ORFs are assigned plasmid functions, green ORFs are assigned phage-related functions, and gray ORFs could not be assigned a function.

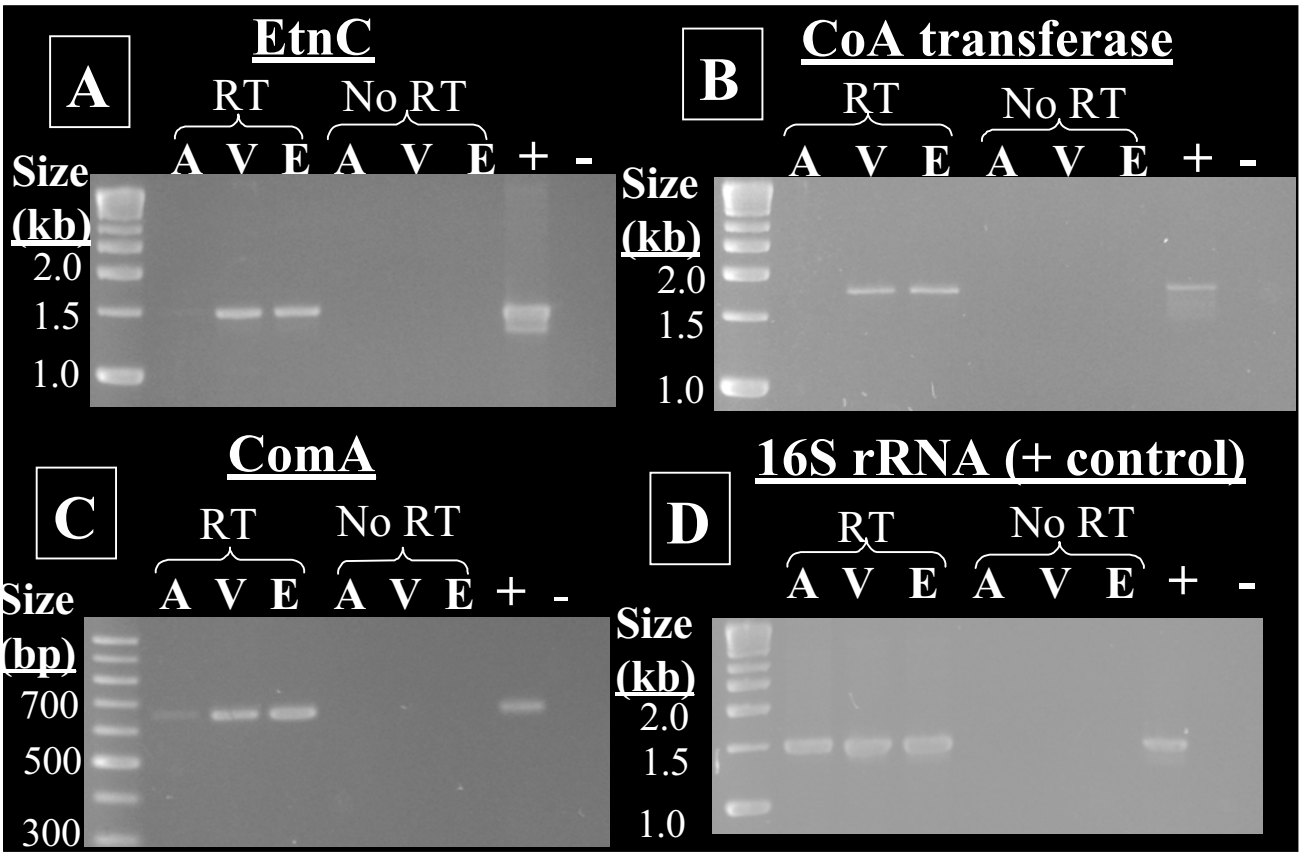

Figure 3. RT-PCR experiments with A) EtnC, B) CoA transferase, C) ComA, and D) 16S rDNA (27f ,1492r)(Lane 1991) primers. Lanes: V, VC-grown JS614 RNA template; E, ETH-grown JS614 RNA template; A, acetate-grown JS614 RNA template; RT, RT-PCR with RNA template; No RT, PCR (no reverse transcriptase) with RNA template; –, No template; +, DNA template.

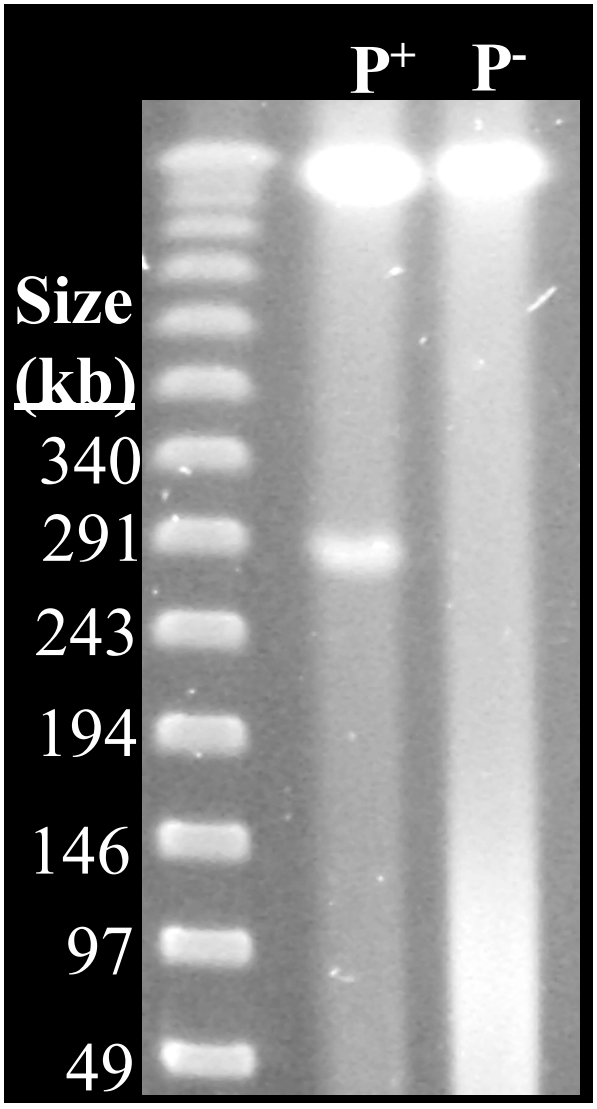

Figure 4. CHEF-PFGE detection of pNoc614 in strain JS614. Lanes: P^+, pNoc614-positive JS614 genomic DNA; P^-, pNoc614-negative JS614 DNA.

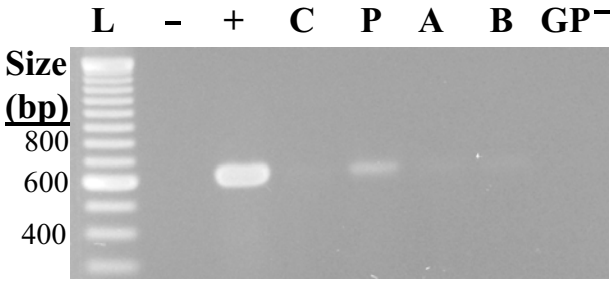

Figure 5. PCR analysis of CHEF purified JS614 DNA. Lane L: 1 kb Ladder; Lane _: No DNA (- control); Lane +: Total JS614 DNA (positive control); Lane C: CHEF-purified chromosomal DNA; Lane A: DNA 1 cm above plasmid; Lane P: CHEF-purified plasmid DNA; Lane B: DNA 1 cm below plasmid; Lane GP^-: Total genomic DNA from pNoc614-negative JS614 strain.

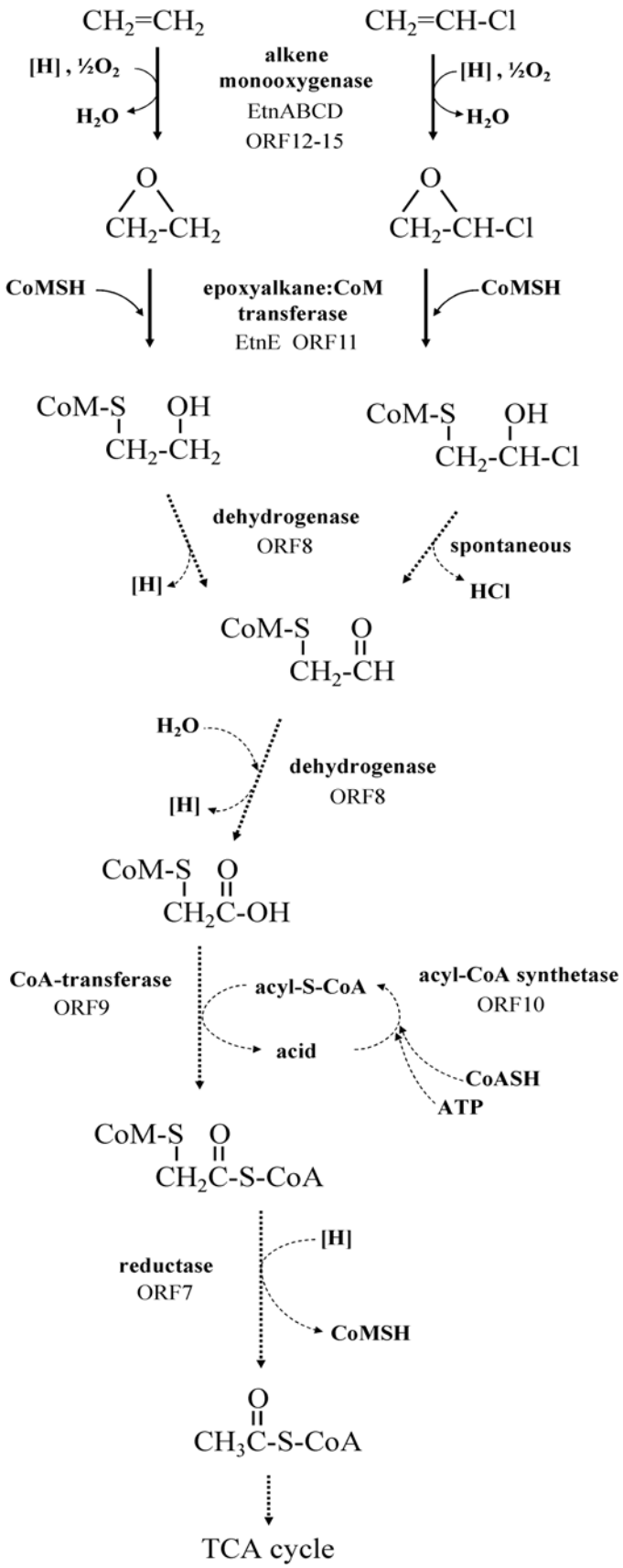

Figure 6. Hypothetical pathway of VC and ETH assimilation in *Nocardioides* JS614.

Appendix F

Mattes, T. E., N. V. Coleman, J. C. Spain, and J. M. Gossett 2004. Characterization of the vinyl chloride and ethene starvation response in *Nocardioides* Strain JS614. Manuscript submitted to *Archives of Microbiology*.

Characterization of the vinyl chloride and ethene starvation response in *Nocardioides* Strain JS614

Authors: Timothy E. Mattes[1*], Nicholas V. Coleman[2], Jim C. Spain[3], and James M. Gossett[4]

1. Department of Civil and Environmental Engineering, 4105 Seamans Center, The University of Iowa, Iowa City, IA, 52242, USA
2. School of Molecular and Microbial Biosciences, University of Sydney, Australia
3. AFRL-MLQL, Tyndall AFB, Florida, 32403, USA.
4. School of Civil and Environmental Engineering, Hollister Hall, Cornell University, Ithaca, NY, 14853, USA

* Corresponding author: Fax: (319) 335-5660
E-mail: tem8@cornell.edu

ABSTRACT

Nocardioides strain JS614 exhibits an extended lag period for resumption of aerobic growth on VC or ETH after these substrates are withheld from the culture for longer than one day. This lag could affect application of JS614 in bioaugmentation and biocatalysis strategies and raises fundamental questions concerning mechanisms controlling the lag. Initial growth experiments indicate the lag is not due to cell death and is limited to starvation recovery on or adaptation to VC or ETH as growth substrates. Assays of alkene monooxygenase (AkMO) and epoxyalkane:Coenzyme M transferase (EaCoMT) activities indicate rapid AkMO inactivation during starvation. Switching ETH-grown JS614 cultures to acetate for 24 h revealed elevated AkMO activities in comparison to starvation. SDS-PAGE and MALDI-TOF MS experiments demonstrated that AkMO subunits were induced by VC and ETH, and were not degraded during starvation. Upon resumption of ETH degradation, SDS-PAGE results suggested that AkMO subunits were synthesized. Addition of acetate along with VC or ETH reduced the lag associated with VC or ETH starvation. We conclude that AkMO inactivation, along with additional undefined mechanisms control the lag period associated with starvation recovery on VC or ETH. Our data suggest that depletion of reducing power contributes to the lag, but that toxic epoxide accumulation or rapid turnover of AkMO subunits are unlikely contributors.

Keywords: starvation, alkene monooxygenase, vinyl chloride, ethene

INTRODUCTION

Vinyl chloride (VC), a known human carcinogen (Bucher 2001) and common groundwater contaminant (Squillace 1999), is derived mainly from incomplete reductive dechlorination of the widely used chlorinated solvents tetrachloroethene (PCE) and trichloroethene (TCE), also common groundwater contaminants (Squillace 1999). VC tends to accumulate in anaerobic groundwater zones but could degrade readily if the VC plume migrates into aerobic groundwater zones (Davis 1990; Edwards 1997; Lee 1998). The recent isolation of several strains of aerobic VC-assimilating bacteria from soil (Coleman et al. 2002), groundwater (Coleman et al. 2002), sediment (Hartmans 1992b), and sewage sludge samples (Hartmans 1992b; Verce 2000; Coleman et al. 2002) suggests that VC-assimilating bacteria play a significant role in aerobic natural attenuation of VC at contaminated sites.

In certain cases, aerobic VC degradation is fortuitous, resulting from non-specific oxygenases produced by organisms growing on a variety of compounds that might be present such as methane, ethene, or BTEX compounds (Fogel 1986; Koziollek 1999; Freedman et al. 2001; Shim et al. 2001). Cometabolic VC oxidation processes are potentially unreliable for enhanced bioremediation of VC due to generation of toxic epoxides, growth substrate requirements and competitive inhibition between the growth substrate and VC. At some VC-contaminated sites, bioaugmentation with organisms capable of growth on VC could support or possibly offer an alternative to bioremediation strategies that rely on cometabolism of VC.

The majority of known, growth-coupled VC degraders are members of the genus *Mycobacterium* (Hartmans 1992b; Coleman et al. 2002). Although such strains are effective degraders, some are phylogenetically related to opportunistic pathogens (Tortoli et al. 1999). As a result, obtaining regulatory approval for *in situ* bioaugmentation with VC-degrading

mycobacteria could be difficult. Similarly, the VC-degrading *Pseudomonas* strains MF1 and DL1 are related to *P. aeruginosa* and thus might also be perceived as pathogens (Alonso et al. 1999). *Nocardioides* strain JS614, on the other hand, is a promising candidate for bioaugmentation applications due to its relatively high rate of VC oxidation and growth yield on VC, in comparison to the mycobacterial and pseudomonad VC-degraders (Coleman et al. 2002). Members of the genus *Nocardioides* are not known to be associated with pathogenesis in animals or plants. Strain JS614 is capable of growth at 37ºC, but its growth optimum is closer to 30ºC (T. Mattes, unpublished results). Strain JS614 could also have potential biocatalysis applications due to its ability to produce epoxides from alkene substrates with a highly active alkene monooxygenase system (Coleman et al. 2002).

The genes that encode enzymes responsible for catabolism of VC and ETH, including an alkene monooxygenase (AkMO) *etnABCD*, and an epoxyalkane:coenzyme M transferase (EaCoMT) *etnE*, have been identified in *Mycobacterium* strain JS60 (Coleman and Spain 2003b) and *Nocardioides* JS614 (Mattes 2004). The monooxygenase catalyzes the initial oxidation of ETH to epoxyethane and VC to chlorooxirane, which are further metabolized by EaCoMT (Coleman et al. 2002).

Nocardioides strain JS614 grows rapidly on VC as a sole carbon source, but displays an extended lag period following a short period of VC starvation. Lag periods in the presence of VC in excess of 40 days were observed when mid-log phase JS614 cultures growing on VC were starved for periods one day or longer (Coleman et al. 2002). In contrast, *Mycobacterium* JS60 and *Pseudomonas* MF1 readily recovered from alkene starvation periods of 7 days without an extended lag period (Verce 2000; Coleman et al. 2002). Mycobacteria are known to fare well

under starvation conditions due to their tendency to accumulate high levels of storage materials and their relatively slow metabolism (Ratledge 1982; de Haan 1993).

Mechanisms controlling the lag period are unknown and could adversely affect practical application of this strain. The main purpose of this study was to characterize the lag period associated with alkene starvation and determine the physiological conditions that reduce or eliminate the lag. The observed lag raises several fundamental scientific questions that have not been well studied in VC and ETH degraders, or in biodegradative microorganisms in general. For example, we were interested in determining if unstable VC/ETH pathway enzyme systems might be contributing to the lag. Here, we present data that suggests inactivation of AkMO followed by a delayed reactivation or induction of AkMO is responsible for the extended lag period following VC and ETH starvation in strain JS614. We also report that the lag period is reduced or eliminated if a readily degradable carbon source is provided along with VC or ETH following the starvation period.

MATERIALS AND METHODS

Chemicals, media, strains and growth conditions. VC (99%) and ETH (99%) were from Matheson. Epoxyethane (99.5%) was from Sigma, Coenzyme M was from Fluka, and NADH was from ACROS organics. All other chemicals were of reagent grade. Cultures of *Nocardioides* JS614 (ATCC BAA-499) or *Mycobacterium* JS60 (ATCC BAA-494) were grown in minimal salts medium (MSM)(Hartmans 1992a), containing VC, ETH, acetate, or epoxyethane or in 1/10-strength trypticase soy broth (1/10-TSB, Difco). Unless indicated otherwise, all cultures were incubated aerobically at 22-25°C, with shaking at 165 rpm.

Analytical Methods. VC, ETH, and epoxyethane were analyzed in headspace samples by gas chromatography with flame-ionization detection using a 1% SP-1000 on 60/80 Carbopack B packed column (Supelco). Acetate was analyzed in liquid samples with a Dionex DX600 ion chromatograph with AS14A analytical and guard ion-exchange columns. Suppressed conductivity detection was carried out in an 8 mM carbonate/ 1 mM bicarbonate eluent at 1 ml/min. UV absorbance (A_{230} and A_{260}) was measured in cell lysates and protein was estimated using the formula: protein (μg/ml)= $(183*A_{230})-(75.8*A_{260})$ as described previously (Coleman et al. 2002).

AkMO assay. Cultures were harvested at mid-exponential phase (approx. OD_{600} 0.2-0.3), the cells were washed twice in KP buffer (K_2HPO_4 20 mM [pH 7.0]), and suspended in 1 ml of the same buffer at an OD_{600} of 5 (approx. protein = 1.0 mg). The cells were transferred to 27-ml serum bottles, ETH (4 μmoles) was added, and the bottles incubated with shaking (300 rpm) at 22ºC. Ethene degradation was analyzed as described above. The observed maximum

ethene degradation rate was assumed to be proportional to the level of AkMO in the original culture. Specific activity was calculated based on protein content.

Preparation of cell extracts. Cultures were harvested at mid-exponential phase, and the cells were suspended without washing in 500 μl MGD buffer (50mM MOPS, 10% glycerol, 1mM dithiothreitol (DTT) [pH 7.2]) at an OD_{600} of 30-60, and flash-frozen in liquid nitrogen for later analysis. Thawed cell suspensions were added to a 2-ml screw-cap tube containing 1.5 ml of cold, 0.1-mm zirconia/silica beads (Bio-spec), wetted with MGD buffer. Cells were lysed by beadbeating (7 cycles of 30s beating, 30s cooling) using a Bio-Spec Mini Beadbeater 8 located in a temperature-controlled room at 4ºC. Lysates were clarified by centrifugation (21,000x *g*, 15 minutes, 4ºC), and the supernatant (referred to hereafter as 'cell extract') was retained and diluted to 0.4 mg of protein/ml in MGD buffer.

EaCoMT assay. Serum bottles (27 ml) containing 900 μl of Tris-Cl (50 mM; pH 8.0), 50 μl cell extract (approx. 0.02 mg protein) and 50 μl freshly prepared coenzyme M (200 mM) were crimp sealed. Epoxyethane (5 μmol) was added, and the bottles incubated with shaking (300 rpm) at 22ºC. Epoxyethane degradation was analyzed as described above.

SDS-PAGE. Cell-free extracts for SDS-PAGE were prepared as described in the EaCoMT assay section, except that the beadbeater lysate supernatant was diluted to 1.5 mg of protein/ml in MGD buffer. SDS-PAGE was performed by the method of Laemmli (Sambrook 2001) using 12% polyacrylamide gels. Proteins were visualized by staining with Coomassie Brilliant Blue and molecular masses were estimated by comparison with low-range standards (Bio-Rad).

MALDI-TOF MS analysis. Following SDS-PAGE, a 50.4 kDa protein band and a protein-negative control band were excised, digested with bovine trypsin (Promega), and a

peptide mass fingerprint (PMF) was obtained using a Bruker BiflexIII MALD/I TOF mass spectrometer in positive-ion/reflector mode. The matrix was a-cyano-4-hydroxycinnamic acid. Peptide masses present in both the sample and negative control were excluded from analysis. The remaining masses were compared to an *in silico* trypsin digest of the putative AkMO alpha subunit protein sequence using the MS-digest program of Protein Prospector(Baker and Clauser).

Growth assays. Cells grown on VC, ETH, or sodium acetate were harvested at mid-log phase, washed and resuspended in 72 ml MSM at OD_{600} 0.2 in 160-ml serum bottles and resuspended in carbon-free medium for 24 hours at 22-25ºC with shaking (165 rpm). Cultures were subsequently supplemented with 200 μmoles of VC, ETH, acetate, or epoxyethane and monitored by GC as described in analytical methods. Some bottles were also amended with rifampicin (35 μg/ml), chloroamphenicol (139 μg/ml), or sodium acetate (1 mM).

RESULTS AND DISCUSSION

Substrate starvation response of strain JS614. The response of JS614 to carbon starvation and subsequent resumption of growth was further evaluated by growing cultures on various substrates, transferring the cells to carbon-free medium for 24 hours, then adding a substrate and monitoring its disappearance (Fig. 1). With VC and ETH as the growth and recovery substrates, cultures exhibited a reproducible approximately 6-day lag period before recovering degradation activity. Both alkenes produced similar starvation responses; therefore, for convenience we used ETH in all subsequent experiments. Starved ETH-grown cultures subsequently supplemented with acetate or epoxyethane degraded the substrates without a lag period, and starved acetate-grown cultures degraded acetate immediately, suggesting that general cellular viability and enzyme activities were not dramatically affected after 24 h starvation, and

that the extended lag period was specific to recovery on alkenes. Acetate-grown cells supplemented with ETH without any starvation period displayed a lag period very similar to that occurring in starved alkene-grown cells, suggesting that the 'starvation' response of JS614 could be due to a lack of enzyme induction, rather than the absence of a carbon source. Taken together, the results point to the AkMO that catalyzes the initial step of the VC and ETH degradation pathways as the main determinant of the extended lag period.

The approximately 6-day lag periods observed here (Fig.1) are much shorter than the >40 day lag observed in a previous study of starved JS614 cultures (Coleman et al. 2002), possibly due to differences in experimental design. In the present study, actively growing cultures were transferred to fresh, carbon-free medium as a means of initiating starvation conditions, whereas in the previous study, cultures were allowed to deplete the substrate in the initial medium. The difference in results suggests that inhibitory factors accumulated (e.g. HCl resulting from VC oxidation) or stimulatory factors were depleted (e.g. nutrients) in the medium during starvation, or alternatively that the rate of onset of starvation affected the subsequent physiological state of the cells.

Maximum-specific AkMO and EaCoMT activities in JS614. To provide a basis for biochemical investigations of the JS614 starvation response, the typical AkMO and EaCoMT activities in JS614 cells grown in various media were measured (Table 1). Since large concentrations of the respective substrates (ETH or epoxyethane) were used, the results are interpreted as maximum-specific activities — a measure of potential activity.

Preliminary studies failed to detect AkMO activity in extracts of alkene-grown JS614 cells, regardless of the addition of NADH, which is the preferred cofactor of AkMOs from *Mycobacterium aurum* L1 and *Mycobacterium* strain E3 (Hartmans 1991; Hartmans 1992b;

Weber 1992), *Rhodococcus rhodochrous* B276 (Miura 1995), and *Xanthobacter* Py2 (Small 1997). The lack of AkMO activity in concentrated JS614 cell extracts is consistent with reports of low AkMO activity in cell extracts from *Mycobacterium aurum* L1 and *Mycobacterium* strain E3 (Hartmans 1991; Hartmans 1992b; Weber 1992), *Rhodococcus rhodochrous* B276 (Miura 1995), and *Xanthobacter* Py2 (Small 1997). The difficulty in observing AkMO activity in crude cell extracts from alkene-oxidizing bacteria might be due to suboptimal ratios of system components (i.e. oxygenase, effector, reductase). Resting-cell assays of AkMO activity, on the other hand, allowed for easy measurement of ETH degradation rates and were reproducible. The AkMO alpha subunit in strain JS614 was expressed in response to VC and ETH, and not expressed in response to acetate (Mattes 2004), providing strong evidence that epoxyethane formation from ETH is due to AkMO and not a fortuitous oxidation by a non-specific oxygenase in VC- and ETH-grown JS614 cells. Therefore we used resting cell assays as an indicator of AkMO activity in all subsequent work

EaCoMT activity has previously been observed in several mycobacteria growing on VC and ETH, and has been implicated in the VC and ETH oxidation pathways in *Mycobacterium* strain JS60 (Coleman and Spain 2003b; Coleman and Spain 2003a). A putative EaCoMT gene (*etnE*) was previously found immediately upstream of the AkMO genes *(etnABCD)* in strain JS614, but an assay for EaCoMT activity was not performed (Mattes 2004). In the present study, CoM-dependent epoxyethane degradation was detected in JS614 cell-extracts, providing additional evidence that EaCoMT catalyzes the second step in alkene assimilation in strain JS614 (Table 1). EaCoMT activity in VC-grown JS614 cell extracts was more than double the highest EaCoMT activity measured in VC-degrading mycobacteria (Coleman and Spain 2003a) which is consistent with the faster growth rate on ethenes. The relatively high level of basal EaCoMT

expression in acetate-grown and 1/10 TSB grown JS614 cell extract is surprising, since EaCoMT expression in acetate-grown *Mycobacterium* JS60 is negligible (Coleman and Spain 2003b), suggesting the second EaCoMT allele in JS614 (Mattes 2004) is functional and constitutively expressed. A putative CoM biosynthesis gene displayed low levels of expression in acetate-grown JS614 cultures (Mattes 2004), an observation that supports this hypothesis.

The high EaCoMT activity in strain JS614 might explain the higher growth yield on VC and ETH, compared to alkene-degrading mycobacteria (Coleman et al. 2002). Chlorooxirane and epoxyethane are both reactive compounds – the aqueous half-life of chlorooxirane is 1.6 minutes (Barbin 1975). Higher EaCoMT activity could lead to more epoxide being converted to the CoM conjugate, and less epoxide being lost to unproductive reactions such as hydrolysis, rearrangement, or nucleophilic attack on cellular components. The EaCoMT activity in JS614 cell extracts was at least two orders of magnitude higher than the EaCoMT activity of resting cells of the same strain (data not shown), most likely due to a limited supply of reduced CoM in whole cells. Therefore, we chose to use cell extracts for all further assays of EaCoMT activity.

Epoxyethane-grown cultures exhibited AkMO and EaCoMT activities higher than basal levels, but much lower than the activities in alkene-grown cells (Table 1). It is possible that epoxyethane is a weak inducer of the VC/ETH pathway enzymes, but interpretation of the results is complicated by the toxicity of epoxyethane. Growth of JS614 on epoxyethane was slow, and it was difficult to attain high cell densities on this substrate (data not shown). The poor growth on epoxyethane at first seems unusual, given that this compound is an intermediate of the ETH assimilation pathway. However, during growth on ETH, it is very unlikely that epoxyethane accumulates to any extent due to the high EaCoMT activity, and thus, the strain is probably

poorly adapted to higher concentrations of the epoxide. Epoxyethane was not detectable in the headspace of JS614 cultures growing on ETH (data not shown).

Effect of ETH starvation on AkMO and EaCoMT activities. Coleman et al. proposed that AkMO activity in the absence of epoxide transforming activity might allow chlorooxirane to accumulate to lethal levels in VC-starved JS614 cultures. An apparent precedent was observed in *Mycobacterium* strain L1, which accumulated VC epoxide when incubated with VC after a short starvation period (Hartmans 1992b). Sublethal levels of epoxide accumulation following addition of VC might result in AkMO inactivation, which could manifest as an extended lag period before resumption of growth. Studies with ETH-assimilating *Mycobacterium* strain E3 indicated that low levels of epoxyethane, epoxypropane, and epoxybutane were capable of irreversibly inactivating the AkMO mediating the epoxidation reaction (Habets-Crützen 1985). Preliminary analysis of enzyme activities in starved ETH-grown cells (Table 1) indicated that AkMO activity was completely lost after starvation, while EaCoMT activity was maintained (albeit at a lower level than in unstarved cells) suggesting that turnover of AkMO is considerably faster than that of EaCoMT in strain JS614. To provide more detail of enzyme activity loss during starvation, the two enzyme activities were assayed at intervals during a 24-h substrate-starvation period (Fig. 2). AkMO dropped to near basal levels within 8 hours of starvation (Fig. 2). EaCoMT activities declined at approximately the same rate as AkMO during the first two hours of starvation, before leveling off to approximately 45% of the initial value (Fig. 2). This observation could explain the lack of a significant lag period when feeding ETH-starved cultures epoxyethane (Fig. 1), and also indicates that, contrary to our previous speculations (Coleman et al. 2002), epoxide accumulation and toxicity is unlikely to be the cause of the extended lag period in strain JS614, since EaCoMT activity was maintained throughout starvation.

Depletion of reducing power could contribute to AkMO inactivation during starvation. Temporary AkMO inactivation resulting from depletion of intracellular NADH levels was observed during epoxypropane production experiments with *Mycobacterium* strain E3 (de Haan 1993). When strain E3 was grown under carbon limitation and amended with propene in resting-cell suspensions, production of epoxypropane ceased after 12 h, an event that coincided with the depletion of NADH in the cells (de Haan 1993). It was determined that addition of a readily degradable carbon source (glucose) facilitated regeneration of intracellular NADH pools and increased epoxypropane production by the AkMO, though the glucose appeared to be converted first to storage material which was subsequently oxidized to regenerate NADH (de Haan 1993).

Interpretation of JS614 AkMO inactivation during starvation is complicated by the multi-component nature and cofactor requirements of AkMO, which might subject AkMO to several potentially simultaneous processes (e.g. depletion of reducing power, irreversible and reversible inactivation, and oxidative damage) that could contribute to inactivation. To examine the possibility that reducing-power depletion impacts AkMO functioning during starvation, AkMO activities were measured in ETH-grown JS614 cultures switched to growth on 20 mM acetate for 24-h. Under this particular physiological condition, AkMO expression should cease since no alkene substrate is present, but oxidation of acetate should provide an ample supply of reducing power for existing AkMO. After 10.3-h incubation with acetate, AkMO activities of ETH-grown JS614 cultures were 10.5%-35.6% higher when compared to AkMO activities during 10.3-h starvation (data not shown) suggesting that depletion of reducing power in starved cells was negatively impacting AkMO activities. Despite this observation, AkMO activities dropped to

basal levels after 24-h (data not shown) suggesting that additional mechanisms are contributing to the observed AkMO activity loss.

In contrast to *Nocardioides* JS614, *Mycobacterium* JS60 readily recovers from alkene starvation periods of 7 days (Coleman et al. 2002) . Mycobacteria are known to fare well under starvation conditions due to their tendency to accumulate high levels of storage materials and their relatively slow metabolism (Ratledge 1982; de Haan 1993) . To further investigate these intergeneric differences in the starvation response, we examined AkMO activities in both JS60 and JS614 during a 24-h starvation period. AkMO activities in starved ETH-grown JS60 cells declined at a lower rate than AkMO levels in ETH-grown JS614 cells, but at approximately the same rate as ETH-grown JS614 cells growing on acetate over the 24-h period (data not shown), suggesting that JS60 is utilizing an alternative carbon source during 24-h starvation that leads to elevated AkMO activities in comparison to starved JS614 cells. Like JS614, JS60 exhibits relatively low AkMO activity after 24-h starvation, further suggesting that additional mechanisms are contributing to AkMO activity loss in starved cells.

Identification of AkMO subunits in JS614 cell extracts. Deduced molecular weights of AkMO subunits and EaCoMT from JS614 (Mattes 2004) were very similar to deduced molecular weights of AkMO subunits and EaCoMT from *Rhodococcus* B276 (Saeki 1994) (Table 2). SDS-PAGE analysis of VC-, ETH-, epoxyethane- and acetate-grown JS614 cell extracts indicated that at least four polypeptides (50.4 kDa, 41.9 kDa, 40 kDa, and 29 kDa) are highly expressed or up-regulated in response to VC, ETH and epoxyethane (Fig. 3). The apparent molecular weights of the 50.4 kDa, 41.9 kDa, and 40 kDa polypeptides correspond with predicted AkMO subunit molecular weights from JS614 and B276, as well as the observed molecular weights of B276 AkMO subunits, allowing us to tentatively identify the proteins as

AkMO subunits in VC-, ETH-, and epoxyethane-grown JS614 cell extracts (Fig.3, Table 2). It is plausible that EtnE and EtnA comigrate during SDS-PAGE due to similar molecular weights. These results are also consistent with epoxyethane being an inducer of AkMO, as was suggested by data in Table 1.

To provide additional evidence that the 50.4 kDa band expressed in response to VC and ETH is EtnC, it was excised and a peptide mass fingerprint (PMF) was obtained by MALDI-TOF MS analysis in comparison to a negative control. The monoisotopic masses of 63 peptide fragments not present in the negative control were compared to monoisotopic masses of a predicted trypsin digest of the EtnC protein sequence. Of these 63 masses, 14 masses matched the predicted digest using a relative mass tolerance of 500 ppm, representing 13 peptide fragments for 46.1% coverage of the protein, indicating a positive match (Table 3). A relative mass tolerance of 500 ppm is more stringent than relative mass tolerances previously employed for protein identification (Henzel et al. 1993), though more accurate mass measurement by MALDI-TOF MS is possible (Jensen et al. 1997). The remaining 49 unmatched peptide masses might correspond to other proteins of the same molecular weight that co-migrated with the AkMO alpha subunit, trypsin autolysis products, keratin or other contaminants.

ETH-induced AkMO subunits are not degraded during starvation. Increased protein degradation (i.e. turnover) during starvation was observed in *E.coli* under starvation conditions (Reeve et al. 1984). It was postulated that starved *E.coli* cultures might use irreversible degradative inactivation to prevent unneeded enzymes from wasting energy or to provide free amino acids for synthesis of starvation-induced proteins, though direct evidence of proteolytic inactivation is scarce and the mechanisms involved are poorly understood (Switzer 1977; Reeve et al. 1984). Since AkMO is an energy-consuming enzyme complex, it is a plausible hypothesis

that starved JS614 cells accelerate turnover of AkMO subunits during starvation to conserve energy. To examine this possibility, AkMO subunits were tracked by SDS-PAGE analysis (Fig.3). Little or no degradation of AkMO subunits was observed after 24-h starvation, indicating that turnover is an unlikely explanation for the observed AkMO activity loss during this time. These results, however, do not rule out oxidative damage (Cabiscol et al. 2000), reversible modification inactivation (Switzer 1977), loss of the di-iron center, and/or unknown cellular processes inactivating one or more AkMO subunits.

After the 24-h starvation period, cultures were supplemented with ETH and cell extracts were prepared after incubation for 5 days, while cultures were still experiencing an extended lag period, and after 7 days, when cultures had fully recovered ETH-degrading ability. Cell extracts from these time points appear to show an increase in the *etnC*, *etnA/*EaCoMT, and *etnD* band intensities suggesting that additional AkMO subunits were synthesized (Fig.3).

Effect of cosubstrates on recovery from ETH starvation. The positive effect of co-substrates on epoxide production in *Mycobacterium* E3 (de Haan 1993), and observations that AkMO subunits were still present after 24-h starvation led us to postulate that addition of a readily degradable substrate, along with VC or ETH, following starvation would decrease the lag period in JS614. Addition of acetate (1 mM) along with ETH resulted in rapid recovery of starved cells (approx. 1 day lag) compared to cultures supplemented with ETH only (approx. 6 day lag) (Fig. 4). After the short lag, cultures amended with acetate gave ETH degradation rates very similar to cultures that had not been subjected to any starvation period. Similar results were seen when glucose, pyruvate or epoxyethane were added along with VC or ETH to starved cultures (data not shown), suggesting that any readily utilizable carbon source can stimulate onset of growth of starved JS614 cells on VC or ETH. Starved ETH-grown cultures

supplemented with ETH, 1 mM acetate, and 139 μg/ml chloramphenicol did not recover ETH-degrading activity during the experiment (Fig. 4), indicating that addition of acetate results in protein synthesis required for recovery of VC- and ETH-degrading activity in starved cells.

Addition of 1 mM acetate also reduced or eliminated the lag period for resumption of growth on ETH by JS614 under other physiological conditions where ETH was withheld for 24 h. For example, if 20 mM acetate were administered during this 24-h "ETH-starvation" period, when the cells were washed and resuspended in MSM-ETH, 200 μmol ETH was degraded within 5 days without lag (data not shown). Furthermore, if the resuspension medium contained 1 mM acetate, the ETH degradation rate was virtually identical to that of unstarved cultures (data not shown).

Acetate clearly reduces or eliminates the extended lag period associated with VC or ETH starvation. Acetate oxidation could facilitate regeneration of reducing power, repair of damaged AkMO subunits, reactivation of covalently modified AkMO subunits, or stimulation of de novo AkMO synthesis. Feeding higher concentrations of acetate to starved cells in the presence of ETH or VC could delay the rapid recovery of AkMO activity due to catabolite repression effects, but this possibility was not addressed in great detail in this study. Preliminary recovery experiments where 5 mM acetate was fed to starved cells in the presence of VC resulted in recovery of AkMO activity within the same time frame (data not shown). Interestingly, small amounts of acetate had no effect on the extended lag period observed for adaptation of acetate-grown JS614 cultures to ETH (data not shown), suggesting that the extended lag period for adaptation of JS614 to growth on alkene-substrates (Fig.1) is controlled by a different mechanism than recovery from short periods of alkene-starvation, perhaps as a result of delayed enzyme synthesis due to stringent regulation of VC and ETH pathway enzyme induction. Recent

evidence suggests that VC and ETH pathway genes in strain JS614 are under the control of a sigma-54 dependent promoter, though no putative activator proteins have yet been discovered (Mattes 2004). Initiation of transcription by sigma-54 promoters can be tightly regulated with very little leaky expression when inactivated, but could also be highly expressed under the right physiological and environmental conditions (Buck et al. 2000). JS614 also did not display extended lag periods following periods of VC starvation in mixed culture (data not shown), suggesting that JS614 relied on waste products or dead cells from other members of the microbial community to maintain energy levels (and presumably enzyme activities) during starvation periods.

The mechanisms controlling the extended lag period in response to VC or ETH starvation in strain JS614 are poorly understood, and could limit the practical applications of this strain. The data presented here suggest that inactivation of AkMO rather than toxic epoxide accumulation during starvation plays a role in the extended lag period before growth on VC or ETH resumes. Possible mechanisms controlling this lag period include depletion of reducing power required by AkMO, turnover of AkMO subunits, reversible or irreversible inactivation of AkMO subunits, oxidative damage to the AkMO reductase, and/or stringent regulation of AkMO synthesis. The extended lag period is reduced or eliminated by addition of small amounts of a readily degradable substrate (e.g. acetate) along with VC or ETH. Based on the data presented in this paper, acetate is likely oxidized to regenerate the reducing equivalent pool, which allows existing AkMO to resume functioning, but could also be utilized for repair of damaged AkMO and/or for energy to synthesize new AkMO. Except for the observation that AkMO subunits are not degraded during starvation, the data presented in this paper do not conclusively implicate or rule out other possible mechanisms that might control the lag period, and therefore further work

is required in this regard. Extended lag periods for adaptation to growth on alkene substrates appear to be controlled by a different mechanism than the lag period associated with alkene starvation, an observation that also warrants further investigation.

ACKNOWLEDGEMENTS

We thank Juli Rubin, Brian Weisenstein, and Linda Rankin for technical assistance. We also thank Anthony Hay, Ruth Richardson, and Steve Zinder for use of their laboratories. The U.S. Strategic Environmental Research and Development (SERDP) program funded this work.

REFERENCES

Alonso A, Rojo F, Martinez JL (1999) Environmental and clinical isolates of *Pseudomonas aeruginosa* show pathogenic and biodegradative properties irrespective of their origin. Environ. Microbiol. 1:421-430.

Baker PR, Clauser KR [http://prospector.ucsf.edu/ucsfhtml4.0/msdigest.htm].

Barbin A, H. Brésil, A. Croisy, P. Jacquignon, C. Malaveille, R. Montesano, and H. Bartsch (1975) Liver-microsome-mediated formation of alkylating agents from vinyl bromide and vinyl chloride. Biochem. Biophys. Res. Comm. 67:596-603

Bucher JR, Cooper, G., Haseman, J. K., Jameson, C. W., Longnecker, M., Kamel, F., Maronpot, R., Matthews, H.B., Melnick, R., Newbold, R., Tennant, R.W., Thompson, C., Waalkes, M. (2001) Ninth report on carcinogens. In. U.S. Dept. of Health and Human Services, National Toxicology Program. [http://ehis.niehs.nih.gov/roc/ninth/known/vinylchloride.pdf]

Buck M, Gallegos M-T, Studholme DJ, Guo Y, Gralla JD (2000) The Bacterial Enhancer-Dependent sigma 54 (sigma N) Transcription Factor. J. Bacteriol. 182:4129-4136

Cabiscol E, Tamarit J, Ros J (2000) Oxidative stress in bacteria and protein damage by reactive oxygen species. Internatl. Microbiol. 3:3-8

Coleman NV, Mattes TE, Gossett JM, Spain JC (2002) Phylogenetic and kinetic diversity of aerobic vinyl chloride-assimilating bacteria from contaminated sites. Appl. Environ. Microbiol. 68:6162-6171.

Coleman NV, Spain JC (2003a) Distribution of the coenzyme M pathway of epoxide metabolism among ethene- and vinyl chloride-degrading *Mycobacterium* strains. Appl. Environ. Microbiol. 69:6041-6046

Coleman NV, Spain JC (2003b) Epoxyalkane:Coenzyme M transferase in the ethene and vinyl chloride biodegradation pathways of *Mycobacterium* strain JS60. J. Bacteriol. 185:5536-5545

Davis JW, and C. L. Carpenter (1990) Aerobic degradation of vinyl chloride in groundwater samples. Appl. Environ. Microbiol. 56:3878-3880

de Haan A, M. R. Smith, W. G. B. Voorhorst and J. A. M. de Bont (1993) Co-factor regeneration in the production of 1,2-epoxypropane by *Mycobacterium* strain E3: the role of storage material. J. Gen. Microbiol. 139:3017-3022

Edwards EA, and Cox, E. E. (1997) Field and laboratory studies of sequential anaerobic-aerobic chlorinated solvent biodegradation. In: Alleman BC, and Leeman, A. (ed) In Situ and On-Site Bioremediation. Battelle Press, Columbus, OH, pp 261-265

Fogel MM, A. R. Taddeo, and S. Fogel (1986) Biodegradation of chlorinated ethenes by a methane-utilizing mixed culture. Appl. Environ. Microbiol. 51:720-724

Freedman DL, Danko AS, Verce MF (2001) Substrate interactions during aerobic biodegradation of methane, ethene, vinyl chloride and 1,2-dichloroethenes. Water Sci. Technol. 43:333-340.

Habets-Crützen AQH, and J. A. M. de Bont (1985) Inactivation of alkene oxidation by epoxides in alkene- and alkane-grown bacteria. Appl Microbiol Biotechnol 22:428-433

Hartmans S, A. Kaptein, J. Tramper, and J. A. M. de Bont (1992a) Characterization of a *Mycobacterium* sp. and a *Xanthobacter* sp. for the removal of vinyl chloride and 1,2-dichloroethane from waste gases. Appl. Microbiol. Biotechnol. 37:796-801

Hartmans S, and J. A. M. de Bont (1992b) Aerobic vinyl chloride metabolism in *Mycobacterium aurum* L1. Appl. Environ. Microbiol. 58:1220-1226

Hartmans S, F. J. Weber, D. P. M. Somhorst, and J. A. M. de Bont (1991) Alkene monooxygenase from *Mycobacterium*: a multicomponent enzyme. J. Gen. Microbiol. 137:2555-2560

Henzel W, Billeci T, Stults J, Wong S, Grimley C, Watanabe C (1993) Identifying Proteins from Two-Dimensional Gels by Molecular Mass Searching of Peptide Fragments in Protein Sequence Databases. Proc. Natl. Acad. Sci. USA 90:5011-5015

Jensen ON, Podtelejnikov AV, Mann M (1997) Identification of the components of simple protein mixtures by high-accuracy peptide mass mapping and database searching. Anal. Chem. 69:4741-4750.

Koziollek P, Bryniok, D., and H. -J. Knackmuss (1999) Ethene as an auxiliary substrate for the cooxidation of *cis*-dichloroethene and vinyl chloride. Arch. Microbiol. 172:240-246

Lee MD, J. M. Odom, and R. J. Buchanan, Jr. (1998) New perspectives on microbial dehalogenation of chlorinated solvents: insights from the field. Annu. Rev. Microbiol. 52:423-452

Mattes T, Coleman, N., Gossett, J., Spain, J. (2004) A linear plasmid carries vinyl chloride biodegradation genes in *Nocardioides* JS614. Submitted

Miura A, and H. Dalton (1995) Purification and characterization of the alkene monooxygenase from *Nocardia corallina* B-276. Biosci. Biotechnol. Biochem. 59:853-859

Ratledge C (1982) Nutrition, growth and metabolism. In: Stanford CRaJ (ed) The Biology of the Mycobacteria. Academic Press, London, pp 185-274

Reeve CA, Bockman AT, Matin A (1984) Role of protein degradation in the survival of carbon-starved *Escherichia coli* and *Salmonella typhimurium*. J. Bacteriol. 157:758-763.

Saeki H, and K. Furuhashi (1994) Cloning and characterization of a *Nocardia corallina* B-276 gene cluster encoding alkene monooxygenase. J. Ferment. Bioeng. 78:399-406

Sambrook J, and D. W. Russell (2001) Molecular cloning: a laboratory manual, 3rd edn. Cold Spring Harbor Laboratory Press, New York

Shim H, Ryoo D, Barbieri P, Wood TK (2001) Aerobic degradation of mixtures of tetrachloroethylene, trichloroethylene, dichloroethylenes, and vinyl chloride by toluene-o-xylene monooxygenase of *Pseudomonas stutzeri* OX1. Appl. Microbiol. Biotechnol. 56:265-269.

Small FJ, and S. A. Ensign (1997) Alkene monooxygenase from *Xanthobacter* strain Py2. J. Biol. Chem. 272:24913-24920

Squillace PJ, M. J. Moran, W. W. Lapham, C. V. Price, R. M. Clawges, and J. S. Zogorski (1999) Volatile organic compounds in untreated ambient groundwater of the United States, 1985-1995. Environ. Sci. Technol. 33:4176-4187

Switzer RL (1977) The Inactivation of Microbial Enzymes in Vivo. Ann. Rev. Microbiol. 31:135-154

Tortoli E et al. (1999) *Mycobacterium tusciae* sp. nov. Int. J. Syst. Bacteriol. 49:1839-1844.

Verce MF, R. L. Ulrich, and D. L. Freedman (2000) Characterization of an isolate that uses vinyl chloride as a growth substrate under aerobic conditions. Appl. Environ. Microbiol. 66:3535-3542

Weber FJ, W. J. H. van Berkel, S. Hartmans, and J. A. M. de Bont (1992) Purification and properties of the NADH reductase component of alkene monooxygenase from *Mycobacterium* strain E3. J. Bacteriol. 174:3275-3281

Table 1. Average maximum-specific enzyme activities (reported in nmol/min/mg protein) of JS614 resting cells and cell extracts, grown on various carbon sources.

Growth substrate	AkMO activity [a,c] (nmol/min/mg protein)	EaCoMT activity [a,b] (nmol/min/mg protein)	
		CoM added	no cofactor
VC	42.9 ± 6.4	6360 ± 2810	50 ± 80
ETH	39.1 ± 4.2	4040 ± 2750	10 ± 10
Acetate	0	350 ± 150	0
1/10 TSB	0	420 ± 190	0
ETH (then starved)	0.2 ± 0.3	1810 ± 1280	0
Epoxyethane	3.5 ± 1.1	940 ± 630	0

[a] Data are the average of at least three independent experiments except for ETH (then starved) which is the average of two independent experiments. Error is the 95% confidence interval.

[b] Cell-extract reactions (1 ml) contained 0.02 mg protein, 5 μmol epoxyethane, and 10 mM CoM. Specific activities were calculated from the epoxyethane depletion rate, after subtraction of the appropriate abiotic rate of epoxyethane loss (5.8±1.3 nmol/min in Tris buffer + CoM). In comparison, average rates of epoxyethane degradation in VC and ETH-grown cell extracts was 108.1±48.4 nmol/min, in acetate and TSB-grown cell extracts was 14.9±1.6 nmol/min, and epoxyethane grown cell extracts was 21.4±6.3 nmol/min. In all cases the biotic rates were statistically higher than the abiotic rates. All errors reported are 95% confidence intervals.

[c] Values were determined in resting-cell assays (KP buffer, pH 7.0). Specific activities were calculated from the ETH degradation rate, after subtraction of the appropriate abiotic rate of ETH loss (1.0±0.5nmol/min in water). The abiotic ETH loss rate was approximately 3.3% of the average ETH degradation rate in VC- and ETH-grown resting cells and was approximately 27% of the ETH degradation rate in epoxyethane-grown resting cells.

Table 2. AkMO subunits in *Rhodococcus* B276

Enzyme or enzyme subunit	Predicted B276 MW (kDa)[a]	Observed B276 MW (kDa)[b]	Predicted JS614 MW (kDa)[c]	Observed JS614 MW (kDa)[d]
EaCoMT	40.6	N/A	40. 5	41.9
AkMO beta subunit	38.4	35	39.1	41.9
AkMO coupling protein	13	14	12.1	12.9
AkMO alpha subunit	57.2	53	57.3	50.4
AkMO reductase	37.3	40	37.4	40.0

[a] The predicted molecular weight (MW) of EaCoMT and AkMO subunits from *Rhodococcus* B276 based upon their gene sequences (Saeki 1994).

[b] Observed MW of AkMO subunits expressed in response to propene in *Rhodococcus* B276 (Miura 1995).

[c] The predicted MW of EaCoMT and AkMO subunits EtnA (beta subunit), EtnB (coupling protein), EtnC (alpha subunit), and EtnD (reductase) from *Nocardioides* JS614 based upon their gene sequences (Mattes 2004).

[d] Observed MW of proteins expressed in response to VC and ETH in *Nocardioides* JS614 (Fig.3) assigned to putative JS614 proteins of similar MW using *Rhodococcus* B276 as a basis for comparison.

Table 3. Peptide Mass Fingerprint data from MALDI-TOF MS analysis of EtnC from JS614, a 50.4 kDa polypeptide excised following SDS-PAGE[a].

$Mass_{meas}$ (Da)	$Mass_{calc}$ (Da)	Δm (Da)	Δm (ppm)	Residues	AkMO alpha subunit amino acid sequence[b]
2799.623	2800.414	0.79	282	16-38	(R)YDWGFDYAKPDPKFPSRYIIPPK(G)
2046.776	2046.898	0.12	60	41-57	(K)DPFRVMMRGYAAMENEK(D)
1915.372	1914.862	-0.51	-266	45-60	(R)VM*M*RGYAAM*ENEKDNR(V)
1940.437	1940.948	0.51	263	71-86	(R)YRNANLAEPRFMEAMK(F)
3310.251	3310.62	0.37	111	81-111	(R)FM*EAMKFAVPALTDAEYQAVCGAGFLISSVK(N)
1367.028	1366.643	-0.39	-282	117-128	(R)QGYAGQM*LDEVR(H)
3553.838	3552.629	-1.21	-340	255-283	(R)HFWHQHMSMDTLVGVVSEYYAVNRPWAYK(D)
1892.964	1892.076	-0.89	-469	302-318	(R)LAPYGLKPPERLPDVAR(F)
2668.689	2668.157	-0.53	-199	342-363	(R)IDPM*GPADYEWFENHYPGWTAR(Y)
1100.67	1100.517	-0.15	-139	364-372	(R)YGGLWDAYR(E)
3809.875	3809.813	-0.06	-16	373-405	(R)EM*SDPSSGRLLMQELPALPPFC@QVCHVPC@VMPR(I)
1824.301	1823.854	-0.45	-245	434-448	(K)LNPTIYTGCANWWER(F)
2282.252	2281.154	-1.10	-481	449-469	(R)FDGM*DLADVILALGYVRPDGK(T)

[a]Protonated monoisotopic masses, sequence assignments and mass errors for peptides that map to the JS614 AkMO alpha subunit are listed.

[b]M*, methionine sulfoxide; C@, S-acrylamidocysteine

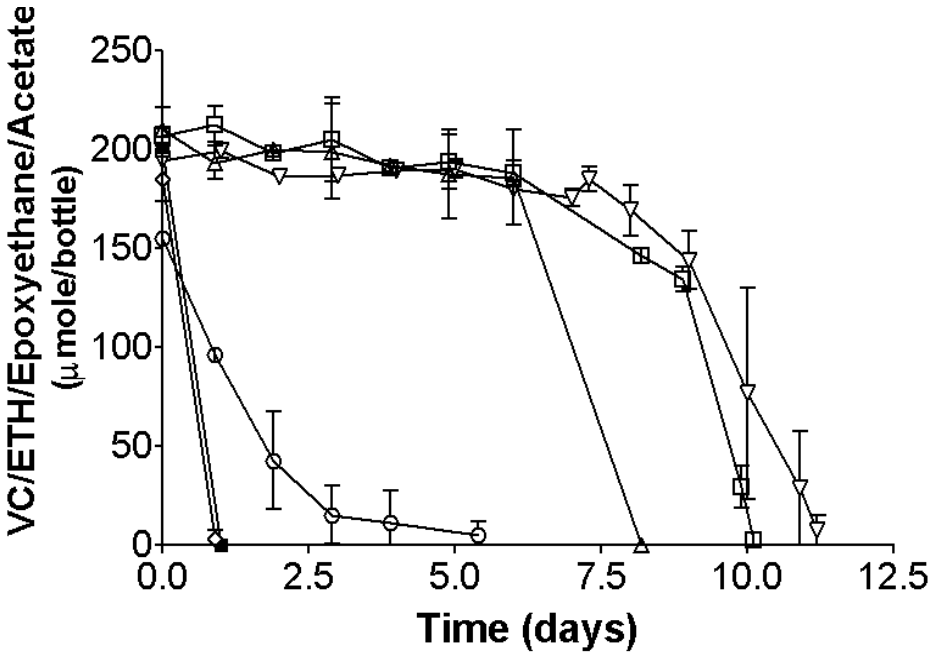

Figure 1. Substrate starvation response of strain JS614. (□) Starved VC-grown cultures supplemented with VC; (△) Starved ETH-grown cultures supplemented with ETH; (○) Starved ETH-grown cultures supplemented with epoxyethane; (◇) Starved ETH-grown cultures supplemented with acetate; (▽) Unstarved acetate-grown cultures supplemented with ETH. (■) Starved acetate-grown cultures supplemented with acetate. Data are the average of 2 replicates, and error bars are the standard deviations.

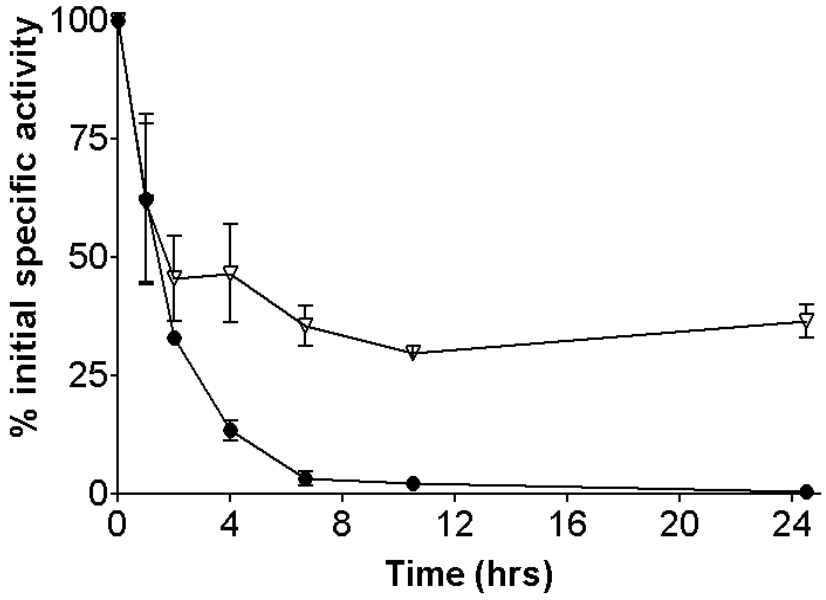

Figure 2. Effect of complete starvation on AkMO and EaCoMT activity. (•) AkMO activity (measured in ETH-grown resting-cell suspensions); (▽) EaCoMT activity(measured in ETH-grown cell-free extracts). Data are the average of 2 replicates, and error bars are the standard deviations.

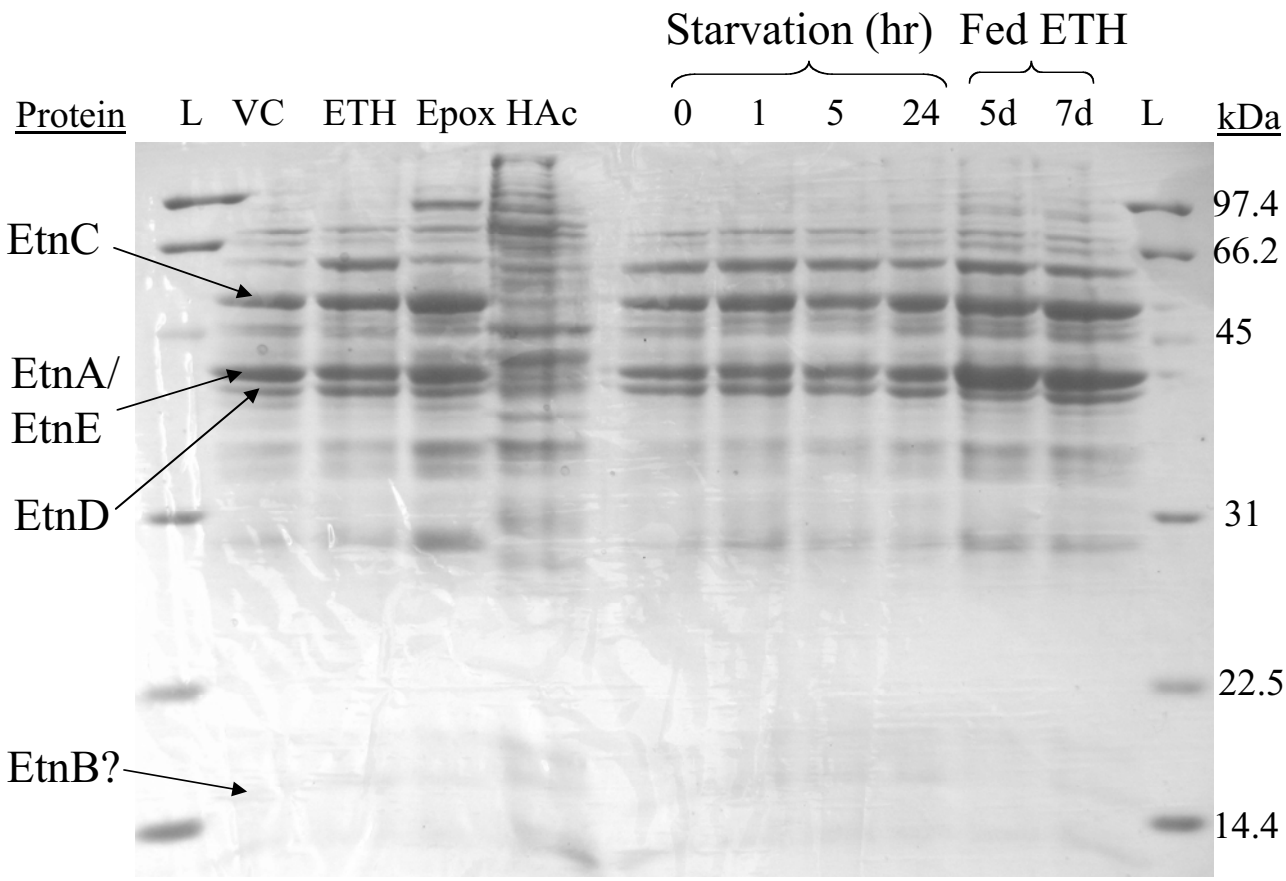

Figure 3. SDS-PAGE of cell-free JS614 cell extracts from various growth conditions. Lane VC: VC-grown JS614; Lane ETH: ETH-grown JS614; Lane EPOX: Epoxyethane-grown JS614; Lane HAc: Acetate-grown JS614; Lane 0: Unstarved ETH-grown JS614; Lane 1: ETH-grown JS614 starved 1 hr; Lane 5: ETH-grown JS614 starved 5 hr; LAne 24: ETH-grown JS614 starved 24 hr; Lane 5d: ETH-grown JS614 starved 24 hr, 5 days after re-feeding ETH; Lane 7d: ETH-grown JS614 starved 24 hr, 7 days after re-feeding ETH. In this experiment, starved JS614 cultures were experiencing an extended lag period 5 days after refeeding ETH, but had fully recovered ETH degradation 7 days after re-feeding ETH. Each lane contains approximately 75 ug protein.

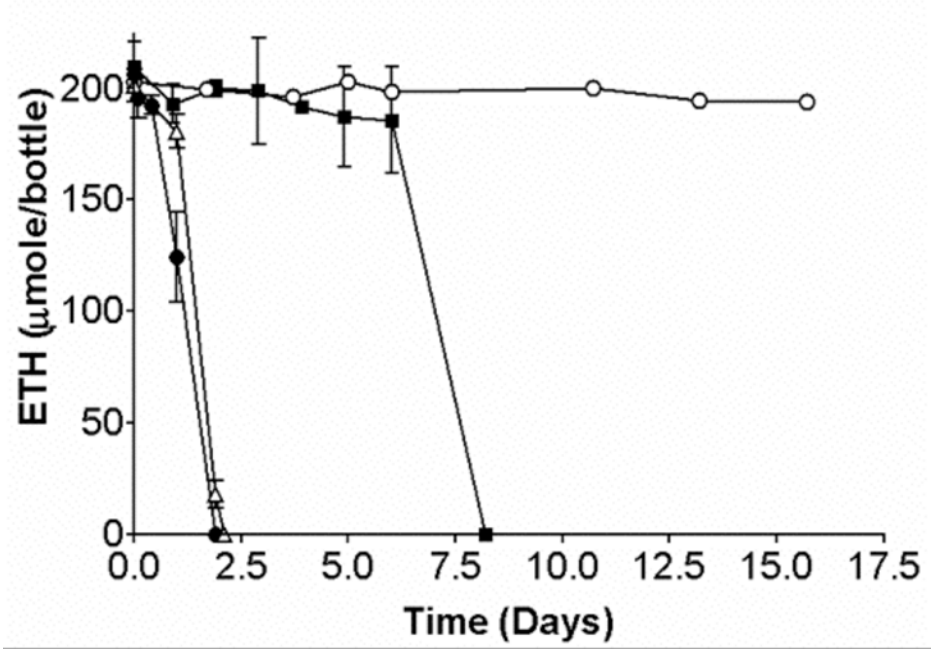

Figure 4. Recovery of ETH degradation after different starvation conditions. (•) Unstarved ETH-grown cultures fed ETH; (Δ) Starved ETH-grown cultures fed ETH + 1 mM acetate; (■) Starved ETH-grown cultures fed ETH (Control); (o) Starved ETH-grown cultures fed ETH + 1 mM acetate + 139 μg/ml chloramphenicol. Data are the average of 2 replicates, and error bars are the standard deviations.